ECOLE DOCTORALE :

Génétique, Cellule, Immunologie,
Infectiologie et Développement (GC2ID)

Molecular Characterisation of Odontoblast during Primary, Secondary and Tertiary dentinogenesis.

Caractérisation Moléculaire de l'Odontoblaste au Cours des Dentinogénèses Primaire, Secondaire et Tertiaire.

Thèse en vue de l'obtention du diplôme de

Doctorat d'Etat

Biologie Orale et Ostéo-articulaire –
Biomatériaux et Biofonctionnalité

Dirigée par :

Professeur Ariane BERDAL (Université de Paris 7 - France)
Professor Anthony J. SMITH (University of Birmingham – United Kingdom)

Auteur:

Stéphane SIMON

Soutenue publiquement :

le 20 novembre 2009

JURY

Mr Le Pr. Pierre MACHTOU, Président
Mme le Pr. Ariane BERDAL
Mr. le Pr. Anthony J. SMITH
Mr le Pr. Gunnar BERGENHOLTZ
Mr le Pr. Henry MAGLOIRE
Mme Le Pr. Dominique MAQUIN
Mr le Dr. Hervé LESOT
Mr le Dr. Richard M. SHELTON

ACKNOWLEDGEMENTS

I wish to express my deepest thanks to my supervisors, Pr Ariane Berdal, Dr Paul Cooper and Professor Tony Smith, for their advice, support and invaluable knowledge throughout my studies.

I wish to express my thanks and respects to Pr G. Bergenholtz and Pr H.Magloire for having accepted to juge this work with indulgence.

I wish to express my thanks and respects to Pr P. Machtou, Pr D.Maquin, Dr H. Lesot and Dr D. Shelton for their participation as members of the jury.

This work was supported by grants from the European Society of Endodontics (ESE) (Annual Research Grant 2004), from the International Federation of Endodontic Association (IFEA) (Annual Research Grant 2005) and from the British Endodontic Society (BES) (Annual research grant 2009)

We would like to thank the School of Dentistry of Birmingham and his Dean, Professor P.J Lumley for the financial support.

We would like to thank Dr Larry Fisher (National Institute of health) for freely providing Anti Mouse Dentin SialoPhosphoProtein Antibody (ref LR153).

To Eleonore, Louise and Sarah.

Thank you so much for your support and your patience. In memory of the very good time we had together at Birmingham for more than two years.

I would never have made it this far without your help and support.

I love you so much...

We are what we think.
All that we are arises with our thought
With our thoughts, we make our world.

Buddha,

(Present from Tony Smith – July 2008)

Abstract :

This research aimed to investigate the molecular regulation of odontoblast behaviour during primary, secondary and tertiary (reactionary and reparative) dentinogenesis.

Using gene microarray analysis and sq-RT-PCR, evidence is presented that the changes in secretory activity of odontoblasts reflect differential transcriptional control and that common regulatory processes may exist between dentine and bone. The p38 gene was shown to be highly expressed in odontoblasts during active primary dentinogenesis, but was drastically down-regulated as cells become quiescent in secondary dentinogenesis. Based on the hypothesis that parallels between development and healing processes in teeth exist, the results suggested that the p38-MAPKinase pathway may be activated during odontoblast stimulation in tertiary dentinogenesis by both p38 phosphorylation and enhanced nuclear translocation, supporting a recapitulation of events from primary dentinogenesis during tertiary dentinogenesis. The feasibility of use of the mouse as an *in vivo* model for studying pulpal healing in response to restorative procedures was also assessed. This approach provides a novel opportunity to exploit use of genetically modified animals to explore cellular and molecular processes during reparative events. Lastly, a transgenic mouse model was used to analyse the possible role of Msx2 transcription factor in odontoblast differentiation. The nature of the tooth phenotype in Msx2 null mutant animals was subsequently analysed.

This study has increased our understanding of the regulation of dentinogenic events, which may allow translation into new therapies aimed at maintenance of the vitality of the pulp.

Key Words :

Odontoblast, Dentinogenesis, MAPKinase pathway, Pulp capping, Msx2, stem cell differentiation.

Résumé :

L'objectif de ce travail a été d'explorer les régulations moléculaires au sein de l'odontoblaste au cours des dentinogénèses primaire, secondaire et tertiaire.
Les résultats obtenus à partir de micro-puces et de PCR semi quantitative ont permis de mettre en évidence un contrôle différentiel transcriptionnel de l'activité sécrétrice de l'odontoblaste. Des processus de régulation commun entre la dentine et l'os sont également discutés. La forte expression du gène p38 au cours de la dentinogénèse primaire, est drastiquement diminuée dans l'odontoblaste mature.
Les résultats suggèrent également que la voie de signalisation p38-MAPKinase pourrait être activée pendant la dentinogénèse tertiaire, par la phosphorylation de la protéine p38 et sa translocation nucléaire, confirmant ainsi la récapitulation d'un processus du développement initiale de la dent dans celui de la cicatrisation pulpaire. L'utilisation de la souris comme nouveau modèle de laboratoire pour étudier la cicatrisation pulpaire est également décrite. Ce nouveau modèle constitue une opportunité réelle car il permet d'utiliser les animaux génétiquement modifiés pour explorer les processus cellulaires et moléculaires impliqués dans la réparation pulpaire. Enfin, un modèle de souris transgénique a été utilisé afin d'analyser l'éventuel rôle du facteur de transcription Msx2 dans le processus de différentiation odontoblastique. Le phénotype dentaire du mutant nul Msx2 -/- est analysé en détail.
Ce travail permet de compléter les connaissances sur la régulation moléculaire de la dentinogénèse, étape importante pour le développement de nouvelles thérapeutiques en terme de conservation de la vitalité pulpaire.

Mots Clefs :

Odontoblaste, Dentinogénèse, MAPKinase, Coiffage pulpaire, Celles souches, Différentiation.

CONTENTS

List of Figures

List of Tables:

1 INTRODUCTION

Significant progress in the field of carious disease management has led to much research into the mineralisation of teeth and the biological behaviour of the dentine-pulp complex. It is apparent that the dentine-pulp complex is able to adapt to a multitude of stimuli invoking defence responses to maintain pulp vitality. The main role of the pulp is to secrete dentine. When tooth development is completed, the pulp maintains the dentine through homeostatic and self-protective mechanisms. The dental pulp is also able to reinitiate dentinogenesis at any time to protect itself from external injuries. However, advances in understanding the basic biology of this tissue have not yet been fully translated into better treatments in day-to-day dental practice beyond only minor carious lesions. When caries has progressed through most of the depth of the dentine, it is generally assumed that it is too late to use regenerative techniques to intervene. When the caries extends to the pulp, a pulpectomy is usually considered in order to prevent painful, infectious complications. However, so far no guidelines clearly define the indications for pulpectomy versus pulp vitality conservation.

Many researchers have been investigating the pulp healing process over several years and recent advances in biotechnology have opened opportunities for development of applications in pulp vitality maintenance, reactionary dentinogenesis and revascularisation of the infected canal.

1.1 Towards a biological approach

The concept of vital pulp therapy is one that focuses on using biological principles to maintain pulp vitality. This requires an understanding of the many patho-physiological processes of the dentine-pulp complex and the development of new materials for clinical use, which exploit the pulpal healing processes and better mimic the physiological tissues being restored. However, this evolution of new therapeutic principles within conservative dentistry dictates that techniques should be developed in which new materials are used in the context of minimising damage to the dental tissues during restorative preparation.

The gradual replacement of amalgams by composites, which are considered to have better aesthetic properties in coronal restorations, has been justified in part by the toxicity of the former both to the patient and environment, although resins are far from being inert themselves. However, adhesive restorations have a biological advantage in minimising the amount of dental tissue needing to be removed during preparation. Apart from the biomechanical advantages of maximal retention of dental tissue, injury to the tissues is minimised and diffusion pathways to the pulp are reduced with the decreased number of open tubules. The improvement in the long-term prognosis offered by these approaches is evident (Murray, About et al. 2000). Therefore, minimalist dentistry, also called “non-invasive” dentistry or Minimal Intervention Therapy, has significant potential (Pashley 1996; Banerjee, Kidd et al. 2003; Ericson, Kidd et al. 2003; Kidd, Banerjee et al. 2003; Kidd 2004; Pashley 2002).

1.2 The dentine-pulp complex

Dentine provides protection to the pulp, a soft connective tissue, which ensures the “vitality” of the tooth (Linde and Goldberg 1993). The “dentine-pulp complex” is so

called because of the intimate relationship of the two tissues that makes it difficult to separate their functional behaviours.

Dentine is a mineralised connective tissue that constitutes the main component of the tooth; it ensures support for the organ and confers elasticity. Seventy percent of dentine is mineralised by hydroxyapatite crystals; it is also composed of 20% organic matrix and 10% water. The organic component is mostly composed of proteins, which play various structural, formative, signalling and homeostatic roles as well as being important in the pulp healing process.

Predentine, present on the formative surface, represents the unmineralised precursor of the dentine matrix. While the composition is similar to that of dentine, changes in some matrix components occur as the mineralisation front is approached (Linde 1984). The dentine is made of various types of collagen such as collagen type I (the major collagenous constituent), V and VI, and of non-collagenous proteins (proteoglycans, glycoproteins, dentin phosphoprotein, etc). Among these molecules, Dentin Sialo-protein (DSP) and Dentin Phospho-protein v are considered to be more specific to dental tissues. Nevertheless, these proteins have also been found in other mineralised tissues such as bone but at significant lower concentrations than in dentine (Goldberg and Smith 2004).

The non-collagenous proteins, secreted from the distal part of the odontoblast process, ensure the transformation of the predentine into dentine, by initiating and controlling the mineralisation of the extracellular matrix (ECM) in the area of the "mineralisation front" (Butler 1998).

Dentine is a permeable tissue that is traversed by tubular structures called dentinal tubules, which extend from the enamel-dentine junction (EDJ) (or the cemental-dentine junction (CDJ) at the root level) to the pulp cavity (chamber or canal). These tubules contain dentinal fluid and the odontoblast processes. The extent of these

odontoblast processes in the tubules remains controversial with some authors claiming that the processes extend from the pulp chamber to the EDJ or CDJ (Maniatopoulos and Smith 1983; Sigal, Aubin et al. 1984; Sigal, Aubin et al. 1985). Others, however, suggest that the odontoblast processes are limited to the internal third of the tubules only (Garberoglio and Brannstrom 1976; Thomas and Carella 1983; Thomas and Carella 1984; Pashley 2002). This structural distinction is important because the presence of cellular extensions in the tubules can influence therapeutic approaches during disease management. Tubules that have been partially occluded by cellular activity will confer different permeability properties on the tissue than those whose dimensions have been increased by carious processes and this will affect treatment planning accordingly.

The circumpulpal dentine is composed of inter-tubular dentine (between tubules) and peri- or intra-tubular dentine (deposited within/around the tubule, which reduces the diameter of the tubule; (Figure 1).

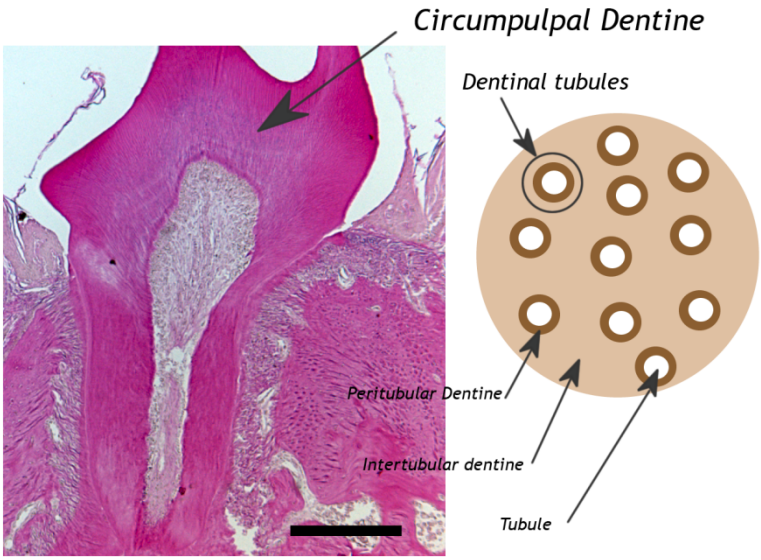

Figure 1: Schematic of the structure of circumpulpal dentine (also called orthodentine). First upper mouse molar. Van Gieson staining. Bar=500µm

The secretion of intra-tubular dentine is continuous throughout the life of the tooth and can be accelerated in certain patho-physiological conditions (such as caries and tooth wear), leading to dentinal sclerosis (Senawongse, Otsuki et al. 2008).

The chemical compositions of inter-tubular and peritubular dentine are different, particularly in terms of their collagen content and responses to etching procedures. These structural differences must be taken into account clinically because, for example, they can cause difficulties for bonding procedures. Protocols must differ between bonding on sclerotic dentine and filling a deep cavity in a relatively young tooth. This structural difference is also important in Endodontics with the introduction of resin-based adhesive systems. Since the dentine structure in the apical region is closer to a fibro-dentine structure than to a tubular one (Mjor, Sveen et al. 2001) questions remain regarding the sealing effectiveness of these systems in the short-, medium- and longer-term where the use of a protocol directly inspired by coronal bonding may not be optimal for endodontic use.

1.2.1 Three types of dentine

Confusion remains regarding the terminology of the different types of dentine, i.e. primary, secondary and tertiary dentines. Many definitions have been proposed in the literature with several of which being contradictory. Although these definitions have not reached a consensus, they have been collated by Goldberg and Smith (Goldberg and Smith 2004) who supported the following definitions:

Primary dentine: this is the earliest dentine formed during tooth development giving rise to the crown and root structure of the tooth. It “patterns” the tooth organ. The most external, relatively thin, layer adjacent to the amelo-dentinal junction is formed as the odontoblasts are completing differentiation resulting in a variable tubular structure and is referred to as mantle dentine.

Secondary dentine: this is physiologically secreted either after the tooth has erupted into the oral cavity, or following apical closure. This dentine is generally responsible for the progressively decreasing space of the canal, which is improperly called "calcification". It is a physiological dentine rather than being pathological in nature; its continuing secretion is responsible for the asymmetrical loss of endodontic volume. This biological process explains the differences in canal volume between a young and an older tooth. The secondary dentine secretion is not uniform, but appears to occur predominantly on the roof and lateral walls of the pulp chamber and not on its floor. The chemical composition and the histological structure of the primary and secondary types of dentine are considered to be identical, although the published evidence for this is limited. Only the rate of secretion differs: 4 µm/day for primary dentine and 0.4 µm/day for secondary dentine (Schour and Poncher 1937; Ziskin, Applebaum et al. 1949; Nanci 2003). The interface between primary and secondary dentine is sometimes demarcated by a subtle calciotraumatic line. However, since both dentines are secreted by the same odontoblasts there will be tubular continuity and thus, there does not appear to be any obvious clinical consequence as to whether primary or secondary dentine is present (**Figure 2**)

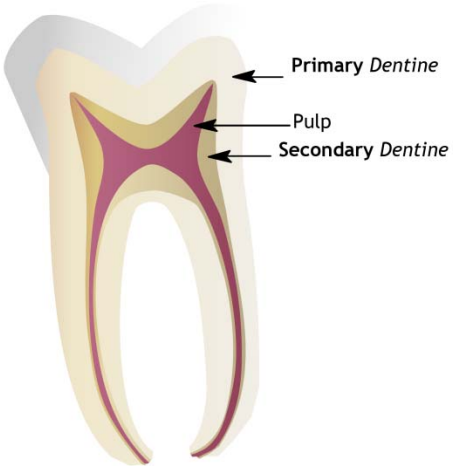

Figure 2: The histological localisation of the two types of physiological (primary and secondary) dentine.

In summary, primary dentinogenesis occurs during development leading to formation of the crown and root of the tooth, whereas secondary dentine is secreted throughout the life of the tooth, and is responsible for reduction in the size of the pulp chamber, root canals and continued deposition of peritubular dentine (Baume 1980).

Tertiary dentine: is secreted in response to external stimuli, such as caries or abrasion, in order to protect the underlying pulp. In the case of moderate stress, which does not result in destruction of odontoblasts, the secreted dentine is termed "reactionary dentine"; when the stress is more intense and odontoblast survival is compromised (i.e., dentine bridge formation at sites of exposure), it is termed "reparative dentine" (**Figure 3**).

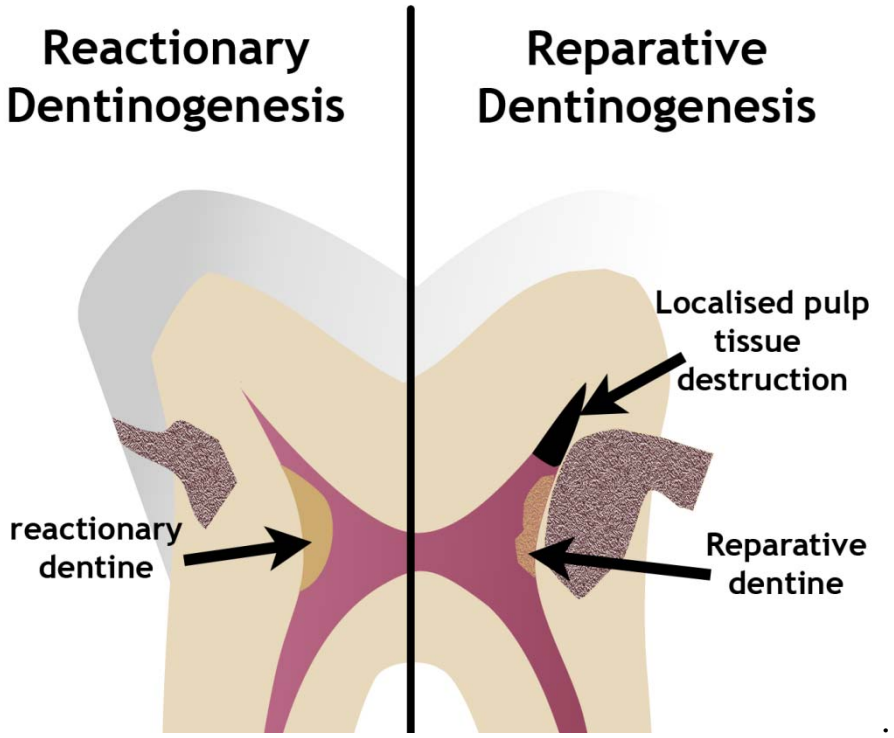

Figure 3: The two types of tertiary dentinogenesis.

Understanding the distinction between the three types of dentine is important, and above all the distinction between secondary (physiological) and tertiary (healing) dentine must be clear, as they are often confused when reported in the literature.

1.2.2 Dentine and bone

Notably, dentine and bone are very similar in their composition, but show some structural differences. Many studies have shown that the compositions of these tissues are more similar than previously appreciated. Indeed, certain molecules that were originally considered to be specific to dentine (such as Dentine sialoprotein; DSP) have been shown to be present in alveolar bone (Butler, Brunn et al. 2003; Huang, Sun et al. 2008). It is therefore more difficult to find specific markers to characterise these tissues. Nevertheless, the profiles of the SIBLINGS protein for example, show differences between the two tissues (Huang, Sun et al. 2008).

On a structural level, bone and dentine exhibit several common features. Cells of both bone and dentine are of a similar mesodermal embryonic origin, which may explain some of the similarities found in their formation and structures. In bone, secretion of the matrix is performed by osteoblasts; once embedded in the mineralised matrix, they appear to change into quiescent cells called osteocytes which communicate with each other through an extensive network of cell processes embedded in canuliculi. In the dentine-pulp complex, odontoblasts remain on the formative surface of the dentine matrix but have a cell process extending through the dentine with many lateral processes. The similarities between the morphologies of dentinal tubules and osteocyte canuliculi have recently been highlighted (Lu, Xie et al. 2007) and recent molecular data demonstrate striking similarities in the behaviour of odontoblasts and bone cells at different stages of their life cycles (Simon, Smith et al. 2009).

1.2.3 Dentinal tubules - a means of communication.

1.2.3.1 The tubular structure

The tubular density of dentine is high (~30,000/mm^2 on average), and these tubules are approximately 1 to 3 micrometers in diameter on average in humans depending on the intratubular dentine thickness; their distribution is unequal throughout the dentine and their density increases near the pulp cavity reflecting the crowding of odontoblasts as they move pulpally during dentinogenesis (Figure 4).

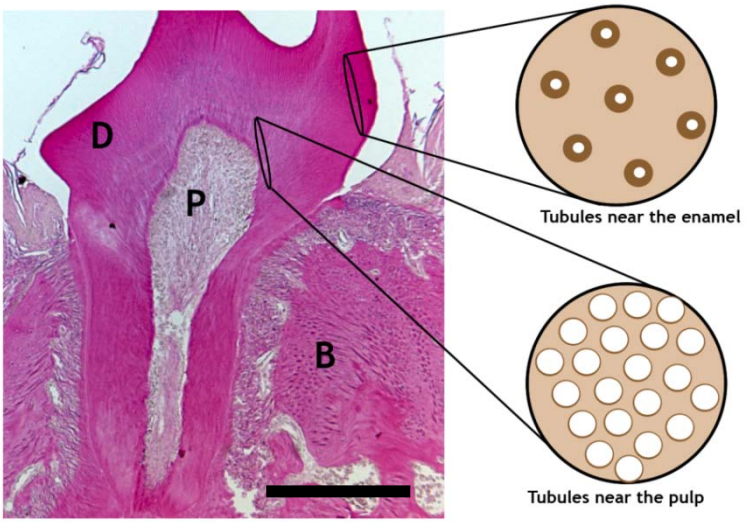

Figure 4 : The density of the dentinal tubules varies according to the depth of the dentine and the proximity to the pulp. Surface area occupied by tubules is 2/3% near the Enamel, but 20-25% near the pulp. (Pashley 1996) (according to (Olgart and Bergenholtz 2003) - D=Dentine, P=Pulp, B=Bone. Bar=500µm

The tubules course in a sinusoidal manner in the crown rather than a rectilinear way, due to a change in the radius of curvature from the outer to the inner aspect of the dentine and each has numerous lateral extensions, which provide a means of communication between them. Thus, much of the area of the dentine matrix is in direct communication with the odontoblasts on its formative surface through their processes contained within the tubules. This has significant clinical implications in

terms of the communication between the inner and outer regions of the tooth and how disease or surgical intervention can impact.

The tubular density differs significantly at outer and inner areas of the dentine. It is estimated that the surface occupied by these tubules represents 1% of the dentinal surface in the periphery of the dentine (under the enamel) and 22% near the pulp (Fosse, Saele et al. 1992). This variable distribution underlines the importance of location when drilling a cavity or making a coronal preparation, due to the opening of a diffusion pathway into the pulp tissue and potentially allowing the ingress of bacteria, toxins, and other adverse agents.

The entire length of the tubules will contain dentinal fluid, which probably represents a cellular transudate from the pulp parenchyma together with any local odontoblast secretions. Two different phenomena are encountered from the moment when open tubules are exposed:

Diffusion *(*Figure 5*):* When two biological environments (i.e., the pulp and the external environment of the oral cavity) are separated by a filter (i.e., the tubular dentine), a concentration gradient is established for agents within these two environments. Diffusion occurs from the most concentrated to the least concentrated milieu in order to equilibrate the concentrations. In the case of teeth, the presence of bacteria at high concentration in the saliva will lead to their passive diffusion to the sterile pulp parenchyma if the permeability barrier of the enamel is absent from the outside of the tooth. Nevertheless, the relatively large diameter of bacteria relative to the diameters of tubules is an obstacle to their movement through the tubules, although toxins and other molecules can still readily pass through.

The phenomenon of intra-pulpal pressure, is greater than that external to the tooth*:* physiologically, the pressure in the pulp relative to that external to the tooth is such that there tends to be an outward flow of fluid if open tubules are exposed,

and thus limits the risk of pulpal contamination from inward diffusion (Figure 6). Fluid mechanics represents a complex science, especially in the context of the irregular architecture within a dentinal tubule, but this outward pressure in the tubule ensures that the tubular dentine matrix does not act as a simple permeable sieve.

1.2.3.2 Dentine permeability and clinical implications

The greater pressure intra-pulpally is directly relevant to clinical procedures in restorative dentistry. In the bonding process, it is recommended to "dry but not dessicate" the dentinal surface. It is worth noting that a few seconds after drying, the dentinal surface is wet again. At this stage, it is not recommended to further dry the surface, otherwise dessication of the dentine may occur causing unnecessary damage to the pulp, which would inevitably lead to post-surgical pain. New generations of adhesives take this into account and tolerate the presence of moisture in the dentine to ensure optimal adhesion.

Dentinal permeability is an unavoidable factor necessary to consider during therapeutic procedures in dentistry. Surgical intervention of teeth will inevitably cause some damage to the pulp; the responding defence processes are numerous and complex and their interplay is not yet fully understood. Nevertheless, they are the basis of the healing process, and post-surgical pain is sometimes encountered after even conservative treatment. It is necessary to recognise the defence processes occurring in the tooth in order to clinically manage post treatment discomfort optimally.

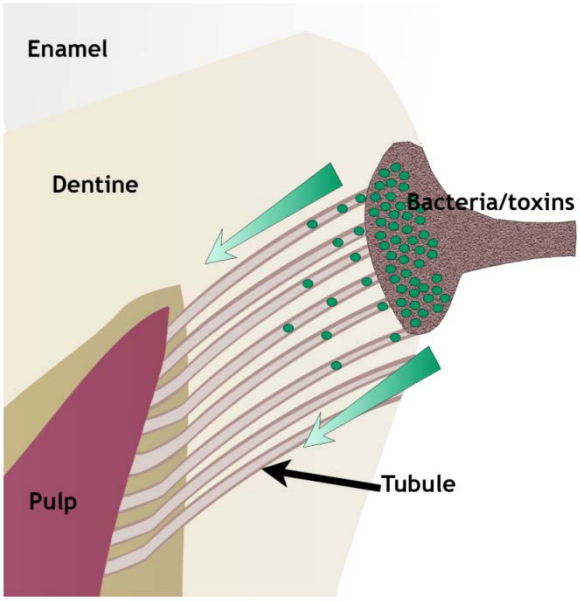

Figure 5 : There is a differential concentration of bacteria/toxins, between the carious dentine and the pulp tissue. Bacteria and toxins tend to diffuse from the highest concentration area to the lowest one through the dentinal tubules. This phenomenon is termed diffusion.

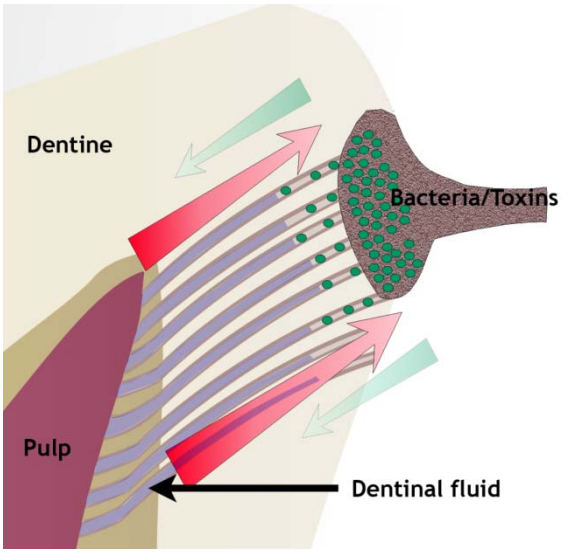

Figure 6 : The difference in the pressure between the intra-pulpal cavity and the outside area is protective of the pulp parenchyma. The external direction of this pressure gradient tends to strongly limit inward diffusion of the bacteria/toxins.

The pulpal hydrodynamic theory (Brannstrom 1963) probably provides our best explanation for pulpal pain. This theory helps explain how one tooth can become very sensitive to cold after dentinal exposure, whereas other teeth in the same

mouth remain painless or why for experimental purposes, application of a few drops of sugar solution can provoke violent pain whereas patients can tolerate much more aggressive stimuli to other teeth? On the basis of histological and physiological observations, Brannström (1963) proposed that dentinal sensitivity is closely associated with very fast and brief movements of dentinal fluid inside the tubules, which may trigger responses within the vascular and neural structures at the pulpal level (Figure 7).

Since Brannström's (1963) seminal publication, new theories have been proposed to extend our understanding of dentinal sensitivity, such as the possibility of partial innervation of the tubules (Carda and Peydro 2006). Recent findings suggest the possible existence of sensory properties for the odontoblast and its role in sensory transmission of stimuli to the tooth (Okumura, Shima et al. 2005; Allard, Magloire et al. 2006).

Although the precise mechanisms of pain transmission in teeth remain to be fully elucidated, our present knowledge already allows understanding of some of the clinical responses encountered in day-to-day practice. It is quite common to find patients complaining of pain after they have received a bonded inlay using an indirect technique. Sensitivity is mainly encountered while chewing and can be explained by the hydrodynamic theory. When chewing, some resin-bonded restorations exhibit a "shock absorber" effect owing to their visco-elastic properties. During each micro-movement, fluid movements in the tubules and in the hybrid layer are triggered and may be responsible for the extra external pressure being exerted on the pulp. Thus, acute pain can be the result of routine restorative treatment.

Movement of the dentinal fluid may explain the unusual pain described by patients presenting with a root crack or fracture. This pain is considered as peculiar since it is not a reaction to pressure, but it is felt during relaxation (opening). In the case of a crack or fissure, the pressure within the tooth during occlusion causes micro-movements and tends to separate the two edges of the crack; therefore, the pulpal interstitial fluid tends to invade the space created. When pressure is released, the two dentinal edges will close up, thus creating increased intra-pulpal pressure resulting in very sharp and transient pain. Therefore, the appropriate treatment for such pathology is to retain the edge gap and provide a tooth covering (for example, with a crown). In this case, endodontic treatment probably has little merit.

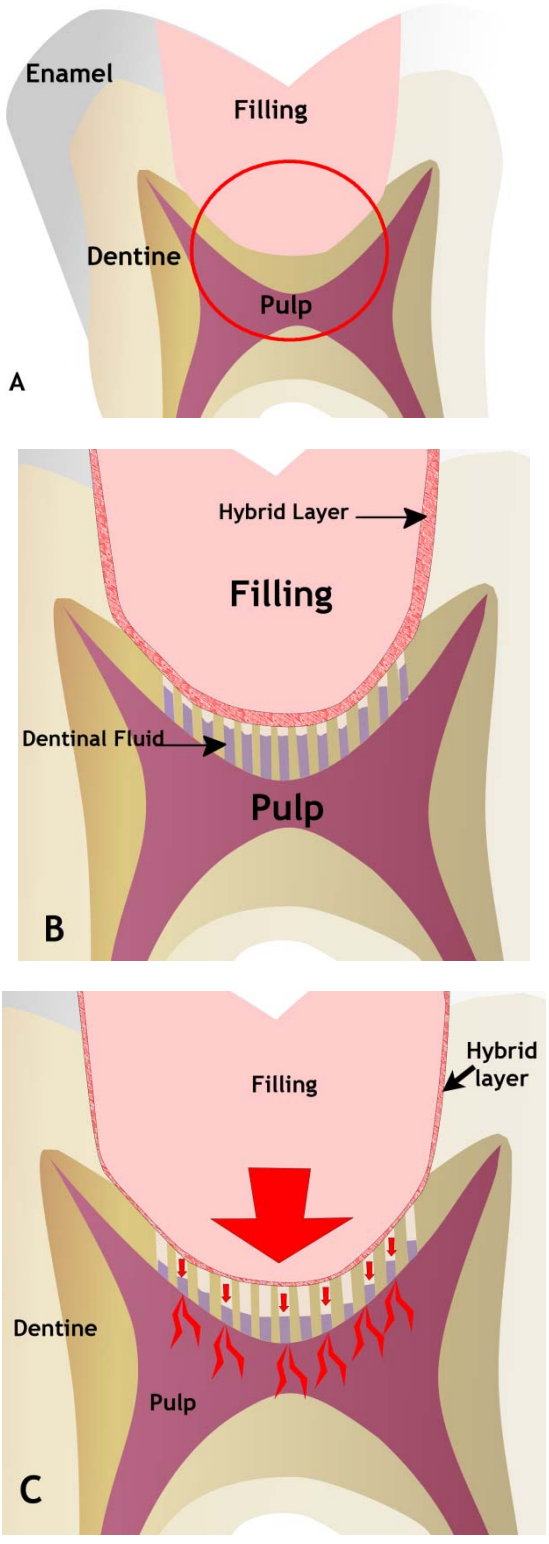

Figure 7 : The principle of Brannström's hydrodynamic theory: (A) The application of forces on the filling can lead to a displacement of the dentinal fluid into the tubules, and create an increased pressure in the pulp, which can cause post-surgical discomfort (B and C).

1.2.3.3 Consequences of new technological developments.

Our knowledge of the dentine-pulp complex provides an important foundation on which to underpin a new era for dentistry with a biological focus. For example, the concept of cavity disinfection is of primary importance to prevent bacterial penetration and diffusion of toxins beneath restorations and this is being exploited in the development of new restorative products. Bonding systems have now been developed, which aim to complement the adhesive properties with antibacterial molecules to control residual and recurrent caries. Protect Bond® (Kuraray®, Germany), in which 12-methacryloyloxy-dodecyl-pyridinium-bromide (MDPB) has been added to the bonding agent, is a relevant example of this new generation of products. New research is underway to consider addition of other molecules which would play a role in stimulating pulpal healing.

1.3 Histological content of the Pulpal tissue

The pulp contains many different cell types several of which show specialisation for particular functions (Figure 8).

1.3.1 Odontoblasts.

These are highly differentiated, post-mitotic cells, and are organised at the periphery of the pulp as a unicellular palisade. The presence of all the elements of the secretory/mineralisation machinery in the cells confirms their intense activity, notably during primary dentinogenesis. At a later stage during secondary dentinogenesis, the cells return to a quiescent state, with a reduced number of cytoplasmic organelles (Jones and Boyde 1984). Odontoblasts are joined by cellular junctions, such as gap junctions, thereby making a palisade of cells that provide a permeability barrier; gap junctions are also responsible for intra-cellular

communication, which may be involved in regulating the pulp healing process (Magloire, Couble et al. 2004).

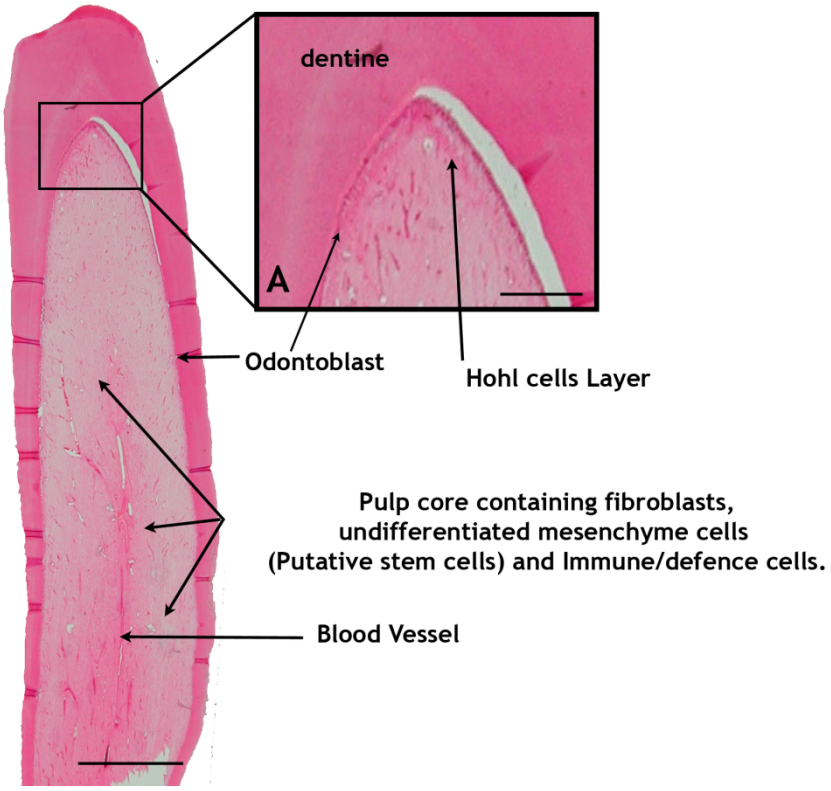

Figure 8: Histology of first upper bovine molar. 7µm section, Haematoxylin and eosin stained. Bar scale=500µm (A): higher magnification view - bar scale - 250µm

Unlike osteocytes, odontoblasts do not become incorporated in the matrix, except for their processes that are embedded in the tubules. This is why dentine must not be considered as an individual tissue but rather as the dentine-pulp complex. The odontoblast processes contain limited organelles (which are believed to be responsible for the later secretion of intra-tubular dentine), but are mostly filled by a dense network of micro-filaments and other micro-tubules.

Increasingly, coronal odontoblasts are regarded as being different from those found in the root (Nanci 2003). The coronal odontoblasts are elongated and pyramidal with

an apical nucleus, whereas radicular odontoblasts are more cuboidal, which is potentially an indication of significantly lower cellular activity. This fact is seldom taken into account, but would explain why therapeutic interventions that have been validated at a coronal level (pulp capping, for instance) will often fail when applied to the radicular pulp (pulpotomy).

1.3.2 Final differentiation process of odontoblasts during development.

Odontoblasts synthesise the components of the predentine (collagen, glycoproteins and other non-collagenous proteins) and are responsible for its mineralisation. As for the other cells of the dental pulp, the odontoblasts are derived from neural crest mesenchymal cells and their differentiation is under the control of the internal dental epithelium (IDE). Differentiation is initiated at each cusp tip and is carried out according to a specific temporo-spatial pattern. In the mouse, the first differentiated odontoblasts appear on the 18th day of embryonic development, on the top of the main cusp of the first lower molar. The differentiation process gradually extends to the apical area and leads to the formation of a gradient of differentiation (Ruch, Lesot et al. 1995).

1.3.2.1 From preodontoblast to functional odontoblast

In the early stages of development, undifferentiated cells derived from the cranial neural crest migrate to the first branchial arch. The oral epithelium plays a key role in the initial pattern of the tooth, by controlling cellular commitment as well as the morphology of the tooth germs (incisor, molar, etc).

Final differentiation of preodontoblasts into odontoblast occurs after a specific number of cell divisions (Ruch, Lesot et al. 1995). All of the cells of the dental papilla have the potential to differentiate into odontoblasts, however, only those in contact with the basal membrane at the interface with the Internal Dental Epithelium (IDE)

undergo terminal differentiation. This consideration has implications in the healing process, in which other signalling processes are responsible for induction of odontoblast-like cell differentiation.

In mice, the pre-odontoblasts, located near the basal membrane (BM), undergo 14 to 15 mitoses before leaving the cell division cycle; the number of cell divisions necessary for this process in humans, however, has not yet been demonstrated. During the last division, the mitotic spindle, originally parallel to the basal membrane, realigns to be perpendicular to this membrane (Osman and Ruch 1976). After the last mitosis, only the cell in contact with the BM is able to enter into the terminal differentiation process, while the other daughter cell (not in contact with the BM), becomes a part of Höhl's cell layer.

1.3.2.2 Cytological modifications and odontoblast differentiation

Differentiation induces nuclear polarisation and cell elongation, implying important cytological changes. The rough reticulum cisternae and the Golgi apparatus are orientated parallel to the long axis of the cell and are localised in its distal area where the process will develop. The cell body of the differentiated secretory odontoblast is approximately 50 to 60 µm long.

Functional odontoblasts are connected by many intercellular junctions; gap junctions ensure rapid transport of ions and small molecules between cells. These junctions are present along the cytoplasmic membrane of the body of the cell, creating cell contact between odontoblasts themselves and between odontoblasts and cells in the sub-odontoblast layer (Sasaki, Nakagawa et al. 1982). Other intercellular junctions, such as desmosomes, enable a mechanical cohesion between the odontoblasts creating a true histological barrier. These junctions are located in the area of the cell body and the process junction (Kagayama, Akita et al. 1995). This distal junction

creates a physical barrier between the compartment of the predentine, and the odontoblast cell-body.

Immature odontoblasts are small and ovoid in shape, having a high nuclear/ cytoplasmic ratio, a rudimentary granular endoplasmic reticulum and a few Golgi cisternae. Cellular modifications appear when cells reach the secretory phase (Goldberg and Smith 2004). Matrix vesicles were initially identified in cartilage of long bone (Bernard 1969), and then later were described in the dentine-pulp complex (Katchburian and Severs 1982). Theses vesicles are located in the extracellular matrix adjacent to the odontoblasts during mantle dentine formation. They disappear once mantle dentine formation is completed and the distal process has started to elongate.

At the ultrastructural level, these vesicles appear as extracellular spherical structures, contain amorphous material more or less electron-dense and surrounded by a membrane. As in bone and cartilage, the membrane of these vesicles is made of 3 layers, and contains various enzymes, especially phosphatases, involved in the mineralisation process. The vesicles are the initial sites of mineralisation in the mantle dentine and are also found in cartilage and bone.

Ultrastructural modifications have also been shown in the secretory cells during primary, secondary and tertiary dentinogenesis related to their functional activity (Couve 1986). Active cell appears elongated, with basal nuclei. They contain many organelles with numerous vesicles, extensive rough endoplasmic reticulum and a well developed Golgi complex located between the nucleus and distal region of the cell. Morphologically the quiescent cell is stubby, cuboidal, and shows only limited cytoplasm. Organelle numbers decrease and this is related to the lower activity of the cells (Nanci 2003).

1.3.2.3 Regulation of odontoblast differentiation

During development, odontoblast differentiation is controlled by reciprocal interactions between the inner dental epithelium and the dental papilla. The extracellular matrix (ECM) and the basal membrane (BM) play a critical role in this regulation, serving as a reservoir of paracrine and autocrine factors.

Only a specific dental BM is able to induce the differentiation of odontoblasts; the preodontoblasts can respond to epigenetic signals only after having carried out a fixed number of cell cycle divisions. Moreover, to play its role, the BM is subject to modifications, regulated by the inner dental epithelium. These changes are fundamental for the regulation of dental development.

The main components of the BM are collagen IV, fibronectin, laminin (Lesot, Osman et al. 1981), nidogen, tenascin, hyaluronic acid and proteoglycans including heparan sulfate (Thesleff, Barrach et al. 1981).

1.3.2.4 Growth factors

Various growth factors and their receptors have been shown to be present at the enamel organ-dental papilla interface by immunohistochemistry and *in situ* hybridisation during tooth development and have been implicated in odontobalst differentiation:

- GH (growth hormone) plays a paracrine and/or autocrine role in dental development (Zhang, Li et al. 1997),

- IGF-1 and -2 (of the family of IGF: Insulin-like Growth Factor) (Begue-Kirn, Smith et al. 1994; Joseph, Savage et al. 1996; Cassidy, Fahey et al. 1997),

- TGFβ-1, - 2 & - 3 (D'Souza, Happonen et al. 1990; Thesleff and Vaahtokari 1992) and BMP-2 -4 and -6 (Vainio, Karavanova et al. 1993) play a role in the

polarisation and the differentiation of odontoblasts (Begue-Kirn, Smith et al. 1994). Notably in adult pulp, TGFβ-1 plays an important role in the regulation of the inflammatory response and tissue regenerative processes.

The sequestration of these growth factors in the dentine matrix and their subsequent fossilisation during the mineralisation process appears key to the pulp healing process where their release from the matrix may be responsible for various signalling events. Their precise localisation in the dentine (Smith, Matthews et al. 1998) and the full scope of their roles, however, remain to be elucidated.

1.3.2.5 Transcription factors :

A second level of regulation exists during dental development through transcription factors. Notably, Msx1 is expressed in polarised preodontoblasts and Msx2 is present in mature odontoblasts (Begue-Kirn, Smith et al. 1994). Msx1 protein and transcripts have been identified in the pulp mesenchyme at early stages of tooth development and their concentrations decreased at the bell stage (Coudert, Pibouin et al. 2005). Msx1 sense RNA is mainly expressed in the dental pulp of the mouse at 15^{th} day of tooth development.

Expression of these transcription factors is under the control of growth factors and they can ultimately have broad ranging effects. Significantly, BMP4 up-regulates Msx1 and Msx2 expression. In turn, transcription factors regulate further growth factor expression; for example, Msx1 up regulates BMP4 synthesis in the mesenchyme and Msx2 regulates Runx2 and Osteocalcin gene expression during odontogenesis (Bidder, Latifi et al. 1998; Blin-Wakkach, Lezot et al. 2001).

Growth factors and transcription factors are thus central to the cascade of molecular and cellular events during tooth development and are responsible for many of the temporo-spatial morphological changes observed in the developing tooth germ.

The second layer of the pulp is a dense zone of cells (the "cell rich layer of *Höhl*", separated from the odontoblasts by an acellular layer called the "cell free zone of *Weil*"). During tooth development, the cellular differentiation process requires a minimum number of mitoses of the odontoblast progenitor cells before they are competent to differentiate to the final cellular phenotype of the odontoblast. The last mitosis has important spatial implications because it occurs perpendicular to the dental basement membrane resulting in two daughter cells : the one adjacent to the basement membrane receives the inductive signal to differentiate to an odontoblast while the other does not and contributes to the *Höhl layer (Ruch, Lesot et al. 1995)*. This layer has long been considered as a potential reservoir of cells, containing incompletely differentiated cells that could be involved in the healing process for reparative dentinogenesis and dentine bridge formation if the odontoblast layer is damaged (Fitzgerald 1979).

The capillary and nerve plexi that exist between both layers are significant; only a few nerve fibres accompany the cytoplasmic extensions into the dentinal tubules and then only for a short distance (Carda and Peydro 2006). Capillaries are closely associated with the odontoblast palisade and provide these cells with the necessary nutrients for their mineralising/synthetic activities.

1.3.3 Pulp fibroblasts

Similar to other connective tissues, the major cell of pulp tissue is the fibroblast. These cells are responsible for the formation and renewal of the extracellular matrix, but at the same time they mediate its controlled remodelling. The extracellular matrix plays an important role in this connective tissue. Its viscosity changes with time (fibrosis increases with the age of the tissue) and during pathophysiological processes. Its visco-elasticity enables it to adapt to potential (and moderate)

variations in pressure, inherent in the inflammatory process. Due to this adaptability, most episodes of pulp inflammation are clinically silent. Pain increases when the intra-pulpal pressure, connected with the vasodilatation inherent in inflammation, can no longer be compensated for.

1.3.4 Immune cells

Dendritic cells have been identified in the pulp tissue (Jontell, Gunraj et al. 1987), even under physiological conditions (Jontell, Okiji et al. 1998). Macrophages are frequently found in healthy pulp (Trowbridge 2002). These phagocytic cells participate in the immune surveillance of the pulp, and enable a rapid response to occur to invading bacteria (Okiji, Kawashima et al. 1992; Okiji, Morita et al. 1992). Products of bacterial origin (such as toxins) diffuse via the tubules, and when in contact with pulp cells, they can behave like antigens; therefore, the immune system of the pulpal parenchyma plays an important role (Heyeraas, Sveen et al. 2001). Recent studies have demonstrated that human dental pulp cells, and particularly odontoblasts, may constitute the first line of defence to cariogenic bacteria entering dentine after enamel disruption (Staquet, Durand et al. 2008). Odontoblasts are proposed to initiate immune/inflammatory events within the dental pulp in response to cariogenic bacteria, by being stimulated by pathogens through Toll-like receptors (TLRs), production of chemokines upon cell stimulation with microbial by-products and induction of dendritic cell migration (Keller, Carrouel et al. 2009). TLR genes are expressed in the healthy human dental pulp that is thus well equipped to combat pathogens entering the tissue. Notably TLR2, CCL2 and CXCL1 are upregulated in odontoblasts both under carious lesions and upon stimulation with pathogen by-products. These molecules are now targets for the design of therapeutic agents able to reduce the immune/inflammatory response to cariogenic bacteria and favour pulp healing (Farges, Keller et al. 2009)

Dendritic cells capture antigens and move these to the lymphatic nodes, where they are presented to T-lymphocytes. Then, these activated T lymphocytes return to the damaged pulp. In this way, the host is immunised and will automatically respond to the future presence of these antigens. Other molecules, such as those of the TGF-β super-family, which have been liberated from the dentine during the mineralisation process, are able to regulate the immune system of the pulp (Farges, Romeas et al. 2003).

Dendritic cells also interact with nerve fibres and blood vessels within the pulp. The neuro-immunological response of the pulp is presumed to be one of the first inflammatory reactions of the dentine-pulp complex (Jontell, Okiji et al. 1998; Farges, Keller et al. 2009).

1.3.5 Dental pulp stem cells

The growing interest in stem cells by the scientific community is a key area in dental research. The description of dental pulp stem cells (DPSC) (Gronthos, Mankani et al. 2000) inside the pulp parenchyma demonstrated that the dental organ provides a "niche" environment for replacement cells. Another population of stem cells has also been reported in the pulp of deciduous teeth. These cells, or SHED (stem cells from human exfoliated deciduous teeth) (Miura, Gronthos et al. 2003), are singularly interesting because they are relatively easy to collect when the deciduous tooth is shed and replaced by the permanent successor.

More recently, a further group of mesenchymal stem cells has been reported in the apical papilla of human immature teeth. These pluripotent cells have been termed Stem Cells of Apical Papilla (SCAP) (Huang, Sonoyama et al. 2008). Since they may be bone marrow-derived cells, SCAPS have potential for osteogenic and dentinogenic differentiation. Growth factor receptor genes are similar on SCAPs and DPSCs. SCAPs

also express neurogenic factors, such as nestin and neurofilament M when stimulated with neurogenic medium (Sonoyama, Liu et al. 2008).

The role of these cells in induced apexogenesis in necrotic immature teeth has been hypothesized. Many investigations have studied the revascularization process to treat immature necrotic teeth. The possibility of canal colonization by SCAPs, which could be introduced to the canal by induction of a blood clot and stimulating and disorganising the apical papilla cells with the file has been investigated by several authors. New therapeutics for necrotic teeth should arise in the future as more understanding of the processes involved become available (Iwaya, Ikawa et al. 2001; Banchs and Trope 2004; Thibodeau, Teixeira et al. 2007; Thibodeau and Trope 2007).

The presence of stem cells in the dental pulp offers exciting possibilities for their exploitation in regenerative medicine both for dental and other diseases. These cells are easier to collect than bone marrow cells, which is currently one of the main sources of post-natal stem cells. Also, they appear to be a promising reservoir of multipotent cells, and as such offer significant potential for use in various non-dental biotechnological applications. The presence of a population of stem/progenitor cells in the dental pulp provides a local source of cells for generating new "odontoblast-like" cells for both natural pulp wound healing or regeneration and direct pulp capping after injury to the tooth. It is still unclear whether these stem cells have a developmental derivation from the dental papilla or if they migrate to the pulp through the vasculature. An important focus of future studies will be a more precise characterisation of these stem cells and their potentiality to allow their most effective application in new regenerative therapies.

The discovery of stem cells in the dental pulp represents a significant advancement for dentistry. Although many questions remain unanswered, the identification of

"post-natal stem cells" in the tooth provides a new platform for development of exciting biological approaches for vital pulp therapy.

1.4 Pulpal responses to injury

Progress in tissue regeneration has enabled researchers to understand better how the odontoblasts and, more generally, the pulp react after injury. The tertiary dentine secreted in the absence of pulpal exposure is commonly reactionary in nature and helps to both restore the structural integrity of the tooth and increase the distance between the injurious agent and the pulp. After the initial secretion and development of the primary dentine, the secretory odontoblast appears to fall into a semi-quiescent, semi-inactive state during which it continues its secretory activity but at a much slower rate. This process of secondary dentinogenesis is responsible for the gradual reduction in size of the pulp chamber, although the molecular control of the odontoblasts responsible for the decrease in activity remains to be elucidated.

During injury to the tooth (caries, trauma or wear), a cascade of pulpal responses will be initiated. The exquisite regenerative or healing potential of the pulp though means that transient histological changes do not necessarily lead to clinically significant manifestations (Seltzer, Bender et al. 1963). Depending on the nature of the injury (whether it is brief or prolonged, or low- or high-intensity), the scope of the pulpal responses will likely differ. Injury of weak or moderate intensity will often be resolved by a brief inflammatory response followed by reactionary dentinogenesis. With injury of a greater intensity, odontoblast death will occur (e.g., deep caries or severe trauma), and as long as inflammation does not become uncontrolled, differentiation of a new generation of odontoblast-like cells may occur leading to dentine bridge formation at sites of exposure: this process is termed reparative dentinogenesis.

1.4.1 Reactionary dentinogenesis

Following injury, odontoblasts are released from their quiescent state and their secretory activity is subsequently up-regulated resulting in deposition of reactionary dentine. Histologically, the calico-traumatic line demarcates this new activity in the dentine matrix (Figure 9). Importantly, because the same cells are responsible for secretion of the reactionary dentine, tubular continuity is seen together with consequent maintenance of dentine permeability. This clearly has consequences with regard to the choice of restorative material, which should not allow leaching of cytotoxic components.

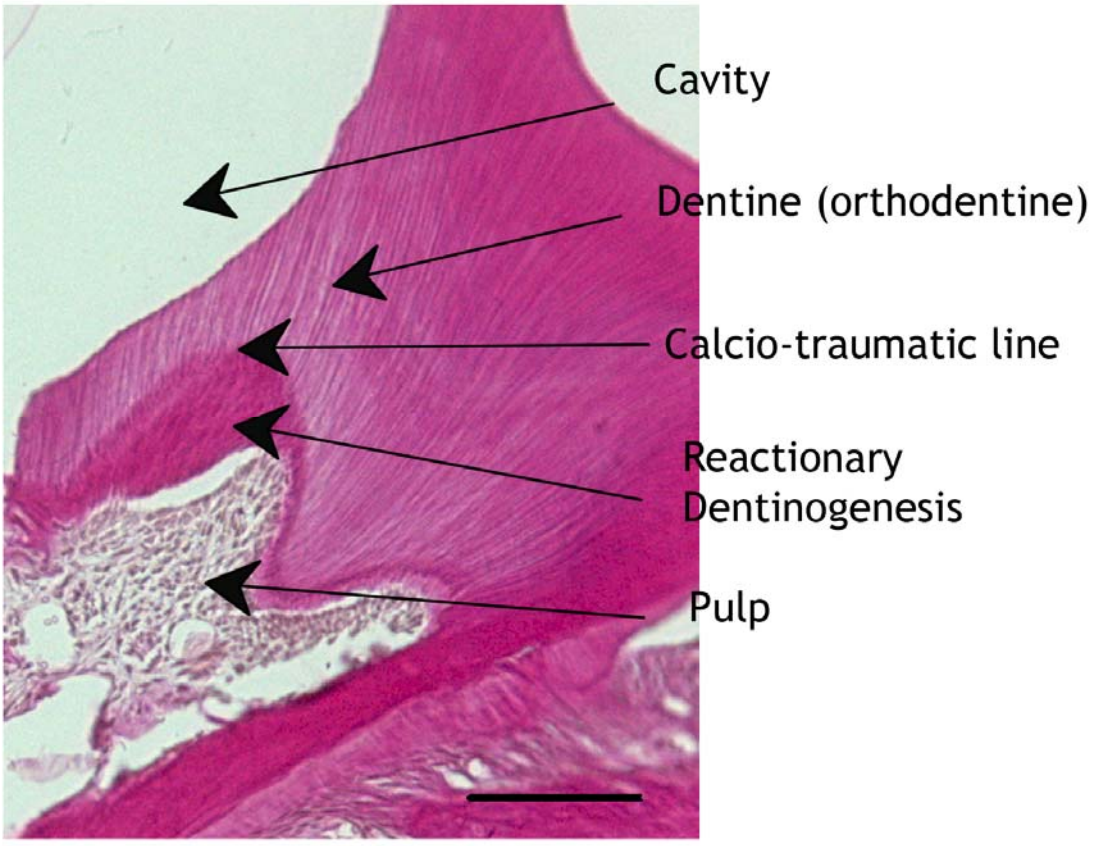

Figure 9 : Longitudinal histological section of a mouse molar which has been treated with a coronal filling. The staining of reactionary dentine is more pronounced than the other dentine matrix. Bar=100µm

Although still poorly understood, it can be postulated that the molecular control processes that are responsible for down-regulating odontoblast activity during the change from primary to secondary dentinogenesis may be reversed to stimulate the odontoblasts again during tertiary dentinogenesis. Decryption of the phenomenon of cell reactivation is necessary, and should facilitate development of new therapeutics that control cell activity.

It is also important to consider the nature of the signalling process between the injurious agent and the odontoblasts. Bacteria and their toxins are key candidates in the direct stimulation of odontoblasts during caries (Durand, Flacher et al. 2006). Also, lipopolysaccharides and other bacterial toxins initiate intra-pulpal inflammatory processes, but other signalling processes may also be critical in the overall balance of pulpal cell responses leading to healing and tissue regeneration (Magloire, Bouvier et al. 1992; Tziafas, Smith et al. 2000; Botero, Shelburne et al. 2006; Smith, Lumley et al. 2008; Choi, Jeong et al. 2009). For example, authors reported recently that TNF-α stimulates differentiation of dental pulp cells toward an odontoblastic phenotype via p38 phosphorylation of the MAP Kinase Pathway (Paula-Silva, Ghosh et al. 2009)

Whilst dentine is a mineralised connective tissue rich in collagen, it is also contains trace amounts of very potent bio-active molecules including cytokines and growth factors, which are sequestrated within the matrix during the mineralisation process and become essentially fossilised therein. During the decay process, demineralisation of the tissue is accompanied by the release of these molecules, which were initially fossilised (Smith 2003). In this pool of substances, many growth factors can be found, especially those of the TGF-β family (Cassidy, Fahey et al. 1997) (Smith, Matthews et al. 1998). These growth factors are extremely potent and have a variety of cell signalling properties which enable them to act at very low concentrations. Once liberated, these factors traverse the tubules to the pulp and induce various cellular

responses, including activation of the odontoblasts (Smith, Tobias et al. 1995). Once stimulated, these formerly quiescent cells enter an active state, and secrete a tertiary reactionary dentine (Figure 10).

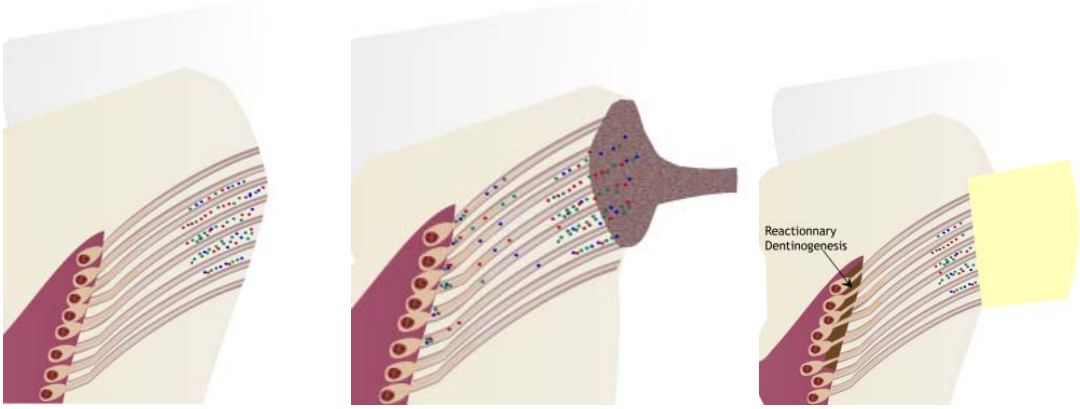

Figure 10 : Numerous matrix proteins (represented by multicoloured dots) are fossilised in the collagen matrix of the dentine during the mineralization process: (a) these factors are released by the dissolution of the mineral matrix (whether pathological or therapeutic); (b) they encounter the odontoblast layer via the tubules; (c) these molecules are considered to be important regulators of signalling pathways in the dentine pulp healing process.

Although the rate of dentine secretion is clearly decreased in the adult, the metabolic activity of the odontoblasts can be up-regulated in response to injury. The members of the TGF-β family present in the dentine may be solubilised by plaque bacterial acids during caries (Smith, Tobias et al. 1995; Smith, Matthews et al. 1998) or by restorative treatments. These molecules could be responsible for the stimulation of odontoblast activity. The organic components secreted in response to injury give rise to the dentine matrix termed “reactionary”, corresponding to an increase in matrix secretion by the stimulated odontoblasts.

From this concept, it is possible to imagine opportunities for therapeutic stimulation, inducing a targeted release of these proteins. For example, cleaning the cavity with EDTA solution, which is well known for its ability to dissolve the mineral phase, would be a potential way to liberate growth factors and to induce the stimulation of

odontoblasts (Smith, Tobias et al. 1990; Smith, Tobias et al. 1994; Smith, Tobias et al. 2001). Etching with orthophosphoric acid, used for conditioning the dentine in bonding procedures, also promotes demineralisation of the dentine and liberation of biological factors. Other products that are presently in the dentist's therapeutic arsenal might come back into favour with new indications. For a long time, calcium hydroxide has been used as a protective lining, especially beneath amalgams fillings, but has more recently fallen out of favour. Nevertheless, this material certainly has the ability to release components from the dentine, including growth factors (Graham, Cooper et al. 2006). Unlike the chelating agents which only have brief contact with the dentine, calcium hydroxide remains in place beneath restorations and favours a gentle and continued dissolution, thus releasing growth factors; its action is prolonged and potentially controllable depending on the form of the product.

More recently, the action of Mineral Trioxide Aggregate (MTA® - Dentsply Maillefer) in releasing growth factors has been demonstrated (Tomson, Grover et al. 2007), although the amounts released differ from those liberated by calcium hydroxide. These differences are interesting because they might explain the differential behaviour observed in response to both materials. If the processes underlying this action were better understood, then the use of such linings under coronal restorations might readily find favour again thereby providing a new focus for research in bioactive materials.

1.4.2 Reparative dentinogenesis

Odontoblasts are the only cells that secrete dentine. If they suffer injury, the formation of a dentine bridge at sites of pulpal exposure is still possible, providing that new odontoblast-like cells are "available" in the area. Conventionally, wound healing involves cell migration from the edge of the injury and with cell division, the

superficial cells move to the centre of the injury regenerating and repairing the tissue and allowing its reorganisation.

Odontoblasts are differentiated post-mitotic cells and are unable to divide to produce new secretory cells. When these cells are lost, cellular replacement occurs which involves stem or progenitor cells resident in the pulp (Fitzgerald 1979; Fitzgerald, Chiego et al. 1990) (Figure 11). Following pulp exposure, and after placement of an appropriate material, a dentine bridge is formed in a few weeks (Figure 12) by new odontoblast-like cells. The origin of these odontoblast-like cells in the dentine pulp healing process is not clearly established. Several authors believe that these processes are likely to be the same as those involved in tooth development (Smith and Lesot 2001; Mitsiadis and Rahiotis 2004), however, the derivation of these cells is still unclear with an origin from outside the tooth via the vasculature cannot be excluded.

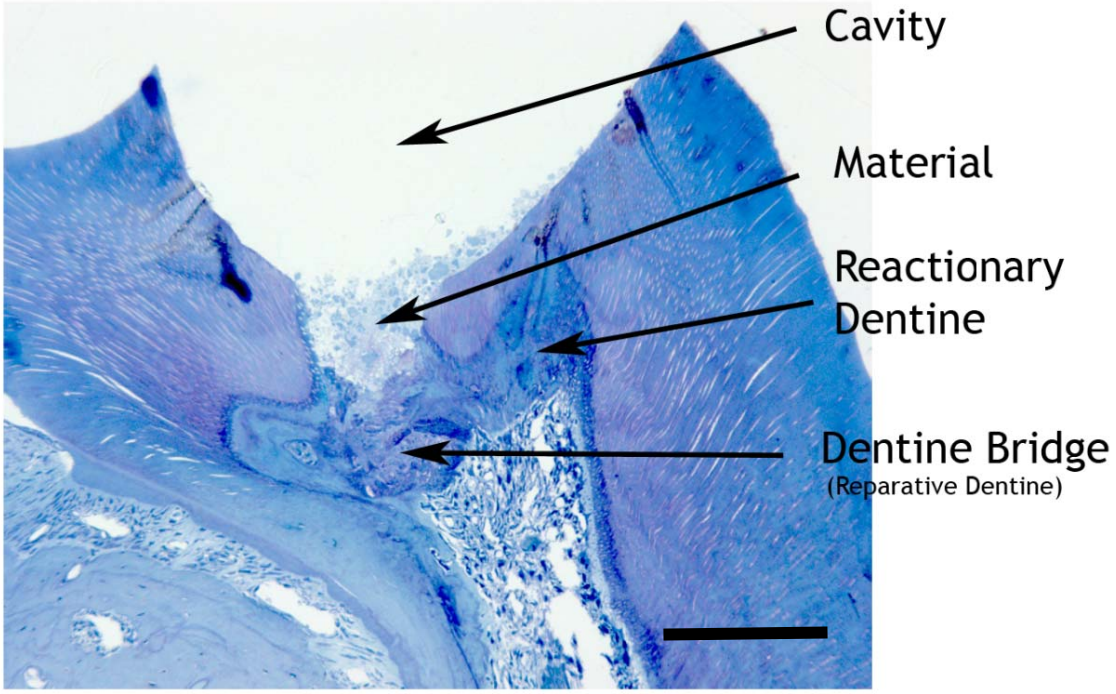

Figure 11 : Dentine bridge formation five weeks after pulp capping with MTA® in a mouse first molar (frontal semi-thin section, x50 magnification, methylene blue - Blue Azur II) Scale bar=200µm.

Various clinical procedures for repair of a pulp exposure have been proposed and calcium hydroxide has long been considered as the material of choice. However, the poor quality of the dentinal bridge and its lack of hermetic seal are potential sources of failure with this material.

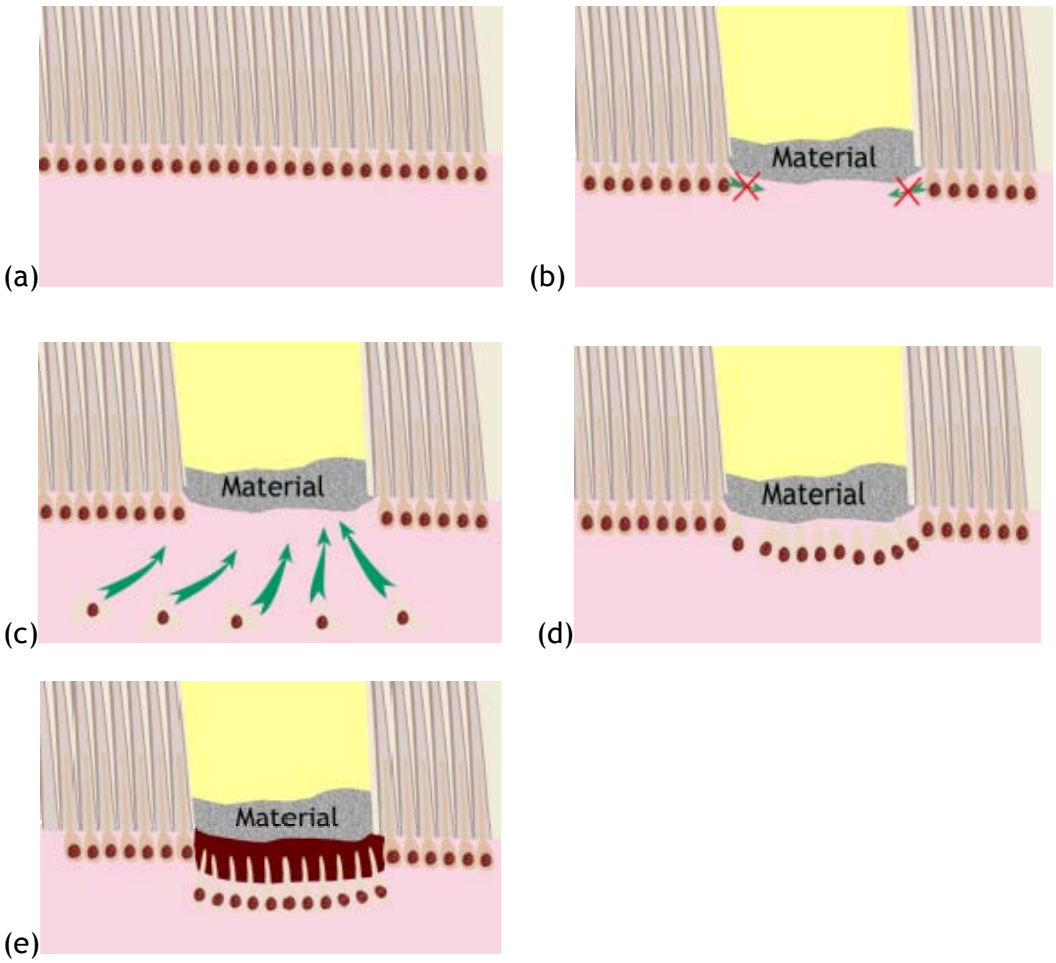

Figure 12 : Reparative dentinogenesis. Contrary to conventional connective tissues, the healing process in the odontoblastic layer does not occur by cell division of other odontoblasts at the edge of the injury (a and b). The attraction of new cells and their differentiation into dentine secreting cells (c) induce the formation of a dentinal bridge in contact with an appropriate material (e).

Currently, a lack of trust in pulp capping due to the inability to predict its prognosis exists and practitioners will frequently therefore remove the pulp of the tooth rather than try to maintain its viability. Although several authors have proposed capping the pulp with the filling material itself, there is no histological evidence that this can

induce dentine bridge formation. Even if, clinically, the results seem to be satisfactory, this approach cannot be considered to be reliable in the long term. This example perhaps illustrates what distinguishes the clinician from the scientist. Whereas clinicians focus on the sealing properties of materials and the prevention of any bacterial or fluid leakage, scientists are more interested in the bio-activity of these materials and their ability to induce a wound healing response. Both are complementary, and it is essential that these two stances are brought together. For the future, existing materials will provide an important stepping stone towards the development of more specific bio-molecules as dentistry develops a biotechnological direction and may encourage greater practitioner uptake of such approaches.

1.4.3 Pulp capping

Following pulp exposure, direct capping using a suitable material can induce a protective response by reparative dentinogenesis resulting in dentine bridge formation. As pulp exposure results in odontoblast loss, the healing process is consequently more complex requiring the recruitment and subsequent differentiation of new dentine secreting odontoblast-like cells. It is therefore probable that the processes involved in pulp repair (reactionary and reparative dentinogenesis) recapitulate those of physiological dentinogenesis, although physiological regulation of odontoblast secretory behaviour may differ in tertiary dentinogenesis (Tziafas, Smith et al. 2000; Smith and Lesot 2001).

Many factors intervene in the prognosis of a pulp capping treatment (Murray, Hafez et al. 2002; Murray, Hafez et al. 2003); lack of inflammation, infection control, and biocompatibility of the used material are reported to be the key factors for improving the clinical outcome (Mjor 2002)(Ward 2002).

As it has also been established that an inflammatory response occurs in pulp tissue as soon as caries reaches the dentine (even at a superficial layer), it appears to be difficult to treat a non-inflamed dental pulp except after a trauma with pulp exposure. Pulp exposure often occurs after trauma and as the pulp is generally free of inflammation, pulp capping in such situations, represents a good approach for treatment. However, it is important to consider management of such cases in the context of the biological behaviour of the pulp, especially in immature teeth which are still developing.

The ultimate goal of pulp capping with a dedicated material is to induce the formation of a barrier of reparative dentine between the pulp and the material of obturation, by allowing the pulp cells to express their dentinogenic potential (Schroder 1985). In 1965, Kakehashi demonstrated the systematic formation of a dentine bridge after pulp exposure in laboratory "germ-free" animals (Kakehashi, Stanley et al. 1965). This study highlights the ability of the pulp to heal depends on its environment, and can occur in the absence of bacterial infection (Cotton 1974).

Over the years, many materials have been used for pulp capping with calcium hydroxide having long been considered the gold standard. Indeed, a search of PubMed *(search keywords: calcium hydroxide and pulp capping)* currently reveals more than 650 references (July 2009). Characterised by a very basic pH (Faraco and Holland 2001), calcium hydroxide no longer seems to be the ideal material for the following reasons:

- The induced dentine bridge is inconsistent and porous (Cox, Subay et al. 1996)
- Calcium hydroxide does not adhere to the dentinal walls
- Sealing ability of Calcium Hydroxide is quite poor.
- The material has poor antibacterial properties.

Because of its highly basic pH, calcium hydroxide in direct contact with the pulp locally destroys a layer of pulp tissue, and thus creates an uncontrolled necrotic zone; this necrotic layer induces an inflammatory reaction which persists in time, or formation of intra pulpal calcification.

Currently, there is considerable research focus directed towards identification of other materials able to induce the formation of a well formed dentine bridge (Tarim, Hafez et al. 1998), however, thus far results remain inconsistent. Other approaches including protection of the pulp with the hybrid layer from new adhesive systems have also been studied (Cox, Hafez et al. 1998).

The introduction of Mineral Trioxide Aggregate (MTA) (Abedi, Torabinejad et al. 1996; Pitt Ford, Torabinejad et al. 1996; Torabinejad and Chivian 1999) has perhaps challenged the position of calcium hydroxide as the gold standard pulp capping material. Although our understanding of its composition and biological effects is limited, recent data suggest the better quality of the dentine bridge compared to that obtained with calcium hydroxide (Nair, Duncan et al. 2008). Moreover, cells in direct contact with the dentine bridge express protein markers of odontoblasts (Simon, Cooper et al. 2008). In a recent randomized prospective study on human teeth, Nair et al. concluded that clinically MTA was more appropriate than calcium hydroxide and should be considered as the new gold standard (Nair, Duncan et al. 2008).

Several *in vivo* studies have shown that MTA induces the creation of a dentine bridge of good quality, with an effective hermetic seal, which can merge with the dentinal walls at the edge of the defect (Simon, Cooper et al. 2008). The advantage of the quality of the dentine bridge obtained with MTA versus calcium hydroxide as a pulp capping agent has been recently demonstrated in a randomised clinical trial (Nair, Duncan et al. 2008).

In spite of the unpublished composition of the material by the manufacturer, recent data suggest that Portland cement resembles the active ingredient of this material and exhibits similar properties (Estrela, Bammann et al. 2000; Holland, de Souza et al. 2001; Abdullah, Ford et al. 2002; Funteas, Wallace et al. 2003; Saidon, He et al. 2003).

1.4.3.1 Pulp Capping and pulp repair:

In most injury situations, pulp exposure is inevitably associated with an inflammatory response and the following steps ensue:

- Haemostasis and formation of a blood clot
- Inflammatory response
- Cell proliferation and/or recruitment
- Tissue remodelling

The healing process in connective tissues is always characterised by these successive steps. Failure to resolve the inflammatory process leads to chronic inflammation, and eventually to pulp necrosis. Pulp tissue adjacent to an exposure is characterised by the presence of necrotic debris, of blood clot formation, and a cellular response involving significant infiltration of neutrophils. Yamamura characterised the chronology of the healing process in the dog after pulp capping with calcium hydroxide (Yamamura 1985) as follows: exudative phase (3 to 5 days), proliferative phase (3 to 7 days), formation of osteodentine (5 to 14 days), formation of tubular dentine (14 days and more). After 3 to 6 days, the inflammatory layer is replaced by granulation tissue. This tissue is arranged along the wound, and contains many fibroblasts and newly formed blood capillaries (Fitzgerald 1979). New extracellular matrix and nodules of mineralisation are seen during healing (Schroder and Granath 1972). The first mineral deposits are found in matrix vesicles, indicating significant similarities between reparative dentinogenesis and the formation of mantle dentine

(Hayashi 1982). At 11 days, the newly formed matrix surrounds cuboidal cells, and a few cells present the first features of odontoblast differentiation (Mjor, Dahl et al. 1991). At 14 days, cells are reorganised in a palisade of cells similar to that seen in primary or secondary dentine (Mjor, Dahl et al. 1991). At 1 month, the dentine bridge and a necrotic layer associated with an inflammatory response in the adjacent pulp tissue can be seen (Fitzgerald 1979). At the ultrastructural level, "tunnel defects" are clearly visible in the dentine bridges of 89% of the cases studied (Cox, Subay et al. 1996).

Reparative dentinogenesis is a complex process comprising a cascade of biological processes;

Interactions of pulpal cells with growth factors, cytokines and other molecular mediators during the healing process are at the origin of each of the three steps of reparative process:

1- Progenitor cells recruitment
2- Cellular differentiation
3- Up regulation of cell synthetic and secretory activity.

1.4.3.2 Progenitor cells of the "second generation" odontoblasts:

Many cellular processes initially observed during embryonic development appear to be recapitulated *in situ* during wound healing and particularly for pulp repair. These phenomena lead to the production of reactionary or reparative dentine depending on whether the pulp has been exposed or not (Smith, Cassidy et al. 1995)

Reparative dentinogenesis during pulp healing requires progenitor cell recruitment and subsequently, the differentiation of these cells into odontoblast-like cells. The newly formed odontoblast-like cells result from the proliferation and differentiation of a population of stem/progenitor cells, probably residing within dental pulp (Ruch 1998). Fitzgerald *et al.*, (1990) studied the migration and the proliferation of cells in

the pulp after capping with calcium hydroxide in the monkey. They stressed that the migration of cells occurred from the central pulp tissue to the pulp/material interface. They also showed that two DNA replications were necessary before the migration of these cells and their differentiation.

Despite our knowledge of tooth development, our understanding of these stem/progenitor cells is still limited. Pulp cells cultured under certain conditions can differentiate into cells with an odontoblast-like phenotype and have the capacity to form nodules of mineralisation *in vitro* (Couble, Farges et al. 2000), although it is unclear whether a sub-population of cells or all pulp cells can exhibit this behaviour. More is known of the multipotent cells of bone marrow (BMSCs), and their potential to differentiate into osteoblasts, chondrocytes, adipocytes, myocytes and neuronal cells (Bennett, Joyner et al. 1991; Krebsbach, Kuznetsov et al. 1997; Azizi, Stokes et al. 1998; Ferrari, Cusella-De Angelis et al. 1998; Pittenger, Mackay et al. 1999). In the pulp, the origin of replacement odontoblast-like cells has not yet been clearly identified. For a long time, the cell rich layer of Höhl was regarded as a reservoir of progenitor cells, although several origins for these stem/progenitor cells have now been proposed including a local origin in the pulp mesenchyme and a remote one derived from the bone marrow. Pericytes in the pulp have also been proposed as candidate repair cells, although whether such cells originate from within the pulp or are transported there through the vasculature is unclear (Yamamura 1985; Shi and Gronthos 2003; Lovschall, Mitsiadis et al. 2007).

Pluripotent cells have been described in the dental pulp (Gronthos, Mankani et al. 2000; Gronthos, Brahim et al. 2002). These cells called DPSCs (Dental Pulp Stem Cells) are able to form dentine-like tissue after ectopic transplantation; they can also differentiate into adipocytes or neuronal cells. These DPSCs are probably progenitor cells and able to undergo self-renewal.

To date, involvement of DPSCs in the pulp healing process has not been definitively demonstrated. The definitive characterisation of the origin of the cells responsible for the healing process in pulp would allow elucidation of their specific behaviour in the repair process, and help to inform the most appropriate treatment after pulp exposure.

1.4.3.3 Pulp Healing and Growth factors:

During dentine degradation, cytokines and growth factors are released from dentine. (Smith 2002b; McLachlan, Sloan et al. 2004; McLachlan, Smith et al. 2005; Smith, Lumley et al. 2008). These cytokines play a key role in the regulation of progenitor cell recruitment, cell proliferation and differentiation of new dentine secreting cells. The members of the TGF-β family have clearly been identified in dental tissue healing events (Rutherford, Wahle et al. 1993; Nakashima 1994; Rutherford, Spangberg et al. 1994; Cassidy, Fahey et al. 1997; Baker, Sugars et al. 2009). The differentiation of new odontoblast-like cells has also been reported after pulp capping with bFGF (Basic Fibroblast Growth Factor), TGF-β1 (Lovschall, Fejerskov et al. 2001) and BMP-7 (Jepsen, Albers et al. 1997).

Direct application of growth factors to pulp tissue offers an interesting therapeutic approach, however, it is important that we first derive a clear understanding of the biological and molecular processes involved in their action before attempting to develop a reliable, reproducible and efficacious new clinical therapy based on their use (Tziafas, Smith et al. 2000).

1.4.3.4 Clinical Implication

Reactionary and reparative dentinogenesis are two very different pathways for pulp repair. The description above of the two types of tertiary dentinogenesis highlights the need for different therapeutic strategies for pulp healing depending on which pathway is involved. Clinically, the choice of regenerative endodontic therapeutic

approaches will necessarily be based on the extent of pulpal disease and particularly, on odontoblast survival.

Translation of biological knowledge into the clinical setting can be simply adoption of a more biological thought process during treatment planning, however it is not always that easy. For instance, the impact of tooth structure on biological events can be fairly readily appreciated, such as in the thickness of the residual dentine separating a cavity from the pulp, which can be an important factor in its protection.

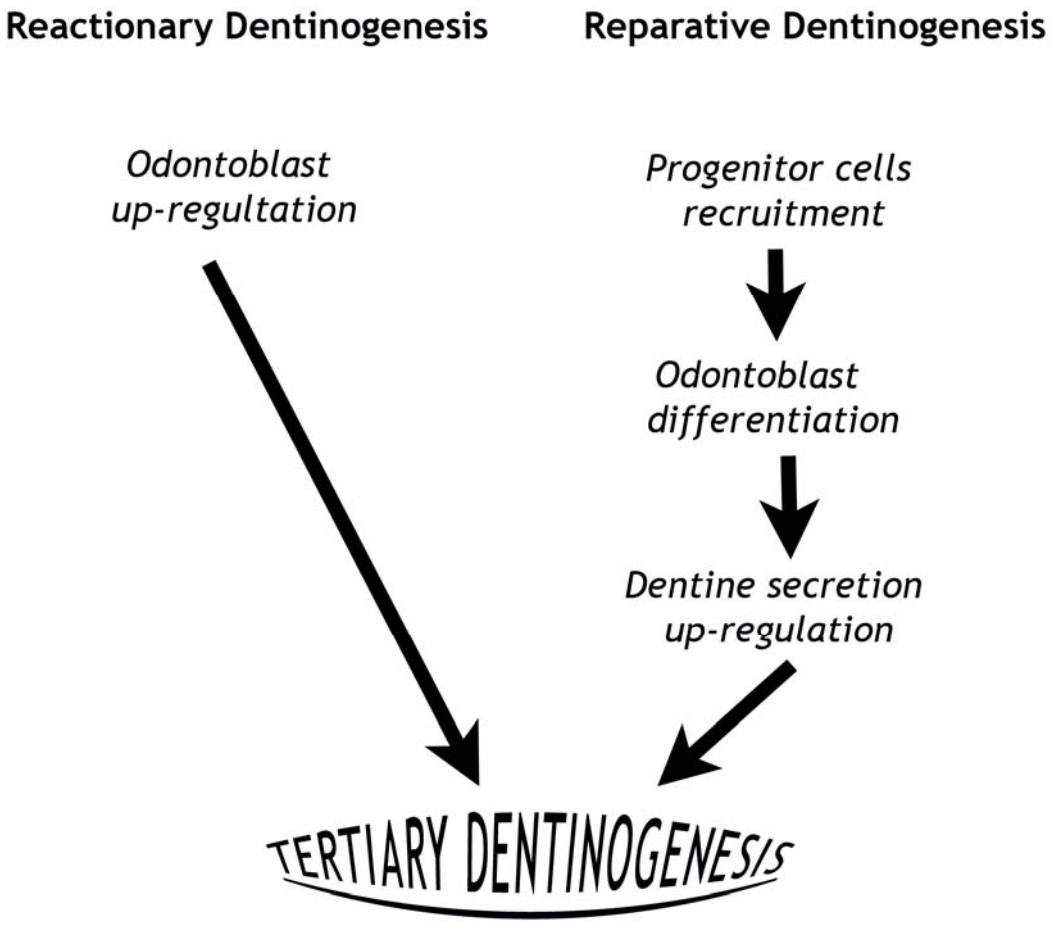

Figure 13 : The differing steps of the two pathways of tertiary dentinogenesis. According to Smith (Smith 2002a)

In deeper cavities, where the thickness of the cavity floor is less than 0.5 mm, the number and the length of the "opened" tubules is such that the communication with the pulp is possibly comparable to that of an actual cavity exposure (Smith, 2002). Also, clinically it can be very difficult, if not impossible, to know the inflammatory status of the pulp, and the cytological state of the odontoblasts since pulpal histology does not necessarily correlate well with clinical presentation; this makes it very difficult to effectively treatment plan in such situations and there is an urgent need for more reliable means of diagnosis of the activity of carious lesions and the level of pulpal inflammation. While thermal or electrical tests provide information on the innervation of the pulp, there is a need for tests which evaluate the vasculature and in particular, the effects thereon of any inflammation that may be present. Unfortunately, the hard tissue shell enclosing the pulp constrains use of techniques such as Laser Doppler scanning or scintography which provide valuable information in other medical specialities.

1.5 MSX2 Homeobox Gene

1.5.1 Msx2

Msx2 or msh homeobox gene 2 encodes a member of the muscle segment homeobox gene family. The Msx2 gene is located on the long (q) arm of mouse chromosome 5 between positions 34 and 35, from base pair 174,084,180 to base pair 174,090,507.

Msx genes (Muscle Homeobox Segment obstructs) are mammalian homologues of the *Drosophila* muscle segment homeobox gene; they encode for transcription factors. Msx-class homeobox genes are characterized by a distinct and highly conserved homeodomain and have been identified in a wide variety of metazoans from vertebrates to coelenterates (Davidson 1995). There is evidence that they participate in inductive tissue interactions that underlie vertebrate organogenesis, including those that pattern the neural crest. Three homeogenes have been isolated in the

mouse, Msx1, Msx2 and Msx3, but only two homeogenes (Msx1, Msx2) have been identified in humans and mutation of these genes has been related to dimorphism (Ivens, Flavin et al. 1990).

Msx2 is known to be induced by BMPs and notably BMP4, which play critical roles in bone formation and osteoblast differentiation(Harada and Rodan 2003). *Msx2*-deficient mice develop reduced bone formation, decreases in osteoblast numbers, impaired chondrogenesis, abnormal calvarial development, and defects in the ectodermal organs including the teeth, hair, and mammary glands (Satokata, Ma et al. 2000; Aioub, Lezot et al. 2007). In contrast, transgenic mice overexpressing *Msx2* show enhanced growth of calvariae (Liu, Kundu et al. 1995). Mutations in the *MSX2* gene in humans, which affects DNA binding activity, causes defects in skull ossification (Wilkie, Tang et al. 2000; Wuyts, Reardon et al. 2000). Furthermore, an autosomal dominant disorder, Boston-type craniosynostosis, results from a gain-of-function mutation of *MSX2* at proline 148 (Ma, Golden et al. 1996; Winograd, Reilly et al. 1997). These findings suggest a positive role for Msx2 in bone development and formation. In contrast to these genetic studies, *in vitro* studies have shown that Msx2 negatively regulates the transcription of the osteoblast-specific genes such as osteocalcin (Towler, Rutledge et al. 1994; Ryoo, Hoffmann et al. 1997). In addition, Msx2 has been shown to bind to Runx2 and inhibit its transcriptional activity (Shirakabe, Terasawa et al. 2001). These studies suggest that Msx2 serves as a negative regulator for osteoblast differentiation.

Msx2 is expressed in many craniofacial structures prior to embryonic day E14, but is expressed in a more restricted pattern at later stages, primarily in developing teeth. Msx2 and osteocalcin are expressed in reciprocal patterns during craniofacial development *in vivo*, and Msx2 expression in pre-odontoblasts clearly precedes osteocalcin expression in odontoblasts (Bidder, Latifi et al. 1998). In incisors, Msx2 is widely expressed in the tooth, primarily in ovoid pre-odontoblast cells and subjacent

dental papilla cells. In appositional bell-stage molars, expression of Msx2 is observed in adjacent pre-odontoblast cells and odontoblasts within the same tooth. Msx2 is also expressed in adjacent immature ovoid pre-odontoblast cells. In less mature teeth populated only by immature ovoid pre-odontoblast cells, Msx2 is widely expressed (Maas and Bei 1997).

Msx2 acts as a transcriptional repressor in dental cells (Zhou, Lei et al. 2000). Like Msx1, the Msx2 homeoprotein plays a key role in osteoblast differentiation and phenotypic expression, via the BMP osteoinductive pathways (Ryoo, Hoffmann et al. 1997) and is involved in the regulation of diverse cell activities, including proliferation, differentiation and apoptosis.

1.5.2 MSX2 and genetic disease

More than 10 mutations in the MSX2 gene have been identified in people with enlarged parietal foramina type 1. These mutations include a change of one amino acid in the MSX2 protein and deletions of one or more nucleotides from the gene. These genetic changes result in the production of an unstable MSX2 protein that cannot bind to DNA. A non-functional MSX2 protein impairs the regulation of cell growth and division (proliferation), cell differentiation and the balance of cell survival and destruction in specific areas of the skull. These cell functional disturbances imply dysregulation of bone formation (ossification), resulting in formation of enlarged parietal foramina.

A mutation in the MSX2 gene is associated with craniosynostosis type 2 disease (also known as Boston type) [(Ma, Golden et al. 1996) for review see (Mavrogiannis, Taylor et al. 2006)]. Craniosynostosis involves early bone closure in the skull, leading to a misshapen head. Skull malformations, including a protruding forehead (frontal bossing), a short wide head that is pointed at the top (turribrachycephaly), or a

cloverleaf-shaped skull (Kleeblattschaedel deformity) are commonly seen in patients suffering from craniosynostosis type 2.

Only one mutation has been found to cause craniosynostosis type 2 and this occurs when the amino acid proline is replaced with the amino acid histidine at position 148. Craniosynostosis type 2 has been found to affect multiple members of a single multi-generational family (Wilkie 1997).

1.6 Aim of this research

Overall this research aimed to investigate the molecular characterisation of odontoblasts during primary, secondary and tertiary (reactionary and reparative) dentinogenesis.

The specific objectives of this project were four fold:

1. To analyse and compare the transcriptome of bovine odontoblasts between early and late stage of post-natal tooth development cells using gene microarrays with subsequent confirmation by sq-RT-PCR.

2. Parallels between development and healing processes in teeth have been suggested. Based on this hypothesis, gene (particularly p38) regulation and protein activation were investigated using an *in vitro* model of tertiary dentinogenesis (involving young and mature cells).

3. *In vivo* investigation is important for an understanding of the interplay of various cellular and molecular processes during wound healing. Currently the published *in vivo* models for pulp healing are limited in their ability to exploit transgenic technologies. In a third part of this work, we aimed to design a new laboratory model for pulp capping in the mouse. With such a validated model, transgenic animals could be used to investigate the role(s) of specific genes.

4. In the final part of this research, we used a transgenic mouse model to analyse the possible role of Msx2 transcription factor in odontoblast differentiation. The precise description of the tooth phenotype in Msx2 null mutant animals was subsequently analysed.

2 Materials and Methods

2.1 Part one: Odontoblast maturity and dentinogenesis

2.1.1 Aim of the project.

So far there is no histological difference described between primary and secondary dentine except at the interface between both tissues delimited by a calciotraumatic line (Thewlis 1940); the two types of dentine are secreted by the same cells, albeit at different times and rates. Odontoblasts are actively secreting during primary dentinogenesis, but become largely less active during secondary dentinogenesis.

We therefore hypothesize that the changes in secretory activity of odontoblasts throughout their life cycle reflect differential transcriptional control and that regulatory processes involved in bone homeostasis may also occur in regulation of dentine secretion. The expression profiles of several genes (DSPP, DMP1, Collagen I) were used as well established markers of odontoblasts and their expression levels may reflect the cell secretory behaviour. So far, comparison of the gene profile of the odontoblast at different stages of its life cycle has not been described. Based on the hypothesis that differential dentine secretion is associated with changes in transcriptional activity within the cell, we have investigated the transcriptomes of odontoblasts involved in primary and secondary dentinogenesis and subsequently used this information to identify key regulatory intracellular pathways involved in this process.

The aim of the first part of our work was therefore to search for the potential specificities between primary and secondary dentine odontoblast transcriptomes.

2.1.2 Methods

2.1.2.1 Selective odontoblast isolation, RNA extraction and cDNA synthesis from cells during primary and secondary dentinogenesis stages.

First permanent incisors, (erupted and with root formation completed), and fourth incisors (still impacted and at an early stage of development) were dissected from two 30 month old cows immediately after slaughter. The root of each tooth was sectioned with a bone saw under cooling with DMEM culture medium (DEPCO, UK). Pulp tissue was subsequently removed, leaving the odontoblast layer remaining attached to the dentine (McLachlan, Smith et al. 2003). Odontoblasts were directly lysed *in situ* by the addition of SV RNA lysis buffer (Promega, UK) into the pulp chamber of the tooth and extracted pulpal tissue was immersed in the same buffer prior to homogenisation and RNA extraction. To support selective isolation of odontoblasts, histological analysis was performed. Four teeth (two after pulp removal and two after odontoblast lysis) were fixed for 24 hours with 10% (w/v) neutral buffered formalin, then demineralised in 10% formic acid for $\geq$7 days. Samples were dehydrated through a series of graded alcohols and xylene, and finally embedded in paraffin wax. Serial sections of 5μm thickness were cut and stained with Mayer's haematoxylin and eosin.

Total RNA was extracted using the SV Total RNA Isolation kit (Promega, UK) and was eluted in a final volume of 30 μl of sterile water as recommended by the manufacturer. Subsequently, 1–2 μg of DNase-digested total RNA was used for oligo(dT) (Ambion, UK) reverse transcription to generate single-stranded cDNA using the Omniscript kit (Qiagen, UK). Both RNA and cDNA concentrations were determined from absorbance values at a wavelength of 260nm using a BioPhotometer (Eppendorf, UK).

2.1.2.2 RT-PCR Analysis

Semi-quantitative RT-PCR assays were performed using the RedTaq PCR system (Sigma, UK). For all analyses, 50 ng of single-stranded cDNA was used to seed 25 μl PCRs

containing; 12.5 μl RedTaq ready reaction mix, 10.5 μl dH2O, 1 μl each of 25mM forward and reverse primers (**Table 1**). Notably, primers for the putative bovine DSPP transcript were derived from the bovine genome sequencing project contig (NW_001506143.1) not currently localized to a chromosome. This sequence had 78% identity over 431bp with the pig DSPP sequence (Acc. No. AY161863.1). To provide further evidence that this assay represented this key dental specific transcript, amplification was assayed from a range of bovine tissues and data indicated that products were only detected in cells derived from the dentine pulp-complex (Figure 14) . Reactions were amplified in a Thermal Cycler (Mastercycler Gradient, Eppendorf, UK) for between 20 and 30 cycles. Following an initial denaturation step of 5 min at 94 °C, a typical amplification cycle consisted of 94 °C for 20 s, 61 °C for 20 s and 72 °C for 20 s ending with a 10-min extension at 72 °C. Following the designated number of cycles, 6 μl of the reaction was removed and the product was separated and visualised on a 1.5% agarose gel containing 0.5 mg/ml ethidium bromide after which gels were scanned and images captured using EDAS 120 software (Kodak, UK). Scanned gel images were imported into AIDA image analysis software (FUJI, UK) and the volume density of amplified products calculated and normalised against the GAPDH housekeeping gene control values.

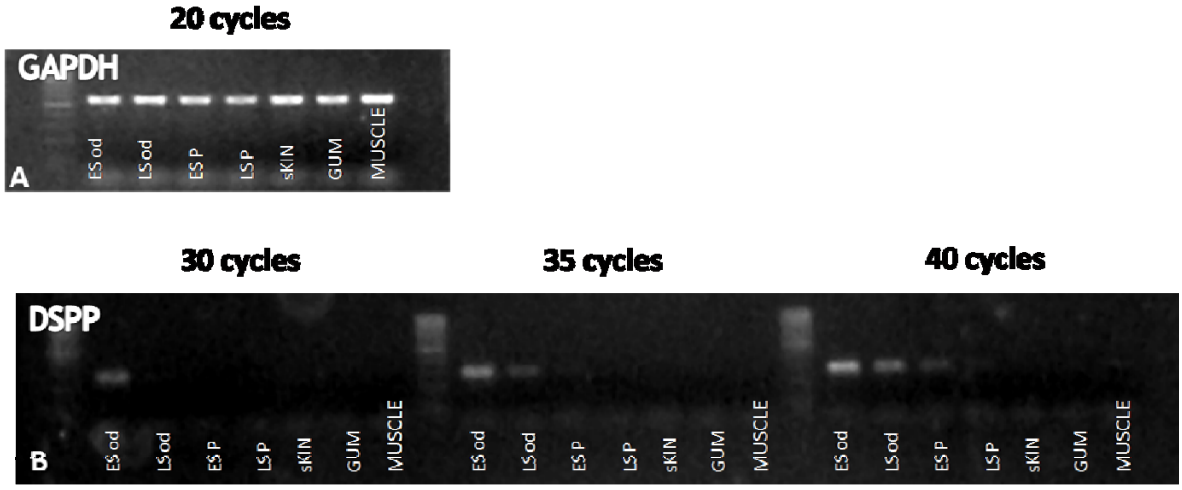

Figure 14: Sq-RT-PCR analysis showing differential expression of (GAPDH) (A) and DSPP genes in Early stage (ES) and Late Stage (LS) Odontoblasts (od), pulp cells (P), skin, gingiva and muscle from bovine tissues. This Sq-RT-PCR was performed to confirm the specificity of the bovine DSPP transcript assay designed from the bovine genome sequencing project contig (NW_001506143.1).

Gene	Forward	reverse	Accession number	Size
GAPDH	GCCAAGAGGGTCATCATCTC	CCCAGCATCGAAGGTAGAAG	NM_001034034	316 bp
DMP-1	GCATCAGGTGGCCAAAGTAT	GAAATCCCATGCAACGTTCT	NM_174038	304 bp
Collagen 1	GGCTCTCCTGGTGAACAACGT	GTAGTAGCGGCCACCATCCTG	NM_074520	312 bp
DSPP	TTTTCCTCCTTCCTTTATGCAA	TTCATTGCCTGACCTAATGC	NW_001506143.1	307 bp
TGF Beta1	TGAATCCTTCAAACGTGCTG	CATTTTGATGCCTTCCTGCT	M36271	320 bp
TGF Beta1 R	TGAATCCTTCAAACGTGCTG	CATTTTGATGCCTTCCTGCT	NM_174621	331 bp
BMP4	TCGTTACCTCAAGGGAGTGG	GTGGGAACACAACAGGCTTT	NM_001045877	359 bp
PGAP1	CCATCTCCGCTTATCTTCCA	GACAAAGCATGGAACCCTGT	XM_580837	328 bp
OSTEOCALCIN	TGACAGACACACCATGAGAACCC	AGCTCTAGACTGGGCCGTAGAAG	NM_174249	337 bp
ADM	AGGGGAGGCAGTGTTCTCTT	GGGGAGGGGAACAATACAAT	NM_173888	385 bp
AMELOGENIN	AGCAGACTCCCCAGAATCAC	GAATATCGGAGGCAGAGGTG	NM_001014984	338 bp
IBSP	CACCGAAATGAAGACGGTTT	GAAAGGGTGGTGTTCTCAGC	NM_174084	349 bp
DECORIN	AACTCTTTTGCTTGGGCTGA	TTTGTTGTTTTGCAGGTCCA	NM_173906	340 bp
ALKALINE PHOSPHATASE	TGAACCTCATCGACATCTGG	AAAGACGTGGGAGTGGTCAG	NM_176858	301 bp
CaSR	CCAACATGACCCTGGGATAC	TTCCAGCGGAAGTACTCGAT	NM_174002	345 bp
SOCSBOX PROTEIN	TCAGTTCAGTGCCAGGATTG	TCACTGCTCTCCTTCCAGGT	NM001034209	327 bp
SPP-1	ACAGCCAGGACGTCAACTCT	GGAAAGCTCGCTACTGTTGG	NM_174187	397 bp
PROTEIN S100	GGGCAAAGAGGGAGACAAGT	AAAGTAAGGTGAGGGGAAGCA	NM_001099042	325 bp
OSTF1	GGTGGAAAGGTACCTGCAAA	AGCACCTTTTTCCAGAAGCA	NM_174409	348bp
PTPRR	GCATTTCCTAAACCCGCATA	CTTCAGATGGCAGAGCATCA	NM_001015662	301 bp
NTRKK2	ACGTGGGACTGAAAAACCTG	AAATTTGCTGATGGCAAACC	NM_001075225	334 bp
MAPK13 (p38)	ACAAAGCCCCAAAAAGGATT	GTGGTATCACGAGGCCATTC	NM_001014947	364 bp
MAP2K6	TCCACTTGCATGAAGATTGC	GCTTCTGCTCTTGGCTGTTT	NM_001034045	400 bp
MKK3	CATCACCATTGGAGACAGGA	CTCCCCGAGAATGTCTTCTG	NM_001083693	358 bp

Table 1: Primer details and conditions for sq-RT-PCR analysis. Primer sequences used in PCR analysis and expected product sizes for each assay. Primers were designed using the Primer3 software (http://frodo.wi.mit.edu/cgi-bin/primer3/primer3_www.cgi) using sequences from the Accession numbers provided.

2.1.2.3 Microarray analysis

Microarray analysis (Affymetrix, UK) was performed to compare the transcriptomes of the two odontoblast populations as previously described (McLachlan *et al.* 2005). 100ng of total RNA were double amplified to generate cDNA and 25µg of cRNA synthesized using the *in vitro* transcription (IVT) reaction prior to fragmentation. 15µg of each of the fragmented cRNAs were solubilized in a hybridization cocktail, which was subsequently incubated in duplicate with GeneChip Bovine Genome arrays (900561) for 16hrs at 45°C. All hybridisation control parameters were within Affymetrix recommended guidelines. Bioinformatics analysis was conducted with three software programmes (D-chip http://biosun1.harvard.edu/complab/dchip/, Onto-Express and Pathway express (http://vortex.cs.wayne.edu/projects.htm).

2.1.2.4 Immunohistochemical analysis

Immunohistochemistry was performed on 5 µm sections mounted on SuperFrost®Plus (Manzel Glase - Germany) slides. Deparaffined and rehydrated sections were incubated for 30 min in 3% H_2O_2/PBS to quench endogenous peroxidase activity, and then rinsed for 10 min in Phosphate Buffered Saline (PBS). Nonspecific protein binding was blocked by incubation for 30 min in 5% goat serum in PBS. Specimens were incubated for 1hour at room-temperature in a humidified chamber with a polyclonal rabbit anti-mouse DSPP (Dentin Sialophosphoprotein) antibody, (kindly provided by Dr Larry Fisher, National Institute of Health, Ref LF 153), a rabbit anti-mouse phospho-p38 MAPK (T180/Y182) Antibody (R &D systems-USA) or anti-bovine DMP-1 Antibody (kindly provided by Dr Larry Fisher, National Institute of Health, Ref LF 148). Sections were washed three times in PBS at room-temperature prior to treatment for 30 minutes at room temperature with the secondary biotin-labelled goat anti rabbit

IgG antibody (Streptavigen Multilink Kit - Biogenex UK). Subsequently, sections were incubated for 30 min at room temperature with peroxidase linked to avidin (Vectastain ABC kit, Vector Laboratories, Burlingame, CA, USA). After rinsing with three changes of PBS, the immunoreactivity was visualized by development for 2 to 5 min with 0.1% 3,3-diaminobenzidine and 0.02% hydrogen peroxide (DAB substrate kit, Vector Laboratories). Sections were counterstained with Mayer's haematoxylin, mounted with permanent mounting medium (XAM® - BDH Laboratory – England) and examined by light microscopy. A positive control was performed on untreated mouse teeth and a negative control on mouse oral mucosa. A further negative control involving omission of primary antibody was also performed on mouse or bovine tooth sections.

2.2 Part Two: Tertiary dentinogenesis and p38 MAPKinase pathway

2.2.1 Aim of the project

Understanding cell behaviour in dentine formation is critical to our future development of new regenerative therapies for teeth. During tooth repair and tertiary dentinogenesis, the healing process may recapitulate developmental events (Smith and Lesot 2001). In this situation, odontoblasts are "re-activated" to restore a greater rate of secretion of dentine (reactionary); they may also die and then pulpal progenitors can differentiate into odontoblast-like cells (reparative). It is therefore important to understand the cellular and molecular changes which occur in odontoblasts at different stages of their life-cycle to facilitate clinical exploitation of the reactivation of quiescent odontoblasts for dentine repair and exploit pharmacological tools to manage and control this healing process.

The transcriptome of the odontoblast evolves as these cells mature. Among the several genes whose expression changed during odontoblast maturation, we found the *p38* gene to be highly expressed in primary odontoblasts but completely silent in secondary odontoblasts.

Based on these observations we hypothesized that p38 might be involved in regulating odontoblast activity, and initiated the present study to determine whether p38 is up-regulated and phophorylated when odontoblasts are stimulated (Figure 15).

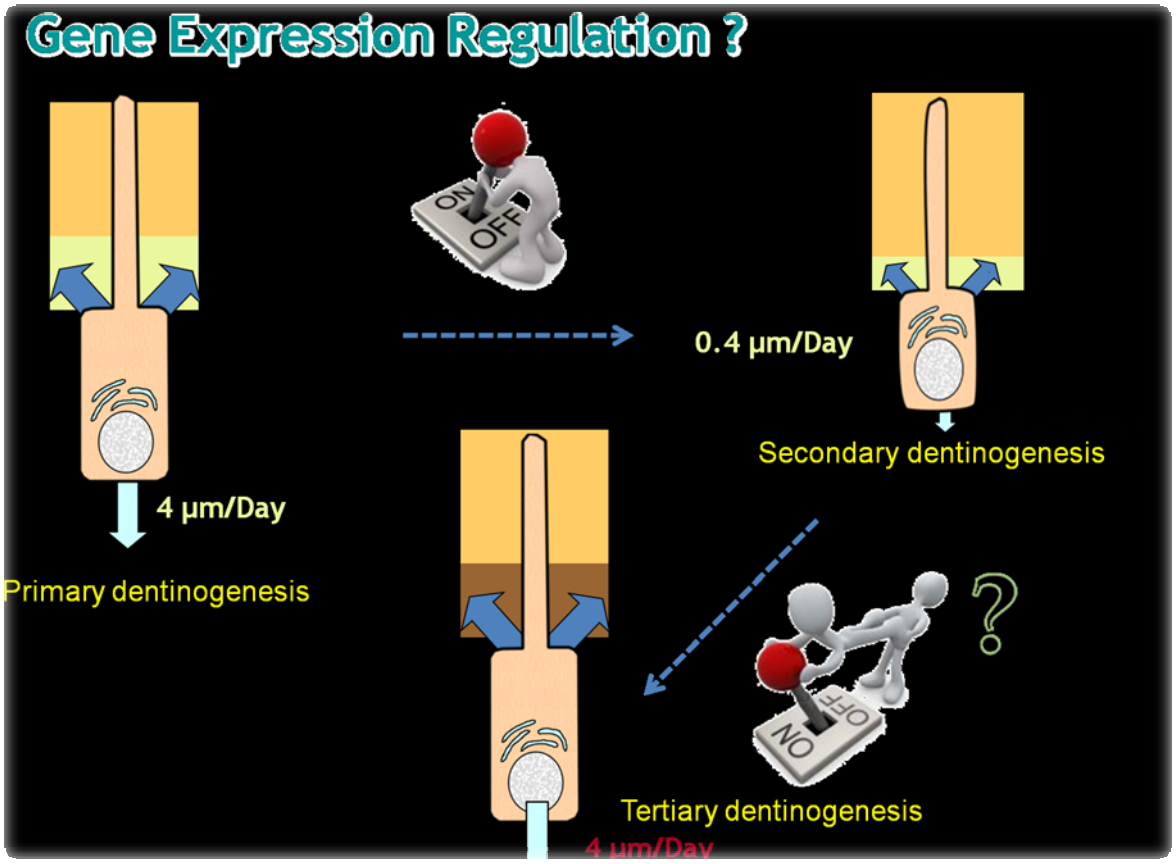

Figure 15: Hypothesis of gene regulation in odontoblasts during primary, secondary and tertiary dentinogenesis

2.2.2 Methods

2.2.2.1 Isolation of Human dentine matrix proteins

Dentine matrix proteins were isolated as previously described (Graham, Cooper et al. 2006). Briefly, dentine matrix components were extracted from powdered dentine using 10% EDTA (pH 7.2) supplemented with the protease inhibitors n-ethylmaleamide (10 mM) (Sigma, UK) and phenyl-methyl-sulphonyl fluoride (PMSF, 5 mM) (Sigma, UK). Extractions were carried out with agitation over 14 days at 4ºC, and with the extraction solution changed daily. Extracts were transferred to dialysis tubing (Scientific Laboratory Supplies, UK) and dialyzed exhaustively for 10 days against repeated changes of distilled water. Dialyzed extracts were lyophilised using

a Modulyo freeze-dryer (Edwards, UK). The lyophilised EDTA dentine matrix extracts were stored at -20ºC prior to use.

2.2.2.2 Cell culture

Mouse odontoblast-like cells (MDPC-23) (Hanks, Fang et al. 1998) were seeded and cultured in 96-well plates (Appleton-Woods, UK) at a density of 25,000 cells per well in Dulbecco's modified Eagle's medium (DMEM) supplemented with 10% fetal calf serum (FCS), 1% penicillin/streptomycin (Sigma, UK), and 200 mM glutamine (Sigma, UK). Cells were cultured in a humidified incubator in a 5% carbon dioxide atmosphere at 37ºC for 24 hours prior to stimulation.

2.2.2.3 Cell stimulation

Cells were stimulated for 15 min, 1 h, 3 h, and 24 h with TNF-α (100 ng/ml; Cellomics, UK), rh-TGFβ1 carrier-free (0.2 ng/ml; R&D systems, UK), EDTA-extracted dentine matrix proteins (DMPs) (1 μg/ml), or adrenomedullin (10^{-11} M; Sigma, UK). As controls, cells were stimulated for 30 minutes before TGF-β1 stimulation with either: anti-TGF-β1 antibody (10 μg/ml; R&D systems, UK); anisomycin (40 ng/ml; Sigma, UK), which induces p38 phosphorylation; the p38 inhibitor SB203580 (0.6 μg/ml; Sigma, UK); or *Streptococcus mutans* (SM) (10^9 bacteria/ml based on chains of 10 cocci). Alternatively, control cells were pre-stimulated with combinations of: TGFβ1 + TNFα, ADM + SM, TGFβ1 + SM, or DMPs + SM (all at concentrations previously described).

2.2.2.4 P38 phosphorylation ELISA

Phosphorylated p38 expression was measured using a cell-based, p38-MAPK ELISA kit (Raybiotech, Norcross, GA, USA). After stimulation, cells were fixed for 20 min in 10%

formalin at room temperature (RT) with shaking, and then treated with a quenching buffer for 20 min at RT. After immersion in a blocking solution, cells were incubated with the primary anti-phospho-p38 antibody (Thr180/Tyr182) for 2 h at RT, and then with HRP-conjugated anti-mouse IgG antibody for 1h. TMP-One-Step reagent was then added to each well and the plates were incubated for 30 min at room temperature. After stopping the reaction, the absorbance of each well was read immediately at 450nm with a spectrophotometer (Universal Plate Reader ELx800, Bio-Tek Instruments Inc). All experiments were performed in triplicate.

2.2.2.5 P38 phosphorylation and translocation analysis.

To determine whether the various treatments activated p38, we examined both the phosphorylation and nuclear translocation of this protein using high-content analysis. After stimulation, cells were fixed in 1% formaldehyde in phosphate buffered saline (PBS) for 1 hour. The fixed plates were processed at Imagen Biotech (Manchester, UK) by permeabilisation and stained with anti-phospho-p38 antibody (Thermofisher, USA, Cat# K0100041). Plates were analyzed on an Arrayscan (Cellomics, Thermofisher, USA) using the compartmental analysis algorithm (Figure 16).

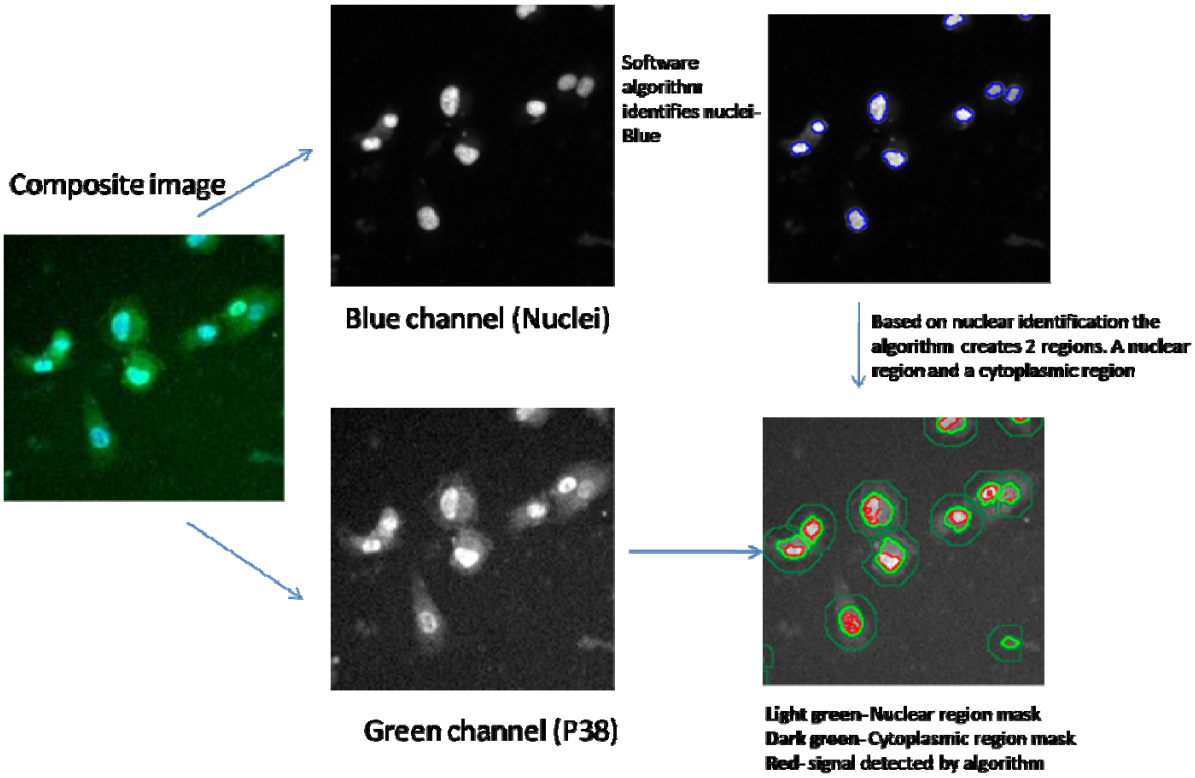

Figure 16: Principles of the cell analysis performed using an Arrayscan (Cellomics, Thermofisher, USA) and the compartmental analysis algorithm.

2.3 Part 3: Designing a new laboratory model for pulp repair:

2.3.1 Aim of the project

As pulp exposure results in odontoblast loss, the healing process is consequently more complex requiring the recruitment and subsequent differentiation of new dentine secreting cells. To date, the origin(s) of the recruited cells, the differentiation process, and the cellular and molecular reactions involved are not clearly defined. Similarities have been reported between the wound healing response and embryonic developmental events. It is therefore probable that the processes involved in pulp repair recapitulate those of initial odontogenesis, specifically during odontoblast differentiation (Tziafas, Smith et al. 2000; Smith and Lesot 2001).

Despite significant study (Smith, Tobias et al. 1990; Decup, Six et al. 2000; Goldberg, Six et al. 2001; Smith, Tobias et al. 2001; Six, Lasfargues et al. 2002), the molecular signaling of cell differentiation during reparative dentinogenesis is not yet fully characterised. Several studies have characterized the effects of growth factors and/or matrix proteins on reparative dentinogenesis using animal models. Similarities in phenotype of primary odontoblasts and "odontoblast-like cells" differentiating during the healing process have been clearly demonstrated (D'Souza, Bachman et al. 1995; About and Mitsiadis 2001). However, the markers used have so far not allowed the initial stages of cell recruitment to be followed, nor the presumptive precursors to be precisely defined, such as pulp fibroblasts, pericytes (Shi and Gronthos 2003), or pluripotent cells of bone marrow (Shi, Robey et al. 2001; Sloan and Smith 2007). Study of ^{3}H-thymidine incorporation during reparative dentinogenesis has not allowed elucidation of the origin and the nature of these replacement cells (Fitzgerald, Chiego et al. 1990).

To date, several animal models of reparative dentinogenesis, including the rat, dog, monkey and ferret, have been used, however, to our knowledge a mouse model has yet to be reported. The mouse represents an interesting and well characterized laboratory model, specifically with regards to transgenic manipulation. These models are predicted to be extremely informative in studies on the molecular signalling involved in pulp healing. The small size of the animal, however, complicates surgical procedures during pulp-capping, as traditional instrumentation is not suitable for use on molar teeth whose diameter is ~1.4mm. Miniaturization of these procedures is therefore necessary to exploit the mouse as a laboratory model for pulp-capping research.

The aim of our study was to demonstrate the utility of the mouse as a model for the study of reparative dentinogenesis.

2.3.2 Methods

2.3.2.1 Animal experimentation

All animal experiments were conducted by an authorized person in accordance with French regulations. Nineteen young adult mice (3 months-old) were used (Table 1). Following anaesthesia by intra-peritoneal injection of 2,2,2 tribromoethanol 2-methyl 2-butanol (Avertine® - Sigma Aldrich Germany) (0,017ml/g), a cavity was drilled with a carbide bur (Dia 0,04mm) (Komet- France) on the palatal aspect of the first upper left molar, in the centre of the tooth according to the mesio-distal plane until the pulp was visible through the transparency of the dentine floor of the cavity. A pulp exposure was subsequently mechanically created using an endodontic hand file of 0.15mm diameter with a 4% taper (C+file®, Dentsply-Maillefer France); this approach enabled control of pulp exposure size to around 150µm (size of the tip of the file). Pulp capping was performed using Mineral Trioxide Aggregate (Pro-Root MTA®, Dentsply-Maillefer France) mixed with sterile water following the manufacturer's

recommendations. MTA was placed in contact with the pulp using the tip of a probe, and slightly condensed with a sterile paper point (XX-Fine, Henry Schein, France), Subsequently, the cavity was sealed with light cured composite resin (Point4®, Kerr) associated with a one-step adhesive system (Prime and Bond ®NT™, Denstply Caulk). Animals were placed in individual cages until they recovered from anaesthesia, and to aid recovery Paracetamol (0.06mg/g/day) was delivered in their drinking water for 72 hours. As a control, the pulp capping procedure was performed in the absence of MTA on first upper molars of 2 animals i.e. the composite resin was placed directly in contact with the pulp.

Prior to dental tissue extraction, animals were euthanized, after deep anaesthesia, by intracardiac perfusion with 4% paraformaldehyde (Sigma) (PFA) in Phosphate Buffered Saline PBS 0.1M (pH =7.4) through the left ventricle, using a monostaltic pump for 5 minutes (Touzart and Matignon, Vitry, France). Treated animals were euthanized at increasing time points following the clinical procedure, as follows :

- Two treated animals at 3 days post operatively
- Two animals at 1 week post operatively
- Two animals at 2 weeks post operatively
- Eight treated animals and the two “controls” at 5 weeks post operatively
- And finally two animals at 11 weeks after treatment.

Following removal of most of the soft tissues, heads of animals were immersed in 4% para-formaldehyde for 6 hours at 4°C.

2.3.2.2 Histology:

The whole maxillae of ten experimental animals and the two control animals were dissected, rinsed in PBS for 20 minutes, and decalcified for 7 weeks in a 4.17% Ethylene diamine tetra acetic Acid (EDTA) solution with 0.2% para-formaldehyde

(pH=6.8) with agitation at 4°C. The solution was renewed every two days for the first week, and then every week until the decalcification was complete as confirmed by X-ray analysis. Samples were dehydrated through increasing concentrations of ethanol and embedded in paraffin or Epon resin blocks according to standard procedures. The samples embedded in paraffin were cut with a microtome (Leica - Germany) in sections of 7µm, and then stained with haematoxylin and eosin (H&E). Samples embedded in Epon resin were cut in sections of 0.5µm and stained using a solution of mixed Methyl Blue and Blue Azur II (50%:50%). Sections were mounted in Depex (Sigma, France) and observed by light microscopy.

2.3.2.3 Immunohistochemistry

Immunohistochemistry was performed on sections mounted on SuperFrost®Plus (Manzel Glase, Germany) slides. Deparaffinized and rehydrated sections were incubated for 30 min in 3% H_2O_2/PBS to quench endogenous peroxidase activity, and then rinsed for 10 min in PBS. Non-specific protein binding was blocked by incubation for 30 min in 5% goat serum in PBS. Specimens were incubated overnight at 4°C in a humidified chamber with the polyclonal rabbit anti-mouse DSPP (Dentin SialoPhosphoProtein) antibody, (kindly provided by Dr Larry Fisher, National Institute of Health, Ref LF 153). Sections were washed three times in PBS at room temperature prior to treatment for 30 minutes at room temperature with the secondary biotin-labelled goat anti rabbit antibody (Streptavigen Multilink Kit, Biogenex, UK). Subsequently, sections were incubated for 30 min at room temperature with peroxidase linked to avidin (Vectastain ABC kit, Vector Laboratories, Burlingame, CA, USA). After rinsing with three changes of PBS, the immunoreactivity was visualized by development for 2 to 5 min with 0.1% 3,3-diaminobenzidine and 0.02% hydrogen peroxide (DAB substrate kit, Vector Laboratories). Sections were counterstained with Mayer's haematoxylin, mounted in permanent mounting medium (XAM® - BDH Laboratory, England) and examined by

light microscopy. A positive control was performed on untreated mouse teeth and a negative control on mouse oral mucosa. A further negative control involving omission of primary antibody was also performed on mouse teeth.

2.3.2.4 Scanning Electron Microscopy:

For scanning electron microscopy (SEM) examination, two specimens (five weeks post operative) were embedded in self-curing epoxy resin (Araldite; Ciba Geigy, Basel, Switzerland, Evanston, Ill). Specimens were prepared with a water-cooled low speed Isomet diamond saw (Buehler Ltd, Evanston, Ill) and polished with an automatic polishing device (Pedemax-2; Struers, Copenhagen, Denmark) with waterproof silicon carbide papers of decreasing abrasivity (600, 1200, 2400, and 4000 grit) and with soft tissue disks with fine diamond suspensions (3μm, 1μm, and 0.03μm) in combination with DL-lubricant cooling solution (Struers, Copenhagen, Denmark). On the two specimens, the three roots were removed and specimens ground and polished until the opening of the pulp chamber was reached.

After polishing, specimens were immersed in 5% sodium hypochlorite solution for 5 minutes, ultrasonicated in water for five minutes, etched with orthophosphoric acid (Bisico-France) for 15 seconds and washed with deionised water for 30 seconds.

Specimens were rinsed with a solution of 0.2 M sodium cacodylate buffer at pH 7.4 for 1 hour with 3 changes, and then dehydrated through increasing concentrations of ethanol (25% for 1hour, 50% for 1 hour, 75% for 1 hour, 95% 2x1hour, and 100% over night). Finally, the specimens were sputter-coated with gold palladium using a sputter coater (SC500; Biorad, Microscience Division, Elexience, France) at 20 mA. Specimens were observed under a field emission SEM (JSM-6400 F Scanning Microscope; JEOL, Ltd., Tokyo, Japan) at an accelerating voltage of 15 to 20 kV and a working distance from 6 to 10 mm. The SEM was equipped with an energy dispersive X-Ray spectrometer system (Tracor 5500). Signals in the energy region for phosphorus

(P), and calcium (Ca) were recorded and compared between the primary dentine and the reparative dentine of the dentine bridge. The two samples were analysed, and reparative dentine composition was compared to orthodentine (in another area, but on the same sample). The energy scale of the X-Ray detector was calibrated using a cobalt standard.

2.4 Part four: Msx2 and odontoblasts

2.4.1 Aim of the project

Studies of the dental and alveolar bone tissues from early postnatal stages up until 6 month age in $Msx2^{-/-}$ animals have shown that Msx2 has effects on many types of cells and stages and is not limited to the periodontal ligament (Aioub, Lezot et al. 2007). Because failure of eruption has been described in patients with an Msx2 mutation (Garcia-Minaur, Mavrogiannis et al. 2003) this gene may well be involved in the process of root formation, eruption and, indirectly, in odontoblast differentiation.

The role of Msx2 in tooth development is important and Msx homeogenes studied seem to have different impacts during postnatal development and adulthood, whereas their expression patterns overlapped during early patterning (Berdal, Molla et al. 2009).

Several cells, such as dental epithelial (Satokata, Ma et al. 2000; Zhou, Lei et al. 2000; Bei, Stowell et al. 2004)and mesenchymal cells (Bidder, Latifi et al. 1998; Yamashiro, Tummers et al. 2003), appear to be potential targets for Msx2 and odontoblasts could also be a target of the Msx2 homeoprotein. A detailed analysis (morphological and histological) of Msx2 null mutant animals has highlighted defects in amelogenesis, dentinogenesis and bone including osteoporosis development (Aioub, Lezot et al. 2007).

Implications of Msx2 in odontoblast differentiation at later stages of development and particularly during secondary dentinogenesis were explored to decipher its possible impact on odontoblast differentiation during root formation and/or dentine secretion and mineralisation.

2.4.2 Methods

2.4.2.1 Animal generation and sampling

Msx2 gene knock-in (KI) mutants were generated by the insertion of the bacterial lacZ gene within the Msx2 gene coding sequences (Lallemand, Nicola et al. 2005). Heterozygous males and females were mated (on a CD1 Swiss genetic background). Their litters were used to compare wild-type, transgenic heterozygous and homozygous mice. The expression pattern of Msx2 in the dental pulp of the first upper molar was investigated in Msx2 homozygous and heterozygous KI mice at 7, 14, 21, 28 post natal days, and at 4 months, and compared to Wild type teeth. Each experimental group comprised 5 mice, giving a total number of 115 animals.

For genotyping, primers were selected for PCR analysis of genomic DNA extracted from the tails in order to determine the genotype. Amplification conditions were 95 °C (10 s), 65 °C (30 s) and 72 °C (1 min) for 30 cycles. Amplification products were identified on 2% agarose gels. All experiments were performed in accordance with the French National Consultative Bioethics Committee for Health and Life Science, following the ethical guidelines for animal care. All experiments were performed by staff that had been trained and accredited to perform *in vivo* studies.

2.4.2.2 Histology analysis

Following anaesthesia by intra-peritoneal injection of 2,2,2 tribromoethanol 2-methyl 2-butanol (Avertine® - Sigma Aldrich Germany) (0,017ml/g), intra-cardiac perfusions were performed on animals with a fixative solution containing 4% paraformaldehyde

(Sigma, la Verpillière, France) in phosphate-buffered saline (PBS) pH 7.4. Post-fixation was ensured by immersion of dissected half-mandibles in the fixative solution overnight at 4°C. After rinsing in PBS, the half-maxillae were processed for histology by decalcification at 4°C for up to 60 days (depending on the anatomical size of the samples) in a pH 7.4 PBS solution containing 4.13% EDTA (Sigma, UK) and 0.2% paraformaldehyde. After extensive washing in PBS, the samples were dehydrated in increasing concentrations of ethanol and toluene and were finally embedded in paraffin (Paraplast plus, Sigma, France). Serial longitudinal sections of the half-maxillae were cut with a microtome (RM 2145; Leica, Rueil-Malmaison, France). The 7-µm-thick sections were deparaffinised, rehydrated and stained by the Van Gieson protocol. Sections were mounted in Depex (Sigma – France) and observed by light microscopy. (Leica, France).

2.4.2.3 Immunohistochemistry (anti-DSPP and anti-β-Gal):

Immunohistochemistry was performed on 5 µm sections mounted on SuperFrost®Plus (Manzel Glase, Germany) slides. Deparaffinised and rehydrated sections were incubated for 30 min in 3% H_2O_2/PBS to quench endogenous peroxidase activity, and then rinsed for 10 min in Phosphate Buffered Saline (PBS). Non-specific protein binding was blocked by incubation for 30 min in 5% goat serum in PBS. Specimens were incubated for 1 hour at room-temperature in a humidified chamber with a polyclonal rabbit anti-mouse DSP (Dentin Sialoprotein) antibody, (kindly provided by Dr Larry Fisher, National Institute of Health, Ref LF 153), or polyclonal rabbit anti-mouse BetaGalactosidase Antibody (ABCam, US) dilution 1/5000. Sections were washed three times in PBS at room-temperature prior to treatment for 30 minutes at room temperature with the secondary biotin-labelled goat anti rabbit IgG antibody (Streptavigen Multilink Kit - Biogenex UK). Subsequently, sections were incubated for 30 min at room temperature with peroxidase linked to avidin (Vectastain ABC kit, Vector Laboratories, Burlingame, CA, USA). After rinsing with three changes of PBS,

the immunoreactivity was visualized by development for 2 to 5 min with 0.1% 3,3-diaminobenzidine and 0.02% hydrogen peroxide (DAB substrate kit, Vector Laboratories). Sections were counterstained with Mayer's haematoxylin, mounted with permanent mounting medium (XAM® - BDH Laboratory – England) and examined by light microscopy. A positive control was performed on untreated mouse teeth and a negative control on mouse oral mucosa. A further negative control involving omission of primary antibody was also performed on mouse tooth sections.

2.4.2.4 Analysis of cell division by BrdU incorporation

Two post natal 14 days old Msx2 -/- mice were intraperitonealy injected with a $60x10^{-3}$ mg/g BrdU (Sigma France) solution 24 hours before euthanasia. Maxillae were then fixed and processed as previously described (see part 2.3.2.2) and immunohistochemistry was performed on 7µm sections mounted on Superfrost+ slides with anti BrdU antibody (Sigma, France) diluted at 1/1000.

Deparaffinised and rehydrated sections were incubated for 30 min in 3% H_2O_2/PBS to quench endogenous peroxidase activity, and then rinsed for 10 min in Phosphate Buffered Saline (PBS). Non-specific protein binding was blocked by incubation for 30 min in 5% goat serum in diluent solution (PBS + 1% Bovine Serum Albumin + 0.05% Tween). Specimens were then treated with 0.1% Trypsin solution for 10 minutes, followed by immersion in 2N HCl solution for 30 minutes. After abundant washing, slides were incubated for 1hour at room-temperature in a humidified chamber with a mouse monoclonal anti-BrdU antibody (dilution 1/1000) (Sigma, France Ref8434). Sections were washed three times in PBS at room-temperature prior to treatment for 30 minutes at room temperature with the biotinylated secondary antibody. Subsequently, sections were incubated for 30 min at room temperature with 1/20 solution of extravidin peroxidase solution (Mouse Extravidin Peroxidase Staining Kit, SIGMA, France). After rinsing with three changes of PBS, the immunoreactivity was

visualized by development for 2 to 5 min with 0.1% 3,3-diaminobenzidine and 0.02% hydrogen peroxide (DAB substrate kit, Vector Laboratories). A negative control was performed on sections of untreated (no BrdU injection) mouse teeth.

2.4.2.5 In Situ Hybridization

Collagen I sense and antisense RNA probes were prepared from full-length cDNA, subcloned into Bluescript plasmid and linearised with Xhol or Pstl endonucleases (Activity 0.405µg/µl).

In summary, non-radioactive *in situ* hybridisation was performed on 7µm sections. Sections were deparaffinised, dehydrated and hybridised with 50µl of probe (3ng/µl) in a humidified chamber overnight. The reaction was revealed by reaction with anti-digoxigenin alkaline phosphatase-conjugated Fab fragment. The sections were stained with haematoxylin and dehydrated before mounting under a coverslip and subsequent light microscopic examination.

Protocol.

Day1 :

1- Section preparation :
   - Xylene 2 x 5min
   - Ethanol 100% 5min
   - Ethanol 95% 5min
   - Ethanol 80% 5min
   - Ethanol 70% 5min
   - Rinse 3 times with DEPC water for 5min
   - Rinse in PBS 2 x 5min
2- Immersion in para-formaldehyde solution (PFA)(4% in PBS) -10min
3- Pretreatment with proteinase K for 5 min in RNase free TE buffer at 37ºC
4- Rinse with DEPC water 3 times
5- Immersion in PFA 4% in PBS solution for 10min
6- Rinse with DEPC water
7- PBS 1X 5min
8- Pre-hybridisation with hybridisation buffer
9- Denaturation of the probes at 80ºC for 10min
10- Hybridisation of cuts with 50µl of diluted probe
11- Hybridization overnight at 60 ºC

Day 2 :

12- First rinse with SSC4X + 50% formamide and 0.1% Tween for 15min at 60 ºC
13- Rinse with SSC2X + 10mMDTT solution at 60 ºC for 15min (2 times)

14- Rinse with SSC 1X + 10mMDTT solution at 60 ºC for 15min (2 times)
15- Rinse with SSC 0.1X + 10mMDTT solution at 60 ºC for 15min (2 times)
16- Rinse in MABT at Room Temperature 30min (2 times)
17- Rinse with NTE (10%NaCl 5M, 1% tris HCl 1M, 1% 0.5MEDTA) in DEPC water + 2.5% RNase
18- Incubation for 4hours with blocking solution (MABT 1x (20ml), blocking reagent (2g), inactivated goat serum (20ml), Tween 20 (100µl), made up with distilled water to 100ml)
19- Incubation with anti-Digoxigenin antibody (1/200 in blocking solution) over night at room temperature in a humidified chamber

Day 3:

20- Rinse 2 times in MABT for 5min
21- Rinse 10min in fresh NTMT at room temperature
22- Revelation of Antibody activity in moist dark room with NBT/BCIP (30min)
23- Rinse 10min at room temperature in NTMT
24- Rinse with double-distilled water.
25- Counterstained with haematoxylin and mounted in Depex$^{(R)}$ after dehydration of sections with increasing concentrations of ethanol solutions.

Abbreviations:

DEPC: deionized, diethylpyrocarbonate treated water

PBS: Phosphate buffered Saline

TE Buffer: Tris-EDTA buffer

PFA : 4% Paraformaldehyde in PBS

SSC 20X: 0.3M trisodium citrate and 3.0M sodium chloride solution in high purity dH_2O

DTT: Dithiothreitol solution

MAB5x : Maleic acid (23.22g) + NaCl (17.53g) + Water (up to 400ml)

MABT : MAB solution + tween (0.1%)

NTE: 100mM Tris; 2.0M NaCl; 10mM EDTA; pH 7.4

NBT/BCIP: Solution of NBT Nitro blue tetrazolium chloride (18.75 mg/ml)+ BCIP (5-Bromo-4-chloro-3-indolyl phosphate,toluidine salt) in 67% DMSO

2.4.2.6 MSX2 over-expression in immortalised cells

Molecular effects of over-expression of Msx2 were studied in MDPC23 (immortalised odontoblast-like cells) and OD21 (immortalised pulp-like cells) (Hanks, Fang et al. 1998) after transfection of the cells with CMV-Msx2 plasmid for protein over-expression

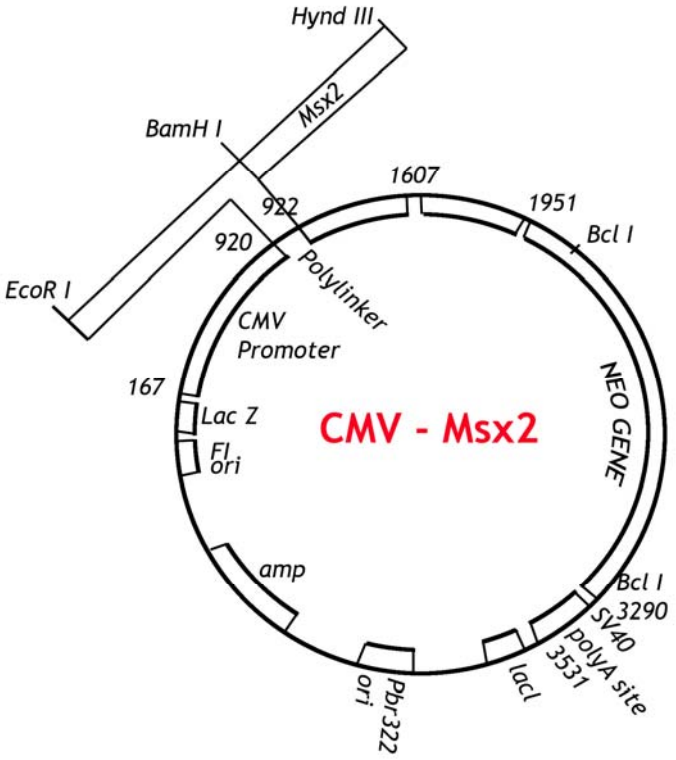

Figure 17 : Plasmid CMV-Msx2. Base plasmid pcB6. Cloning site: 5'-EcoRI 3'-HyndIII; Amino Acids Contained: 3-268. Plasmid designed for protein expression in eukaryotic cells. Cloning strategy: isolate/EcoRI/HindIII fragment from plasmid #129 and cloned directly. Bacterial Strain: DH5α. Selectable marker AMP.

MDPC-23 cells were seeded and cultured in 6-well plates (Appleton-Woods, UK) at a density of 25,000 cells per well in Dulbecco's modified Eagle's medium (DMEM) supplemented with 10% fetal calf serum (FCS), 1% penicillin/streptomycin (Sigma, UK), and 200 mM glutamine (Sigma, UK). Cells were cultured in a humidified

incubator in a 5% carbon dioxide atmosphere at 37ºC for 24 hours prior to transfection.

Plasmid pvB6 (concentration 1.01µg/µl) (see Figure 17 for plasmid construction and identification) was introduced into cells by lipofectamin transfection (EFFECTEN KIT- Qiagen – France). After medium removal, cells were incubated with 0.4µg of plasmid DNA, 3.2µl of Enhancer, Buffer (top up to 100µl), 10µl of Effectene Reagent, and 1.6ml of culture medium for 6 or 48 hours. Cells were finally washed with DMEM medium, and lysed for further molecular biological analysis.

2.4.2.7 Real Time quantitative PCR analysis

Total RNA was extracted using the SV Total RNA Isolation kit (Promega, UK) and was eluted in a final volume of 30 µl of sterile water as recommended by the manufacturer. After total RNA quantification, equal amounts of RNA (1 µg) were transcribed into cDNA using a SuperScript II RNase H Reverse Transcriptase (Invitrogen) with oligo-dT and hexa-nucleotide random primers. Gene expression levels were determined by real-time PCR using primers (Table 2). Optimal conditions and cDNA dilutions were determined for each gene. q-PCR experiments were performed in a Roche light Cycler, in triplicate using FastStart DNA Master SYBR Green I (Roche, Neuilly-sur-Seine, France). Amplification reactions were carried out in a total volume of 15 µl at 0.9µl of 300 nM (each- Forward and Reverse) primers), 5 µl of cDNA, and 7.5µl of FastStart Universal SYBR Green Master buffer (Roche, Neuilly-sur-Seine, France) and 0.7µl of water. The PCR cycling programme consisted of one cycle at 95 degrees C, 20 s and 45 cycles at 95 degrees C, 3 s and 30 s at 60 degrees C. A final cooling step of 3 min at 40°C was included for handling of the samples, because the LightCycler had no cooling block like many commercially available thermocyclers. Data collection was performed during the annealing phase of each amplification cycle, and the fluorescent signal was monitored through the F2

channel. Data were analysed with LightCycler software by the Fit Point method to minimise noise and obtain the best correlation coefficient possible between standards. Positives were defined as samples having a C_t of less than 40 cycles and significant fluorescent gain when compared to the standard of GAPDH concentration.

Mouse Gene		Primers	Size (bp)	Tm (°C)
MSX2	F	CCTGAGGAAACACAAGACCA	278	60
	R	AGTTGATAGGGAAGGGCAGA		
GAPDH	F	CCCATCACCATCTTCCAGGAGC	450	56
	R	CCAGTGAGCTTCCCGTTCAGC		
Collagen I	F	AAAAGGGTCATCGTGGCTTC	499	58
	R	ACTCTGCGCTCTTCCAGTCA		
DSPP	F	ACAAGAGTGGGACCCTGTTT	399	58
	R	TACAGTGTGGGCGTTACAAC		

Table 2: Primer details and conditions for q-RT-PCR analysis. Primer sequences used in PCR analysis, and expected product size for each assay. Primers were designed using the Primer3 software (http://frodo.wi.mit.edu/cgi-bin/primer3/primer3_www.cgi).

3 Results

3.1 Microarray :

3.1.1 Selective extraction of odontoblasts RNA.

Histological examination of fixed teeth confirmed that only odontoblasts were retained following pulp tissue removal and that RNA extracted from these lysed cells was therefore preferentially derived from odontoblasts (Figure 18).

3.1.2 Semi-quantitative RT-PCR analysis

RT-PCR analysis was performed in triplicate on individual samples (i.e., technical replicates) and in duplicate for different samples (i.e., biological replicates). In initial RT-PCR analyses, gene expression analysis clearly indicated differential regulation of transcripts in cells at the two stages of dentinogenesis studied. DSPP and collagen Iα gene expression were down-regulated in the late stage odontoblast population compared to that of the early stage. The proteins encoded by these transcripts are key components of the dentine matrix and the down-regulation of the expression of these genes concurs with the less active deposition rate of the late stage cells. The expression of a further 6 genes (BMP4, DMP1, TGF-β1, TGF-β1R, PGAP1, (Post-glycosylphosphatidylinositol attachment to proteins 1, Osteocalcin) was also analysed in extracted odontoblast and pulpal RNA samples. The differential gene expression data supported the purity of the isolated cell and tissue populations (McLachlan, Smith et al. 2003). Confirmatory RT-PCR analysis of transcript levels for selected genes identified as being differentially expressed by microarray analysis between the late stage (LS) and early stage (ES) populations also supported the validity of our isolation technique (Figure 19). On a second stage, based on the results of microarray and analysis of the data, several transcripts were selected and analysed by RT-PCR including ADM,

Amelogenin, IBSP, DCN, Alkaline phosphatase, CaSR, SOCSBOX, SPP1 (similar to OPN), PROTS100-A1, OSTF-1, p38-MAPK, NTRK2, MAP2K6, PTPRR (Figure 20).

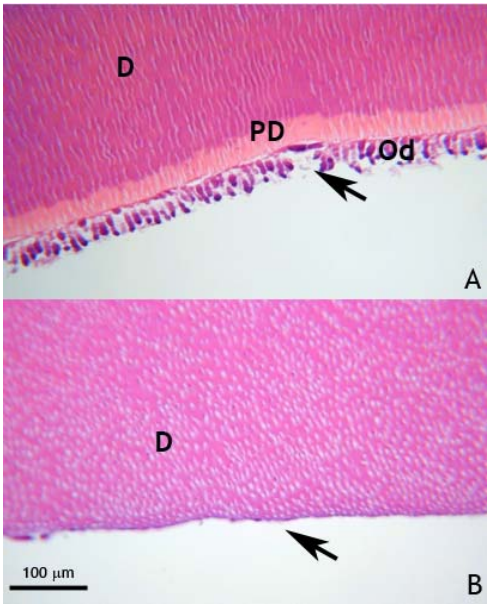

Figure 18 *:* Histological assessment of selective extraction of odontoblasts after lysis. 5μm thickness, haematoxylin and eosin staining. (A) Tooth after pulp parenchyma removal – only the odontoblast layer remains in place (black Arrow). (B) Tooth after pulp parenchyma removal and *in situ* odontoblast lysis. These images support the selective lysis of odontoblasts for RNA extraction. (D: Dentine, PD: Predentine, Od: Odontoblast Layer).

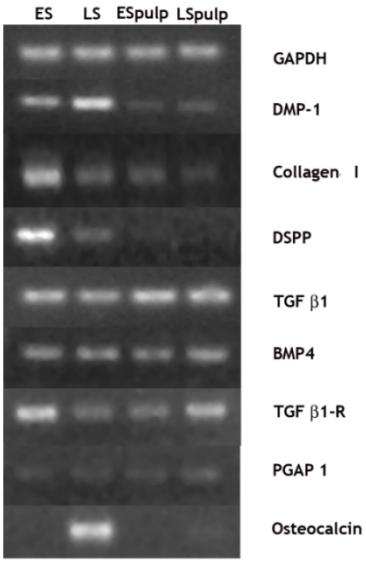

Figure 19: Changes in DMP-1, Collagen I, DSPP, TGF β1, BMP4, TGFβ-1, PGAP-1 and Osteocalcin gene expression in ES (early stage odontoblasts), LS (Late stage odontoblasts), ES pulp (early stage dental pulp) and LS pulp (late stage dental pulp). DMP-1 and Osteocalcin gene expression were up-regulated in the mature odontoblasts, whereas Collagen I, DSPP, TGF-β1 and TGF -β1-R gene expression were down-regulated. BMP4 and PGAP 1 gene expression were unchanged. In the dental pulp, minimal up-regulation of expression of TGFβ1 receptor gene was evident.

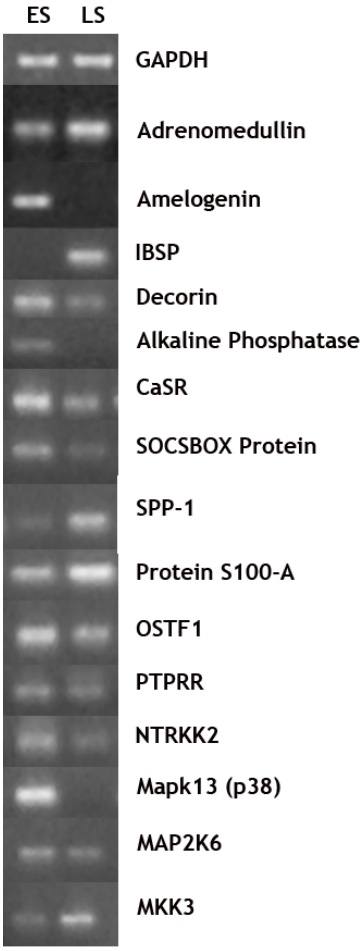

Figure 20: Post-array Sq-RT-PCR analysis showing differential expression in Early stage (ES) and Late Stage (LS) odontoblasts. This sq-RT-PCR was performed to validate the microarray results and to characterize transcript levels of genes involved in the p38 MAP Kinase Pathway (PTPRR, NTRKK2, MAPK13, MAP2K6, MKK3.

3.1.3 Microarray analysis.

Microarray analysis supported the initial RT-PCR results obtained for Collagen I α 1 chain and DMP1 gene expression. Of the 24000 genes analyzed using microarrays, 1338 genes were differentially expressed in the two populations by >2 fold (574 genes with $p<0.05$) and among those, 216 genes by >5 fold, (paired analysis, $p<0.05$) (See Appendix 1 for the full list of regulated genes). The relatively large number of differentially expressed genes was unexpected. However, such a magnitude of differential changes concur with

data previously reported for the proteomic analysis of bone cells (Cho, Lee et al. 2006). Transcripts were classified using a gene ontology classification (Figure 21).

The data analysis highlighted differential expression of a significant number of genes, not previously associated with odontoblasts or dentinogenesis. These previously un-associated genes also highlighted various regulatory mechanisms which may modulate ES and LS odontoblast activity including those of MAPKinase, apoptosis, TGF-β, and FGF pathways. Notably, a potentially important pathway identified from this analysis was that involving MAP Kinase (MAPK), with transcriptional changes identified in 6 component genes, including PTPRR, NTRK2, MAP2K6, CD14, MAPK13 (p38)M and FGF1 (Table 3 and Figure 22). Other pathways also appeared to be implicated as being differentially regulated with variable number of genes involved, such as TGF-β, GnRH and calcium signalling pathways.

3.1.4 Post-array sq-RT- PCR analysis of differentially regulated genes

As sq-RT- PCR screening of all differentially regulated genes was not feasible, 14 genes of interest were selected for further confirmatory analysis. Selection criteria were based on the level of differential regulation (high score with statistical significance), their known or alternatively previously uncharacterised role in dentinogenesis, their potential involvement in previously unexplored pathways (eg MAP Kinase pathway) or their reported involvement in the mineralisation process (e.g CASR).

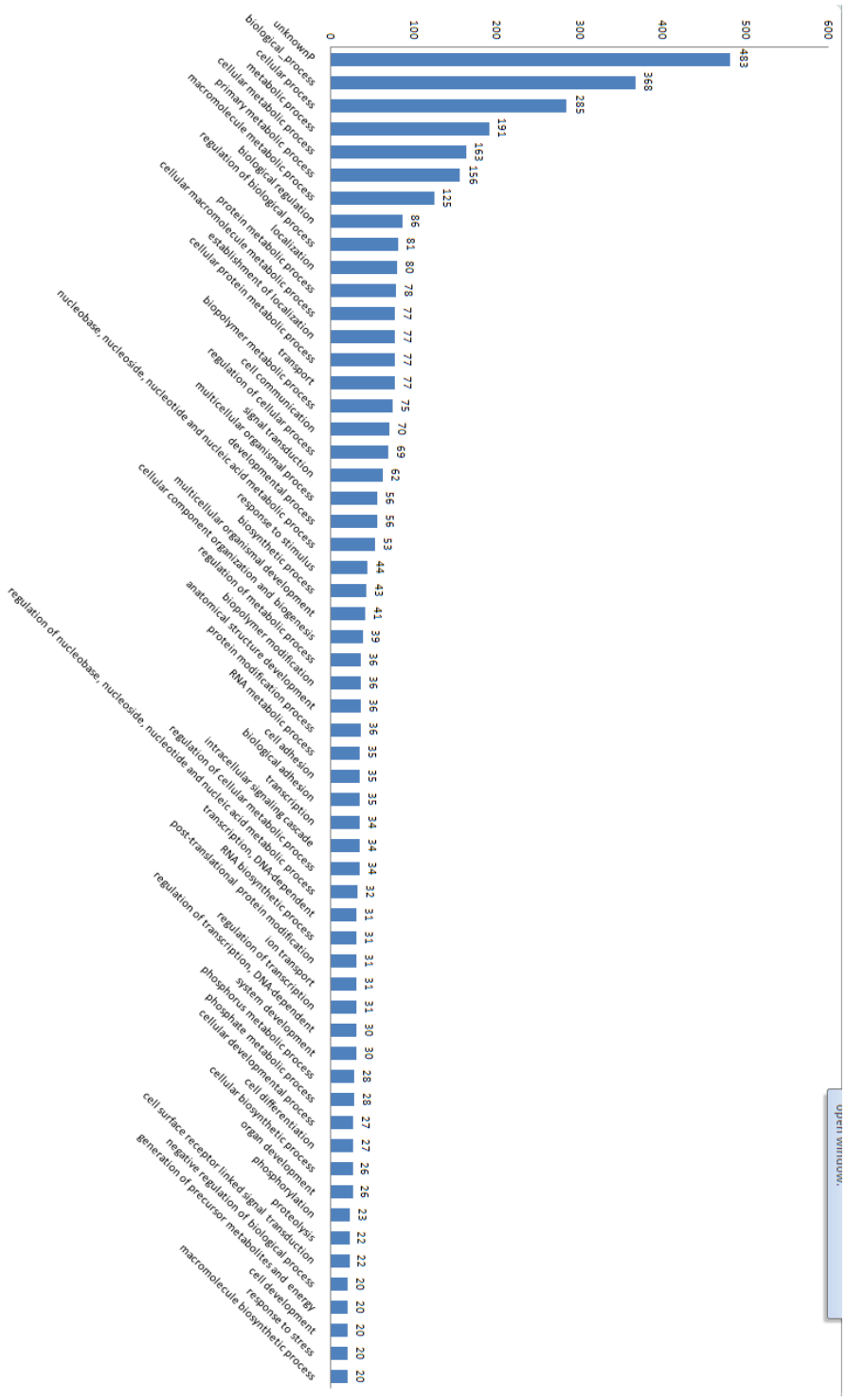

Figure 21: Ontological classification of genes up- and down-regulated between young and mature odontoblasts. Only processes involving more than 20 genes are shown.

MAPK PATHWAY

probe set	GENE ID	baseline mean (LS)	experiment mean (ES)	Change	fold change	lower bound o	upper bound of FC	Gene Title
Bt.1069.1.A1_a	PTPRR	666,73	1757,93	**-1091,2**	2,64	2,36	2,98	protein tyrosine phosphatase, receptor type, R (PTP in the Pathway)
Bt.12217.1.S1_	NTRK2	10,7	136,5	**-125,8**	12,76	6,2	100000000	Neurotrophic tyrosine kinase, receptor, type 2 (Tyr K A/B in Pathway)
Bt.561.1.S1_at	MAP2K6	323,94	1233,75	**-909,81**	3,81	3,28	4,48	mitogen-activated protein kinase kinase 6
Bt.13789.1.A1_	CD14	154,8	12,37	**142,43**	-12,52	-8,45	-23,53	CD14 molecule
				0				
Bt.800.1.S1_at	MAPK13	6,28	559,48	**-553,2**	89,06	40,69	100000000	mitogen-activated protein kinase 13 (p38 MAPK)
Bt.5038.1.S1_a	FGF1	1229,9	20,37	**1209,53**	-60,37	-37,88	-146,24	fibroblast growth factor 1 (acidic)

TGF Beta Pathway

probe set	GENE ID	baseline mean (LS)	experiment mean (ES)	Change	fold change	lower bound o	upper bound of FC	Gene Title
Bt.23178.1.S1_	DCN	776,34	4372,5	**-3596,16**	5,63	4,96	6,51	decorin
Bt.405.1.S1_at	FST	300,19	21,36	**278,83**	-14,05	-7,42	-125,3	follistatin
Bt.12760.1.S1_	INHBA	28,24	932,21	**-903,97**	33,01	15,56	100000000	inhibin, beta A (Activin)

Calcium Signaling Pathway

probe set	GENE ID	baseline mean (LS)	experiment mean (ES)	Change	fold change	lower bound o	upper bound of FC	Gene Title
Bt.1165.1.S1_a	ADCY7	345,04	1801,94	**-1456,9**	5,22	4,61	5,99	adenylate cyclase 7 (ADCY in pathway)
Bt.23606.1.S1_	ITPR1	6647,25	2032,66	**4614,59**	-3,27	-2,48	-4,72	inositol 1,4,5-triphosphate receptor, type 1 (IP3R in pathway)

GnRH Pathway

probe set	GENE ID	baseline mean (LS)	experiment mean (ES)	Change	fold change	lower bound o	upper bound of FC	Gene Title
Bt.1165.1.S1_a	ADCY7	345,04	1801,94	**-1456,9**	5,22	4,61	5,99	adenylate cyclase 7 (AC in pathway)
Bt.23606.1.S1_	ITPR1	6647,25	2032,66	**4614,59**	-3,27	-2,48	-4,72	inositol 1,4,5-triphosphate receptor, type 1 (IP3R in pathway)
Bt.561.1.S1_at	MAP2K6	323,94	1233,75	**-909,81**	3,81	3,28	4,48	mitogen-activated protein kinase kinase 6
Bt.800.1.S1_at	MAPK13	6,28	559,48	**-553,2**	89,06	40,69	100000000	mitogen-activated protein kinase 13 (p38 MAPK)

Table 3: Data extracted from Microarray analysis data files, after transcriptome analysis Early Stage cells (ES) versus Late Stage cells (LS). Negative fold change indicates that gene expression was down-regulated from ES to LS whilst a positive fold change indicates the gene expression was up-regulated. These genes were selected from the list of 574 for which expression was up or down regulated between both populations of odontoblasts with a fold change >2 and with $p<0.05$.

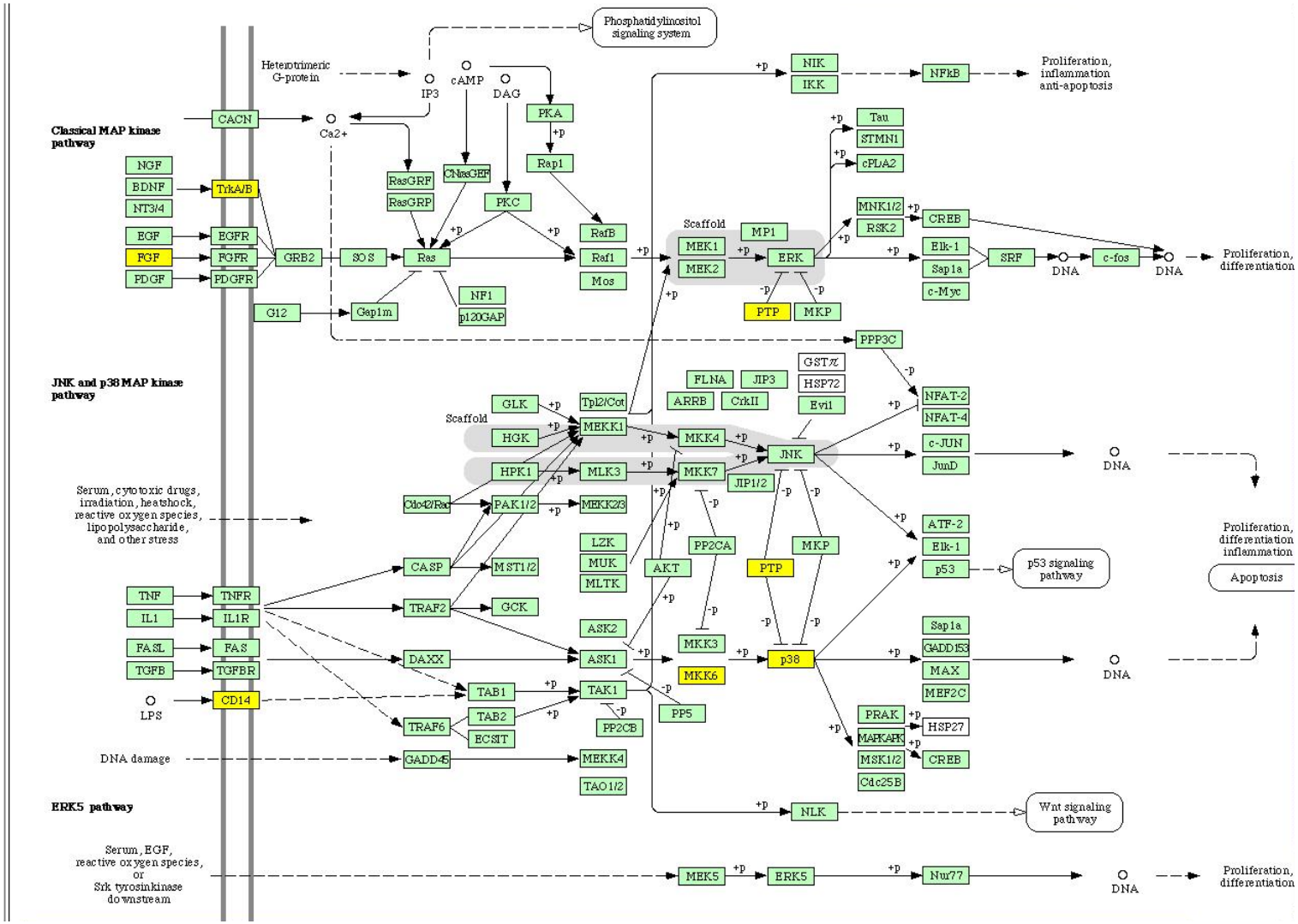

Figure 22: The p38-MAPKinase pathway (Pathway-Express software http://vortex.cs.wayne.edu). Differentially egulated genes as identified by microarray analysis are highlighted in yellow.

Alkaline phosphatase and amelogenin transcripts were more abundant in early stage odontoblasts; these results concur with their previously described patterns of expression (Hotton, Mauro et al. 1999; Papagerakis, MacDougall et al. 2003). DMP1 RNA was detected in both cell samples, but was significantly more abundant in the late stage population. This observation was also in accordance with published results (Lu, Xie et al. 2007). ADM, IBSP (Bone Sialoprotein), SPP1 (Osteopontin), Osteocalcin and M1K3 gene expression were also up-regulated in late stage cells as shown previously for osteocalcin (Papagerakis, Berdal et al. 2002), whereas in contrast TGF-β1 and SOCSBOX were down-regulated in these cells. Other genes investigated, including BMP4, TGF-βR1, PGAP 1, OSTF1, were not evidently differentially regulated.

3.1.5 Immunohistochemical analysis

3.1.5.1 DMP1 expression:

DMP1 protein expression and localisation was examined by immunohistochemical staining using an anti-DMP1 antibody on unerupted bovine first molar histological sections. The differential staining of cells in the cuspal area compared to the apical area in this immature tooth clearly shows that odontoblasts are functioning differently in the coronal as compared to apical regions based on DMP1 immunoreactivity. To identify odontoblasts and confirm their activity in the secretory phase, Anti-DSP antibody staining was used as a positive control (Figure 23).

3.1.5.2 Phosphorylated p38 MAPK analysis:

As this pathway was highlighted as being potentially differentially regulated in LS compared to ES odontobalsts by both microarray and RT-PCR analyses, p38 protein expression and activity were investigated by performing immunohistochemical staining using an anti-phosphorylated p38 antibody on an erupted mouse maxillary incisor. The greater immunoreactivity of cells in the immature apical area compared to the incisal

area clearly shows that phosphorylated-p38 is differentially expressed in young and old odontoblasts, further corroborating the gene expression findings previously identified (Figure 24).

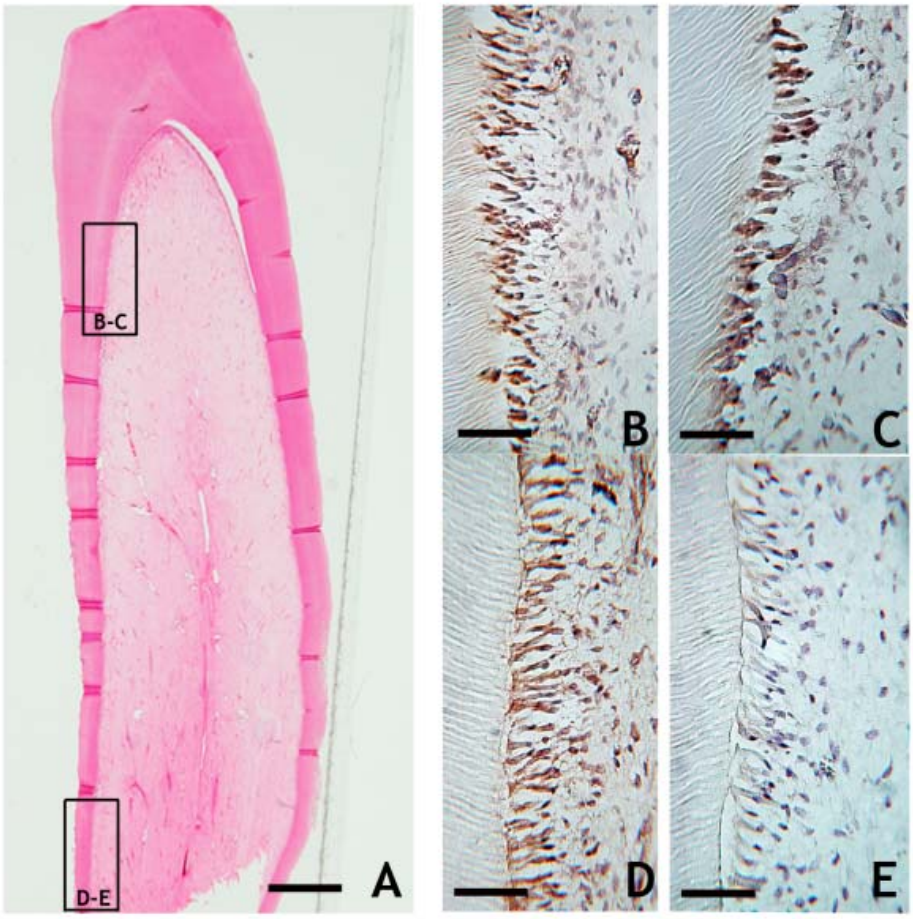

Figure 23: (A) Histology of a bovine unerupted first upper molar cusp, 5μm thickness section, haematoxylin and eosin staining, bar=500μm. (B-C) Immunohistochemistry with anti-DSP antibody on odontoblasts in the coronal area (B) and apical area (C). Expression of protein is visibly unchanged in both sections highlighting the secretory activity of the cells. (D-E) Immunohistochemistry using the anti-DMP1 antibody in odontoblasts in the coronal (D) and apical areas (E). The differential expression of DMP1 protein between both populations of cells corroborates the reported gene expression data (B,C,D,E : Bar=100μm).

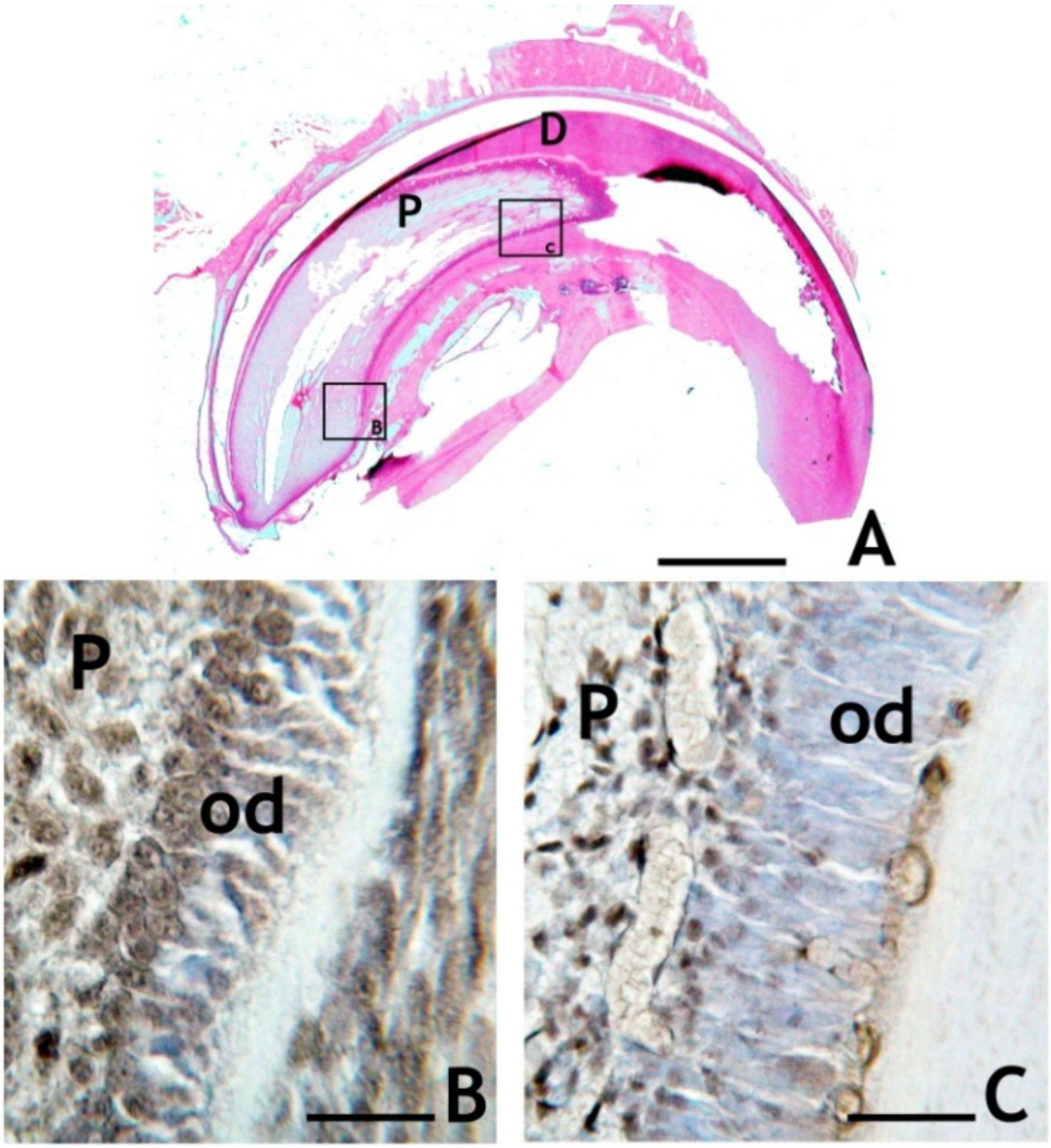

Figure 24: Mouse upper incisor (A) 5μm thickness, haematoxylin and eosin staining. (B) Immunohistochemical analysis using anti-mouse phosphorylated p38 antibody in apical area of the erupted mouse tooth. Nuclear staining of odontoblasts is evident, and phosphorylated-p38 is apparently also present in the cells of the pulpal parenchyma. (C) Immunohistochemistry using the same antibody performed on cells nearer the incisal tip, with mature odontoblasts. Staining is enhanced in the apical area, indicating the higher concentration and activity of p38 protein in the young cells compared to that of the mature ones. Cytoplasm of mature cells is free of staining, and nuclear staining is strong indicating that p38 is potentially acting as a transcription factor. P= Pulp – od= Odontoblasts – D = dentine (A) Bar= 1 mm (B) Bar= 50 μm (C) Bar=75 μm.

3.2 Tertiary dentinogenesis and p38 MAPKinase pathway

3.2.1 P38 Phosphorylation ELISA

Anisomycin is known to stimulate the MAPKinase pathway by activating p38 (Geiger, Wright et al. 2005). In the present study, phosphorylated protein was expressed at a basal level in untreated MDPC-23 odontoblast-like cells and was further activated in cells following anisomycin stimulation, with a peak level reached at 15 min. Expression levels then progressively decreased, returning to basal levels by 24 hours. Exposure of cells to the p38 inhibitor SB203580 caused no detectable reduction in p38 protein expression (Figure 25).

Similar expression profiles were observed after cells were stimulated with TGF-β1, ADM, or TNF-α. Incubation of cells with anti-TGF-β1-receptor alone reduced protein expression levels compared to the control. Pre-incubation of cells with antibody before incubation with rh-TGF-β1 led to no increase in protein activation, confirming previous findings that activation of the p38-MAPK pathway depends on TGF-β1 receptor binding.

Significantly, use of extracted Dentine Matrix Proteins (DMPs) for stimulation also induced p38 phosphorylation, albeit with a different temporal profile. At 15 minutes, p38 protein was expressed at levels only two-fold above control, whereas expression was increased almost 5-fold with ADM or TNF-α, and nearly 6.5-fold with TGF-β1 exposure. However, peak expression levels, which approached those achieved with other molecules, were reached only after 1 hour. At 3 hours, the protein expression level after DMP stimulation was higher than with other treatments, and at 24 hours phospho-p38 remained 25% over-expressed compared to that of the control, at which time expression levels in cells treated with other molecules had returned to baseline.

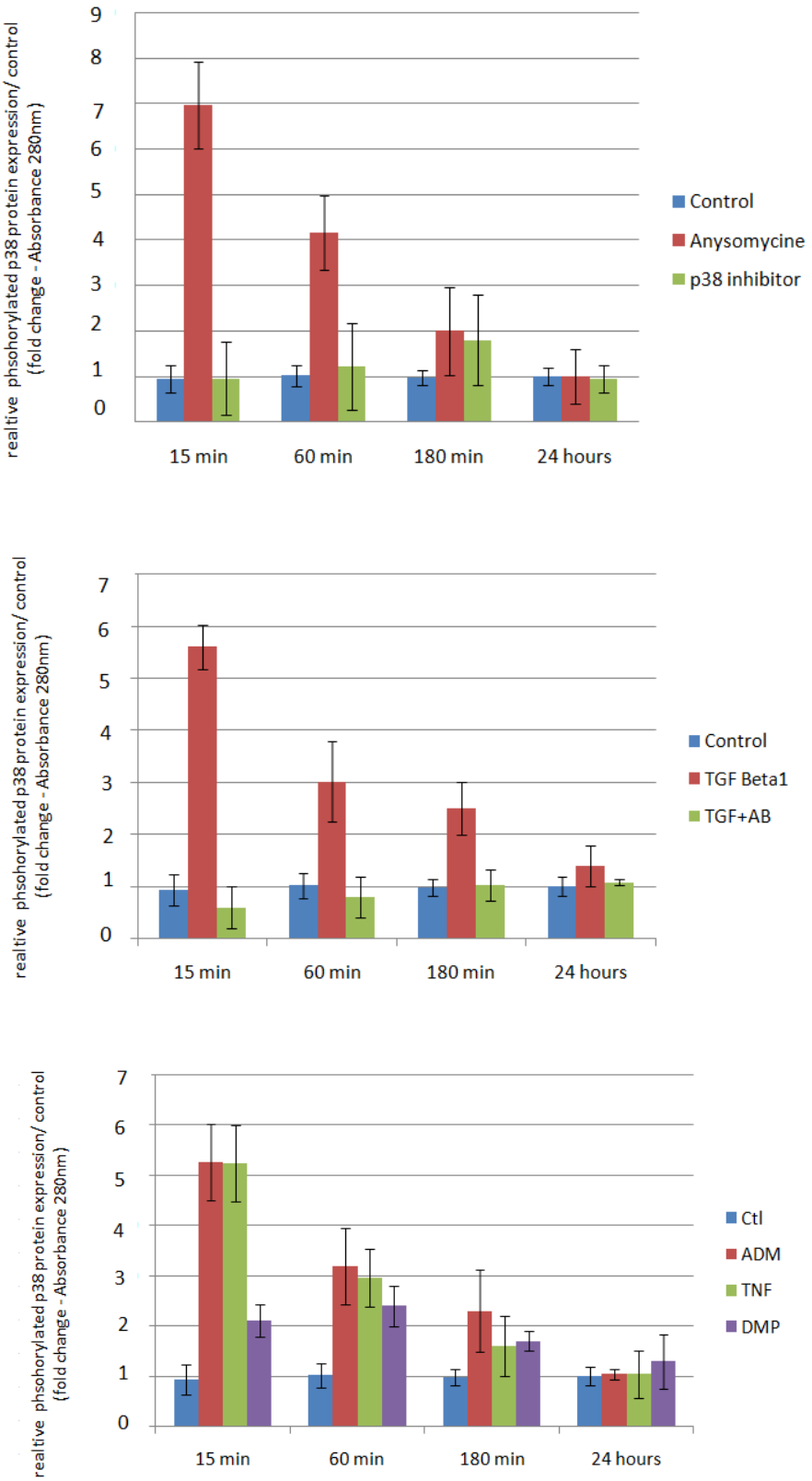

Figure 25: Phosphorylated p38 protein expression at a basal level in untreated MDPC-23 cells and after cell treatment with anisomycin, SB203580 (p38 phosphorylation inhibitor), TGF-β1, TGF-ß1+antiTGF-β1 antibody, ADM, TNF-α, Dentine Matrix Proteins for 15, 60, 180mins and 24hours. Bars are +/- S.E.M. y units:relative phosphorylated p38 protein expression/control (fold change - (Absorbance 280nm))

3.2.2 Segmental analysis of cytoplasmic and nuclear expression of phosphorylated-p38

All molecules previously used induced an activation and translocation of the protein, albeit at different levels. With TNF-α, phospho-p38 protein appeared nearly completely translocated, however, following stimulation with *Streptococcus Mutans*, only half the activated protein was present in the nucleus. Notably, TGF-β1 was most effective for both p38 activation and protein translocation. Dentine Matrix Proteins and ADM exhibited similar effects, inducing activation of the protein resulting in 75% of the protein being translocated after one hour exposure.

When the stimulatory molecules were applied in combination, to potentially better mimic the *in vivo* situation, protein activation was increased. TNF-α together with TGF-β1 increased phospho-p38 expression by 55% compared to TNF-α exposure alone, and by 15% compared to TGF-β1 exposure alone. Growth factors applied in combination with *Streptococcus Mutans* also led to a synergistic effect compared to *Streptococcus Mutans*or growth factors stimulation alone (Figure 26).

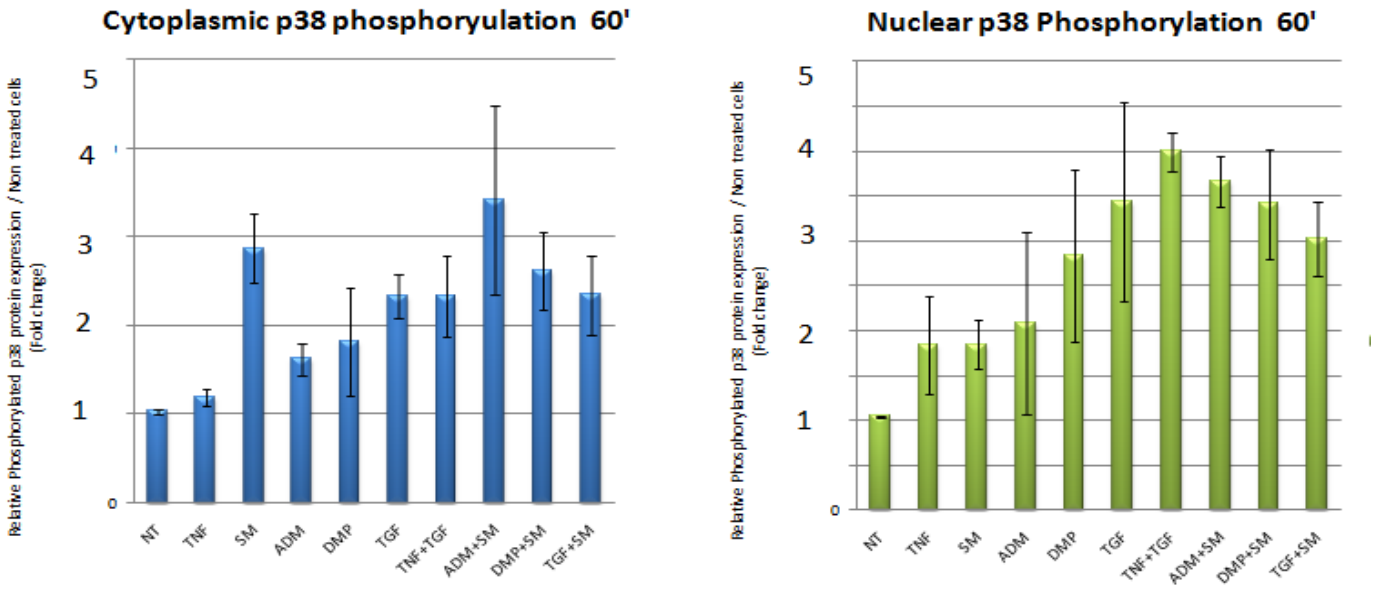

Figure 26: Phoshorylated p38 protein expression in cytoplasmic and nuclear localisations of MDPC-23 cells, after stimulation with TNF-α, Streptococcus mutans (SM), ADM, DMPs, TGF-β1, TNFα+TGF-β1, ADM+SM, DMP+SM, TGF-β1+SM for 60 minutes. (DMP = dentine matrix protein preparation, SM = Streptococcus mutans). Y Axis units : Relative Phosphorylated p38 protein expression / Non treated cells (Fold change)- Bars are +/- S.E.M. *: statistically significant difference from control.

3.3 MSX2 proteins and dentinogenesis.

3.3.1 Histology observations:

No differences were observed for the first upper molar morphology of wild type and heterozygous transgenic mice. In contrast, tooth morphology was strongly disrupted in null mutant animals with crown morphology and root formation demonstrating clear alterations. Changes were also observed in the dentine thickness (Figure 27).

3.3.1.1 At 7 days post-natally

Dentine thickness was slightly increased in null mutant animals, and on the side of the cusp, a convex dome was observed instead of the concave shape seen in Wild Type (WT) teeth.

In Msx2 -/- mouse teeth, a slight mineralization defect was noticeable on the top of the first molar cusp. The mantle dentine thickness was also noticed to be greater than in wild type animals.

On Msx2 null mutant animals, the course of the coronal dentine tubules was more sinusoidal than those of Wild type (WT) animals; many lateral branches were clearly visible and in higher number than in WT, although it was difficult to see any true communication between them. The density of the lateral branching was greatest in between cuspal areas rather than on the cusps themselves (Figure 28).

Root formation had already started in WT animals whereas it had not begun in -/- animals.

The alterations in dentine morphology and tubular orientations confirm the disturbances in dentinogenesis in the absence of the MSX2 protein. In the odontoblast palisade layer, nuclear polarization was inverted in many cells. Such inversion of polarity was rarely observed in WT or +/- samples (Figure 29).

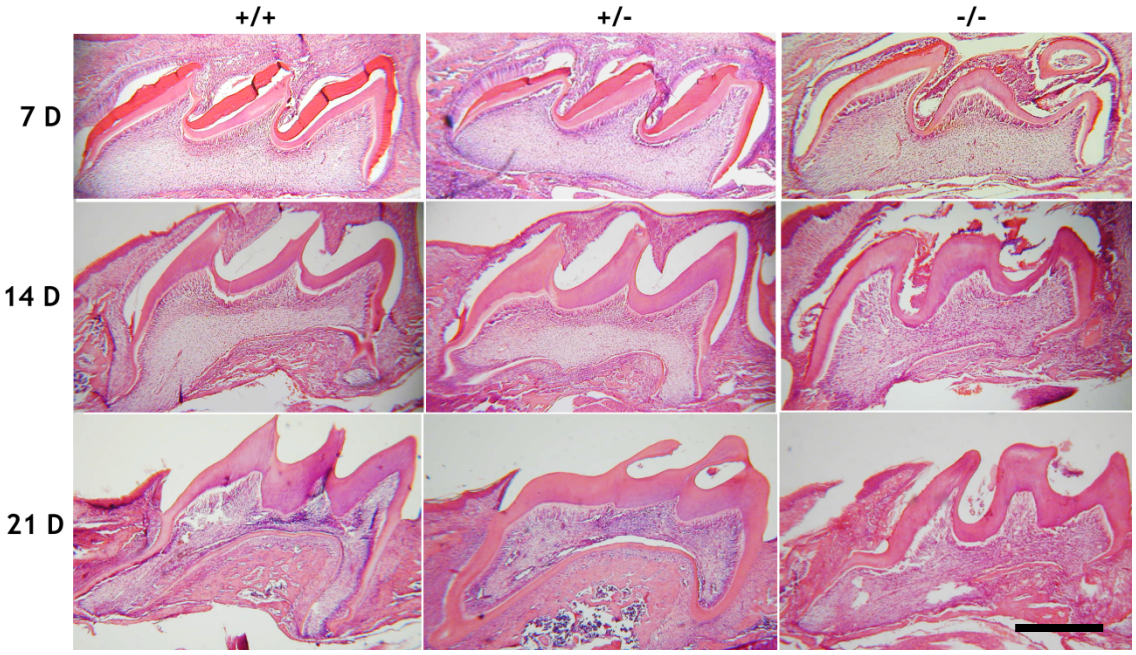

Figure 27: Histology of the first upper molar in WT, +/- and -/- mice, at 7, 14 and 21 post-natal days. 7µm thickness sections with haematoxylin and eosin staining. Bar=500µm

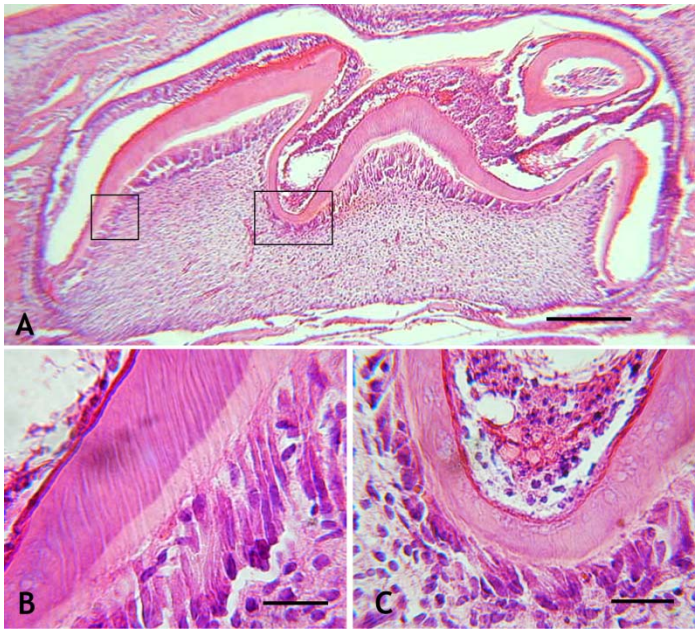

Figure 28: First upper molar in Msx2 -/- 7 days post natal. 7µm thickness, haematoxylin and eosin staining. (A): Bar= 250µm (B)-(C): Higher magnification; Bar= 50µm.

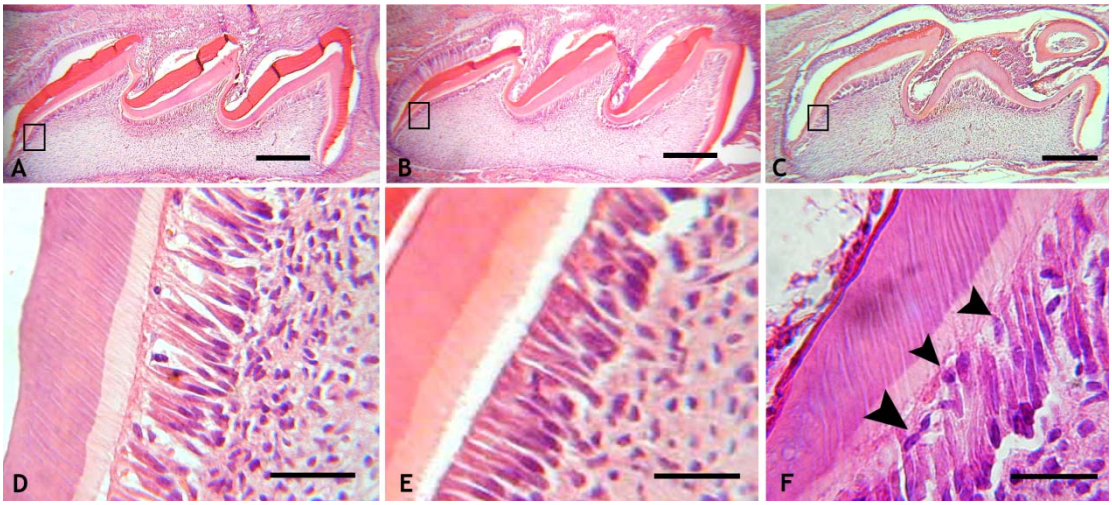

Figure 29: First upper molar in +/+ (A and D), +/- (B and E), -/- (C and F). 7 days post natal days. 7µm thickness, haematoxylin and eosin staining. (D, E and F) higher magnification of odontoblast layer. Note inverted polarisation of odontoblasts in -/- animals (black arrows). (A, B, C), bar=200µm - (D, E, F), bar= 70µm.

3.3.1.2 At 14 days post natal :

Between 7 and 14 days post-natally, an obvious line of defective matrix secretion was readily seen in the dentine. Within this area of defective matrix secretion, some cellular inclusions were also observed. Subsequent matrix secretion on the pulpal aspect of the dentine appeared relatively normal at the histological level, although the dentinal tubule course appeared more disturbed after the defect area than before (Figure 30).

This perturbation to matrix secretion was not specific to the first upper molar and was also seen in the second and third molars (Figure 31). This observation allowed us to hypothesize that the stimulus for this disturbance to dentinogenesis is probably time dependant, because the disturbance occurred at the same time of post natal development in the three molars.

In Msx2 -/- animals, the odontoblast palisade layer appeared slightly disorganized compared to WT animals. Whereas root formation had begun in WT and +/- animals, this process was strongly disrupted in null mutant animals. On the mesial root, a 90° change in orientation occurred as soon as root formation started. At 14 days, this directional

change in root formation was noticeable, showing a 'kinking' of the root. Root length was shorter in -/- animals compared to WT or +/- ones. There was no predentine observed in the cuspal areas of the teeth in -/- animals. Inclusions were also detected in the thickness of dentine matrix. No nuclei were visible inside these inclusions, but the size and morphology of these inclusions led us to speculate that cells may have been present and vital in these vacuoles.

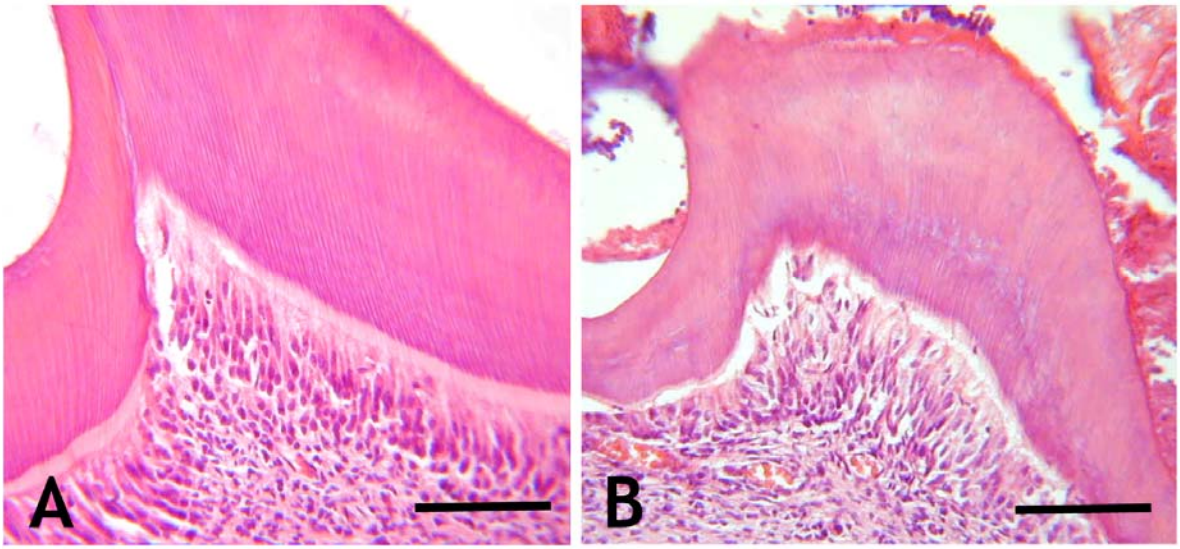

Figure 30: Comparison of dentine structure on +/+ (A) and Msx2 -/- (B) first upper molar 14 days post natal mice. 7µm thickness with haematoxylin and eosin staining. Bar = 100µm

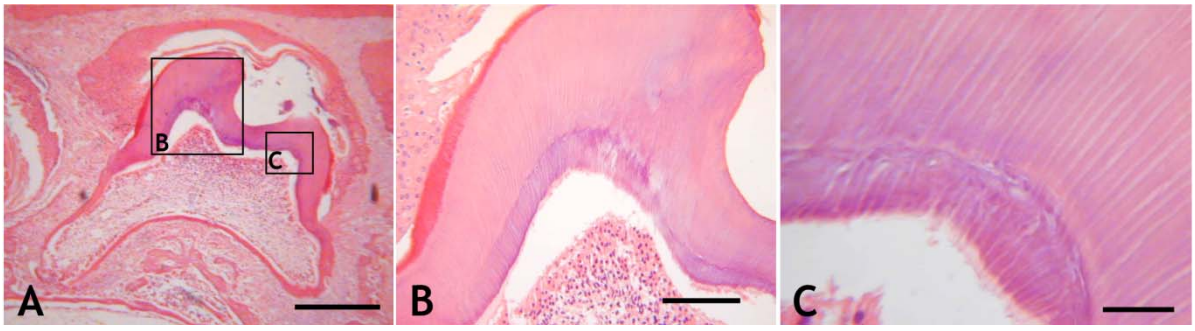

Figure 31: Dentine structure in the coronal area of the second upper molar of 14 days post-natal Msx2 -/- mice. A line is clearly visible in the thickness of the coronal dentine, which may represent a landmark of an episode of dysregulation of odontoblast secretory activity. 7µm thickness, haematoxylin and eosin staining. A: Bar= 300µm, B: Bar=100µm, C: Bar=50µm.

3.3.1.3 At 21days post natal :

The line of disturbed dentine matrix structure described above was still clearly visible at 21 days post-natally. Inclusions in the dentine were also noticeable and the odontoblast layer was highly disorganized. In Msx2 -/- animals, secondary dentinogenesis seemed to result in secretion of a combination of orthodentine, and reparative dentine with cellular inclusion (osteodentine). No predentine was present in the coronal area of the tooth.

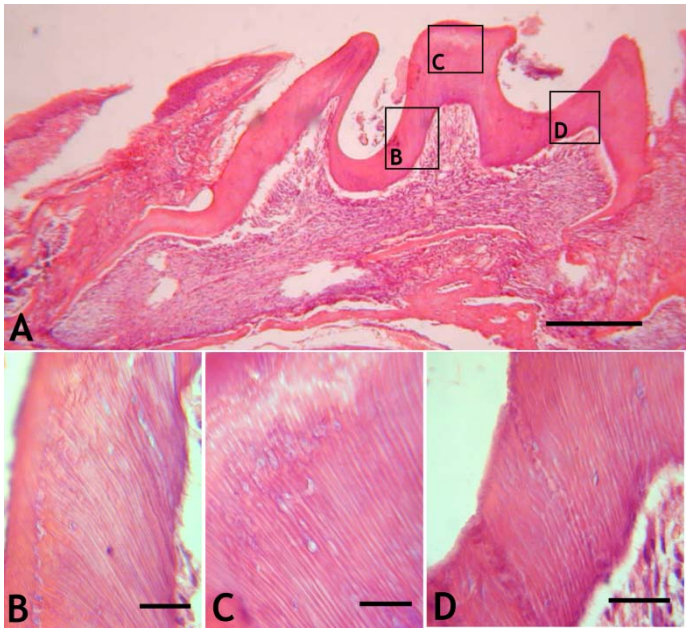

Figure 32: Dentine structure of a first upper molar from a 21 days post natal Msx2 -/- mouse showing different areas of the crown of the tooth. Abnormalities of dentine structure were obvious, with the presence of vacuoles in the mineralized tissue thickness, which may be a landmark of cellular inclusions. 7µm thickness, haematoxylin and eosin staining. A: Bar= 200µm, B, C, D: Bar=50.

3.3.1.4 4 month old animals:

The mesial cusp had been completely lost at 4 months, possibly due to abrasion of the enamel-free tooth. The line of disturbance of matrix secretion was still visible in the dentine and seemed to separate the two types of secreted (primary and secondary) dentine (Figure 33). In the apical area of the tooth, no true root formation was seen and

only a mass of mineralized tissue with cellular inclusions (usually called osteodentine) had been secreted. A new predentine layer was noticed in few sections, leading us to speculate that an alternation in orthodentine/osteodentine secretion may have been occurring.

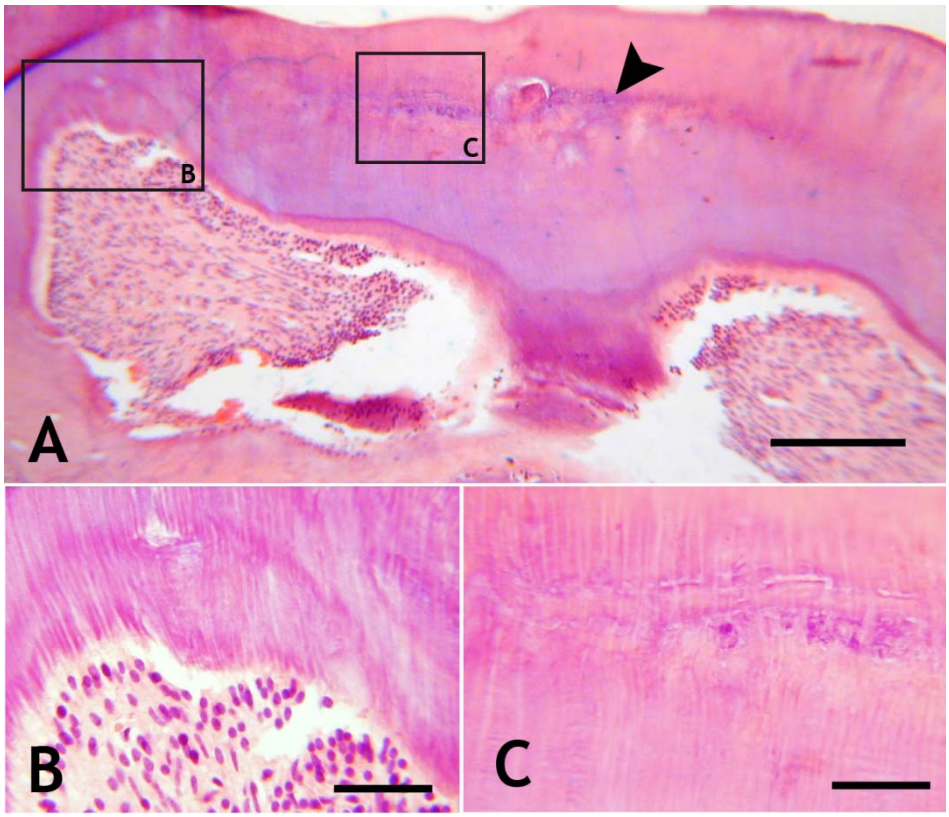

Figure 33: Dentine structure of first upper molar in a 4 month old Msx2 -/- mouse. (A) The line of disturbed matrix secretion in the dentine is still clearly visible (black arrow) (B and C) : dentine structure at higher magnification. 7µm thickness, haematoxylin and eosin staining. A: Bar= 150µm, B,C: Bar=50µm.

3.3.2 Beta galactosidase immunohistochemistry:

The n-lacZ gene encoding prokaryotic β-galactosidase (β-Gal) enzyme was used as a reporter gene for Msx2 screening. Hertwig Root Sheath cells were strongly stained, delimiting a pale zone, free of β-Gal staining in the apical papilla area (Figure 35). Expression of Msx2 protein in HERS cells confirmed Yamashiro's previous data on RNA

expression, obtained using *in situ* hybridization in rat teeth.(Yamashiro, Tummers et al. 2003) as β-Gal was highly expressed in central pulp parenchyma. A few odontoblasts also expressed the reporter protein, however, there were regional variations apparent (Figure 34). Higher expression was noticed in root odontoblasts compared to coronal cells. Interestingly, odontoblasts showing no polarization (nucleus in distal position) were systematically stained. Protein expression seemed to decrease with cell maturity (Figure 34: Immunohistochemical analysis using anti-mouse beta-galactosidase antibody on first upper molars of 7 days post natal Msx2 +/-mice. Nuclear staining of a few odontoblasts and pulp cells is evident. Counterstained with haematoxylin. A: Bar=150µm, B,C,D: Bar= 60µm.). Epthelial cell rests of Malassez cells also showed strong immunoreactivity for MSX2 (Figure 36 &Figure 37).

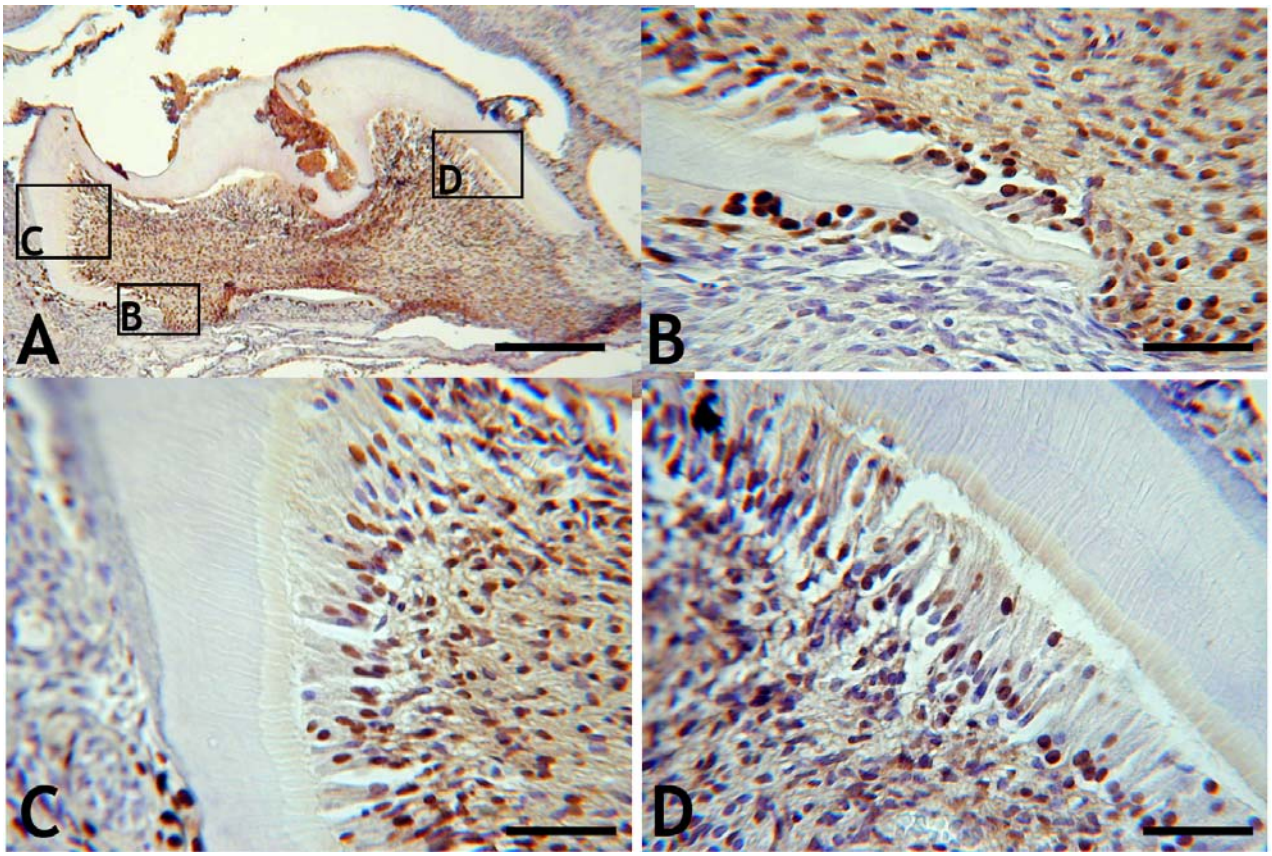

Figure 34: Immunohistochemical analysis using anti-mouse beta-galactosidase antibody on first upper molars of 7 days post natal Msx2 +/-mice. Nuclear staining of a few odontoblasts and pulp cells is evident. Counterstained with haematoxylin. A: Bar=150µm, B,C,D: Bar= 60µm.

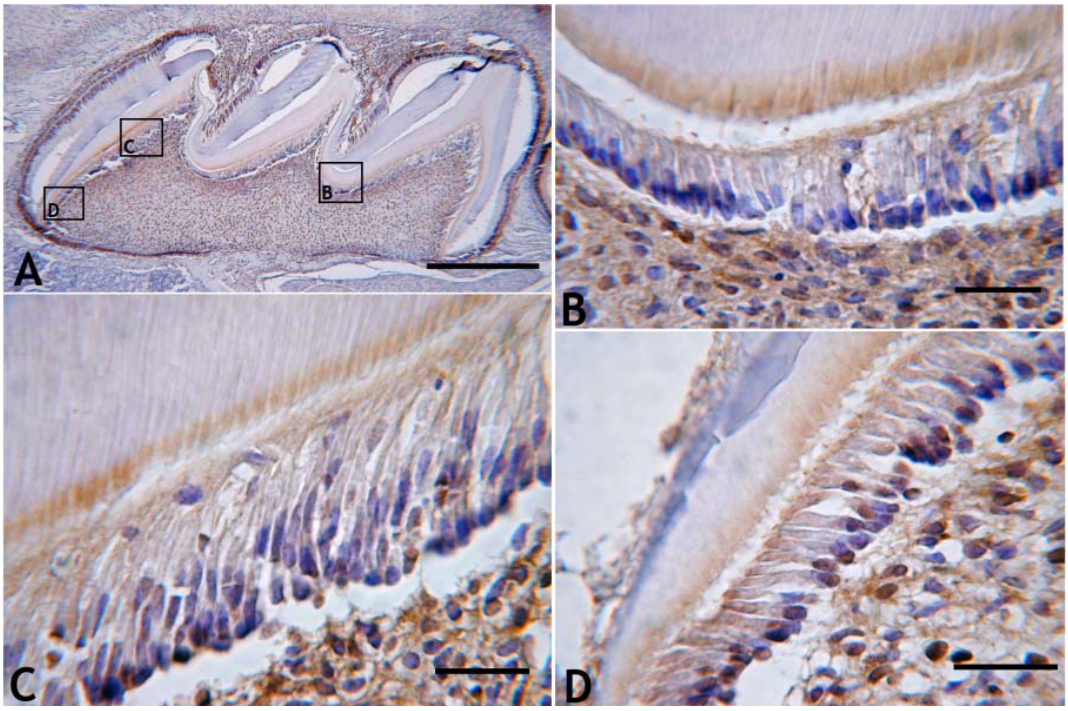

Figure 35: Immunohistochemical analysis using anti-mouse beta-galactosidase antibody on first upper molar of a 14 days post natal Msx2 -/- mouse. Nuclear staining of a few odontoblasts and pulp cells is evident and also in Hertwig's Epithelial Root Sheath cells (B). Counterstained with haematoxylin. A: Bar=150µm, B,C,D: Bar= 60µm.

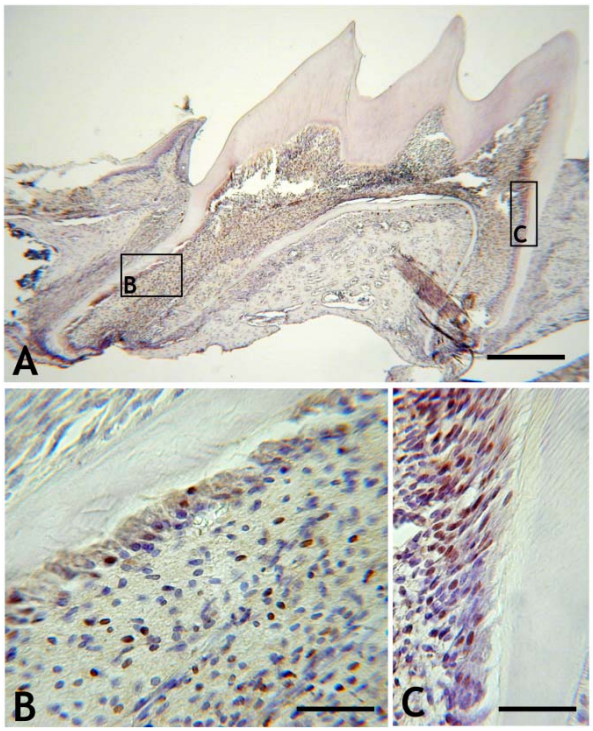

Figure 36: Immunohistochemical analysis using anti-mouse beta-galactosidase antibody on first upper molars of 21 days post natal Msx2 +/- mice. Counterstained with haematoxylin. A: Bar=150µm, B,C,D: Bar= 60µm.

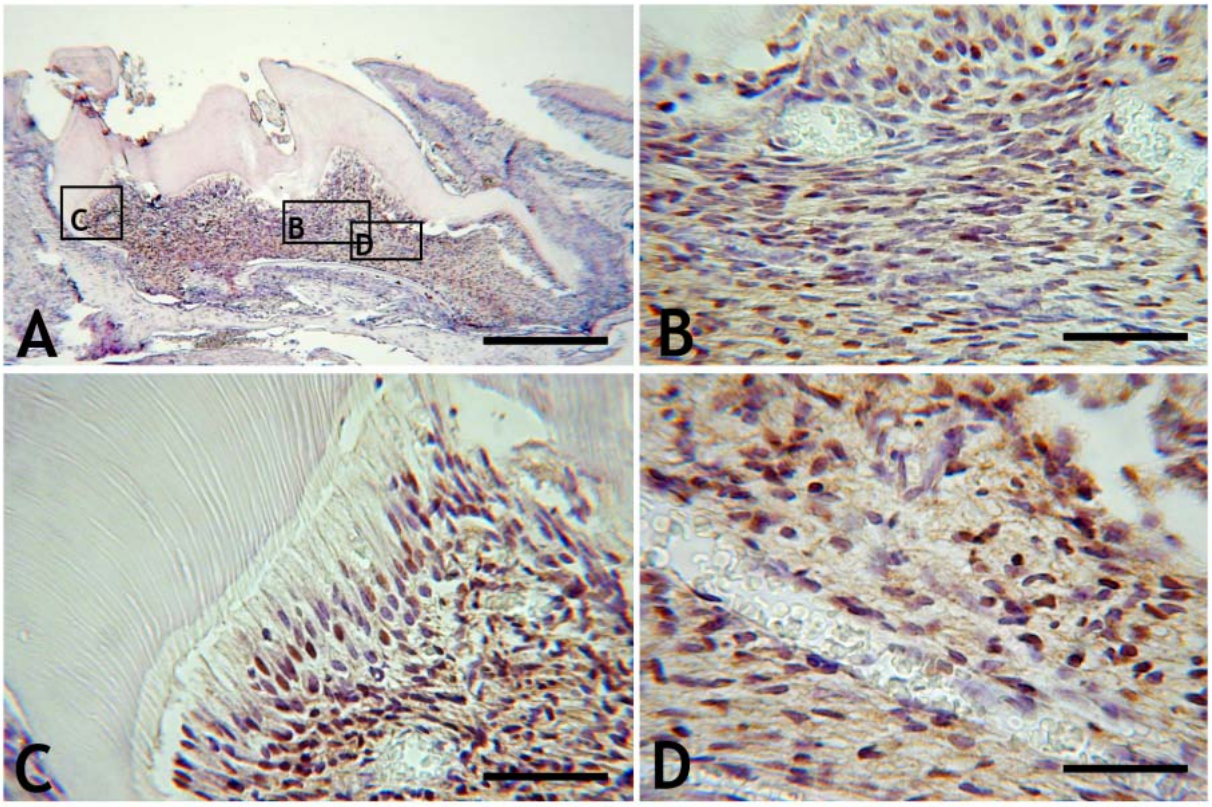

Figure 37: Immunohistochemical analysis using anti-mouse beta-galactosidase antibody on first upper molar of 21 days post natal Msx2 -/- mice. Counterstained with haematoxylin. A: Bar=150µm, B,C,D: Bar= 60µm.

3.3.3 Dentine Sialoprotein (DSP) Immunohistochemistry

DSP was normally expressed in odontoblasts of -/- mice. Whereas nuclei were not clearly visible inside the dentine inclusions observed in these animals, DSP immunoreactivity was strong in these vacuoles/disturbances of matrix secretion (Figure 38 , Figure 39). The immunoreactive areas co-localising with the inclusions described above were also evident in other areas, which appeared to be randomly localized in various regions of the dentine thickness. This was an important observation, indicating that even if these inclusions represented sites of cells which were no longer vital, they may have been entrapped during the dentinogenic process prior to death potentially by lack of nutritive supply (in contrast to

osteocytes). Interestingly, there appeared to be a true gradient of immunoreactivity observed between the dentine secreted "before the line of disturbed matrix secretion" and the dentine secreted "after" this point.

A few pulp calcifications which were positive for DSP were visible within the central pulp.

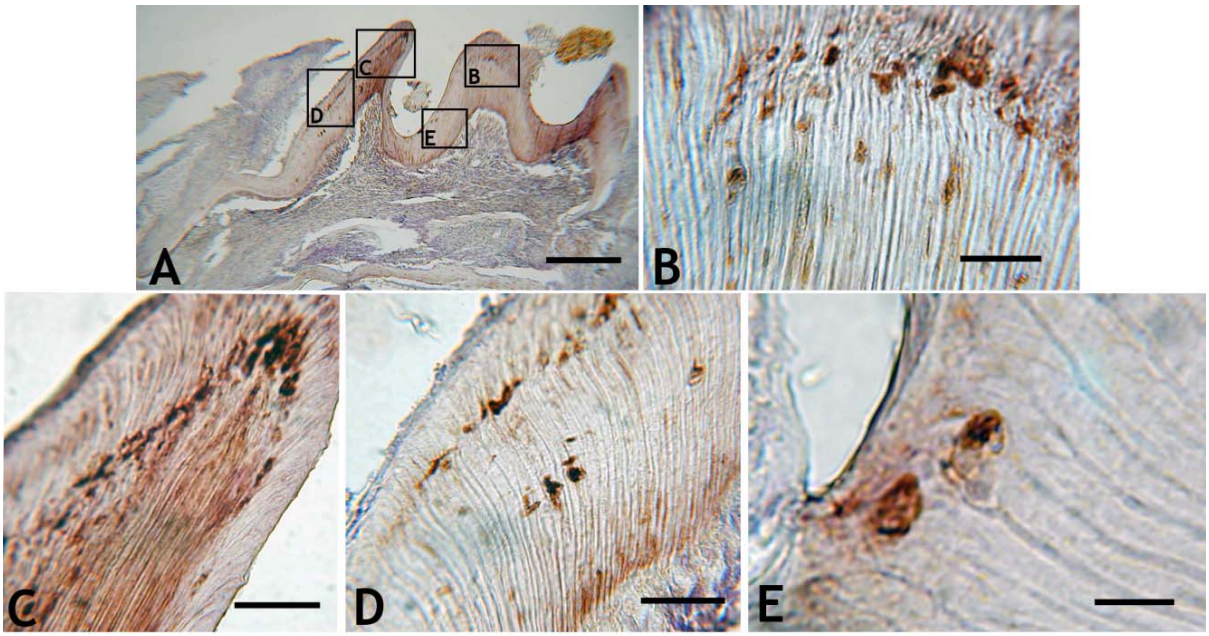

Figure 38: Immunohistochemical analysis using anti-mouse DSP antibody on a first upper molar of 21 days post natal Msx2 -/- mouse. Counterstained with haematoxylin. A: Bar=150µm, B,C,D: Bar= 60µm, E: Bar=20µm.

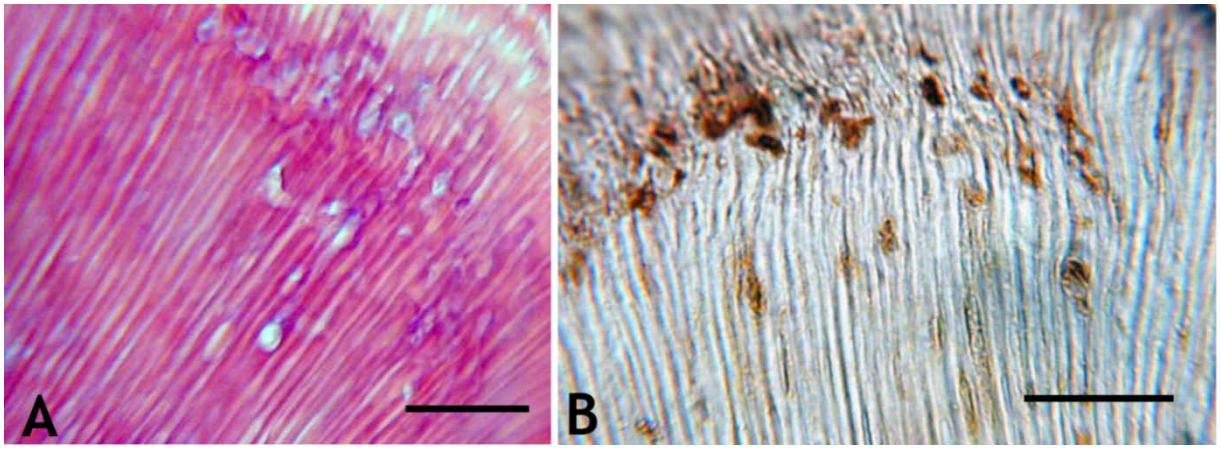

Figure 39: Coronal area of a first upper molar of a 21 days post natal Msx2 -/- mouse,. A: 7µm thickness, haematoxylin and eosin staining. B: Immunohistochemical analysis using anti-mouse DSP antibody. Counterstained with haematoxylin. Bar 70µm. DSP immunoreactivity is clearly visible for the embedded material in the dentine thickness.

3.3.4 BrdU IHC

BrdU was injected 12 hours before euthanasia of the animals and subsequently IHC was performed on 7µm sections to identify the cells undergoing cell division. An appreciable number of proliferating cells were visible in the interradicular bone area, however, no odontoblast cell division was noticed (Figure 40).

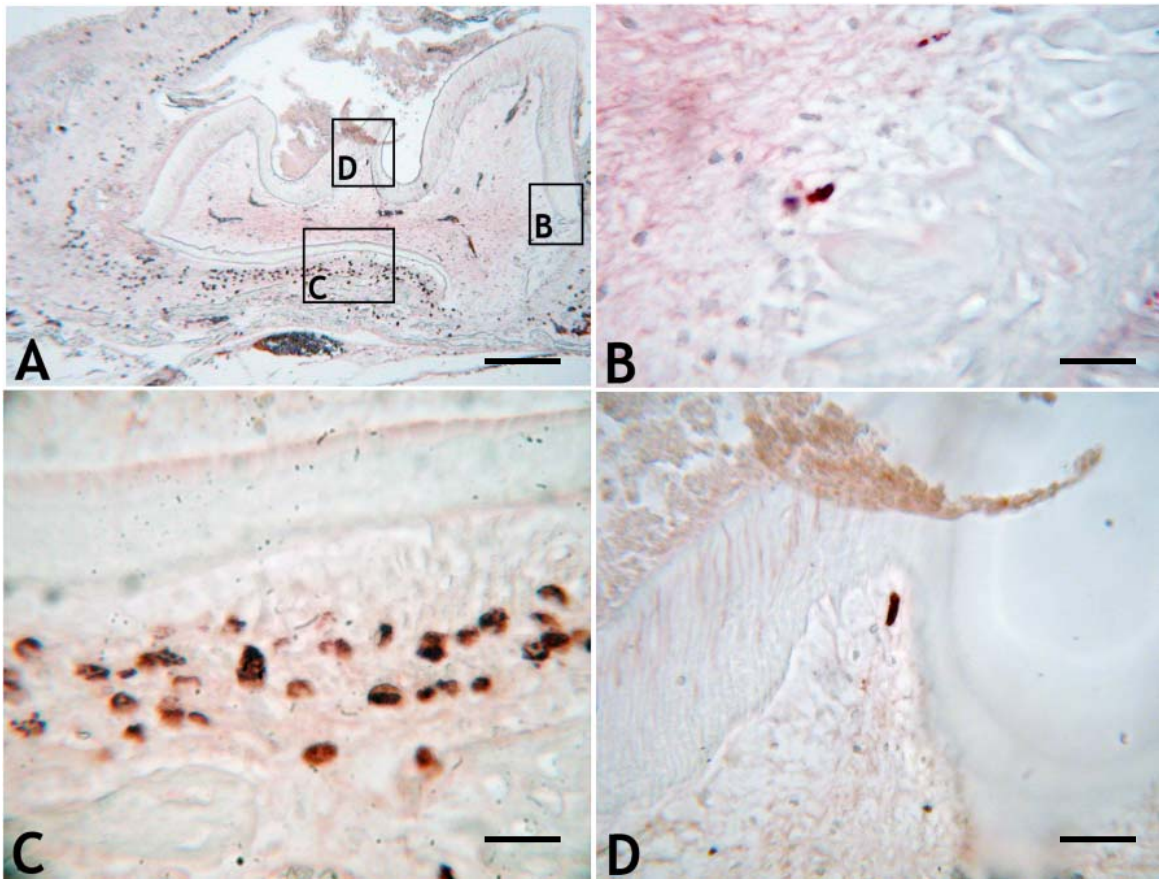

Figure 40: Immunohistochemical analysis using anti-mouse BrdU antibody on 14 days post natal Msx2 -/- animals, 12 hours after BrdU injection., no odontoblast cell division was noticeable. However, several cells mitoses were clearly highlighted in the bone area. A: Bar= 250µm, B,D: Bar= 100µm, C:Bar= 50µm.

3.3.5 *In Situ* Hybridization for Collagen I α1.

In situ hybridization was performed to evaluate cell activity and vitality. All of the odontoblasts (even those not polarised) in the teeth of -/- animals were stained for Collagen I α1 RNA confirming their secretory activity (Figure 41).

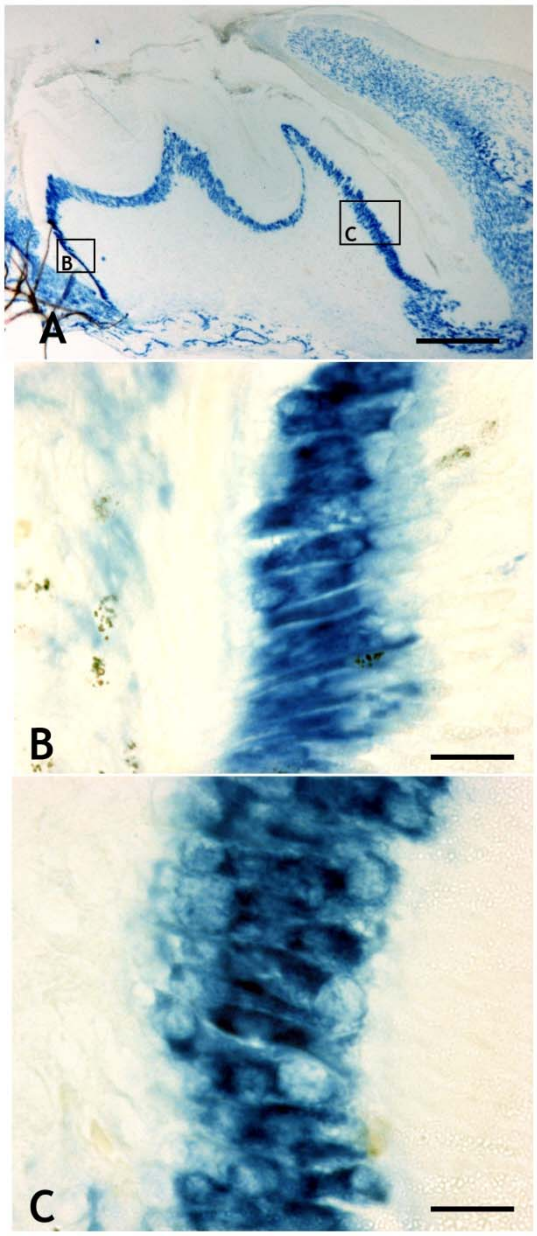

Figure 41: *In Situ* Hybridization of collagen Iα1 chain on first upper molar of a 14 days post natal Msx2 -/- mouse. Secretory activity of odontoblasts (even inverted polarity cells) was observed. A: bar=200μm, B: bar = 50μm C: bar= 20μm.

3.3.6 Quantitative RT-PCR (Q-RT-PCR)

Q-RT-PCR was initially undertaken on RNA of pulp mesenchyme extracted from +/+, +/- and -/- mice. Secondly, Q-RT-PCR were performed on MDPC-23 (immortalised mouse odontoblast-like cells) and OD21 (immortalised mouse pulp-like cells) before and after over-expression of MSX2 induced by lipofectamine transfection of CMV-Msx2 plasmid.

Data confirmed the absence of expression of MSX2 in the null mutant mesenchyme cells, and higher MSX2 expression after transfection in both cell types (Figure 42).

DSPP was up regulated in +/- mesenchyme. A minimal down regulation was evident when comparing +/- and -/-. These results confirmed recent data (Molla et al. submitted; personal communication). No significant regulation of DSP RNA levels was noticed after Msx2 over-expression in MDPC-23 cells and OD21 (Figure 43).

Osteocalcin was up-regulated in +/- and in -/- pulp mesenchyme compared to wild type. These results were in agreement with previous data (Molla et al. submitted). Interestingly, Osteocalcin seemed to be also over-expressed in cells after Msx2 over-expression. No significant change in regulation of gene expression was noticed after Msx2 over-expression in immortalized pup cells (Figure 44).

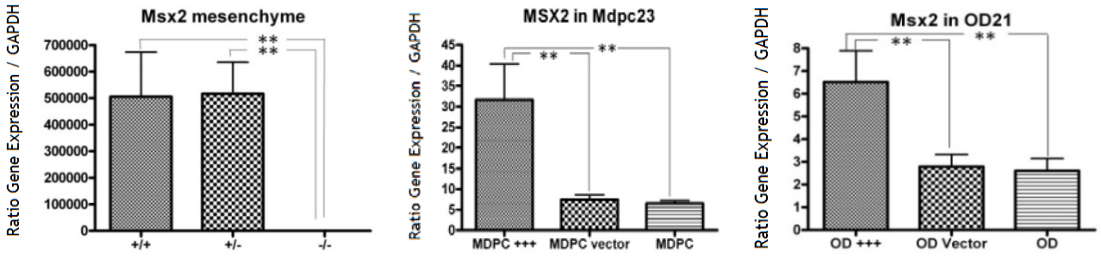

Figure 42: Quantitative RT-PCR analysis of Msx2 mRNA isolated from (A) incisor pulp mesenchymal cells of 3 months old Msx2 +/+, +/- and -/- mice, (B) MDPC23 cells (MDPC), MDPC 23 after transfection with Msx2 probe (+++) or lipofectamin® vector only (MDPC vector), (C) OD21 (OD) and OD21 after transfection with Msx2(OD+++) probe or lipofectamin® vector only (OD vector). Y axis units: ratio Msx2/GAPDH (: statistically significant (p<0,05)).**

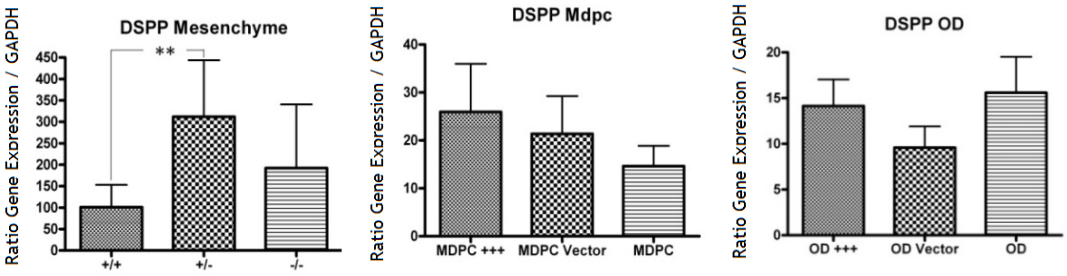

Figure 43: Quantitative RT-PCR analysis of DSPP mRNA isolated from (A) incisor pulp mesenchymal cells of 3 months old Msx2 +/+, +/- and -/- mice, (B) MDPC23 cells (MDPC), MDPC 23 after transfection with Msx2 probe (+++) or lipofectamin® vector only (MDPC vector), (C) OD21 (OD) and OD21 after transfection with Msx2(OD+++) probe or lipofectamin® vector only (OD vector). (: statistically significant) Y axis units: ratio DSPP/GAPDH (**: statistically significant (p<0,05)).**

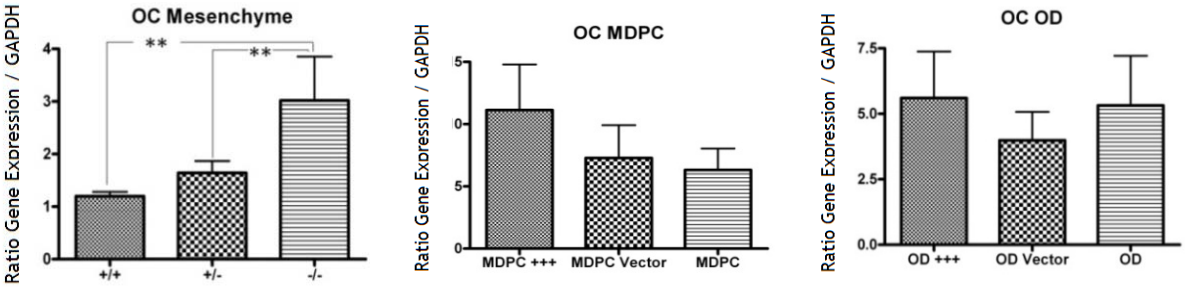

Figure 44: Quantitative RT-PCR analysis of Osteocalcin (OC) mRNA isolated from (A) incisor pulp mesenchymal cells of 3 months old Msx2 +/+, +/- and -/- mice, (B) MDPC23 cells (MDPC), MDPC 23 after transfection with Msx2 probe (+++) or lipofectamin® vector only (MDPC vector), (C) OD21 (OD) and OD21 after transfection with Msx2(OD+++) probe or lipofectamin® vector only (OD vector). Y axis units: ratio OC/GAPDH (: statistically significant (p<0,05)).**

3.4 Design and use of a new laboratory model for pulp repair:

3.4.1 Surgical procedure

Following the surgical procedure, one animal did not recover from the anaesthesia and died 4 hours after treatment. The eighteen surviving mice recovered within 6 to 10 hours, and were then housed individually, with food and water *ad libitum*. Paracetamol (0.06mg/g/day) was delivered in water for two days for analgesia.

3.4.2 Light microscopy observations:

All specimens were cut in a longitudinal plane with control of the positioning of specimens performed using the opposing first molar of the same maxilla as a landmark. Histological examination confirmed the successful completion of the procedure, the localisation of the cavity and the diameter of the pulp exposure at around 150μm.

In the majority of the treated teeth (16/18), the perforation of the pulp was located in the mesial half of the tooth in front of the mesial root canal. The cavity was generally centred on the buccal-palatal aspect. In the two other specimens (5 weeks post operative), the floor of the pulp chamber was perforated during the surgical procedure and these specimens were considered failures.

In the negative control in which no MTA was used for pulp capping, the histology of the pulp appeared normal, but neither a dentine bridge nor any signs of healing of the exposure were evident even 5 weeks after treatment. No histological signs of inflammation were observed in either of the control specimens (Figure 45).

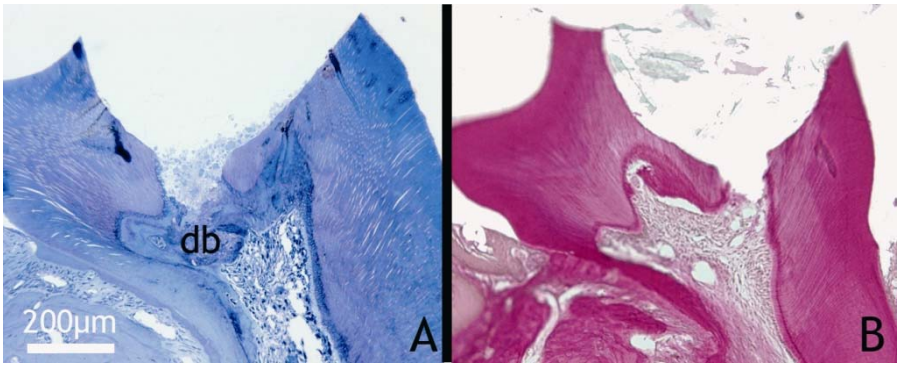

Figure 45: (A)_Histology of a mouse first upper molar capped with MTA, 11 weeks post operatively. 0.5µm thickness sections were stained with Methyl Blue/Azur II blue (50%:50%). The dentine bridge (db) was clearly visible, with inclusion of dentine chips. Dentine chips were probably impacted into the pulp tissue during pulp exposure. (B) Mouse first upper molar treated without MTA, 5weeks post operatively. No dentine bridge was visible. Histologically, the pulp tissue appears healthy with no inflammation evident. 7µm thickness cut sections stained with haematoxylin and eosin.

By two weeks post-operatively, a line with a high affinity for histological dyes was observed. This line precisely followed the contours of the capping material and this Junctional Extra-cellular Matrix (JEM) may represent an abrupt structural change in the extracellular matrix in contact with the capping material (Figure 46). This JEM appears as a structural reorganisation of the matrix in this area, and not a necrotic layer as described in many publications about pulp capping with calcium hydroxide. More investigations are needed to characterise this junctional area, which may reflect changes in cell secretory behaviour during dentine bridge formation at the material interface.

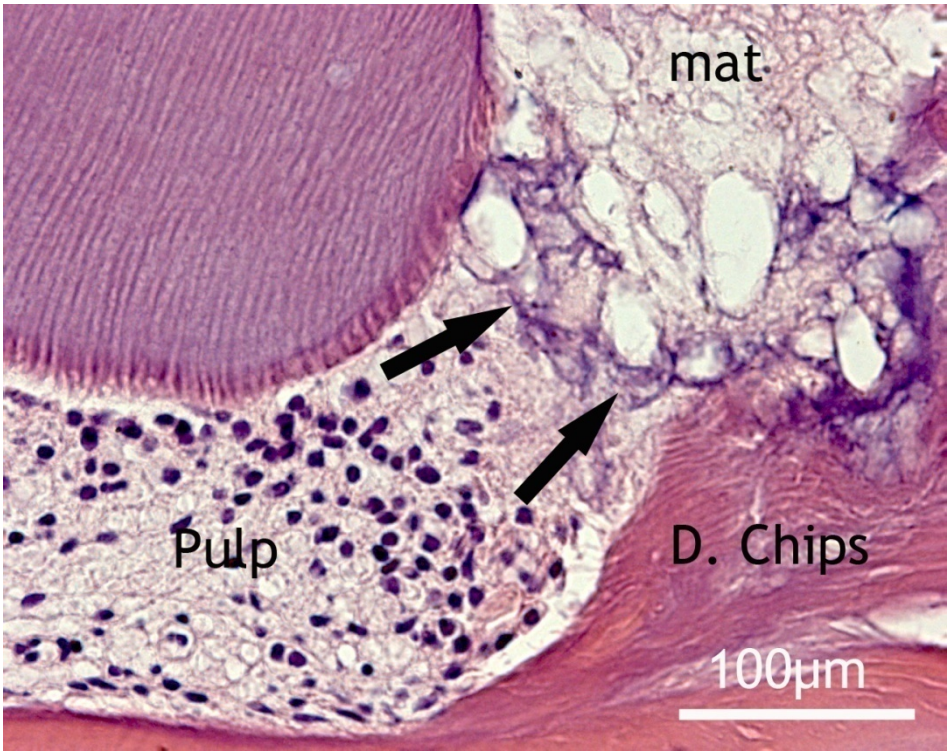

Figure 46: Histology at 2 weeks post-operatively. Haematoxylin and eosin (H&E) staining. The inflammation has already decreased, and few cells are present in contact with the material involved in tissue reorganisation. A specific line (→), with a high affinity for stain, demarcates the material and the pulp tissue. This line is in intimate contact with the material. At this stage no bacteria or inflammatory cells were visible.

At five weeks post operatively, a dentine bridge was visible in all of the experimental specimens. The dentine bridge was in close contact with the dentine walls and no gap was apparent between the two structures. The pulp cells were in close association with the new hard tissue, however, a polarised cell morphology was not apparent. In three specimens, dentinal tubules were visible in the matrix of the dentine bridge; these tubules were not linear and their course appeared interrupted (Figure 47 A).

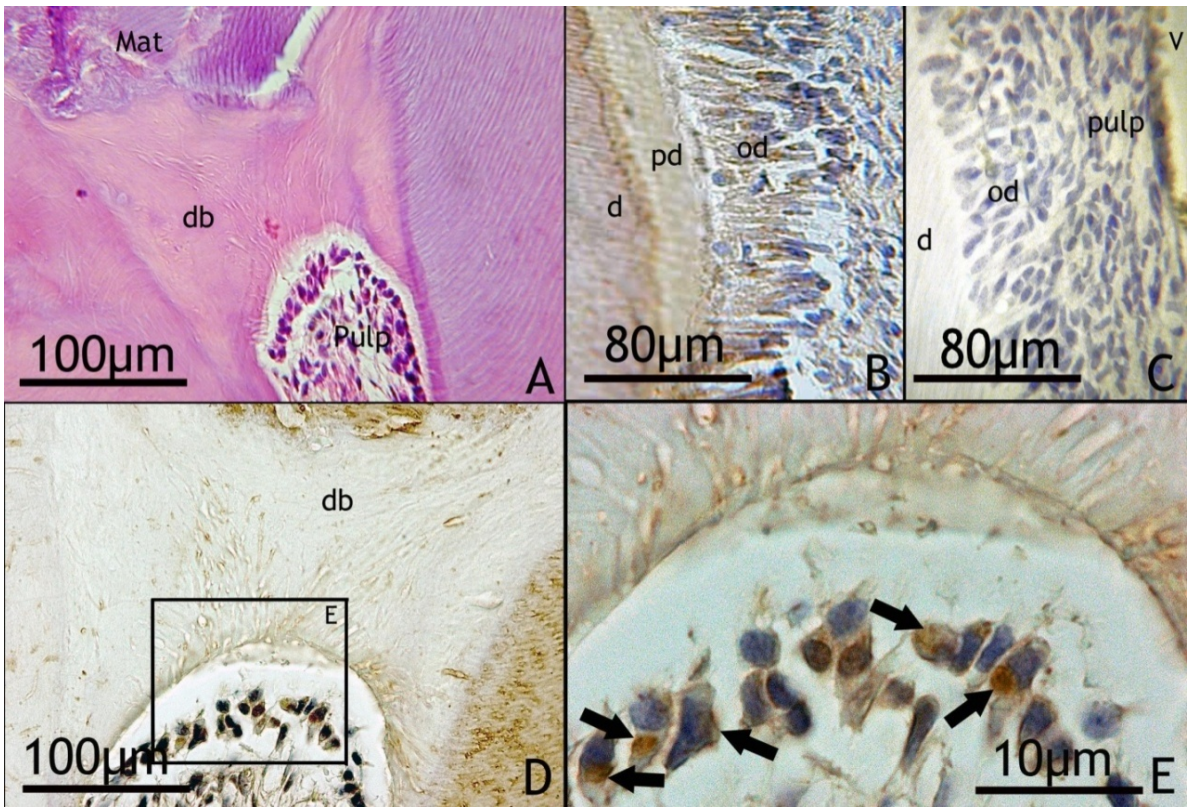

Figure 47: Mouse first upper molar, 5 weeks after pulp capping with MTA. (A) H&E staining. The dentine bridge (db) appears very clearly between material (mat) and the pulp; there is no visible gap between dentine bridge and dentine walls. In the thickness of the dentine bridge, a few tubules are evident; their course is not straight as in orthodentine (x 50). (B) Immunohistochemistry with the DSPP antibody of untreated mouse molar pulp (positive control). Staining of odontoblasts is evident, and DSPP is apparently also present in the extracellular matrix of the pulp (x50). (C) Negative control staining with omission of primary antibody (DSPP). (D) Immunohistochemistry with DSPP antibody of first upper molar tooth capped with MTA, 5 weeks post operatively (x50). Dentine bridge staining is very weak compared to orthodentine. (E) At higher magnification, DSPP expression is clearly visible in the cells in close contact with the dentine of the bridge (x100).

In most of the specimens, several dentine chips were included within the dentine bridge, but did not appear to adversely affect the healing process. The embedding of this debris has previously been described in the literature as being part of the healing process.

3.4.3 Immunohistochemical analysis

The immunoreactivity for Dentin SialoPhosphoprotein (DSPP) associated with the dentine bridge was clearly evident (Figure 47). Cytoplasmic staining of the formative

cells is also characteristic of dentine secreting odontoblast-like cells. Orthodentine was also stained as was the intratubular (peritubular) dentine. It was also noticeable that the dentine bridge was stained less intensely than the adjacent orthodentine. The negative controls demonstrated absence of staining.

3.4.4 Scanning Electron Microscopy (SEM) analysis

An inner view of the pulp chamber roof revealed the presence of the dentine bridge. Higher magnification observation showed an intimate contact between the dentine bridge and the dentinal wall of the tooth. The structure of the reparative dentine of the bridge had a globular morphology and appeared different from the tubular othodentine structure (Figure 48).

X-Ray spectrophotometeric analysis allowed comparison of phosphorus and calcium levels in different areas of the tooth (Figure 49). The calcium and phosphorus levels of both types of dentine (reparative and orthodentine) were analysed in the teeth and the Ca/P ratios of both tissues were similar confirming the calcification of the dentine constituting the bridge. The calcium levels were slightly lower for reparative dentine (62.52 % (Sample1) and 65.53 % (Sample 2)) than for orthodentine (73.64% (Sample 1) and 72.53% (Sample 2)), suggesting that the reparative dentine samples were less calcified than the orthodentine.

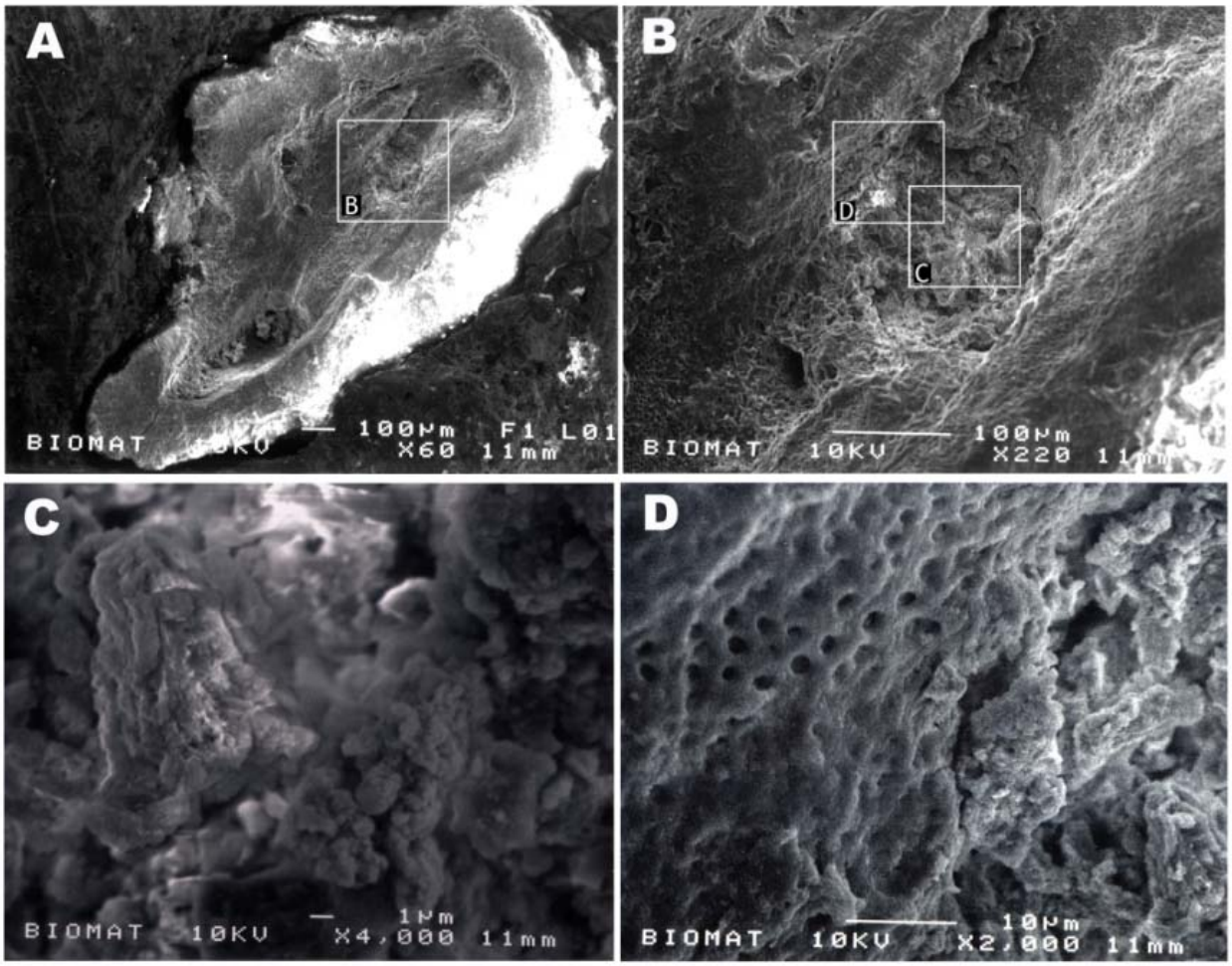

Figure 48: SEM observation of a mouse molar 5 weeks post operatively capped with MTA. Roots and pulp chamber floor were removed and the the pulp chamber roof was observed under different magnifications. (A) Magnification x60; dentine bridge appears clearly on the surface of the roof. (B) Observation of the dentine bridge at higher magnification (x200) (C) x4000 ultrastructure of the dentine bridge is different compared to orthodentine; it is more globular in appreance. (D) SEM observation at magnification x2000 of the limit between dentine wall and dentine bridge. No gap was visible.

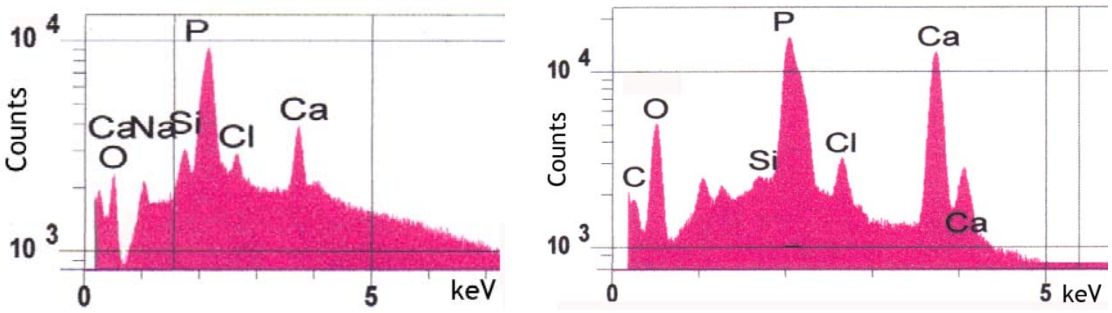

Figure 49: Results of X-ray spectrophotometeric analyses of orthodentine (left) and the reparative dentine of the dentine bridge (right).

4 Discussion

4.1 Regulation of odontoblast secretion and clinical implications.

Odontoblasts are actively secreting cells during primary dentinogenesis, but become largely quiescent during secondary dentinogenesis. Under physiological conditions, the reduction in size of the pulp chamber and canal size is gradual, and explains why teeth of elderly people show a diminution in the size of the root canal system compared to teeth from younger individuals. Under pathological conditions, odontoblasts can up-regulate their secretion again in response to an injurious challenge to secrete tertiary reactionary dentine at similar rates to primary dentine formation. This reactionary dentine is usually only secreted focally at sites of injury and therefore shows only limited distribution.

It is probable that the processes involved in pulp repair (reactionary and reparative dentinogenesis) recapitulate those of physiological dentinogenesis, although regulation of odontoblast secretory behaviour may differ in tertiary dentinogenesis (Tziafas, Smith et al. 2000; Smith and Lesot 2001).

Pulp exposure often occurs after trauma and as the pulp is generally free of inflammation, pulp capping in such situations represents a good approach for treatment. However, it is important to consider management of such cases in the context of the biological behaviour of the pulp, especially in immature teeth which are still developing.

Luxation has been reported to result in pulp necrosis for 8% of immature permanent teeth (Andreasen and Pedersen 1985), although reduction in canal size occurs commonly when pulp vitality is preserved (Andreasen, Zhijie et al. 1987). Pulp canal obliteration after trauma has been recognized for many years and seems to occur

more frequently in immature teeth after luxation or avulsion (Jacobsen and Kerekes 1977).

In one of our published case report (Simon, P.J et al. 2009) the pulp healing process was interesting due to the differential behaviour of two consecutive teeth (#21 and #11) where avulsion occurred in the former, but pulpal complications were more obvious in the latter and following pulp capping. The reduction in size of the root canal system in tooth #11 reflects dys-regulation in the control of odontoblast secretory activity, although it is not possible to identify the etiology or nature of this dysfunction.

Traditionally, after completion of root formation secondary dentinogenesis is regarded as proceeding at a much slower rate than primary dentinogenesis gradually reducing the size of the pulp chamber and root canal system over many years. In the cited clinical case, the radiographic appearance suggested that two years after treatment dentinogenesis appeared to have slowed down in the luxated tooth while in tooth #11, dentinogenesis was still actively taking place implying dys-regulation of the normal physiological control of odontoblast secretory activity in this tooth. We still have limited understanding of how odontoblast behaviour changes from primary, through secondary to tertiary reactionary dentinogenesis, although dentinal tubule continuity strongly indicate that the same cells are responsible for all three of these stages. Morphological evidence also provides the basis of our understanding of the down-regulation of odontoblast secretion during secondary dentinogenesis and its up-regulation again during reactionary tertiary dentinogenesis.

In the present work, our data suggest that there is a change in gene expression profile from primary to secondary dentinogenesis, and that this change may be reversible as odontoblast secretion is up-regulated during reactionary dentinogenesis. Clearly, an important goal was to characterise the transcriptional control of

odontoblast secretory behavior to understand what are the necessary cues for the down-regulation of the rate of dentine secretion during secondary dentinogenesis and its up-regulation during tertiary dentinogenesis.

In the described case, pulp capping of tooth #11 with MTA might be expected to have led to a focal deposition of tertiary dentine around the site of application while radiographically there appeared to be active secretion of circumpulpal dentine throughout the root canal. Without extraction of the tooth and subsequent analysis, it is not possible to determine if this represents lack of transition from primary to secondary dentinogenesis in the tooth following the original trauma and pulp capping or whether widespread tertiary dentinogenesis has been induced by the treatment. It is tempting to speculate that the physiological cues for down-regulation of odontoblast secretion normally leading to secondary dentinogenesis were absent or overridden in this tooth.

This case highlights why pulp capping is still a relatively controversial treatment in endodontics. Indication and prognosis are difficult to establish, and recommendations are often based on a rather limited scientific evidence base. Pulp capping is traditionally recommended on young teeth only, due to the greater reparative potential of younger pulp tissue, its better blood supply and cell density; retrospective studies, however, show clearly that age of the patient cannot be considered as a limiting factor (Haskell, Stanley et al. 1978; Barthel, Rosenkranz et al. 2000; Al-Hiyasat, Barrieshi-Nusair et al. 2006).

Based on these observations, it appeared interesting to investigate the molecular changes in odontoblasts at different stage of maturity to better understand the behaviour of this population of cells during physiological and pathological dentinogenesis. Microarray and RT-PCR gene expression analysis in two populations of bovine odontoblasts allowed us to highlight molecular changes during maturation of

these secretory cells. To complement these gene expression studies, we highlighted the involvement of the MAPK pathway by regulation of p38 protein secretion and regulation.

Based on these results and on the hypothesis that pulp healing could involve recapitulation of developmental processes, we secondly investigated regulation of the MAPK pathway in tertiary reactionary dentinogenesis using an *in vitro* model (stimulation of immortalised odontoblast-like cells with a preparation of isolated dentine matrix proteins).

Thirdly, we were interested in reparative tertiary dentinogenesis, and we designed a pulp healing model using the mouse. Such a model was anticipated to provide a starting point for using transgenic animals in the future to investigate gene regulation with approaches such as use of gene reporters, conditional mutant or null mutant animals.

Finally, we investigated the probable role of Msx2 transcription factor in the process of odontoblast differentiation or regulation of secretion. Working on null mutant and heterozygous animals, and based on previous observations already published in our laboratory, we investigated the phenotype of the first upper molar of Msx2 null mutant mice. The next stage of this work in the future would be to undertake pulp capping in null mutant or heterozygous animals to decipher the possible role of Msx2 in odontoblast differentiation and/or the role of this protein in regulation of cell behaviour during tertiary dentinogenesis.

The Msx2 transgenic model was used as a starting point for investigation of dentinogenesis. Others transgenic mice, such as the DMP1 null mutant, or p38 protein null mutant for example may provide further valuable models to increase our knowledge of pulp healing processes, and to facilitate development of new therapeutic strategies in endodontics, which include tissue engineering.

4.2 Molecular characterization of young vs mature odontoblasts

4.2.1 Transcriptome comparison of young and mature odontoblasts

Dentinogenesis is a continuous process of matrix deposition throughout the life of a tooth, albeit occurring at different rates. Odontoblasts, a monolayer of cells at the periphery of the pulp, firstly secrete the unmineralised dentine matrix (predentine) and then subsequently, are responsible for the mineralisation of this matrix (dentine). The presence of a permanent layer of predentine between the formative odontoblasts and mineralized dentine highlights the continuing activity of these cells. Three types of dentine are commonly described in the literature with the primary and secondary forms being physiologically secreted, whereas tertiary (reactionary or reparative) being synthesized in response to injury (Goldberg and Smith 2004).

However, so far there is no histological difference described between primary and secondary dentine except at the interface between both tissues which is generally delimited by a calciotraumatic line (Thewlis 1940); In this area, dentine has a lower affinity for Periodic Acid-Schiff staining (Symons 1961; Symons 1962). Because of the post-mitotic nature of the odontoblast, the two types of dentine are secreted by the same cells, albeit at different times and rates. Although, both types of dentinogenesis are reported to differ in their rate of matrix deposition (4µm/day for primary and approximately 0.4µm/day for secondary) (Schour and Poncher 1937; Ziskin, Applebaum et al. 1949), this may reflect modulation in secretory activity of the odontoblasts rather than irreversible phenotypic change. Odontoblasts are actively secreting during primary dentinogenesis, but become largely less active during secondary dentinogenesis. They can up-regulate their secretory activity again in response to an injurious challenge to secrete tertiary reactionary dentine at similar rates to primary dentine (Wennberg, Mjor et al. 1982). Thus, odontoblasts are the first target cells for external stimuli which include thermal variations, biomechanical

forces, molecular products derived from microorganisms and inflammatory cells during patho-physiological responses to the environment of the tooth including the carious process.

The interface between primary and secondary dentine remains controversial in the literature. To date the boundary between the two types of odontoblast behaviour has been based on anatomical landmarks. For some authors, the completion of root formation is the end point of primary dentinogenesis whereas for others, tooth eruption is the starting point of secondary secretion (Nanci 2003). So far, the absolute point of change in odontoblast activity reflecting the change from primary to secondary dentinogenesis is ill-defined. Without phenotypic landmarks, it is difficult to delineate the temporo-spatial pattern of the two types of dentinogenesis which may occur concomitantly in the same tooth, depending on its stage of development.

In addition, understanding cell behaviour in dentine formation is critical to our future development of new regenerative therapies for teeth. During tooth repair and tertiary dentinogenesis, the healing process may recapitulate developmental events (Smith and Lesot 2001). In this situation, odontoblasts are "re-activated" to restore a greater rate of secretion of dentine (reactionary); they may also die and then pulpal progenitors can differentiate into odontoblast-like cells (reparative). It is therefore important to understand the cellular and molecular changes which occur in odontoblasts at different stages of their life-cycle to facilitate clinical exploitation of the reactivation of quiescent odontoblasts for dentine repair and exploit pharmacological tools to manage and control this healing process.

The identification of the odontoblast phenotype has received much attention over the years, and has established at the molecular level, the different roles played by odontoblasts in dentine formation (Butler 1995; Linde 1995), their cell-cell communications (He, Niu et al. 2004), mechano-transduction mechanisms (He, Niu et

al. 2004; Magloire, Couble et al. 2008) and their role in innate immunity (Staquet, Durand et al. 2008). We therefore hypothesize that the changes in secretory activity of odontoblasts throughout their life cycle reflect differential transcriptional control and that regulatory processes involved in bone homeostasis may also occur in regulation of dentine secretion. The expression profiles of several genes (DSPP, DMP1, Collagen I) were used as well established markers of odontoblasts and their expression levels may reflect the cell secretory behaviour. So far, comparison of the gene profile of the odontoblast at different stages of its life cycle has not been well characterized. Based on the hypothesis that differential dentine secretion is associated with changes in transcriptional activity within the cell, we have investigated the transcriptomes of odontoblasts involved in primary and secondary dentinogenesis and subsequently used this information to identify key regulatory intracellular pathways involved in this process.

The differential gene expression that we observed in primary and secondary dentinogenesis highlights modifications in transcriptional control of the odontoblasts and the need to identify the nature of the underlying regulatory mechanisms, both to characterize cell phenotype and to better understand how cell secretory behaviour can be regulated during tertiary dentinogenesis for therapeutic purposes. Such a strategy has been applied to studies of bone cell lineage and has contributed to discrimination of the respective functions of osteoblasts and mature osteocytes.

The relatively high number of genes differentially regulated between both populations of odontoblasts was an unexpected observation and therefore confirmation by RT-PCR of selected genes using experimental replicates was applied. Initially, DMP1 expression was demonstrated as this gene is commonly used as a phenotypic marker of odontoblasts differentiation (Butler 1995; Unterbrink, O'Sullivan et al. 2002). Notably, DMP1's role in dentinogenesis has received considerable attention, and it has been implicated in regulation of DSPP expression regulation

during dentinogenesis (Ye, MacDougall et al. 2004). Our analysis supported DMP1 as being a marker of maturity of odontoblasts, results which were also confirmed by immunohistochemistry on bovine teeth.

The presently studied stages of odontoblasts potentially parallel the situation in bone where the osteoblast is the active-forming cell, while the osteocyte does not deposit bone. Both are secretory and mineralizing cells, and increasingly, it is difficult to characterise distinct or differential profiles of matrix components for either tissue. Differential expression of the same components in these two tissues implies their similarity rather than an absolute difference in composition. Such differences are also apparent between different skeletal sites, such as flat and long bones (Watahiki, Yamaguchi et al. 2008). A functional analogy between the odontoblast and osteoblast-life cycles has been recently highlighted by authors who interestingly, proposed a new nomenclature for odontoblasts sub-dividing them into three populations of pre-odontoblasts, odontoblasts and odontocytes (Kim and Simmer 2007; Larmas 2008).

In bone, preosteoblasts are differentiating cells. Osteoblasts secrete bone matrix and some of them subsequently become embedded in the mineralised matrix (Opperman 2000). These osteocytes, are morphologically different, being much less active in matrix deposition and are characteristically dendritic cells. Despite much focus on the osteoblast, the osteocyte derived from it has received less interest until recently (Kubota, Wakabayashi et al. 2003; Stains and Civitelli 2003; Bonewald 2004; Cho, Lee et al. 2006). Osteocytes differ from osteoblasts in their respective functions and regulatory mechanisms, notably those related by the SOST gene and Wnt pathway for recruitment of osteoblast progenitors. A central role of osteocytes is to regulate bone mass by the transduction of biomechanical loading into molecular signals controlling osteoblast and osteoclast number (Bonewald 1999; Bonewald 2002; Bonewald 2004). Although parallels can be drawn between bone and dentine, there are several

differences. Bone cells are continuously renewed by reiterative cycles of proliferation and differentiation on bone surfaces while odontoblasts are post-mitotic cells. During physiological dentinogenesis, the odontoblast secretes dentine matrix and the cell moves pulpally leaving its process embedded in the matrix. The odontoblast cell body is never entrapped in its matrix, unlike osteocytes, except occasionally in the pathological situation of "osteodentine". Finally, bone resorption is a physiological process under the control of osteoblast and osteocyte signals, while dentine resorption occurs in specific physio-pathological situations, such as root resorption and internal resorption. The present transcriptome data may provide a framework to underpin the analogy between, on the one hand, young odontoblasts and osteoblasts and, on the other hand, osteocytes and mature odontoblasts. Interestingly, DMP-1 is also a constitutive bone matrix protein and is differentially expressed in pre-osteoblasts and mature osteoblasts (increased by 36.8 in mature cells) (Cho, Lee et al. 2006). In odontoblasts, expression was up-regulated by 3.21 fold in late stage cells. This protein therefore appeared to be a marker of maturity in both cell types.

Similar observations were also made for Bone Sialoprotein, which was increased by 24.3 fold in mature bone cells (Cho, Lee et al. 2006), while by 800 fold in odontoblasts, Osteopontin (8.6 fold increase in bone (Gravallese 2003; Morinobu, Ishijima et al. 2003)), 4616 fold in odontoblasts and Osteocalcin (8.0 fold in bone cells (Ducy, Desbois et al. 1996; Eghbali-Fatourechi, Lamsam et al. 2005), 715 fold in odontoblasts). Osteocalcin has previously been reported to be selectively localised in peritubular dentine produced by odontoblasts during secondary dentinogenesis (Papagerakis, Berdal et al. 2002). It appears that several markers of osteocytes are also up-regulated in mature odontoblasts compared to relatively younger cells.

Nevertheless, not all the markers appear to be differentially regulated in the same way in bone and dentine forming cells. SOST gene (coding for Sclerostin protein) is one example of differential gene expression between these cells. In bone, Sclerostin

is the product of the SOST gene and is expressed predominantly by osteocytes (Winkler, Sutherland et al. 2003; van Bezooijen, Roelen et al. 2004; Bellido, Ali et al. 2005). Sclerostin stimulates the recruitment of osteoblast progenitors via the Wnt pathway and mutations in humans result in high bone mass disorders, such as Van Buchem's disease (Balemans, Ebeling et al. 2001). In odontoblasts, the differential expression of the SOST gene appears to be the inverse to that in bone. SOST gene was highly expressed in young cells whilst it was strongly down-regulated in more mature cells (differential expression by 465 fold). This inverse SOST bone-dentine relationship may parallel divergence in odontoblast/osteoblast recruitment in a physiological context. Throughout growth and homeostasis, bone formation results from a continuous differentiation of new osteoblasts on the bone surface. In contrast, the odontoblast layer is composed of post-mitotic cells which contribute to the continuing deposition of dentine, without emergence of newly differentiated cells in a physiological context. In conclusion we have shown here that, as in bone cells, the transcriptome of odontoblasts evolves with the stage and the maturity of the cells. The temporal expression of all of these genes may correlate with a change in secretory activity of odontoblasts as their functional status changes (Lu, Xie et al. 2007), as previously suggested by Larmas (Larmas 2008). In bone, osteocalcin and osteopontin are two well characterized markers of fully differentiated and mature osteoblasts and osteocytes (Park, Shin et al. 2001). We found the same differential expression between mature and young odontoblasts. It is interesting to compare the young odontoblast (primary dentinogenesis) to the osteoblast and the mature odontoblast (secondary dentinogenesis) to the osteocyte which may support the nomenclature for these cells as being pre-odontoblasts, odontoblasts and odontocytes (Larmas 2008).

By comparison of the published data on dentine secretion rates (Schour and Poncher 1937; Hoffman and Schour 1940) and the gene expression patterns presented here,

we can conclude that the functional status of the odontoblast evolves, and the less active deposition by the cell during secondary dentinogenesis is associated with important changes in its transcriptome. It should be noted, however, that the markers of osteocytes were not systematically regulated in the same way in odontoblasts. We still need to be cautious in suggesting new nomenclature for these cells and not to confuse the concept of two populations of cells with a continuum of changes in the transciptome, which appear to be associated with the secretory status of the cell and may have functional consequences. In future studies, it would be interesting to compare the gene expression patterns reported here with those of odontoblasts or odontoblast-like cells taking part in tertiary dentinogenesis where secretory activity becomes up-regulated again (Wennberg, Mjor et al. 1982; Smith and Lesot 2001). However, such studies may be complex in view of the diversity of cellular responses during tertiary dentinogenesis (Smith, Cassidy et al. 1995; Smith, Lumley et al. 2008).

Histological similarities between odontoblasts and bone cells are also apparent. Osteocytes communicate with other osteocytes and the bone surface via cytoplasmic processes that cross through the mineralised bone (Marotti 1996; Tatsumi, Ishii et al. 2007). The presence of the processes in the canaliculi is clearly similar to the situation with the odontoblast, even though the odontoblast has only one main process with many lateral ramifications. The three dimensional structures of canalicular/tubular systems in odontoblasts and osteocytes are similar with a striking similarity between the morphological distribution of canaliculi/tubules in dentine and bone (Lu, Xie et al. 2007). Osteocytes and osteoblasts have been described as functional mechano-receptors, responsible for capturing information on the bone surface and controlling bone balance by transmitting the information to other osteoblasts and osteoclasts (Tatsumi, Ishii et al. 2007). The odontoblast has also been described as a receptor cell, and might assume *per se* both the transduction and

responses to mechanical stimuli by increasing dentine production and mineralisation. Although its potential role as a mechano-receptor is reported (Dhopatkar, Sloan et al. 2005), the further molecular elucidation of its related mechano-transduction pathways could help to highlight its potential roles in pathological conditions such as internal dentinal resorption. If further similarities between odontoblasts and bone cells are identified, there is the possibility that the available data on bone research could be translated to new applications for dentine-pulp complex repair.

Finally, the concept that primary dentine secretion occurs before tooth eruption whilst secondary dentine secretion occurs following eruption, may need revision based on our observations. Notably DMP1 immunohistochemistry indicated that during development, odontoblasts undergoing secondary dentinogenesis (in the cusp area) and odontoblasts secreting primary dentine (in the apical area) may coexist in the same tooth. Morphological appearance or anatomical localisation appear insufficient criteria to define the functional status of an odontoblast in regard to primary or secondary dentinogenesis.

In bone, following injury, progenitor cells need to be recruited to differentiate into osteoblasts for bone repair. In contrast to the odontoblast, the osteocyte is unable to reverse its maturation state and change its status from a quiescent to an actively secreting cell. One of the unique features of the odontoblast is that it may be re-activated after injury and secrete reactionary dentine at similar rates to primary dentine. As similarities have been described between development and the healing process (Tziafas, Smith et al. 2000; Smith and Lesot 2001), we sought to investigate the variation in protein secretory processes concomitant with the switch from early stage to late stage odontoblasts to examine whether key pathways could be identified, which might be targets for the switch from secondary to tertiary dentinogenesis. The MAPK/ERK pathway is a signal transduction pathway that couples intracellular responses to the binding of growth factors to cell surface receptors. This

pathway is complex and includes many signalling mediators. It is also well established that the MAPK signalling pathway is involved in cellular differentiation. Microarray data identified 6 genes (PTPRR, NTRK2, MAP2K6, CD14, MAPK13 (p38) and FGF1) involved in the p38 pathway as being differentially regulated.

Notably, the role of TGF-β1 is well established in odontoblast differentiation during primary development and in tertiary dentinogenesis (D'Souza, Flanders et al. 1992; D'Souza, Cavender et al. 1998; Smith and Lesot 2001; Unterbrink, O'Sullivan et al. 2002) and significantly, recent publications indicate that TGF-β1 may regulate the MAPK pathway (Ning, Song et al. 2002; Zhao, Chen et al. 2004). The role of the MAPK pathway therefore warrants further investigation to try to better understand its role during the odontoblast maturation process and its possible involvement in the reactivation of odontoblast secretory activity during tertiary dentinogenesis. Characterization of such key pathways involved in odontoblast secretion may provide exciting targets for development of novel regenerative therapies. Finally, the growing body of information suggesting similarities between pulp cells and bone cells may help us to better understand the physiology and pathology of the mineralised tissues of the body and allow greater comparison of data derived from bone and dental studies.

4.2.2 Dentinogenesis definitions and the choice of our research model:

An important outcome of this research has been re-evaluation of the limited evidence supporting the concept of the definitions for primary and secondary dentinogenesis. Initially, we tried to use the terms primary and secondary dentinogenesis widely to allow the reader to appreciate the context of the data we report. Finally, we have tried to refer more to early and late stage odontoblasts to

perhaps emphasise the paucity of reliable markers to distinguish the interface between what have become known as primary and secondary dentines in the literature. The presence of a calciotraumatic line may be more characteristic of human teeth than other species and even in the human, demarcation of this line can be quite subtle in some teeth. It is also important not to confuse this with the calciotraumatic line seen at the interface with reactionary tertiary dentine, which is sometimes confused with "secondary" dentine at sites, such as beneath worn incisal edges and occlusal surfaces. The "marriage" of traditional anatomical and histological knowledge with data derived from newer molecular technologies is sometimes not easy, but there is no doubt that we are moving into exciting times as we deepen our understanding of cell behaviour in the hard tissues and the functional significance of this knowledge.

Indeed, the distinction between primary and secondary dentinogenesis was a starting point of our work and led us to re-evaluate the present established doctrine on the differences between primary and secondary dentinogenesis. Analysis of the published literature showed very limited data to support the definitions that have now become established in the textbooks. Much of the information is morphological in nature, eg, rate of dentine matrix secretion (based on thickness of dentine laid down in a certain period of time) suggesting secondary is slower than primary dentinogenesis (Smith 2002a); continuity of dentinal tubules suggesting that the same cells are responsible for primary and secondary dentinogenesis. There appears to be a lack of data in the literature to underpin a robust definition of primary and secondary dentinogenesis, which may explain why some regard the change between the two as when the tooth erupts in the mouth and others define it as the completion of apexogenesis. The presence of a calciotraumatic line may not always provide a reliable marker to distinguish the two populations of odontoblasts in primary and secondary dentinogenesis, because such lines can be seen wherever there is disruption of

odontoblast physiological behaviour, e.g., neonatal line, at times of systemic disease, at the initiation of reactionary dentinogenesis etc.

While a calciotraumatic line can be detected in the crown of the bovine tooth, its position represents a much earlier stage than might be anticipated for any primary/secondary dentine interface. We can only speculate about the cause of this line, but suspect it may represent an event such as weaning/lactation or other physio/patho-logical event. No such line was evident in the bovine incisor from a later stage perhaps emphasising a possible weaker relationship between the presence of such a line and a change in odontoblast secretory activity (i.e., as defined as primary and secondary dentinogenesis) in bovine teeth. Our experience generally with various bovine teeth is that although a gradual reduction in size of the pulp chamber with age is observed (equates to what has been termed secondary dentinogenesis), calciotraumatic lines are very variable features of these teeth and probably are not a reliable marker of the interface between primary and secondary dentines.

Perhaps clearer evidence of altered secretory behaviour in the odontoblast with age is demonstrated by the ultrastructural changes reported in odontoblasts (Takuma and Nagai 1971; Couve 1986), which suggest a life cycle for these cells with secretory, transitional and aged stages although these stages have not been aligned to the presence of any calciotraumatic lines.

Based on our observation, we feel that the presence of a calciotraumatic line is not necessarily strongly associated with a change in secretory activity of odontoblasts following crown and root formation, i.e., what has been defined as the interface between primary and secondary dentines.

In the present studies only crowns of the teeth were used for cell isolation. Most authors appear to consider that primary dentinogenesis stops when the tooth erupts, whereas others define this limit as the time of completion of apexogenesis. Based on this observation, we selected our tooth samples from two opposite points: erupted teeth with fully formed roots as a model for what has been termed secondary dentinogenesis, and a very early stage of development of the tooth (unerupted, no root formation, but calcified tissue formation in progress in the crown to ensure that differentiated and secreting odontoblasts were present. We sourced bovine teeth from 30 month old animals because both types of teeth are present in the same animal thereby minimising inter-species differences.

4.2.3 DMP1 as a marker of odontoblast maturity

In attempting to identify molecular markers to help to make a clear distinction between primary and secondary odontoblasts, we had the choice between several proteins for which the corresponding mRNAs were appreciably changed. Among those, BSP gene expression was increased by 714 fold and OPN by 968 fold in late stage cells. Nevertheless, we focussed on DMP1 which was only 3 fold increased and on DSP.

There were two major reasons why we consider DMP1 to be a more reliable marker of cell maturity. Firstly, DMP-1 is one of the rare markers of mature odontoblasts that has already been identified (Larmas 2008), while neither OPN nor BSP have been previously highlighted in this context.

DMP-1 immunohistochemistry on bovine molars was performed initially to investigate the expression of this gene in the crown tissues of unerupted teeth. Because the molar was unerupted and only crown formation was taking place, it is assumed that the cells were only involved in what is traditionally regarded as primary

dentinogenesis. By performing immunohistochemistry on these tissues, we expected a basal expression of the protein, and not the observed gradient along the cells of the crown. Because of this unexpected result, we were concerned by the definitions of primary and secondary dentinogenesis and their putative markers.

Secondly, the microarray data utilises fluorescence intensities of the probes in its expression level calculations. From the absolute data (fluorescence of the probe) for each sample (ES and LS), we calculated the relative data, based on the ratios between ES cell and LS cell values.

- DMP 1: *ES value* : 5722 *LS value*: 18371 *Ratio:* 3.21 (*Absolute value of variation:* 12649)
- IBSP (BSP): *ES value* 11.05 *LS value*: 7900 *Ratio*: 714 (*Absolute value of variation*: 7889)
- SPP1 (OPN) : *ES value*: 4.77 *LS Value:* 4621 *Ratio*: 968.80 (*Absolute value of variation*: 4616)

Based on these observations, DMP1 expression showed the greatest absolute change between young and mature cells and exhibited the highest basal level of expression. However, our data also indicated that BSP and OPN were appropriate markers of mature cells, because their expression was relatively low in young odontoblasts. The greater differential expression for DMP-1 may also be anticipated to be reflected in protein expression and hence DMP-1 was the favoured target for immunohistochemistry. Thus, for these two reasons it appeared to us that it was more appropriate at this stage to use DMP1 as it may be a more robust marker for mature cells and certainly highlights the need to reconsider our concepts of primary and secondary dentinogenesis.

4.3 Phospho-p38 regulation and odontoblast stimulation

Reactionary dentinogenesis is the secretion of a tertiary dentine matrix by surviving odontoblasts in response to an appropriate stimulus (Smith, Cassidy et al. 1995). The dentine matrix is permeable by virtue of its tubular structure and therefore following injury to the tooth and/or subsequent restorative procedures, this may allow molecules to diffuse and contact the pulp. Such substances may include bacteria, toxins and/or dentine matrix proteins (DMPs). Because the pulp is enclosed by a rigid, mineralised tissue shell, dentine matrix degradation by acid bacterial products begins before the disease process reaches the pulp. Notably, growth factors derived from the dentine have been shown to reach and stimulate the odontoblast layer, inducing new dentine secretion in those areas of the dentine-pulp complex that are in direct tubular connection with the traumatic agent (Mjor 1983).

It has been suggested that, during tooth repair and tertiary reactionary dentinogenesis, the healing process recapitulates developmental events (Smith and Lesot 2001). TGF-β1 has been shown to play an important role in tooth development (Cam, Lesot et al. 1997; Lesot, Lisi et al. 2001), particularly in odontoblast differentiation (Begue-Kirn, Smith et al. 1992; Begue-Kirn, Smith et al. 1994). TGF-β1 is also sequestrated within the dentine matrix (Cassidy, Fahey et al. 1997), and may be released during carious disease or by restorative agents commonly used in dentistry that dissolve mineralised components, such as ethylene diamine tetra-acetic acid (EDTA), calcium hydroxide (Graham, Cooper et al. 2006) or mineral trioxide aggregate (Tomson, Grover et al. 2007). Notably, TGF-β1 has also been demonstrated *in vivo* and *in vitro* to stimulate odontoblast mineralisation (Smith, Tobias et al. 1994; Sloan and Smith 1999; Duque, Hebling et al. 2006).

It would be clinically valuable to be able to activate quiescent odontoblasts for dentine repair and thus, it is important to understand the regulatory control of

cellular and molecular signalling in these cells. However, only limited information currently exists on these molecular events which occur during reactionary dentinogenesis. In a previous study, we provided evidence that changes in the secretory activity of odontoblasts reflect differential transcriptional control and that, therefore, the transcriptome of the odontoblast evolves as the cell matures (Simon, Smith et al. 2009). Among the dataset of genes whose expression changed during odontoblast maturation, we identified the *p38* transcript to be abundantly expressed in odontoblasts during primary dentinogenesis whilst being significantly down-regulated in secondary dentinogenesis. Based on these observations, we hypothesized that p38 signalling might be involved in regulating odontoblast activity, and the present study aimed to determine whether the p38 protein is up-regulated and phophorylated upon odontoblast stimulation.

The MAPK/ERK pathway is a signal transduction pathway that couples intracellular responses to the binding of growth factors to cell surface receptors and has been implicated in odontoblast differentiation (Wang, Hu et al. 2006). The role of TGF-β1 in odontoblast differentiation during primary development and in tertiary dentinogenesis is well established (D'Souza, Flanders et al. 1992; D'Souza, Cavender et al. 1998; Smith and Lesot 2001; Unterbrink, O'Sullivan et al. 2002; Baker, Sugars et al. 2009) with several recent publications indicating that TGF-β1 regulates the MAPK pathway (Ning, Song et al. 2002; Zhao, Chen et al. 2004). As similarities have been described between primary development and the healing process (Tziafas, Smith et al. 2000; Smith and Lesot 2001), we wished to investigate the role of the MAPK pathway in these processes and to determine whether odontoblasts might be stimulated in a model of reactivation of dentine secretion during reactionary dentinogenesis.

Stimulation of odontoblast-like cells with several growth factors, as an *in vitro* model of tertiary dentinogenesis, or with *Streptococcus mutans*, as an *in vitro* model of

caries, caused an increase in p38 phosphorylation and its nuclear translocation. This enhancement of translocation is significant, as apart from the HSP27 pathway, most components of the p-38 MAPKinase pathway reside in the nucleus, where p38 acts as a transcription factor.

TNF-α, ADM, and TGF-β1 showed similar patterns of p38 activation, whereas isolated dentine matrix proteins appeared to induce a different pattern of p38 activation. The cocktail of growth factors in the preparation of isolated dentine matrix proteins appeared to have a weaker, but a more enduring effect on cells than did the growth factors or bacterial stimulants alone. The effect of these dentine matrix proteins on p38 protein persisted past the point where the effect of growth factors alone had culminated. It is likely that this response profile better mirrors the events occurring in carious disease, in which dentine matrix components are released in combination. In view of the fact that tissue regeneration is a balance between inflammation and repair, the comparatively weaker effect of dentine matrix proteins may serve the biological role of protecting the dental pulp by preventing pulpal inflammation.

Bacterial contamination of the pulp is usually described as the most important factor in pulp disease. In our experiments, when cells were stimulated with *Streptococcus mutans*, only half of the activated protein was translocated. Based on this observation, we hypothesize that bacteria might stimulate the cytoplasmic pathway better, whereas growth factors might directly induce transcription. It should be noted that bacteria alone were not able to induce odontoblast activation, but that they exhibit a synergistic effect when combined with growth factors. It is thus critical, when evaluating the healing and toxic effects of various agents, that they be tested both alone and in combination. Further study is needed to determine the effect of a range of concentrations of dentine matrix proteins and other agents, to allow the development of a more accurate and reliable *in vitro* model of the carious disease process.

Notably, our results are in agreement with the differential phospho-p38 expression that has been observed during tertiary dentinogenesis. As has been suggested by several authors, this finding may indicate that the behaviour of odontoblasts during tertiary dentinogenesis recapitulates the development of the primary cells (Tziafas, Smith et al. 2000; Smith and Lesot 2001). Understanding cellular behaviour in response to carious disease may allow the development of new approaches in regenerative dentistry that utilize biological and pharmacological control of cell behaviour, much as p38 phosphorylation is currently exploited as a target of anti-inflammatory drugs. Better understanding of the regulation of the p38 pathway during tertiary dentinogenesis might also allow the development of new therapies, in particular for novel pharmaceuticals which facilitate bonding systems to better control the healing process and enhance the secretory activity of odontoblasts.

4.4 The mouse as an experimental model for pulp capping.

Several species of animal have been used for pulp-capping studies including the monkey (Pitt Ford, Torabinejad et al. 1996), dog (Tziafas, Kolokuris et al. 1992) ferret (Smith, Tobias et al. 1994), and rat (Decup, Six et al. 2000). The monkey and dog are large animals, and are therefore expensive, requiring special care facilities. Moreover, the rules concerning animal experimentation increasingly present difficulties for this kind of work, especially using non-human primate species. For these reasons, the numbers of animals studied is often restricted, potentially influencing the experimental outcomes, reproducibility and subsequent interpretation of data.

A pulp-capping protocol has been described in the rat model, using the mesial face of the first maxillary molar, after gingivectomy (Decup, Six et al. 2000) or on the occlusal face (Lovschall, Tummers et al. 2005). The molar of the rodent is particularly interesting, because it presents morphological similarities with its human

counterpart: it has three roots, three cusps and thus shows analogous conditions of vascularisation and innervation. While the rat offers a number of advantages as an experimental model, the availability of genetically-altered models for this species is more restricted than for the mouse.

Validation of the mouse as an experimental model now opens the way for use of transgenic studies in reparative dentinogenesis; such a model should enable more precise definition of the cellular and molecular mechanisms involved in the process of dentine-pulp repair. Potentially, animals with a modified genome (with reporter gene or gene deletion) could thus be used to:

- characterise the phenotype of the replacement odontoblast-like cells and determine their origin through cell lineage-studies in transgenic mutated mice (Chai, Jiang et al. 2000) ;

- decipher the cell differentiation process at the molecular level by using transgenic null mutant mice for potentially determinant factors (e.g. DSPP null mutant mice (Sreenath, Thyagarajan et al. 2003) Msx2 null mutant mice (Aioub, Lezot et al. 2007) to better understand the process of differentiation; and

- evaluate effects of novel bioactive molecules.

It is with this new knowledge and an understanding of these processes that new therapeutic strategies can be developed to promote pulp vitality and healing. Within the constraints of the regulations of animal experimentation, this model will also facilitate use of adequate numbers of sample for robust data collection.

A limitation of the model presented is that it currently uses healthy teeth, whilst in the clinical situation pulp inflammation is generally present. However, future experiments could simulate caries-like situations by incorporating bacterial infection models using whole live bacteria or bacterial components. In addition, the presence of dentinal chips or debris arising from the creation of a pulp exposure may

contribute to reparative responses in the pulp. Although this may complicate data interpretation, it does reflect the clinical situation where dentine fragments (Tziafas, Kolokuris et al. 1992) and dissolution products (Smith 2002b) contribute to overall pulpal responses. Reproducibility of the pulp-capping procedure was regarded as an important element in the viability of the model especially in view of the small size of the mouse tooth. The histological observations confirmed the reproducibility of our surgical procedure.

Contrary to many of the studies reported with calcium hydroxide (Schroder and Granath 1972; Horsted, El Attar et al. 1981; Fitzgerald, Chiego et al. 1990), neither a necrotic layer, nor a persistent inflammatory zone were noticed. The completion of the pulp-capping in a very short time, and adaptation of a clean procedure (sterilisation of the material) limited the duration of the pulp exposure to the oral cavity and thus, bacterial contamination. Moreover, the use of a light cured composite bonded with a one-step bonding system avoided any bacterial leakage post-restoration (Pradelle-Plasse, Besnault et al. 2003). Even at 11 weeks, the coronal filling was still intact and did not show any evidence of deterioration of the tooth-restoration interface.

In our study, continuous bridge formation was observed, in good continuity with the dentine of the walls of the cavity and the discontinuity between the bridge and the dentinal wall, often described with the use of calcium hydroxide, was not apparent. This result confirms several published reports with other animal models after capping with MTA and also clinical reports (Holland, de Souza et al. 2001; Aeinehchi, Eslami et al. 2003; Dominguez, Witherspoon et al. 2003; Asgary, Parirokh et al. 2006; Nair, Duncan et al. 2007).

Two weeks post-operatively, the first signs of the healing process were observed as the presence of a zone of matrix in direct contact with the capping material. This

zone followed the contours of the material precisely and was visible on all stained sections. The structural modification of the matrix at this level may play an important role in the process of differentiation of the second generation of odontoblast-like cells, as suggested by experiments using growth factors (Rutherford, Wahle et al. 1993). This could reflect recapitulation of developmental events in which signals from the inner dental epithelium mediated by the dental basement membrane are responsible for induction of odontoblast differentiation. In the mature tooth, epithelial cells and a basement membrane are absent, however, in the healing process of the pulp, similar signalling processes for odontoblast differentiation may exist but be of different derivation (Smith and Lesot 2001). The structural modification of the matrix in the area adjacent to the material at the exposure site might play a key role in the process of differentiation of the second generation of odontoblast-like cells. We speculate that the matrix in this area may substitute for the role of the basement membrane during odontoblast differentiation in tooth development.

The modifications of the matrix at this level may include:

- adsorption of dentinal matrix proteins (and predentine), produced by odontoblasts prior to cavity preparation
- incorporation of serum components leaked into the pulpal parenchyma, at the time of surgery possibly resulting from inflammation
- local cellular secretion either by various pulpal cell populations or newly differentiated odontoblast-like cells.

This study has allowed the chronological monitoring of the healing process. The initial inflammatory phase was very short (the first two days) (data not shown), which concurs with the results published by various authors in preceding studies of

other species (Abedi, Torabinejad et al. 1996; Torabinejad and Chivian 1999). The subsequent dentine bridge formation showed evidence of a dentinogenic response.

The staining of the new odontoblast-like cells with DSP antibody, confirmed the secretion of a matrix with at least some dentine characteristics, namely the secretion of Dentin Sialoprotein. However, further characterisation of the matrix with other markers (such as MEPE, nestin, alkaline phosphatase for example) may also be beneficial.

The SEM and X-Ray spectrometric analyses allowed confirmation that the dentine bridge was calcified, although it appeared that the reparative dentine was probably less calcified than orthodentine. These observations are of interest and are potentially novel as most of our knowledge on reparative dentine is based on histological evidence that requires decalcification of the hard tissues and therefore may generate processing artefacts. The Ca/P ratios of the reparative dentine may be indicative of the presence of other forms of calcium phosphate rather than hydroxyapatite alone, emphasising the pathological nature of the process of reparative dentinogenesis.

4.5 MSX2 homeoprotein and the dentine pulp complex:

4.5.1 MSX2 repression and dental abnormalities

The important role that Msx genes play in tooth development has already been described and is exemplified by mice lacking Msx gene function. Msx2-deficient mice exhibit late defects in tooth development (Maas and Bei 1997; Aioub, Lezot et al. 2007). So far, the role of the Msx2 protein in odontoblast differentiation has only been investigated at the early stages of tooth development, as the role of homeobox transcription factor are predicted to affect the initial stages of tooth formation (Begue-Kirn, Smith et al. 1994; Bidder, Latifi et al. 1998). The main conclusions of

these studies were that Msx2 and Osteocalcin were expressed in reciprocal patterns during tooth development, and Msx2 expression in pre-odontoblasts clearly precedes Osteocalcin expression in odontoblasts. As a result, it has been suggested that Msx2 suppresses Osteocalcin expression at stages immediately preceding odontoblast terminal differentiation (Bidder, Latifi et al. 1998). Our q-PCR results confirmed the reverse trascriptional regulation of Osteocalcin by Msx2, as Osteocalcin was highly over-expressed in null mutant pulp cells. Over-expression did not seem to induce any regulation of the presently analysed dentine protein secretion, except a slight change in osteocalcin.

A transcriptional repression of Msx2 on matrix protein related gene expression is potentially instrumental for the regulation of odontoblast behaviour as established for the osteoblast (Cheng, Shao et al. 2008)

Our histological observations, performed on post-natal tissues, appear to demonstrate that Msx2 protein is still expressed in pulp cells throughout the life of the tooth as suggested by the β-galactosidase data. Indeed, most of the cells of the pulpal parenchyma and a few odontoblasts, especially the ones showing reverse polarisation, (those which will probably be entrapped in the dentine matrix), still expressed Msx2 in adult animals.

In regard to the putative cell inclusions, we wondered whether the cells were included in the matrix prior to or after their death. The high expression of DSP protein in these inclusions may be evidence that before being embedded inside the dentine matrix, cells were still vital and active.

During odontoblast differentiation, after 15 mitoses (in the mouse), one cell aligns adjacent to the basal membrane and differentiates into an odontoblast, and the other becomes incorporated within the cell layer of Höhl (Ruch, Lesot et al. 1995). It has been also hypothesised that because the pulp reduces in size during secondary

dentinogenesis, some cells die thus avoiding the over population of the pulp with cells (Baume 1980).

In MSX2 null mutant animals, the odontoblast layer appeared clearly disturbed with a probable over population of cells which may be explained by three hypotheses :

- In the absence of MSX2 protein, the physiological cell death programme does not occur appropriately,
- In the absence of MSX2 protein, odontoblast recruitment is still occurring from a progenitor pool, inducing an over population of cells, which finally become embedded in the secreted dentine matrix.
- In the absence of MSX2 protein, the odontoblast is no longer a post-mitotic cell and division may occur. Nevertheless, with BrdU incorporation studies, we showed that no cell significant division occurred in the odontoblast layer. Whilst the time of BrdU injection (12 hours before animal death) is probably too short to be conclusive, this last hypothesis does not seem to be robust.

Histologically, coronal dentinogenesis was clearly disturbed, except in the first layer of dentine secretion (before 7 days). The dentine thickness was altered in comparison to the wild type animals as was the thickness of enamel indicating a form of amelogenesis imperfecta (Aioub, Lezot et al. 2007); Mola et al., submitted). The moderate amount of circumpulpal dentine produced in such a context of extreme dental abrasion related to the quasi absence of enamel, suggested a reduced defence ability of the pulp in the null mutant animals.

Root formation was also clearly altered; the roots were short, the pulp chamber was abnormally large, reflecting taurodontism. The dentinal walls were extremely thin, and the root surface presented many irregularities. Odontoblasts were not polarised at all in contrast to the gradient of odontoblast polarisation present along the root as observed in the normal tooth. Odontoblasts in the apical third of the root are

generally less polarised than those in coronal third and cells on the pulp chamber floor are generally cuboidal showing a less obvious polarisation (Nanci 2003). The *in situ* hybridisation we performed in this study was on a 14 days post-natal mouse tooth. Root formation had not clearly started at this stage of development. Hybridization for collagen I performed on a later stage of tooth development could be helpful to characterise the nature of these cells. Indeed, secretion of collagen I by the apical cells may provide some evidence of the odontoblast phenotype, based on the known over expression of collagen Iα in odontoblasts and osteoblasts compared to fibroblasts (Leblond and Wright 1981; Leblond 1989; Heersche, Reimers et al. 1992).

At this stage of our observations, we have not been able to identify if these changes are related to an absence of odontoblastic differentiation, or a defect in secretion and dentinogenesis in the root. Although no evident morphological abnormality was observed in heterozygous animals, histologically there were appreciable changes in the null mutant.

Secondary dentinogenesis was significantly affected in the null mutant. Sinusoidal tubules, increased branching and morphological disturbances of the odontoblast layer provide evidence of disturbances in dentinogenesis. The most important observation was the line or zone of disturbed matrix secretion in the dentine. This line seemed to appear at seven days post-natally and might be compared to the calciotraumatic line described in mature teeth and generally considered as the limit between primary and secondary dentinogenesis.

As stated earlier in this thesis (see Introduction), no established physiological understanding has still been given for the transition from primary to secondary dentinogenesis. From the present observations in Msx2 -/- animals, we speculate that Msx2 is involved (directly or indirectly) in the process of secondary dentinogenesis, as primary dentinogenesis seems to occur normally, except in terms of tooth

morphology. It was not possible, however, to identify the specific processes responsible for induction of these disturbances in dentinogenesis.

In the microarray data we obtained from bovine odontoblasts, the MSX2 gene was not identified in the list of differentially regulated genes between young and mature odontoblasts however this may reflect species variation.

4.5.2 MSX2 and pulp repair

In further studies, it would be interesting to determine the influence of Msx2 on the pulp repair process. Our first hypothesis was that Msx2 should be a determinant factor for the differentiation of the progenitor cells whose niches lie within the radicular pulp, via intercellular interactions and regulation with growth factors such as BMP4 and/or TGFβ1. This hypothesis is based on the data obtained in our laboratory on the dental phenotype of Msx2, and the demonstration by Bei (Bei, Stowell et al. 2004) that abrogation of Msx2 inhibits the expression of BMP4. This is supported by the established role of the growth factors of the TGF-β superfamily in the process of osteo-odontoblastic differentiation in the context of development and repair.

TGF-β1 could be directly involved in the regulation of cell proliferation, migration, and extracellular matrix production in the human dental pulp and eventually in the repair process occurring after tooth injury. It is clear that TGF-β plays a key role in dental repair (Smith, Matthews et al. 1998; Sloan, Couble et al. 2001; Baker, Sugars et al. 2009). This role is not well defined, and the members of the TGF-β family implicated in this process are not fully identified although TGF-β1 and TGF-β3 seem to provide the best candidates. In further studies, it would be interesting to investigate the potential relationship between Msx2 and TGF-β in mature cells and in

the pulp healing process, as has been described in tooth development (Begue-Kirn, Smith et al. 1994).

Indeed, many parallels have been shown between development and wound healing (Smith 2002b; Goldberg and Smith 2004). This hypothesis also applies to dentinal repair. The description of a possible role of Msx2 in the early stages of odontogenesis mainly at the level of the odontoblast (Begue-Kirn, Smith et al. 1994; Maas and Bei 1997; Bidder, Latifi et al. 1998), encourages us to investigate whether this relationship persists during the differentiation of odontoblast-like cells after pulp capping of dental pulp.

In a preliminary study, pulp capping with MTA was performed on the first upper molars of null mutant Msx2 mice. Histological procedures were implemented to investigate the presence or absence of dentinal bridge and the cytological aspect of pulpal responses. This preliminary study was curtailed by issues with animal experimentation during my stay in the UK, but in the few samples examined it appeared that no dentine bridge had been secreted 5 weeks after pulp capping, but the dental pulp was still vital, and reactionary dentinogenesis was visible on the pulp chamber floor opposite to the site of pulp exposure. More samples are needed to confirm these observations, but they may indicate a role for MSX2 in pulp repair (inflammation, progenitor recruitment and/or odontoblast differentiation) which will require further study.

5 Conclusion

Research on pulp regeneration is growing and provides exciting possibilities for more biological approaches to endodontic therapy in the future. However, for significant progress to be made in translation to the clinic we need a much deeper understanding of the molecular control of odontoblast secretion and identification of the physiological cues responsible for regulation of odontoblast behaviour. Pulpectomy represents a radical treatment for the non-necrotic pulp, but pulpotomy or pulp capping are only likely to find broader use if we can extend our knowledge of pulp regenerative processes. Such developments will likely bring significant progress to the area of vital pulp therapy.

Our work focussed on odontoblast behaviour during the three phases of dentinogenesis. These observations on molecular characterisation allowed us to clearly demonstrate transcriptional regulation of the dentinogenic cells at different stage of maturity. Based on the hypothesis of a parallel between development and healing process, we were secondly interested in investigating the reversibility of a molecular signalling process (p-38 MAPK pathway) which was shown to be absent in mature cells compared to younger cells. The phosphorylation of the protein and its translocation to the nucleus after cell stimulation allowed us to confirm this hypothesis. Based on these first results, it would be interesting to analyse in further studies the regulation of others genes that have been shown to be up- or down-regulated during the maturation of the cells.

Differentiation and transcriptional regulation of cells are also key processes during reparative dentnogenesis, since differentiation is one step of the complex system for pulp repair when the primary odontoblasts have been destroyed.

Transcriptional regulation in odontoblasts has clearly been demonstrated in the present study. Neverthless, further data are needed to fully understand the complete healing process. *In vitro* models are ideally used for initial investigations, but *in vivo* models are also necessary for pulp repair research. The mouse as a laboratory model for pulp capping is a new tool now available for transgenic investigations offering the possibility to screen *in vivo* the role of a gene (or pathway) by using a reporter gene or a deletion construct in the genome.

Msx2 transcription factor was the first gene we investigated in odontoblast differentiation. The analysis of the Msx2 null mutant tooth phenotype in post-natal animals confirmed the possible role of this protein in odontoblast differentiation and/or mineralisation. The next step will be to analyse the role of this protein during reparative dentinogenesis by undertaking pulp capping in Msx2 transgenic mice. Our preliminary findings were encouraging, although further studies are required to delineate the role of this molecule in the complex pulp repair process and to exploit it in new clinical therapies.

A key point of the repair process is the balance between infection, inflammation and tissue healing. To complement of our understanding of the healing process, more data are also needed on pulp inflammation and its clinical quantification. With these new tools, new diagnostic models and devices may be designed and furthermore, true indications and contra-indications of such new procedures could then be robustly assessed. As a result, pulp capping or other clinical strategies, such as pulpotomy, may be considered as viable alternative treatments to root canal treatment when the pulp is still vital (Figure 50).

Figure 50: 14 months post operatively after endodontic treatment on tooth# 36. Necrotic pulp in the mesial root canal was treated endodontically and a conventional filling applied. Pulp vitality maintenance in the distal root allowed pulp capping of the tissue with a dedicated material (Pro Root MTA®-Dentsply Mailelfer). More than 12 months later, tooth still responds to pulp vitality tests. This kind of treatment may become treatment of choice in the future.

REFERENCES:

Abdullah, D., T.R. Pitt Ford, et al. (2002). "An evaluation of accelerated Portland cement as a restorative material." Biomaterials **23**(19): 4001-10.

Abedi, H., M. Torabinejad, et al. (1996). "The use of Mineral Trioxide Aggregate cement (MTA) as a pulp capping material. (abstract)." J Endod **22**: 199.

About, I. and T. A. Mitsiadis (2001). "Molecular aspects of tooth pathogenesis and repair: in vivo and in vitro models." Adv Dent Res **15**: 59-62.

Aeinehchi, M., B. Eslami, et al. (2003). "Mineral trioxide aggregate (MTA) and calcium hydroxide as pulp-capping agents in human teeth: a preliminary report." Int Endod J **36**(3): 225-31.

Aioub, M., F. Lezot, et al. (2007). "Msx2 -/- transgenic mice develop compound amelogenesis imperfecta, dentinogenesis imperfecta and periodental osteopetrosis." Bone **41**(5): 851-9.

Al-Hiyasat, A. S., K. M. Barrieshi-Nusair, et al. (2006). "The radiographic outcomes of direct pulp-capping procedures performed by dental students: a retrospective study." J Am Dent Assoc **137**(12): 1699-705.

Allard, B., H. Magloire, et al. (2006). "Voltage-gated sodium channels confer excitability to human odontoblasts: possible role in tooth pain transmission." J Biol Chem **281**(39): 29002-10.

Andreasen, F. M. and B. V. Pedersen (1985). "Prognosis of luxated permanent teeth--the development of pulp necrosis." Endod Dent Traumatol **1**(6): 207-20.

Andreasen, F. M., Y. Zhijie, et al. (1987). "Occurrence of pulp canal obliteration after luxation injuries in the permanent dentition." Endod Dent Traumatol **3**(3): 103-15.

Asgary, S., M. Parirokh, et al. (2006). "SEM evaluation of neodentinal bridging after direct pulp protection with mineral trioxide aggregate." Aust Endod J **32**(1): 26-30.

Azizi, S. A., D. Stokes, et al. (1998). "Engraftment and migration of human bone marrow stromal cells implanted in the brains of albino rats--similarities to astrocyte grafts." Proc Natl Acad Sci U S A **95**(7): 3908-13.

Baker, S. M., R. V. Sugars, et al. (2009). "TGF-beta/extracellular matrix interactions in dentin matrix: a role in regulating sequestration and protection of bioactivity." Calcif Tissue Int **85**(1): 66-74.

Balemans, W., M. Ebeling, et al. (2001). "Increased bone density in sclerosteosis is due to the deficiency of a novel secreted protein (SOST)." Hum Mol Genet **10**(5): 537-43.

Banchs, F. and M. Trope (2004). "Revascularization of immature permanent teeth with apical periodontitis: new treatment protocol?" J Endod **30**(4): 196-200.

Banerjee, A., E. A. Kidd, et al. (2003). "In vitro validation of carious dentin removed using different excavation criteria." Am J Dent **16**(4): 228-30.

Barthel, C. R., B. Rosenkranz, et al. (2000). "Pulp capping of carious exposures: treatment outcome after 5 and 10 years: a retrospective study." J Endod **26**(9): 525-8.

Baume, L. J. (1980). "The biology of pulp and dentine. A historic, terminologic-taxonomic, histologic-biochemical, embryonic and clinical survey." Monogr Oral Sci **8**: 1-220.

Baume, L. J. (1980). Definitions and Classifications of the Pulpodentinal Tissues. The Biology of Pulp and Dentine. H. M. Meyers. Philadelphia. **8:** 60-62.

Begue-Kirn, C., A. J. Smith, et al. (1994). "Comparative analysis of TGF beta s, BMPs, IGF1, msxs, fibronectin, osteonectin and bone sialoprotein gene expression

during normal and in vitro-induced odontoblast differentiation." Int J Dev Biol **38**(3): 405-20.

Begue-Kirn, C., A. J. Smith, et al. (1992). "Effects of dentin proteins, transforming growth factor beta 1 (TGF beta 1) and bone morphogenetic protein 2 (BMP2) on the differentiation of odontoblast in vitro." Int J Dev Biol **36**(4): 491-503.

Bei, M., S. Stowell, et al. (2004). "Msx2 controls ameloblast terminal differentiation." Dev Dyn **231**(4): 758-65.

Bellido, T., A. A. Ali, et al. (2005). "Chronic elevation of parathyroid hormone in mice reduces expression of sclerostin by osteocytes: a novel mechanism for hormonal control of osteoblastogenesis." Endocrinology **146**(11): 4577-83.

Bennett, J. H., C. J. Joyner, et al. (1991). "Adipocytic cells cultured from marrow have osteogenic potential." J Cell Sci **99 (Pt 1)**: 131-9.

Berdal, A., M. Molla, et al. (2009). "Differential impact of MSX1 and MSX2 homeogenes on mouse maxillofacial skeleton." Cells Tissues Organs **189**(1-4): 126-32.

Bernard, G. W. (1969). "The ultrastructural interface of bone crystals and organic matrix in woven and lamellar endochondral bone." J Dent Res **48**(5): 781-8.

Bidder, M., T. Latifi, et al. (1998). "Reciprocal temporospatial patterns of Msx2 and Osteocalcin gene expression during murine odontogenesis." J Bone Miner Res **13**(4): 609-19.

Blin-Wakkach, C., F. Lezot, et al. (2001). "Endogenous Msx1 antisense transcript: in vivo and in vitro evidences, structure, and potential involvement in skeleton development in mammals." Proc Natl Acad Sci U S A **98**(13): 7336-41.

Bonewald, L. F. (1999). "Establishment and characterization of an osteocyte-like cell line, MLO-Y4." J Bone Miner Metab **17**(1): 61-5.

Bonewald, L. F. (2002). "Osteocytes: a proposed multifunctional bone cell." J Musculoskelet Neuronal Interact **2**(3): 239-41.

Bonewald, L. F. (2004). "Osteocyte biology: its implications for osteoporosis." J Musculoskelet Neuronal Interact **4**(1): 101-4.

Botero, T. M., C. E. Shelburne, et al. (2006). "TLR4 mediates LPS-induced VEGF expression in odontoblasts." J Endod **32**(10): 951-5.

Brannstrom, M. (1963). A hydrodynamic mechanism in the transmission of pain producing stimuli through the dentin. Snesory mechanisms in dentine. D. J. Anderson. London, Pergamon Press**:** 73-9.

Butler, W. T. (1995). "Dentin matrix proteins and dentinogenesis." Connect Tissue Res **33**(1-3): 59-65.

Butler, W. T. (1998). "Dentin matrix proteins." Eur J Oral Sci **106 Suppl 1**: 204-10.

Butler, W. T., J. C. Brunn, et al. (2003). "Dentin extracellular matrix (ECM) proteins: comparison to bone ECM and contribution to dynamics of dentinogenesis." Connect Tissue Res **44 Suppl 1**: 171-8.

Cam, Y., H. Lesot, et al. (1997). "Distribution of transforming growth factor beta1-binding proteins and low-affinity receptors during odontoblast differentiation in the mouse." Arch Oral Biol **42**(5): 385-91.

Carda, C. and A. Peydro (2006). "Ultrastructural patterns of human dentinal tubules, odontoblasts processes and nerve fibres." Tissue Cell **38**(2): 141-50.

Cassidy, N., M. Fahey, et al. (1997). "Comparative analysis of transforming growth factor-beta isoforms 1-3 in human and rabbit dentine matrices." Arch Oral Biol **42**(3): 219-23.

Chai, Y., X. Jiang, et al. (2000). "Fate of the mammalian cranial neural crest during tooth and mandibular morphogenesis." Development **127**(8): 1671-9.

Cheng, S. L., J. S. Shao, et al. (2008). "Msx2 exerts bone anabolism via canonical Wnt signaling." J Biol Chem **283**(29): 20505-22.

Cho, J. Y., W. B. Lee, et al. (2006). "Bone-related gene profiles in developing calvaria." Gene **372**: 71-81.

Choi, B. D., S. J. Jeong, et al. (2009). "Temporal induction of secretory leukocyte protease inhibitor (SLPI) in odontoblasts by lipopolysaccharide and wound infection." J Endod **35**(7): 997-1002.

Cotton, W. R. (1974). "Bacterial contamination as a factor in healing of pulp exposures." Oral Surg Oral Med Oral Pathol **38**(3): 441-50.

Couble, M. L., J. C. Farges, et al. (2000). "Odontoblast differentiation of human dental pulp cells in explant cultures." Calcif Tissue Int **66**(2): 129-38.

Coudert, A. E., L. Pibouin, et al. (2005). "Expression and regulation of the Msx1 natural antisense transcript during development." Nucleic Acids Res **33**(16): 5208-18.

Couve, E. (1986). "Ultrastructural changes during the life cycle of human odontoblasts." Arch Oral Biol **31**(10): 643-51.

Cox, C. F., A. A. Hafez, et al. (1998). "Biocompatibility of primer, adhesive and resin composite systems on non-exposed and exposed pulps of non-human primate teeth." Am J Dent **11 Spec No**: S55-63.

Cox, C. F., R. K. Subay, et al. (1996). "Tunnel defects in dentin bridges: their formation following direct pulp capping." Oper Dent **21**(1): 4-11.

D'Souza, R. N., T. Bachman, et al. (1995). "Characterization of cellular responses involved in reparative dentinogenesis in rat molars." J Dent Res **74**(2): 702-9.

D'Souza, R. N., A. Cavender, et al. (1998). "TGF-beta1 is essential for the homeostasis of the dentin-pulp complex." Eur J Oral Sci **106 Suppl 1**: 185-91.

D'Souza, R. N., K. Flanders, et al. (1992). "Colocalization of TGF-beta 1 and extracellular matrix proteins during rat tooth development." Proc Finn Dent Soc **88 Suppl 1**: 419-26.

D'Souza, R. N., R. P. Happonen, et al. (1990). "Temporal and spatial patterns of transforming growth factor-beta 1 expression in developing rat molars." Arch Oral Biol **35**(12): 957-65.

Davidson, D. (1995). "The function and evolution of Msx genes: pointers and paradoxes." Trends Genet **11**(10): 405-11.

Decup, F., N. Six, et al. (2000). "Bone sialoprotein-induced reparative dentinogenesis in the pulp of rat's molar." Clin Oral Investig **4**(2): 110-9.

Dhopatkar, A. A., A. J. Sloan, et al. (2005). "British Orthodontic Society, Chapman Prize Winner 2003. A novel in vitro culture model to investigate the reaction of the dentine-pulp complex to orthodontic force." J Orthod **32**(2): 122-32.

Dominguez, M. S., D. E. Witherspoon, et al. (2003). "Histological and scanning electron microscopy assessment of various vital pulp-therapy materials." J Endod **29**(5): 324-33.

Ducy, P., C. Desbois, et al. (1996). "Increased bone formation in osteocalcin-deficient mice." Nature **382**(6590): 448-52.

Duque, C., J. Hebling, et al. (2006). "Reactionary dentinogenesis after applying restorative materials and bioactive dentin matrix molecules as liners in deep cavities prepared in nonhuman primate teeth." J Oral Rehabil **33**(6): 452-61.

Durand, S. H., V. Flacher, et al. (2006). "Lipoteichoic acid increases TLR and functional chemokine expression while reducing dentin formation in in vitro differentiated human odontoblasts." J Immunol **176**(5): 2880-7.

Eghbali-Fatourechi, G. Z., J. Lamsam, et al. (2005). "Circulating osteoblast-lineage cells in humans." N Engl J Med **352**(19): 1959-66.

Ericson, D., E. Kidd, et al. (2003). "Minimally Invasive Dentistry--concepts and techniques in cariology." Oral Health Prev Dent **1**(1): 59-72.

Estrela, C., L. L. Bammann, et al. (2000). "Antimicrobial and chemical study of MTA, Portland cement, calcium hydroxide paste, Sealapex and Dycal." Braz Dent J **11**(1): 3-9.

Faraco, I. M., Jr. and R. Holland (2001). "Response of the pulp of dogs to capping with mineral trioxide aggregate or a calcium hydroxide cement." Dent Traumatol **17**(4): 163-6.

Farges, J. C., J. F. Keller, et al. (2009). "Odontoblasts in the dental pulp immune response." J Exp Zoolog B Mol Dev Evol **312B**(5): 425-36.

Farges, J. C., A. Romeas, et al. (2003). "TGF-beta1 induces accumulation of dendritic cells in the odontoblast layer." J Dent Res **82**(8): 652-6.

Ferrari, G., G. Cusella-De Angelis, et al. (1998). "Muscle regeneration by bone marrow-derived myogenic progenitors." Science **279**(5356): 1528-30.

Fitzgerald, M. (1979). "Cellular mechanisms of dentinal bridge repair using 3H-thymidine." J Dent Res **58**: 2198-2206.

Fitzgerald, M., D. J. Chiego, Jr., et al. (1990). "Autoradiographic analysis of odontoblast replacement following pulp exposure in primate teeth." Arch Oral Biol **35**(9): 707-15.

Fosse, G., P. K. Saele, et al. (1992). "Numerical density and distributional pattern of dentin tubules." Acta Odontol Scand **50**(4): 201-10.

Funteas, U. R., J. A. Wallace, et al. (2003). "A comparative analysis of Mineral Trioxide Aggregate and Portland cement." Aust Endod J **29**(1): 43-4.

Garberoglio, R. and M. Brannstrom (1976). "Scanning electron microscopic investigation of human dentinal tubules." Arch Oral Biol **21**(6): 355-62.

Garcia-Minaur, S., L. A. Mavrogiannis, et al. (2003). "Parietal foramina with cleidocranial dysplasia is caused by mutation in MSX2." Eur J Hum Genet **11**(11): 892-5.

Geiger, P. C., D. C. Wright, et al. (2005). "Activation of p38 MAP kinase enhances sensitivity of muscle glucose transport to insulin." Am J Physiol Endocrinol Metab **288**(4): E782-8.

Goldberg, M., N. Six, et al. (2001). "Application of bioactive molecules in pulp-capping situations." Adv Dent Res **15**: 91-5.

Goldberg, M. and A. J. Smith (2004). "Cells And Extracellular Matrices Of Dentin And Pulp: A Biological Basis For Repair And Tissue Engineering." Crit Rev Oral Biol Med **15**(1): 13-27.

Graham, L., P. R. Cooper, et al. (2006). "The effect of calcium hydroxide on solubilisation of bio-active dentine matrix components." Biomaterials **27**(14): 2865-73.

Gravallese, E. M. (2003). "Osteopontin: a bridge between bone and the immune system." J Clin Invest **112**(2): 147-9.

Gronthos, S., J. Brahim, et al. (2002). "Stem cell properties of human dental pulp stem cells." J Dent Res **81**(8): 531-5.

Gronthos, S., M. Mankani, et al. (2000). "Postnatal human dental pulp stem cells (DPSCs) in vitro and in vivo." Proc Natl Acad Sci U S A **97**(25): 13625-30.

Hanks, C. T., D. Fang, et al. (1998). "Dentin-specific proteins in MDPC-23 cell line." Eur J Oral Sci **106 Suppl 1**: 260-6.

Harada, S. and G. A. Rodan (2003). "Control of osteoblast function and regulation of bone mass." Nature **423**(6937): 349-55.

Haskell, E. W., H. R. Stanley, et al. (1978). "Direct pulp capping treatment: a long-term follow-up." J Am Dent Assoc **97**(4): 607-12.

Hayashi, Y. (1982). "Ultrastructure of initial calcification in wound healing following pulpotomy." J Oral Pathol **11**(2): 174-80.

He, W. X., Z. Y. Niu, et al. (2004). "TGF-beta activated Smad signalling leads to a Smad3-mediated down-regulation of DSPP in an odontoblast cell line." Arch Oral Biol **49**(11): 911-8.

Heersche, J. N., S. M. Reimers, et al. (1992). "Changes in expression of alpha 1 type 1 collagen and osteocalcin mRNA in osteoblasts and odontoblasts at different

stages of maturity as shown by in situ hybridization." Proc Finn Dent Soc **88 Suppl 1**: 173-82.

Heyeraas, K. J., O. B. Sveen, et al. (2001). "Pulp-dentin biology in restorative dentistry. Part 3: Pulpal inflammation and its sequelae." Quintessence Int **32**(8): 611-25.

Hoffman, M. M. and I. Schour (1940). "Quantitative studies in the development of of the rat molar, I. The growth pattern of the primary and secondary dentin. (from birth to 500 days of age)." Anat Rec **78**: 238-252.

Holland, R., V. de Souza, et al. (2001). "Healing process of dog dental pulp after pulpotomy and pulp covering with mineral trioxide aggregate or Portland cement." Braz Dent J **12**(2): 109-13.

Horsted, P., K. El Attar, et al. (1981). "Capping of monkey pulps with Dycal and a Ca-eugenol cement." Oral Surg Oral Med Oral Pathol **52**(5): 531-53.

Hotton, D., N. Mauro, et al. (1999). "Differential expression and activity of tissue-nonspecific alkaline phosphatase (TNAP) in rat odontogenic cells in vivo." J Histochem Cytochem **47**(12): 1541-52.

Huang, B., Y. Sun, et al. (2008). "Distribution of SIBLING proteins in the organic and inorganic phases of rat dentin and bone." Eur J Oral Sci **116**(2): 104-12.

Huang, G. T., W. Sonoyama, et al. (2008). "The hidden treasure in apical papilla: the potential role in pulp/dentin regeneration and bioroot engineering." J Endod **34**(6): 645-51.

Ivens, A., N. Flavin, et al. (1990). "The Human homeobox gene Hox7 maps to chromosome 4p16.1and may be implicated in Wolf Hirschhorn syndrome." Hum Gen **84**: 473-476.

Iwaya, S. I., M. Ikawa, et al. (2001). "Revascularization of an immature permanent tooth with apical periodontitis and sinus tract." Dent Traumatol **17**(4): 185-7.

Jacobsen, I. and K. Kerekes (1977). "Long-term prognosis of traumatized permanent anterior teeth showing calcifying processes in the pulp cavity." Scand J Dent Res **85**(7): 588-98.

Jepsen, S., H. K. Albers, et al. (1997). "Recombinant human osteogenic protein-1 induces dentin formation: an experimental study in miniature swine." J Endod **23**(6): 378-82.

Jones, S. and A. Boyde (1984). Dentin and Dentinigenesis. A. Linde. Boca Raton, CRC Press. **1:** 81-134.

Jontell, M., M. N. Gunraj, et al. (1987). "Immunocompetent cells in the normal dental pulp." J Dent Res **66**(6): 1149-53.

Jontell, M., T. Okiji, et al. (1998). "Immune defense mechanisms of the dental pulp." Crit Rev Oral Biol Med **9**(2): 179-200.

Joseph, B. K., N. W. Savage, et al. (1996). "In situ hybridization evidence for a paracrine/autocrine role for insulin-like growth factor-I in tooth development." Growth Factors **13**(1-2): 11-7.

Kagayama, M., H. Akita, et al. (1995). "Immunohistochemical localization of connexin 43 in the developing tooth germ of rat." Anat Embryol (Berl) **191**(6): 561-8.

Kakehashi, S., H. R. Stanley, et al. (1965). "The Effects Of Surgical Exposures Of Dental Pulps In Germ-Free And Conventional Laboratory Rats." Oral Surg Oral Med Oral Pathol **20**: 340-9.

Katchburian, E. and N. J. Severs (1982). "Membranes of matrix-vesicles in early developing dentine. A freeze fracture study." Cell Biol Int Rep **6**(10): 941-50.

Keller, J. F., F. Carrouel, et al. (2009). "Toll-like receptor 2 activation by lipoteichoic acid induces differential production of pro-inflammatory cytokines in human odontoblasts, dental pulp fibroblasts and immature dendritic cells." Immunobiology.

Kidd, E. A. (2004). "How 'clean' must a cavity be before restoration?" Caries Res **38**(3): 305-13.

Kidd, E. A., A. Banerjee, et al. (2003). "Relationships between a clinical-visual scoring system and two histological techniques: a laboratory study on occlusal and approximal carious lesions." Caries Res **37**(2): 125-9.

Kim, J. W. and J. P. Simmer (2007). "Hereditary dentin defects." J Dent Res **86**(5): 392-9.

Krebsbach, P. H., S. A. Kuznetsov, et al. (1997). "Bone formation in vivo: comparison of osteogenesis by transplanted mouse and human marrow stromal fibroblasts." Transplantation **63**(8): 1059-69.

Kubota, K., K. Wakabayashi, et al. (2003). "Proteome analysis of secreted proteins during osteoclast differentiation using two different methods: two-dimensional electrophoresis and isotope-coded affinity tags analysis with two-dimensional chromatography." Proteomics **3**(5): 616-26.

Lallemand, Y., M. A. Nicola, et al. (2005). "Analysis of Msx1; Msx2 double mutants reveals multiple roles for Msx genes in limb development." Development **132**(13): 3003-14.

Larmas, M. (2008). "Pre-odontoblasts, odontoblasts, or "odontocytes"." J Dent Res **87**(3): 198; author reply 199.

Leblond, C. P. (1989). "Synthesis and secretion of collagen by cells of connective tissue, bone, and dentin." Anat Rec **224**(2): 123-38.

Leblond, C. P. and G. M. Wright (1981). "Steps in the elaboration of collagen by odontoblasts and osteoblasts." Methods Cell Biol **23**: 167-89.

Lesot, H., S. Lisi, et al. (2001). "Epigenetic signals during odontoblast differentiation." Adv Dent Res **15**: 8-13.

Lesot, H., M. Osman, et al. (1981). "Immunofluorescent localization of collagens, fibronectin, and laminin during terminal differentiation of odontoblasts." Dev Biol **82**(2): 371-81.

Linde, A. (1995). "Dentin mineralization and the role of odontoblasts in calcium transport." Connect Tissue Res **33**(1-3): 163-70.

Linde, A. and M. Goldberg (1993). "Dentinogenesis." Crit Rev Oral Biol Med **4**(5): 679-728.

Liu, Y. H., R. Kundu, et al. (1995). "Premature suture closure and ectopic cranial bone in mice expressing Msx2 transgenes in the developing skull." Proc Natl Acad Sci U S A **92**(13): 6137-41.

Lovschall, H., O. Fejerskov, et al. (2001). "Pulp-capping with recombinant human insulin-like growth factor I (rhIGF-I) in rat molars." Adv Dent Res **15**: 108-12.

Lovschall, H., T. A. Mitsiadis, et al. (2007). "Coexpression of Notch3 and Rgs5 in the pericyte-vascular smooth muscle cell axis in response to pulp injury." Int J Dev Biol **51**(8): 715-21.

Lovschall, H., M. Tummers, et al. (2005). "Activation of the Notch signaling pathway in response to pulp capping of rat molars." Eur J Oral Sci **113**: 312-317.

Lu, Y., Y. Xie, et al. (2007). "DMP1-targeted Cre expression in odontoblasts and osteocytes." J Dent Res **86**(4): 320-5.

Ma, L., S. Golden, et al. (1996). "The molecular basis of Boston-type craniosynostosis: the Pro148-->His mutation in the N-terminal arm of the MSX2 homeodomain stabilizes DNA binding without altering nucleotide sequence preferences." Hum Mol Genet **5**(12): 1915-20.

Maas, R. and M. Bei (1997). "The genetic control of early tooth development." Crit Rev Oral Biol Med **8**(1): 4-39.

Magloire, H., M. Bouvier, et al. (1992). "Odontoblast response under carious lesions." Proc Finn Dent Soc **88 Suppl 1**: 257-74.

Magloire, H., M. L. Couble, et al. (2004). "Odontoblast primary cilia: facts and hypotheses." Cell Biol Int **28**(2): 93-9.

Magloire, H., M. L. Couble, et al. (2008). "Odontoblast: a mechano-sensory cell." J Exp Zoolog B Mol Dev Evol.

Maniatopoulos, C. and D. C. Smith (1983). "A scanning electron microscopic study of the odontoblast process in human coronal dentine." Arch Oral Biol **28**(8): 701-10.

Marotti, G. (1996). "The structure of bone tissues and the cellular control of their deposition." Ital J Anat Embryol **101**(4): 25-79.

Mavrogiannis, L. A., I. B. Taylor, et al. (2006). "Enlarged parietal foramina caused by mutations in the homeobox genes ALX4 and MSX2: from genotype to phenotype." Eur J Hum Genet **14**(2): 151-8.

McLachlan, J. L., A. J. Sloan, et al. (2004). "S100 and cytokine expression in caries." Infect Immun **72**(7): 4102-8.

McLachlan, J. L., A. J. Smith, et al. (2005). "Gene expression profiling of pulpal tissue reveals the molecular complexity of dental caries." Biochim Biophys Acta **1741**(3): 271-81.

McLachlan, J. L., A. J. Smith, et al. (2003). "Gene expression analysis in cells of the dentine-pulp complex in healthy and carious teeth." Arch Oral Biol **48**(4): 273-83.

Mitsiadis, T. A. and C. Rahiotis (2004). "Parallels between tooth development and repair: conserved molecular mechanisms following carious and dental injury." J Dent Res **83**(12): 896-902.

Miura, M., S. Gronthos, et al. (2003). "SHED: stem cells from human exfoliated deciduous teeth." Proc Natl Acad Sci U S A **100**(10): 5807-12.

Mjor, I. A. (1983). Dentin and pulp. Reaction patterns in human teeth. B. Raton, CRC Press**:** 63-156.

Mjor, I. A. (2002). "Pulp-dentin biology in restorative dentistry. Part 7: The exposed pulp." Quintessence Int **33**(2): 113-35.

Mjor, I. A., E. Dahl, et al. (1991). "Healing of pulp exposures: an ultrastructural study." J Oral Pathol Med **20**(10): 496-501.

Mjor, I. A., O. B. Sveen, et al. (2001). "Pulp-dentin biology in restorative dentistry. Part 1: normal structure and physiology." Quintessence Int **32**(6): 427-46.

Morinobu, M., M. Ishijima, et al. (2003). "Osteopontin expression in osteoblasts and osteocytes during bone formation under mechanical stress in the calvarial suture in vivo." J Bone Miner Res **18**(9): 1706-15.

Murray, P. E., I. About, et al. (2000). "Postoperative pulpal and repair responses." J Am Dent Assoc **131**(3): 321-9.

Murray, P. E., A. A. Hafez, et al. (2003). "Histomorphogenetic analysis of odontoblast-like cell numbers and dentin bridge secretory activity following pulp exposure." Int Endod J. **36(2)**: 106-16.

Murray, P. E., A. A. Hafez, et al. (2002). "Comparison of pulp responses following restoration of exposed and non-exposed cavities." J Dent **30**(5-6): 213-22.

Nair, P. N., H. F. Duncan, et al. (2008). "Histological, ultrastructural and quantitative investigations on the response of healthy human pulps to experimental capping with mineral trioxide aggregate: a randomized controlled trial." Int Endod J **41**(2): 128-50.

Nakashima, M. (1994). "Induction of dentin formation on canine amputated pulp by recombinant human bone morphogenetic proteins (BMP)-2 and -4." J Dent Res **73**(9): 1515-22.

Nanci, A. (2003). Dentin-Pulp Complex. Ten Cate's Oral Histology: development structure, and function. A. Nanci. Saint Louis, USA, Mosby**:** 192-239.

Ning, W., R. Song, et al. (2002). "TGF-beta1 stimulates HO-1 via the p38 mitogen-activated protein kinase in A549 pulmonary epithelial cells." Am J Physiol Lung Cell Mol Physiol **283**(5): L1094-102.

Okiji, T., N. Kawashima, et al. (1992). "An immunohistochemical study of the distribution of immunocompetent cells, especially macrophages and Ia

antigen-expressing cells of heterogeneous populations, in normal rat molar pulp." J Dent Res **71**(5): 1196-202.
Okiji, T., I. Morita, et al. (1992). "Pathophysiological roles of arachidonic acid metabolites in rat dental pulp." Proc Finn Dent Soc **88 Suppl 1**: 433-8.
Okumura, R., K. Shima, et al. (2005). "The odontoblast as a sensory receptor cell? The expression of TRPV1 (VR-1) channels." Arch Histol Cytol **68**(4): 251-7.
Olgart, L. and G. Bergenholtz (2003). The dentine-pulp complex: responses to adverse influences. Textbook of Endodontology. G. Bergenholtz, P. Horsted-Bindslev and C. Reit. Oxford, Blackwell Munksgard.
Opperman, L. A. (2000). "Cranial sutures as intramembranous bone growth sites." Dev Dyn **219**(4): 472-85.
Osman, A. and J. V. Ruch (1976). "Topographic distribution of mitosis in the lower incisor and 1st molar in the mouse embryo." J Biol Buccale **4**(4): 331-48.
Papagerakis, P., A. Berdal, et al. (2002). "Investigation of osteocalcin, osteonectin, and dentin sialophosphoprotein in developing human teeth." Bone **30**(2): 377-85.
Papagerakis, P., M. MacDougall, et al. (2003). "Expression of amelogenin in odontoblasts." Bone **32**(3): 228-40.
Park, M. H., H. I. Shin, et al. (2001). "Differential expression patterns of Runx2 isoforms in cranial suture morphogenesis." J Bone Miner Res **16**(5): 885-92.
Pashley, D. H. (1996). "Dynamics of the pulpo-dentin complex." Crit Rev Oral Biol Med **7**(2): 104-33.
Pashley, D. H. (2002). Pulpodentin Complex. Seltzer and Bender's Dental Pulp. . G. H. Hargreaves KM. IL, Quintessence Publishing**:** 63-93.
Paula-Silva, F. W., A. Ghosh, et al. (2009). "TNF-alpha promotes an odontoblastic phenotype in dental pulp cells." J Dent Res **88**(4): 339-44.
Pitt Ford, T. R., M. Torabinejad, et al. (1996). "Using Mineral Trioxide Aggregate as pulp capping material." J Am Dent Assoc **127**(1491-4).
Pittenger, M. F., A. M. Mackay, et al. (1999). "Multilineage potential of adult human mesenchymal stem cells." Science **284**(5411): 143-7.
Pradelle-Plasse, N., C. Besnault, et al. (2003). "Influence of new light curing units and bonding agents on the microleakage of Class V composite resin restorations." Am J Dent **16**(6): 409-13.
Ruch, J. V. (1998). "Odontoblast commitment and differentiation." Biochem Cell Biol **76**(6): 923-38.
Ruch, J. V., H. Lesot, et al. (1995). "Odontoblast differentiation." Int J Dev Biol **39**(1): 51-68.
Rutherford, R. B., L. Spangberg, et al. (1994). "The time-course of the induction of reparative dentine formation in monkeys by recombinant human osteogenic protein-1." Arch Oral Biol **39**(10): 833-8.
Rutherford, R. B., J. Wahle, et al. (1993). "Induction of reparative dentine formation in monkeys by recombinant human osteogenic protein-1." Arch Oral Biol **38**(7): 571-6.
Ryoo, H. M., H. M. Hoffmann, et al. (1997). "Stage-specific expression of Dlx-5 during osteoblast differentiation: involvement in regulation of osteocalcin gene expression." Mol Endocrinol **11**(11): 1681-94.
Saidon, J., J. He, et al. (2003). "Cell and tissue reactions to mineral trioxide aggregate and Portland cement." Oral Surg Oral Med Oral Pathol Oral Radiol Endod **95**(4): 483-9.
Sasaki, T., K. Nakagawa, et al. (1982). "Ultrastructure of odontoblasts in kitten tooth germs as revealed by freeze-fracture." Arch Oral Biol **27**(10): 897-904.
Satokata, I., L. Ma, et al. (2000). "Msx2 deficiency in mice causes pleiotropic defects in bone growth and ectodermal organ formation." Nat Genet **24**(4): 391-5.

Schour, I. and H. G. Poncher (1937). "the rate of apposition of human enamel and dentin as measured by the effects of acute fluorosis." Am J Dis Child **54**: 757-776.

Schroder, U. (1985). "Effects of calcium hydroxide-containing pulp-capping agents on pulp cell migration, proliferation, and differentiation." J Dent Res **64 Spec No**: 541-8.

Schroder, U. and L. E. Granath (1972). "Scanning electron microscopy of hard tissue barrier following experimental pulpotomy of intact human teeth and capping with calcium hydroxide." Odontol Revy **23**(2): 211-20.

Seltzer, S., I. B. Bender, et al. (1963). "The Dynamics Of Pulp Inflammation: Correlations Between Diagnostic Data And Actual Histologic Findings In The Pulp." Oral Surg Oral Med Oral Pathol **16**: 969-77.

Senawongse, P., M. Otsuki, et al. (2008). "Morphological characterization and permeability of attrited human dentine." Arch Oral Biol **53**(1): 14-9.

Shi, S. and S. Gronthos (2003). "Perivascular niche of postnatal mesenchymal stem cells in human bone marrow and dental pulp." J Bone Miner Res **18**(4): 696-704.

Shi, S., P. G. Robey, et al. (2001). "Comparison of human dental pulp and bone marrow stromal stem cells by cDNA microarray analysis." Bone **29**(6): 532-9.

Shirakabe, K., K. Terasawa, et al. (2001). "Regulation of the activity of the transcription factor Runx2 by two homeobox proteins, Msx2 and Dlx5." Genes Cells **6**(10): 851-6.

Sigal, M. J., J. E. Aubin, et al. (1985). "An immunocytochemical study of the human odontoblast process using antibodies against tubulin, actin, and vimentin." J Dent Res **64**(12): 1348-55.

Sigal, M. J., J. E. Aubin, et al. (1984). "The odontoblast process extends to the dentinoenamel junction: an immunocytochemical study of rat dentine." J Histochem Cytochem **32**(8): 872-7.

Simon, S., P. Cooper, et al. (2008). "Evaluation of a new laboratory model for pulp healing: preliminary study." Int Endod J **41**(9): 781-90.

Simon, S., P.J. Lumley, et al. (2009). "Trauma and dentinogenesis : a case report." J Endod(In Press).

Simon, S., A. J. Smith, et al. (2009). "Molecular characterisation of young and mature odontoblasts." Bone **45**(4): 693-703.

Six, N., J. J. Lasfargues, et al. (2002). "Differential repair responses in the coronal and radicular areas of the exposed rat molar pulp induced by recombinant human bone morphogenetic protein 7 (osteogenic protein 1)." Arch Oral Biol **47**(3): 177-87.

Sloan, A. J., M. L. Couble, et al. (2001). "Expression of TGF-beta receptors I and II in the human dental pulp by in situ hybridization." Adv Dent Res **15**: 63-7.

Sloan, A. J. and A. J. Smith (1999). "Stimulation of the dentine-pulp complex of rat incisor teeth by transforming growth factor-beta isoforms 1-3 in vitro." Arch Oral Biol **44**(2): 149-56.

Sloan, A. J. and A. J. Smith (2007). "Stem cells and the dental pulp: potential roles in dentine regeneration and repair." Oral Dis **13**(2): 151-7.

Smith, A. J. (2002a). Dentine formation and repair. Seltzer and Bender's Dental Pulp. K. M. Hargreaves and H. E. Goodies. IL, Quintessence Publishing**:** 41-62.

Smith, A. J. (2002b). "Pulpal responses to caries and dental repair." Caries Res **36**(4): 223-32.

Smith, A. J. (2003). "Vitality of the dentin-pulp complex in health and disease: growth factors as key mediators." J Dent Educ **67**(6): 678-89.

Smith, A. J., N. Cassidy, et al. (1995). "Reactionary dentinogenesis." Int J Dev Biol **39**(1): 273-80.

Smith, A. J. and H. Lesot (2001). "Induction and regulation of crown dentinogenesis: embryonic events as a template for dental tissue repair?" Crit Rev Oral Biol Med **12**(5): 425-37.

Smith, A. J., P. J. Lumley, et al. (2008). "Dental regeneration and materials: a partnership." Clin Oral Investig **12**(2): 103-8.

Smith, A. J., J. B. Matthews, et al. (1998). "Transforming growth factor-beta1 (TGF-beta1) in dentine matrix. Ligand activation and receptor expression." Eur J Oral Sci **106 Suppl 1**: 179-84.

Smith, A. J., R. S. Tobias, et al. (1995). "Influence of substrate nature and immobilization of implanted dentin matrix components during induction of reparative dentinogenesis." Connect Tissue Res **32**(1-4): 291-6.

Smith, A. J., R. S. Tobias, et al. (1994). "Odontoblast stimulation in ferrets by dentine matrix components." Arch Oral Biol **39**(1): 13-22.

Smith, A. J., R. S. Tobias, et al. (2001). "Transdentinal stimulation of reactionary dentinogenesis in ferrets by dentine matrix components." J Dent **29**(5): 341-6.

Smith, A. J., R. S. Tobias, et al. (1990). "In vivo morphogenetic activity of dentine matrix proteins." J Biol Buccale **18**(2): 123-9.

Sonoyama, W., Y. Liu, et al. (2008). "Characterization of the apical papilla and its residing stem cells from human immature permanent teeth: a pilot study." J Endod **34**(2): 166-71.

Sreenath, T., T. Thyagarajan, et al. (2003). "Dentin sialophosphoprotein knockout mouse teeth display widened predentin zone and develop defective dentin mineralization similar to human dentinogenesis imperfecta type III." J Biol Chem **278**(27): 24874-80.

Stains, J. P. and R. Civitelli (2003). "Genomic approaches to identifying transcriptional regulators of osteoblast differentiation." Genome Biol **4**(7): 222.

Staquet, M. J., S. H. Durand, et al. (2008). "Different roles of odontoblasts and fibroblasts in immunity." J Dent Res **87**(3): 256-61.

Symons, N. B. B. (1961). "A histochemical study of the intertubular and peritubular matrices in normal human dentine." Arch Oral Biol **5**: 239-148.

Symons, N. B. B. (1962). "Coronal dentin in upper incisor teeth." J Dent res **41**: 1271 (Abstract).

Takuma, S. and N. Nagai (1971). "Ultrastructure of rat odontoblasts in various stages of their development and maturation." Arch Oral Biol **16**(9): 993-1011.

Tarim, B., A. A. Hafez, et al. (1998). "Biocompatibility of Optibond and XR-Bond adhesive systems in nonhuman primate teeth." Int J Periodontics Restorative Dent **18**(1): 86-99.

Tatsumi, S., K. Ishii, et al. (2007). "Targeted ablation of osteocytes induces osteoporosis with defective mechanotransduction." Cell Metab **5**(6): 464-75.

Thesleff, I., H. J. Barrach, et al. (1981). "Changes in the distribution of type IV collagen, laminin, proteoglycan, and fibronectin during mouse tooth development." Dev Biol **81**(1): 182-92.

Thesleff, I. and A. Vaahtokari (1992). "The role of growth factors in determination and differentiation of the odontoblastic cell lineage." Proc Finn Dent Soc **88 Suppl 1**: 357-68.

Thewlis, J. (1940). "The structure of teeth as shown by X-ray examination." Arch Oral biol **7**: 195-205.

Thibodeau, B., F. Teixeira, et al. (2007). "Pulp revascularization of immature dog teeth with apical periodontitis." J Endod **33**(6): 680-9.

Thibodeau, B. and M. Trope (2007). "Pulp revascularization of a necrotic infected immature permanent tooth: case report and review of the literature." Pediatr Dent **29**(1): 47-50.

Thomas, H. F. and P. Carella (1983). "A scanning electron microscope study of dentinal tubules from un-erupted human teeth." Arch Oral Biol **28**(12): 1125-30.

Thomas, H. F. and P. Carella (1984). "Correlation of scanning and transmission electron microscopy of human dentinal tubules." Arch Oral Biol **29**(8): 641-6.

Tomson, P. L., L. M. Grover, et al. (2007). "Dissolution of bio-active dentine matrix components by mineral trioxide aggregate." J Dent **35**(8): 636-42.

Torabinejad, M. and N. Chivian (1999). "Clinical applications of mineral trioxide aggregate." J Endod **25**(3): 197-205.

Towler, D. A., S. J. Rutledge, et al. (1994). "Msx-2/Hox 8.1: a transcriptional regulator of the rat osteocalcin promoter." Mol Endocrinol **8**(11): 1484-93.

Trowbridge, H. O. (2002). Histology of Pulpal Inflammation. Seltzer's and Bender's Dental Pulp. L. C. Bywaters, Quintessence Publishing Co**:** 227-245.

Tziafas, D., I. Kolokuris, et al. (1992). "Short term dentinogenetic response of dog dental pulp tissue after its induction by demineralized or native dentin, or predentin." Arch Oral Biol **37**: 119-128.

Tziafas, D., A. J. Smith, et al. (2000). "Designing new treatment strategies in vital pulp therapy." J Dent **28**(2): 77-92.

Unterbrink, A., M. O'Sullivan, et al. (2002). "TGF beta-1 downregulates DMP-1 and DSPP in odontoblasts." Connect Tissue Res **43**(2-3): 354-8.

Vainio, S., I. Karavanova, et al. (1993). "Identification of BMP-4 as a signal mediating secondary induction between epithelial and mesenchymal tissues during early tooth development." Cell **75**(1): 45-58.

van Bezooijen, R. L., B. A. Roelen, et al. (2004). "Sclerostin is an osteocyte-expressed negative regulator of bone formation, but not a classical BMP antagonist." J Exp Med **199**(6): 805-14.

Wang, F. M., T. Hu, et al. (2006). "p38 Mitogen-activated protein kinase affects transforming growth factor-beta/Smad signaling in human dental pulp cells." Mol Cell Biochem **291**(1-2): 49-54.

Ward, J. (2002). "Vital pulp therapy in cariously exposed permanent teeth and its limitations." Aust Endod J **28**(1): 29-37.

Watahiki, J., T. Yamaguchi, et al. (2008). "Identification of differentially expressed genes in mandibular condylar and tibial growth cartilages using laser microdissection and fluorescent differential display: chondromodulin-I (ChM-1) and tenomodulin (TeM) are differentially expressed in mandibular condylar and other growth cartilages." Bone **42**(6): 1053-60.

Wennberg, A., I. A. Mjor, et al. (1982). "Rate of formation of regular and irregular secondary dentin in monkey teeth." Oral Surg Oral Med Oral Pathol **54**(2): 232-7.

Wilkie, A. O. (1997). "Craniosynostosis: genes and mechanisms." Hum Mol Genet **6**(10): 1647-56.

Wilkie, A. O., Z. Tang, et al. (2000). "Functional haploinsufficiency of the human homeobox gene MSX2 causes defects in skull ossification." Nat Genet **24**(4): 387-90.

Winkler, D. G., M. K. Sutherland, et al. (2003). "Osteocyte control of bone formation via sclerostin, a novel BMP antagonist." Embo J **22**(23): 6267-76.

Winograd, J., M. P. Reilly, et al. (1997). "Perinatal lethality and multiple craniofacial malformations in MSX2 transgenic mice." Hum Mol Genet **6**(3): 369-79.

Wuyts, W., W. Reardon, et al. (2000). "Identification of mutations in the MSX2 homeobox gene in families affected with foramina parietalia permagna." Hum Mol Genet **9**(8): 1251-5.

Yamamura, T. (1985). "Differentiation of pulpal cells and inductive influences of various matrices with reference to pulpal wound healing." J Dent Res **64 Spec No**: 530-40.

Yamashiro, T., M. Tummers, et al. (2003). "Expression of bone morphogenetic proteins and Msx genes during root formation." J Dent Res **82**(3): 172-6.

Ye, L., M. MacDougall, et al. (2004). "Deletion of dentin matrix protein-1 leads to a partial failure of maturation of predentin into dentin, hypomineralization, and expanded cavities of pulp and root canal during postnatal tooth development." J Biol Chem **279**(18): 19141-8.

Zhang, C. Z., H. Li, et al. (1997). "Evidence for a local action of growth hormone in embryonic tooth development in the rat." Growth Factors **14**(2-3): 131-43.

Zhao, Q., N. Chen, et al. (2004). "Effect of transforming growth factor-beta on activity of connective tissue growth factor gene promoter in mouse NIH/3T3 fibroblasts." Acta Pharmacol Sin **25**(4): 485-9.

Zhou, Y. L., Y. Lei, et al. (2000). "Functional antagonism between Msx2 and CCAAT/enhancer-binding protein alpha in regulating the mouse amelogenin gene expression is mediated by protein-protein interaction." J Biol Chem **275**(37): 29066-75.

Ziskin, D. E., E. Applebaum, et al. (1949). "The effect of Hypophysectomie pont the permanent dentition of rhesus monkey." J Dent Res **28**: 48-54.

Appendix:

Appendix 1:

Full list of regulated genes between young and mature issued from Microarray data analysis with D-Chip Software.

[COMPARE_CRITERIA_V2]
$NUM_OPTION_LINE=5
$ARRAY_LIST_FILE=
$COMPARE_ON_GENE_LIST=
$COMPARE_ON_USE_LIST=1
$AVERAGE_USING_STANDARD_ERROR=Yes
$OMIT_AFFY_CONTROL_GENE=Yes
$NUM_CRITERION=1

$Parenthesis	Combine Baseline and Experiment	E/B>	or B/E>	Use
$No	3,4	1,2 2.000	2.000	Lower Bound

[COMPARE_RESULT]

probe set	GENE ID	baseline mean (LS	periment mean (L	fold change	lower bound of F	upper bound of F	difference of me	Gene Title
Bt.10029.2.S1_at	LOC506032	979,14	340,99	-2,87	-2,5	-3,34	-638,15	similar to Chromosome 17 open reading frame 75
Bt.5879.1.S1_at	---	87,84	1358,46	15,47	13,79	17,61	1270,63	Transcribed locus
Bt.26387.1.A1_at	LOC533760	885,52	12,25	-72,29	-43,88	-204,86	-873,27	Similar to glutamate receptor
Bt.22746.1.S1_at	LOC505366	420,42	11273,33	26,81	20,6	38,39	10852,91	similar to prostate stromal protein ps20
Bt.29409.1.S1_at	---	635,21	18,72	-33,92	-25,55	-50,44	-616,48	Transcribed locus
Bt.9594.1.S1_at	---	2141,41	35,29	-60,69	-37,47	-159,32	-2106,13	Transcribed locus
Bt.22400.1.A1_at	LOC615883	748,28	8022,51	10,72	9,36	12,54	7274,23	similar to SLIT3
Bt.12302.1.S1_at	PLAT	16764,37	562,19	-29,82	-21,11	-50,75	-16202,18	plasminogen activator, tissue
Bt.26824.1.A1_a	MGC128625	703,41	2857,35	4,06	3,93	4,21	2153,93	similar to mitochondrial ribosomal protein L46
Bt.16188.2.S1_at	CYYR1	18,23	279,37	15,32	12,37	20,12	261,14	cysteine/tyrosine-rich 1
Bt.7349.1.S1_at	---	185,43	6992,42	37,71	28,6	55,31	6806,98	Transcribed locus
Bt.7870.1.S1_at	PP	89,01	1877,59	21,09	15,97	31,04	1788,58	pyrophosphatase (inorganic)
Bt.4804.2.A1_at	LOC510972	504,39	4212,72	8,35	7,38	9,61	3708,33	similar to Cyclin-dependent kinase inhibitor 1C (Cyclin-dependent kinase inhibitor p57) (p57KIP2)
Bt.6400.2.S1_a_a	---	1756,52	132,86	-13,22	-10,7	-17,29	-1623,66	---
Bt.12769.1.S1_at	PCK2	550,72	5647,44	10,25	8,71	12,46	5096,72	phosphoenolpyruvate carboxykinase 2 (mitochondrial)
Bt.16583.1.S1_at	MGC126930	4585,1	299,34	-15,32	-11,98	-21,22	-4285,76	similar to Voltage-dependent calcium channel gamma-like subunit (Neuronal voltage-gated calcium channel gamma-like subunit
Bt.28224.1.A1_at	---	305,33	1410,35	4,62	4,29	5	1105,01	Transcribed locus
Bt.28171.1.S1_at	LOC616560	451,95	4892,01	10,82	8,98	13,62	4440,06	hypothetical LOC616560
Bt.12498.1.A1_at	LOC530657	57,71	3752,92	65,04	39,36	186,76	3695,21	similar to alpha 3 type VI collagen isoform 5 precursor
Bt.2025.1.A1_at	---	1318,9	7318,08	5,55	5,01	6,22	5999,18	Transcribed locus
Bt.5247.1.S1_at	PTGIS	4705,94	410,34	-11,47	-9,18	-15,26	-4295,61	prostaglandin I2 (prostacyclin) synthase
Bt.4675.1.S1_a_a	MX1	656,5	3229,73	4,92	4,5	5,42	2573,23	myxovirus (influenza virus) resistance 1, interferon-inducible protein p78 (mouse)
Bt.5453.1.S1_at	---	663,4	4873,89	7,35	6,37	8,68	4210,5	Transcribed locus
Bt.9569.1.S1_at	TACSTD1	117,79	1712,09	14,54	12,3	17,76	1594,31	tumor-associated calcium signal transducer 1
Bt.18593.1.A1_at	---	1,07	282,26	263,48	53,38	100000000	281,19	Transcribed locus
Bt.15822.1.S1_at	MGC159776	378,6	2,78	-136,17	-33,5	-100000000	-375,82	similar to Proto-oncogene tyrosine-protein kinase FGR (P55-FGR) (C-FGR)
Bt.3100.1.A1_at	IGFBP5	16824,86	1909,36	-8,81	-7,46	-10,77	-14915,5	insulin-like growth factor binding protein 5
Bt.13853.1.S1_at	MGC139227	1079,45	164,06	-6,58	-5,82	-7,56	-915,4	similar to cell adhesion kinase beta
Bt.1533.1.S1_at	LOC444872	683,65	3373,36	4,93	4,67	5,23	2689,71	perlecan
Bt.20605.1.S1_at	---	247,14	5152,25	20,85	17,99	24,78	4905,11	Transcribed locus
Bt.15548.1.A1_at	---	28,88	564,2	19,54	13,8	33,41	535,32	---
Bt.24618.1.S1_at	DBP	1268,75	175,1	-7,25	-6,33	-8,47	-1093,65	D site of albumin promoter (albumin D-box) binding protein
Bt.27332.1.A1_at	---	227,96	1734,73	7,61	6,53	9,11	1506,77	---
Bt.4898.1.S1_at	BASP1	137,09	2281,7	16,64	12,63	24,36	2144,61	brain abundant, membrane attached signal protein 1
Bt.29065.1.A1_at	---	7824,15	951,48	-8,22	-6,87	-10,23	-6872,67	Transcribed locus
Bt.2359.1.A1_at	FYN	755,24	4029,09	5,33	4,77	6,05	3273,85	FYN oncogene related to SRC, FGR, YES
Bt.12065.1.S1_at	LOC618071	938,83	26,55	-35,35	-23,62	-70,14	-912,27	Hypothetical LOC618071
Bt.11662.1.A1_at	LOC523311	391,15	6454,83	16,5	12,59	23,91	6063,68	hypothetical LOC523311
Bt.7133.1.S1_at	LOC515547 /// L	785,83	6903,98	8,79	7,18	11,3	6118,15	ornithine decarboxylase /// similar to Ornithine decarboxylase (ODC)
Bt.223.1.S1_at	AMBN	1140,94	7936,22	6,96	5,93	8,4	6795,28	ameloblastin (enamel matrix protein)
Bt.11641.1.S1_at	MGC129051	852,24	13383,38	15,7	12,49	21,12	12531,15	similar to thrombospondin 4 precursor
Bt.23178.1.S1_at	DCN	776,34	4372,5	5,63	4,96	6,51	3596,16	decorin
Bt.16213.1.S1_at	MGC148630	559,39	6986,8	12,49	11,21	14,1	6427,41	hypothetical protein LOC613320
Bt.27207.1.A1_at	---	360,48	2685,81	7,45	6,73	8,34	2325,33	Transcribed locus
Bt.16972.1.A1_at	---	5,5	1063,18	193,33	97,48	11333,66	1057,68	Transcribed locus
Bt.7393.1.S1_at	LOC513362	263,64	3400,03	12,9	10,54	16,58	3136,39	Similar to nephronectin
Bt.16740.1.A1_at	MGC143240	122,91	1600,01	13,02	9,62	20,1	1477,1	similar to laminin S B3 chain
Bt.22729.2.A1_at	BoLA /// LOC507	133,4	3490,63	26,17	14,88	107,88	3357,23	MHC class I heavy chain /// major histocompatibility complex, class I, A
Bt.29415.1.A1_at	---	6337,24	492,71	-12,86	-9,55	-19,64	-5844,53	Transcribed locus
Bt.5326.2.S1_at	LOC539364	577,14	6284,79	10,89	9,42	12,88	5707,64	similar to TIS21
Bt.7128.1.S1_at	---	796,65	29,51	-26,99	-14,9	-142,22	-767,14	Transcribed locus
Bt.5163.1.A1_at	---	802,58	4287,41	5,34	4,75	6,1	3484,83	Transcribed locus, weakly similar to NP_001847.3 1 type XVI collagen precursor [Homo sapiens]

probe set	GENE ID	baseline mean (LS	periment mean (E	fold change	lower bound of F	upper bound of F	difference of me	Gene Title
Bt.2590.1.A1_at	LOC520939	57	624,62	10,96	8,35	15,92	567,63	similar to Kruppel-like zinc finger transcription factor
Bt.23770.1.A1_at	---	182,43	1243,81	6,82	5,96	7,96	1061,38	Transcribed locus
Bt.984.1.S1_at	---	1344,11	7261,92	5,4	4,76	6,25	5917,81	Transcribed locus
Bt.24280.1.A1_at	LOC616194	4258,75	1140,79	-3,73	-3,47	-4,04	-3117,96	similar to Placental protein 25 (PP25)
Bt.3251.1.S1_at	LOC515749	1193,56	111,84	-10,67	-8,09	-15,64	-1081,71	similar to alpha-catenin related protein
Bt.9760.1.S1_at	CX26	286,29	3183,9	11,12	9,47	13,46	2897,61	connexin 26 protein
Bt.24305.1.A1_at	---	2461,02	586,71	-4,19	-3,8	-4,67	-1874,31	Transcribed locus
Bt.14201.1.S1_at	MGC134244	630,17	2644,69	4,2	3,81	4,66	2014,52	hypothetical protein MGC134244
Bt.22210.1.S1_at	CGREF1	330,7	4945,3	14,95	11,43	21,57	4614,6	cell growth regulator with EF-hand domain 1
Bt.25849.1.S1_at	MGC148634	211,7	2743,48	12,96	9,66	19,64	2531,77	similar to C1q and tumor necrosis factor related protein 6
Bt.25918.1.A1_at	---	5,8	4424,23	763,36	157,68	100000000	4418,44	Transcribed locus
Bt.20593.2.S1_at	MGC140018	800,35	6489,43	8,11	7,07	9,48	5689,08	similar to Peptidyl-prolyl cis-trans isomerase C (PPIase) (Rotamase) (Cyclophilin C)
Bt.16109.1.S1_at	---	15,24	301,49	19,78	11,94	57,19	286,25	Transcribed locus
Bt.2592.1.A1_x_a	BOLA	891,81	18,44	-48,37	-24,77	-984,29	-873,38	Classical MHC class I antigen
Bt.8802.1.S1_at	MGC155170	390,15	2121,27	5,44	4,69	6,46	1731,12	hypothetical LOC508425
Bt.21589.1.S1_at	LOC512019	1222,92	8217	6,72	5,64	8,28	6994,08	similar to angiopoietin-related protein-2
Bt.8909.1.S1_at	LOC525869	109,82	986,85	8,99	7,03	12,4	877,03	similar to Ankycorbin (Ankyrin repeat and coiled-coil structure-containing protein) (Retinoic acid-induced protein 14) (Novel retinal pigment
Bt.25703.1.A1_at	MGC139970	3278,51	1013,97	-3,23	-2,98	-3,52	-2264,54	similar to plexin domain containing 2 precursor
Bt.5379.1.S1_at	LOC512072	335,8	3107,87	9,26	7,85	11,26	2772,07	similar to protein tyrosine phosphatase, receptor type, F
Bt.26846.1.A1_at	LOC507856 /// M	3308,93	361,82	-9,15	-7,74	-11,14	-2947,1	similar to La ribonucleoprotein domain family, member 6
Bt.23786.1.A1_at	MGC165813	2195,99	710,01	-3,09	-2,86	-3,36	-1485,97	hypothetical LOC531552
Bt.7176.1.S1_at	SPON1	31,45	633,45	20,14	12,01	62,06	602,01	spondin 1, extracellular matrix protein
Bt.24841.1.S1_at	LOC790463 /// SI	520,07	3511,71	6,75	5,79	8,09	2991,64	splA/ryanodine receptor domain and SOCS box containing 1 /// similar to SPRY domain-containing SOCS box protein SSB-1
Bt.2096.2.S1_at	LOC505206	24,25	680,2	28,05	17,4	71,89	655,95	similar to pincher
Bt.21369.1.S1_at	---	2923,44	666,39	-4,39	-3,94	-4,95	-2257,05	Transcribed locus
Bt.24383.1.S1_at	MGC151582	1477,93	123,11	-12	-8,86	-18,54	-1354,81	similar to PSGC2903
Bt.13546.2.S1_at	---	124,98	13,28	-9,41	-7,18	-13,61	-111,71	Transcribed locus
Bt.21041.1.S1_at	---	1036,66	120,36	-8,61	-6,75	-11,88	-916,29	Transcribed locus
Bt.2801.1.S1_at	LOC539976	589,04	4001,93	6,79	5,76	8,26	3412,88	hypothetical LOC539976
Bt.16941.1.A1_at	MPZL1	3,16	172,81	54,72	18,4	100000000	169,65	myelin protein zero-like 1
Bt.14853.1.A1_at	MGC137223	1924,4	361,79	-5,32	-4,69	-6,13	-1562,6	similar to RAB3A interacting protein isoform alpha 1
Bt.231.1.S1_at	TXN	1606,67	5163,98	3,21	2,99	3,47	3557,31	thioredoxin
Bt.26992.2.S1_at	---	452,5	1377,93	3,05	2,82	3,31	925,43	Transcribed locus
Bt.9559.2.S1_at	APP	375,5	6719,52	17,89	14,66	22,93	6344,02	amyloid beta (A4) precursor protein
Bt.692.1.S1_at	LOC539385	8455,65	1484,81	-5,69	-4,87	-6,84	-6970,84	hypothetical LOC539385
Bt.20542.1.S1_at	LOC514246	3881,41	754,52	-5,14	-4,5	-5,99	-3126,89	similar to Transcription factor jun-B
Bt.21071.2.A1_at	---	5380,88	1137,66	-4,73	-4,15	-5,48	-4243,22	Transcribed locus
Bt.24157.1.A1_at	MGC152175	325,05	10,21	-31,84	-20,38	-72,41	-314,84	similar to DKFZP564O0823 protein
Bt.22545.1.S1_a_	MGC148755	976,13	5125,71	5,25	4,69	5,96	4149,58	similar to fibulin-1 C
Bt.4461.1.S1_at	CKMT1	15,16	2218,01	146,29	58,55	100000000	2202,85	creatine kinase, mitochondrial 1 (ubiquitous)
Bt.9914.1.S1_at	MGC128163	253,65	1459,76	5,76	4,86	7,04	1206,11	similar to dolichyl-phosphate mannosyltransferase polypeptide 3
Bt.7655.1.S1_at	MGC148333	253,16	2007,56	7,93	6,62	9,88	1754,4	similar to Y-box protein ZONAB-B
Bt.24793.1.S1_at	---	128,87	658,59	5,11	4,46	5,97	529,72	Transcribed locus
Bt.28140.1.S1_at	KCTD15	242,6	1423,71	5,87	5,12	6,88	1181,1	potassium channel tetramerisation domain containing 15
Bt.12649.1.S1_at	MGC129108	531,76	2386,08	4,49	3,94	5,19	1854,32	similar to myo-inositol monophosphatase A3
Bt.209.3.S1_at	LYS	134,22	3,23	-41,52	-18,78	-100000000	-130,99	lysozyme C, non-stomach isozyme
Bt.1818.1.S1_at	LOC514360	14,8	846,24	57,19	25,4	100000000	831,44	similar to desmoplakin isoform II
Bt.16710.1.A1_at	---	1439,68	4710,09	3,27	3	3,59	3270,41	Transcribed locus
Bt.350.1.S1_s_at	BLA-DQB	2806,75	31,84	-88,14	-29,58	-100000000	-2774,91	MHC class II antigen
Bt.22108.1.S1_at	---	527,26	1992,45	3,78	3,47	4,14	1465,2	Transcribed locus
Bt.13885.1.S1_at	---	2045,81	490,85	-4,17	-3,78	-4,63	-1554,96	Transcribed locus
Bt.9570.1.S1_at	LOC786672	2300,31	549,44	-4,19	-3,84	-4,6	-1750,87	similar to tumor necrosis factor, alpha-induced protein 2
Bt.4850.1.S1_at	MGC140785	741,09	2368,3	3,2	2,94	3,5	1627,21	Similar to 5-nucleotidase, cytosolic III
Bt.4952.2.S1_a_a	LOC784507	91,28	344,11	3,77	3,38	4,25	252,83	similar to RPL22L1 protein
Bt.16445.1.A1_at	LOC618444	1109,24	13,36	-83,02	-42,37	-1995,12	-1095,88	hypothetical LOC618444
Bt.5550.1.S1_at	IMPG1	643,72	26,18	-24,59	-12,77	-319,89	-617,54	interphotoreceptor matrix proteoglycan 1
Bt.11826.1.S1_at	LOC614589	1092,85	3302,37	3,02	2,8	3,28	2209,51	similar to Zinc finger CCCH type antiviral protein 1 (Zinc finger CCCH domain-containing protein 2
Bt.10076.1.S1_at	RCSD1	336,26	2069,56	6,15	5,12	7,69	1733,3	RCSD domain containing 1
Bt.25616.1.S1_at	LOC782069	18,09	287,27	15,88	10,12	36,64	269,18	hypothetical protein LOC782069
Bt.5021.1.S1_at	FBN1	122,42	825,96	6,75	5,64	8,37	703,53	fibrillin 1
Bt.17317.1.S1_at	LOC534505	26,24	1109,42	42,28	16,59	100000000	1083,18	similar to Carboxypeptidase X 2 (M14 family)
Bt.1646.1.S1_at	EIF3S6IP	2242,53	5133,3	2,29	2,18	2,41	2890,77	eukaryotic translation initiation factor 3, subunit 6 interacting protein
Bt.21975.1.S1_at	PRF1	554,98	35,06	-15,83	-9,96	-38,26	-519,92	perforin 1 (pore forming protein)
Bt.26011.1.A1_at	---	1130,09	101	-11,19	-9,01	-14,72	-1029,09	Transcribed locus

probe set	GENE ID	baseline mean (LS	periment mean (L	fold change	lower bound of F	upper bound of F	difference of me	Gene Title
Bt.28461.1.S1_at	LOC408017	441,13	6374,19	14,45	9,44	30,63	5933,06	insulin receptor
Bt.9728.1.S1_at	ATP1B3	6880,18	2173,3	-3,17	-2,91	-3,47	-4706,89	ATPase, Na+/K+ transporting, beta 3 polypeptide
Bt.19739.1.A1_at	---	104,8	552,57	5,27	4,48	6,38	447,76	Transcribed locus
Bt.20354.1.S1_at	---	2472,34	5464,76	2,21	2,11	2,31	2992,42	CDNA clone MGC:166326 IMAGE:8229867
Bt.24456.1.S1_at	---	440,8	4205,68	9,54	8,09	11,61	3764,88	Transcribed locus
Bt.19120.1.A1_at	---	224,5	17,55	-12,79	-8,59	-24,93	-206,95	Transcribed locus
Bt.2331.1.A1_at	MGC148675	7193,16	1330,47	-5,41	-4,74	-6,28	-5862,69	similar to receptor activity-modifying protein 1
Bt.9605.1.S1_at	ms4A8B	59,78	756,84	12,66	8,64	23,58	697,06	membrane spanning 4-domain subfamily A member 8B
Bt.21563.1.S1_at	LOC520730	6,74	293,17	43,52	15,74	100000000	286,43	similar to KIAA0869 protein
Bt.24343.1.A1_at	CLDN1	118,1	1759,94	14,9	11,19	22,24	1641,84	claudin 1
Bt.20531.1.A1_at	MGC151713	3327,98	924,54	-3,6	-3,23	-4,05	-2403,44	similar to KIAA0668 protein
Bt.6954.1.S1_at	LOC505149	5685,14	740,21	-7,68	-6,16	-10,18	-4944,93	similar to regulatory erythroid kinase long form
Bt.3797.1.S1_at	FMOD	848,79	6834,58	8,05	6,72	10,02	5985,79	fibromodulin
Bt.21409.2.S1_at	COL11A1	44,7	681,75	15,25	9,58	37,14	637,05	collagen, type XI, alpha 1
Bt.2191.2.S1_at	---	81,3	810,93	9,97	8,94	11,26	729,63	---
Bt.24713.1.S1_at	---	1336,19	227,79	-5,87	-4,86	-7,38	-1108,4	Transcribed locus
Bt.2559.1.S1_at	CETN2	5305,46	1132,08	-4,69	-4,28	-5,17	-4173,38	centrin, EF-hand protein, 2
Bt.12510.2.S1_at	LOC509824	32,81	473,63	14,43	10,85	21,47	440,82	Similar to Os08g0528700
Bt.1774.1.S1_at	LOC513493	646,46	1979,54	3,06	2,8	3,37	1333,08	similar to myosin IXB
Bt.4078.1.S1_at	RCN3	1409,85	4866,71	3,45	3,15	3,81	3456,85	reticulocalbin 3, EF-hand calcium binding domain
Bt.5356.1.S1_s_a	BoLA-DRB3	622,2	44,55	-13,97	-8,85	-32,87	-577,65	major histocompatibility complex, class II, DRB3
Bt.27032.1.S1_at	---	931,83	34,3	-27,16	-13,12	-100000000	-897,53	---
Bt.4817.1.A1_at	MGC128478	708,67	8924,06	12,59	9,44	18,88	8215,39	similar to claudin 11
Bt.5507.2.S1_at	LOC506218	4277,41	965,75	-4,43	-3,85	-5,19	-3311,66	similar to Sorting nexin 9
Bt.22199.1.S1_at	MGC155271	21,02	256,77	12,22	8,19	23,92	235,75	similar to RTP801-like protein
Bt.27481.2.S1_at	SPG3A	411,15	36,53	-11,25	-7,73	-20,6	-374,62	spastic paraplegia 3A (autosomal dominant)
Bt.7018.1.S1_at	MGC159915	356,06	95,57	-3,73	-3,31	-4,25	-260,49	similar to OTTHUMP00000030232
Bt.7646.1.S1_at	LOC613533	407,75	4598,48	11,28	8,7	16,01	4190,73	similar to filamin B, beta (actin binding protein 278)
Bt.21934.1.S1_a	MAP2	2569,99	455,21	-5,65	-4,76	-6,91	-2114,78	microtubule-associated protein 2
Bt.21873.1.S1_at	MGC152070	1930,62	440,71	-4,38	-3,82	-5,12	-1489,92	hypothetical LOC618177
Bt.488.1.S2_at	PLA2R1	161,46	16,01	-10,09	-7,83	-14,1	-145,45	phospholipase A2 receptor 1, 180kDa
Bt.20958.1.A1_at	MGC152553	30,72	892,53	29,06	14,61	1916,43	861,81	similar to ADP ribosylation factor-like protein 7
Bt.4395.1.S1_at	MGC140645	3643,2	1127,12	-3,23	-2,95	-3,57	-2516,08	similar to Phosphoribosyl pyrophosphate synthetase-associated protein 1 (PRPP synthetase-associated protein 1) (39 kDa phosphoribosypyrophosphate synthetase-associated protein) (PAP39)
Bt.23559.1.S1_at	MGC139725	685,65	1607,77	2,34	2,2	2,51	922,12	similar to thiamin pyrophosphokinase 1
Bt.23178.1.S2_at	DCN	923,21	3736,58	4,05	3,54	4,71	2813,36	decorin
Bt.26764.1.A1_at	LEC2	288,27	1998,47	6,93	5,5	9,35	1710,2	Lectomedin 2
Bt.27973.1.S1_at	SLCO3A1	1308,23	3643,36	2,78	2,56	3,05	2335,13	solute carrier organic anion transporter family, member 3A1
Bt.4793.1.S1_at	SLC12A2	1983,04	65,75	-30,16	-22,76	-44,64	-1917,29	solute carrier family 12 (sodium/potassium/chloride transporters), member 2
Bt.26812.1.S1_at	---	1744,68	698,11	-2,5	-2,36	-2,65	-1046,57	Transcribed locus
Bt.18049.1.A1_at	---	532,15	1766,51	3,32	3,01	3,69	1234,36	Transcribed locus
Bt.2698.1.S1_at	FKBP10	894,81	3307,87	3,7	3,27	4,24	2413,06	FK506 binding protein 10, 65 kDa
Bt.26635.2.S1_at	FZD1	8923,15	3053,79	-2,92	-2,68	-3,21	-5869,35	frizzled homolog 1 (Drosophila)
Bt.23900.1.A1_at	---	395,09	1651,09	4,18	3,71	4,77	1255,99	Transcribed locus
Bt.21765.1.S1_at	LOC541106	1716,16	188,36	-9,11	-6,75	-13,94	-1527,8	similar to OTTHUMP00000016853
Bt.9773.1.A1_at	---	2995,09	894,34	-3,35	-3	-3,77	-2100,75	Transcribed locus
Bt.5301.2.S1_a_a	THBS	4,6	201,54	43,85	14,41	100000000	196,95	thrombospondin
Bt.17704.1.S1_at	CHSY1	1066,56	5333,31	5	4,21	6,13	4266,76	carbohydrate (chondroitin) synthase 1
Bt.3513.1.A1_at	---	1457,64	146,84	-9,93	-7,49	-14,62	-1310,79	Transcribed locus
Bt.7220.1.S1_at	BLA-DQB	301,26	4,69	-64,28	-33,08	-1099,07	-296,58	MHC class II antigen
Bt.422.1.S2_at	IGFBP3	3228,51	529,92	-6,09	-5,06	-7,63	-2698,59	insulin-like growth factor binding protein 3
Bt.6933.1.S1_at	LOC613449	204,52	1681,51	8,22	7,09	9,77	1476,99	similar to KIAA0369
Bt.9310.1.S1_at	C16orf5	5317,71	790,14	-6,73	-5,33	-9,1	-4527,57	chromosome 16 open reading frame 5
Bt.12356.1.S1_at	MGC157300	1663,63	6185,09	3,72	3,31	4,24	4521,46	hypothetical LOC534625
Bt.22036.1.S1_at	---	1114,67	202,7	-5,5	-4,62	-6,78	-911,97	Transcribed locus
Bt.1770.2.A1_at	LOC515860	113,89	4140,91	36,36	28,2	51,11	4027,02	similar to peroxidasin homolog
Bt.4392.2.A1_at	---	104,42	543,81	5,21	4,29	6,59	439,39	Transcribed locus
Bt.21760.1.S1_at	---	36,92	518,83	14,05	9,02	31,48	481,91	Transcribed locus
Bt.4267.1.S1_at	MIA	1918,77	8279,27	4,31	3,77	5,03	6360,5	melanoma inhibitory activity
Bt.25478.1.A1_at	LOC529947	151,97	1400,25	9,21	7,62	11,62	1248,28	hypothetical LOC529947
Bt.1220.1.S1_at	---	577,76	31,44	-18,38	-11,38	-47,21	-546,32	Transcribed locus
Bt.20091.1.S1_at	---	438,08	1195,34	2,73	2,61	2,85	757,27	---
Bt.8879.2.S1_at	---	415,82	1725,81	4,15	3,57	4,94	1309,99	Transcribed locus
Bt.13490.1.S1_at	LOC504408	2294,48	965,41	-2,38	-2,21	-2,56	-1329,07	similar to nuclear mitogen- and stress-activated protein kinase-1

probe set	GENE ID	baseline mean (LS	periment mean (L	fold change	lower bound of F	upper bound of F	difference of me	Gene Title
Bt.20226.2.A1_at	---	3437	1232,59	-2,79	-2,55	-3,08	-2204,41	Transcribed locus
Bt.9147.1.A1_at	MEP50	1024,72	3087,59	3,01	2,74	3,34	2062,88	methylosome protein 50
Bt.19337.1.S1_at	---	1736,68	414,78	-4,19	-3,59	-5,01	-1321,9	Transcribed locus
Bt.19578.1.S1_at	LOC618914	1776,85	477,75	-3,72	-3,26	-4,32	-1299,1	hypothetical LOC618914
Bt.16495.2.A1_at	LOC511602	13,27	1760,95	132,7	59,24	100000000	1747,68	similar to alpha-5 type IV collagen
Bt.27248.1.A1_at	MMP16	539,62	2349,21	4,35	4,11	4,63	1809,59	matrix metallopeptidase 16 (membrane-inserted)
Bt.5382.1.S1_at	NT5C2	970,43	2298,67	2,37	2,2	2,56	1328,24	5'-nucleotidase, cytosolic II
Bt.1720.1.S1_at	LOC788823	2221,2	5919,58	2,67	2,46	2,9	3698,38	similar to nucleolar protein No55
Bt.5040.1.S1_at	UQCR	1452,05	4997,42	3,44	3,07	3,9	3545,37	ubiquinol-cytochrome c reductase (6.4kD) subunit
Bt.20793.1.A1_s_	LOC532572	253,1	1822,54	7,2	6,21	8,54	1569,44	similar to Laminin gamma-1 chain precursor (Laminin B2 chain)
Bt.3520.1.S1_at	PYCR1	998,04	2370,13	2,37	2,25	2,51	1372,09	pyrroline-5-carboxylate reductase 1
Bt.22504.2.S1_at	MGC140208	28,47	476,43	16,74	9,91	53,63	447,96	similar to G protein-coupled receptor 56
Bt.22471.1.S1_at	PHF5A	208,43	958,95	4,6	4,01	5,38	750,53	PHD finger protein 5A
Bt.10030.2.S1_a_	TMEPAI	2476,82	565,62	-4,38	-3,76	-5,23	-1911,2	transmembrane, prostate androgen induced RNA
Bt.783.1.S1_at	AOX1	53,13	655,77	12,34	7,83	28,93	602,63	aldehyde oxidase 1
Bt.9549.1.S1_at	LAGY	3830,9	139,59	-27,44	-22,81	-34,42	-3691,31	homeodomain only protein
Bt.21096.1.S1_at	---	849,72	3000,83	3,53	3,13	4,04	2151,11	---
Bt.8904.1.S1_at	---	1717,13	378,38	-4,54	-4,04	-5,17	-1338,75	---
Bt.1403.1.S1_at	NNT	265,76	1085,8	4,09	3,5	4,89	820,04	nicotinamide nucleotide transhydrogenase
Bt.11241.1.S1_at	CDH1	145,72	1294,86	8,89	7,51	10,85	1149,14	Cadherin 1, type 1, E-cadherin (epithelial)
Bt.15717.1.A1_at	LOC512918	1248,1	419,18	-2,98	-2,69	-3,32	-828,92	similar to Sorting nexin-7
Bt.7192.1.S1_at	MRPL17	461,15	1812,71	3,93	3,41	4,63	1351,57	mitochondrial ribosomal protein L17
Bt.692.2.S1_at	LOC539385	3542,88	533,14	-6,65	-5,35	-8,73	-3009,73	hypothetical LOC539385
Bt.25336.1.A1_at	---	36,58	248,99	6,81	5,34	9,34	212,41	Transcribed locus
Bt.1613.1.S1_at	PRSS11	9902,53	2159,57	-4,59	-4,01	-5,34	-7742,97	protease, serine, 11
Bt.2285.1.A1_at	MGC142825	366,8	1565,2	4,27	3,63	5,15	1198,4	similar to Protein kinase C, delta binding protein
Bt.28780.1.A1_at	LOC505234	582,22	1871,3	3,21	2,87	3,65	1289,07	similar to FYVE, RhoGEF and PH domain-containing protein 4 (Actin filament-binding protein frabin) (FGD1-related F-actin-binding protein) (Zinc finger FYVE domain-containing protein 6)
Bt.13347.1.S1_at	LOC504458	964,24	2073,84	2,15	2,01	2,3	1109,6	similar to translocated to HRX in t(11;19) leukemia
Bt.6983.1.S1_at	LOC790129	86,31	1792,8	20,77	17,6	25,32	1706,49	similar to SOX9
Bt.24563.1.S1_at	LOC532952	694,42	103,06	-6,74	-5,17	-9,62	-591,36	similar to membrane-associated guanylate kinase-related 3 (MAGI-3)
Bt.4056.1.S1_at	CRIP2	2677,53	597,23	-4,48	-3,86	-5,34	-2080,31	cysteine-rich protein 2
Bt.3577.1.S1_at	GRAMD3	1694,89	501,85	-3,38	-3,05	-3,78	-1193,05	GRAM domain containing 3
Bt.18689.2.A1_at	LOC538401	1141,41	5003,78	4,38	3,83	5,11	3862,37	similar to Arylsulfatase B precursor (ASB) (N-acetylgalactosamine-4-sulfatase) (G4S)
Bt.27068.1.A1_at	MGC137696	5947,9	1041,33	-5,71	-5,09	-6,49	-4906,58	similar to KIAA0517 protein
Bt.17876.1.A1_at	---	3960,04	837,86	-4,73	-3,97	-5,82	-3122,18	Transcribed locus
Bt.27755.1.S1_at	LOC788643 /// P	691,6	20,16	-34,31	-18,55	-223,58	-671,44	platelet-derived growth factor B /// hypothetical protein LOC788643
Bt.15751.1.S1_at	LOC514185	1167,3	3913,39	3,35	3,05	3,72	2746,1	similar to AMP deaminase
Bt.12552.1.S1_at	LOC513148	2073,47	621,37	-3,34	-2,94	-3,84	-1452,1	similar to Probable ATP-dependent RNA helicase DHX35 (DEAH box protein 35)
Bt.569.1.S1_at	MAP2	1116,48	422	-2,65	-2,43	-2,89	-694,49	microtubule-associated protein 2
Bt.2997.1.A1_at	---	6101,97	167,71	-36,38	-27,71	-52,9	-5934,26	Transcribed locus
Bt.422.1.S1_at	IGFBP3	2453,8	314,33	-7,81	-6,25	-10,37	-2139,47	insulin-like growth factor binding protein 3
Bt.4235.1.S1_at	LOC505942	299,42	792,46	2,65	2,41	2,92	493,04	similar to Collagen alpha 2(IX) chain precursor
Bt.27886.1.S1_s_	LOC783645	290,66	1030,08	3,54	3,11	4,1	739,42	similar to vinculin isoform meta-VCL
Bt.22613.1.A1_at	---	607,39	1791,52	2,95	2,69	3,26	1184,13	Transcribed locus
Bt.1670.1.A1_at	---	213,35	990,87	4,64	3,89	5,73	777,51	---
Bt.9201.1.A1_at	MGC128839	785,03	3369,94	4,29	3,75	5	2584,91	similar to Tetraspanin-14 (Tspan-14) (Transmembrane 4 superfamily member 14) (DC-TM4F2)
Bt.5605.3.S1_at	MGC137530	90,71	389,79	4,3	3,7	5,11	299,07	Similar to Myristoylated alanine-rich C-kinase substrate (MARCKS)
Bt.7538.1.S1_at	---	1872,54	5793,89	3,09	2,75	3,52	3921,35	---
Bt.5084.1.S1_at	CKB	368,33	2402,9	6,52	4,96	9,46	2034,57	creatine kinase, brain
Bt.22679.1.S1_at	MGC137743	1912,86	325,86	-5,87	-4,72	-7,73	-1587	similar to Myosin Id
Bt.24819.1.S1_at	LOC785433	818,18	2558,54	3,13	2,81	3,51	1740,36	similar to formin homology 2 domain containing 3
Bt.27347.1.A1_at	---	178,25	401,43	2,25	2,1	2,43	223,19	Transcribed locus
Bt.9996.1.S1_at	LOC533726	119,92	575,19	4,8	3,97	6,01	455,26	hypothetical LOC533726
Bt.21059.1.S1_at	LOC509490	1141,8	335,3	-3,41	-3,05	-3,86	-806,5	similar to eIF4E-binding protein 3
Bt.3546.1.S1_at	LOC785924	23,1	1032,3	44,68	21,95	100000000	1009,2	similar to transmembrane receptor
Bt.12199.1.A1_at	---	552,59	2091,07	3,78	3,3	4,43	1538,48	Transcribed locus
Bt.3313.1.A1_at	ARHGAP24	2025,63	658,19	-3,08	-2,74	-3,5	-1367,44	Rho GTPase activating protein 24
Bt.6853.1.S1_at	---	999,13	4647,4	4,65	3,84	5,87	3648,27	Transcribed locus
Bt.6516.1.A1_at	LOC540332	1214,69	156,86	-7,74	-5,65	-12,22	-1057,84	similar to Coiled-coil domain containing 85B
Bt.20501.1.S1_at	---	2734,57	574,78	-4,76	-4,21	-5,45	-2159,79	Transcribed locus
Bt.12718.1.A1_at	LOC613972	172,29	8,01	-21,51	-10,62	-100000000	-164,28	Similar to Apolipoprotein D precursor (Apo-D) (ApoD)
Bt.24226.1.S1_at	EEF1A1	1527,26	381,34	-4	-3,4	-4,86	-1145,92	Eukaryotic translation elongation factor 1 alpha 1
Bt.3750.1.S1_at	S100A11	1736,95	4353,17	2,51	2,31	2,74	2616,23	S100 calcium binding protein A11 (calgizzarin)

probe set	GENE ID	baseline mean (LS	periment mean (L	fold change	lower bound of F	upper bound of F	difference of me	Gene Title
Bt.15927.1.S1_at	MGC159964	447,15	3360,09	7,51	6,21	9,48	2912,93	similar to WD repeat domain, phosphoinositide interacting 1
Bt.16326.2.S1_at	LOC515475	226,46	19,04	-11,89	-7,84	-24,38	-207,41	hypothetical LOC515475
Bt.23994.1.A1_at	MGC143207	6160,97	2499,55	-2,46	-2,36	-2,57	-3661,42	Similar to epsilon isoform of 61kDa regulatory subunit of PP2A
Bt.28502.1.S1_at	MGC140374	1175,07	4020,02	3,42	3,08	3,83	2844,95	similar to FAM83D protein
Bt.13587.1.S1_at	LOC521539	588,9	3138,87	5,33	4,35	6,83	2549,96	similar to mannosidase, alpha, class 2A, member 1
Bt.20234.1.S1_at	LOC510926	111,7	6650,37	59,54	43,74	93,1	6538,67	hypothetical LOC510926
Bt.12220.1.S1_a	---	3199,81	894,6	-3,58	-3,15	-4,13	-2305,22	Transcribed locus
Bt.7431.1.S1_a_	LOC787862	870,72	155,26	-5,61	-4,43	-7,6	-715,46	similar to Formin homology 2 domain containing 1
Bt.12054.2.S1_at	LOC511748	1346,38	288,04	-4,67	-3,84	-5,95	-1058,34	similar to Yip1 domain family, member 1
Bt.22090.1.S1_at	---	1124,84	2666,91	2,37	2,19	2,59	1542,07	Transcribed locus
Bt.799.1.S1_at	---	492	1339,34	2,72	2,47	3,03	847,34	Transcribed locus
Bt.25805.1.A1_at	---	13,07	506,35	38,73	15,61	100000000	493,27	Transcribed locus
Bt.462.1.S1_at	PRKAR2B	605,83	81,78	-7,41	-6,04	-9,53	-524,05	protein kinase, cAMP-dependent, regulatory, type II, beta
Bt.6642.1.S1_at	---	751,07	122,69	-6,12	-4,74	-8,6	-628,39	Transcribed locus
Bt.21978.1.S1_at	MGC160122	383,6	43,59	-8,8	-6,09	-15,77	-340,01	similar to KIAA1509 protein
Bt.15847.1.S1_at	MGC128861	3953,77	1444,63	-2,74	-2,51	-3	-2509,14	similar to cerebellar degeneration-related protein 2
Bt.20554.1.S1_at	LOC527410	149,05	456,31	3,06	2,72	3,5	307,25	similar to P-Rex1 protein
Bt.20090.1.S1_at	LOC526006	583,81	70,6	-8,27	-5,82	-14,14	-513,21	similar to human gamma enolase
Bt.16951.1.A1_at	LOC538507	68,67	647,54	9,43	6,7	15,78	578,87	similar to FZD2 protein
Bt.11156.1.S1_at	MGC137074	535,48	3542,51	6,62	5,16	9,18	3007,03	similar to Hypothetical UPF0184 protein C9orf16 homolog
Bt.19643.2.S1_at	LOC520448	338,85	1764,12	5,21	4,36	6,43	1425,27	similar to large-conductance calcium-activated potassium channel beta subunit
Bt.8948.1.S1_at	LOX	1019,96	8283,38	8,12	6,42	11,05	7263,42	lysyl oxidase
Bt.10949.1.S1_at	LOC782141	781,46	2701,48	3,46	3,07	3,95	1920,02	Hypothetical protein LOC782141
Bt.5121.1.S1_at	CASR	25,88	6519,89	251,97	129,82	4234,78	6494,01	calcium-sensing receptor
Bt.9989.1.S1_at	---	2657,85	1150,46	-2,31	-2,16	-2,47	-1507,39	---
Bt.20376.1.S1_at	LOC521932	635,69	2175,33	3,42	3,1	3,81	1539,65	hypothetical LOC521932
Bt.4768.1.S2_at	JAM1	690,29	2135,62	3,09	2,73	3,55	1445,33	junctional adhesion molecule 1
Bt.13734.2.S1_at	---	41,51	611,09	14,72	8,73	46,12	569,58	Transcribed locus
Bt.23494.1.S1_at	LOC516399	587,45	1914,11	3,26	2,86	3,78	1326,65	similar to UDP-glucose:glycoprotein glucosyltransferase 2
Bt.13771.2.S1_at	MGC152529	1221,44	452,67	-2,7	-2,43	-3,02	-768,77	Similar to CD134 homologue
Bt.8327.1.S1_at	LOC507622	2672,59	539,46	-4,95	-4,32	-5,81	-2133,13	similar to chromosome 13 open reading frame 14
Bt.12536.1.S1_at	KCNK2	5028,34	1687,78	-2,98	-2,68	-3,34	-3340,55	potassium channel, subfamily K, member 2
Bt.27717.1.A1_at	---	836,63	166,16	-5,04	-4,17	-6,33	-670,47	Transcribed locus
Bt.2047.1.S1_at	ADM	40,06	1052,64	26,27	20,26	37,29	1012,57	adrenomedullin
Bt.9300.1.A1_at	LOC519626	511,1	147,95	-3,45	-3	-4,06	-363,15	similar to opioid growth factor receptor-like 1
Bt.3236.2.S1_at	LOC782247	48,9	368,02	7,53	5,36	12,52	319,12	similar to RhoGEF protein
Bt.27471.1.S1_at	LOC618415	1081,74	129,09	-8,38	-6,26	-12,64	-952,65	similar to synaptogyrin 3
Bt.5163.2.S1_at	---	110,26	506	4,59	3,74	5,9	395,74	Transcribed locus, weakly similar to NP_001847.3 1 type XVI collagen precursor [Homo sapiens]
Bt.17635.1.A1_at	MGC152587	1460,74	278,85	-5,24	-4,18	-6,99	-1181,89	similar to ELOVL4
Bt.16053.1.S1_at	LOC781625	312,7	55,64	-5,62	-4,44	-7,62	-257,06	similar to plexin D1
Bt.26715.1.S1_at	ST14	1843,41	378,86	-4,87	-3,97	-6,26	-1464,55	suppression of tumorigenicity 14
Bt.14106.1.A1_at	---	184,85	1409,9	7,63	6,62	8,96	1225,05	Transcribed locus
Bt.15732.1.S1_at	MGC157216	3512,82	7805,4	2,22	2,08	2,38	4292,58	similar to HMGIC fusion partner-like 2
Bt.10124.1.S1_at	LOC513129	12,11	581,07	47,97	25,53	388,09	568,96	hypothetical LOC513129
Bt.23555.2.S1_at	---	1371,56	3165,83	2,31	2,12	2,53	1794,27	---
Bt.2453.1.S1_at	LOC505599	2409,93	5653,51	2,35	2,18	2,54	3243,58	similar to RNA polymerase II subunit hRPB17
Bt.4451.1.S1_at	MGC137365	2825,41	1046,95	-2,7	-2,45	-3	-1778,46	similar to four and a half LIM domains 2
Bt.27386.1.A1_at	LOC527956	263,76	805,11	3,05	2,71	3,49	541,34	similar to ankyrin repeat domain 50
Bt.19192.1.S1_at	---	786,83	18,13	-43,4	-23,65	-259,07	-768,7	Transcribed locus
Bt.25952.1.A1_at	---	420,59	1004,37	2,39	2,19	2,62	583,78	---
Bt.12663.1.S1_at	LOC514812	1881,92	7016,37	3,73	3,23	4,4	5134,45	cytokeratin 19
Bt.26708.1.A1_at	LOC537314	2182,24	558,26	-3,91	-3,33	-4,72	-1623,99	similar to leucine rich repeat containing 16
Bt.21454.1.S1_at	GPRC5C	3719,7	1136,15	-3,27	-2,93	-3,7	-2583,55	G protein-coupled receptor, family C, group 5, member C
Bt.2508.1.S1_at	---	343,85	72,38	-4,75	-3,93	-5,99	-271,47	Transcribed locus
Bt.9723.1.S1_at	---	28,57	850,94	29,79	22,63	43,52	822,38	Transcribed locus
Bt.15561.1.S1_at	LOC514259	1159,81	2623,86	2,26	2,11	2,43	1464,05	hypothetical LOC514259
Bt.4441.1.S1_at	LOC509889	523,21	2661,9	5,09	4,04	6,83	2138,69	hypothetical LOC509889
Bt.26316.1.A1_at	---	55,95	666,29	11,91	8,29	20,94	610,34	Transcribed locus
Bt.7288.1.S1_at	SSR4	2171,09	8545,32	3,94	3,48	4,53	6374,23	signal sequence receptor, delta (translocon-associated protein delta)
Bt.10967.1.S1_at	LOC540924	1157,21	4245,25	3,67	3,33	4,08	3088,04	similar to cartilage-associated protein (CASP)
Bt.5959.1.S1_at	LOC526726	11,83	219,89	18,59	8,91	100000000	208,06	similar to Retinal short chain dehydrogenase reductase
Bt.21083.1.S1_at	LOC504658	369,73	2493,92	6,75	5,71	8,2	2124,18	hypothetical LOC504658
Bt.24716.1.S1_at	---	1986,11	8638,22	4,35	3,82	5,05	6652,1	Transcribed locus
Bt.16467.2.A1_at	LOC532960	962,04	244,62	-3,93	-3,34	-4,77	-717,41	similar to KIAA1378 protein

probe set	GENE ID	baseline mean (LS	periment mean (E	fold change	lower bound of F	upper bound of F	difference of me	Gene Title
Bt.25761.1.S1_at	LOC780994 /// TI	801,95	2076,41	2,59	2,34	2,89	1274,45	THO complex 7 homolog (Drosophila) /// hypothetical protein LOC780994
Bt.16051.1.S1_at	LOC513279	281,87	720,15	2,55	2,31	2,85	438,28	similar to KIAA0595 protein
Bt.15732.1.S1_a	MGC157216	1193,06	3141,64	2,63	2,38	2,94	1948,58	similar to HMGIC fusion partner-like 2
Bt.7500.1.S1_at	RAB8B	2454,15	1126,48	-2,18	-2,01	-2,37	-1327,66	RAB8B, member RAS oncogene family
Bt.20193.1.S1_at	GARS	2824,8	6231,42	2,21	2,03	2,4	3406,62	glycyl-tRNA synthetase
Bt.2289.1.S1_at	---	464,66	1022,64	2,2	2,04	2,39	557,98	---
Bt.11192.1.S1_at	MGC139030	2020,75	5216,7	2,58	2,36	2,85	3195,95	similar to inducible poly(A)-binding protein
Bt.1701.2.A1_a_	LOC616222	1445,99	4557,02	3,15	2,98	3,34	3111,03	similar to nonclathrin coat protein zeta-COP
Bt.23779.1.A1_a	---	16,95	1498,1	88,37	47,67	599,56	1481,15	Transcribed locus
Bt.12966.1.S1_at	NOLA2	930,32	5433,35	5,84	5,02	6,98	4503,02	nucleolar protein family A, member 2
Bt.16719.1.A1_a	---	891,03	2155,9	2,42	2,21	2,66	1264,88	---
Bt.23285.1.S1_at	LOC616719	597,98	1451	2,43	2,21	2,68	853,02	hypothetical LOC616719
Bt.26673.1.S1_at	LOC535280	4470,98	131,87	-33,91	-22,38	-69,65	-4339,11	similar to neuroblastoma, suppression of tumorigenicity 1 1
Bt.9288.3.A1_at	LOC510738	17,59	1004,3	57,09	34,52	164,12	986,71	similar to FLJ00258 protein
Bt.2949.1.S1_at	MGC138032	483,77	37,25	-12,99	-8,34	-28,96	-446,51	similar to Growth factor receptor-bound protein 7 (GRB7 adapter protein) (Epidermal growth factor receptor GRB-7) (B47)
Bt.9708.2.S1_at	CUTC	2019,38	604,17	-3,34	-2,9	-3,92	-1415,21	cutC copper transporter homolog (E. coli)
Bt.11259.1.S1_at	ISG12(A)	11418,3	1870,74	-6,1	-5,41	-6,98	-9547,57	similar to putative ISG12(a) protein
Bt.1645.1.S1_at	PTGDS	4636,71	932,24	-4,97	-4,14	-6,19	-3704,47	prostaglandin D2 synthase 21kDa (brain)
Bt.2520.1.S1_at	LOC523846	151,26	726,99	4,81	4,17	5,65	575,73	similar to testican-2
Bt.9248.1.A1_at	TNFRSF19L	132,49	2490,54	18,8	13,37	31,47	2358,05	tumor necrosis factor receptor superfamily, member 19-like
Bt.1954.1.S1_at	---	2250,07	942,61	-2,39	-2,2	-2,61	-1307,46	Transcribed locus
Bt.22079.1.A1_a	---	223,16	947,19	4,24	3,62	5,11	724,04	Transcribed locus
Bt.1336.1.S1_at	LOC617340	567,85	37,94	-14,97	-7,84	-153,79	-529,91	similar to putative emu2 protein
Bt.8874.1.S1_at	LOC514296	682,94	2468,91	3,62	3,07	4,37	1785,98	hypothetical LOC514296
Bt.12811.1.S1_a	UACA	4748,53	1778,46	-2,67	-2,46	-2,91	-2970,07	uveal autoantigen with coiled-coil domains and ankyrin repeats
Bt.14272.1.A1_a	---	1412,58	5121,27	3,63	3,33	3,97	3708,69	Transcribed locus
Bt.17605.1.A1_a	---	146,63	737,58	5,03	4,09	6,49	590,95	Transcribed locus
Bt.15667.1.S1_at	LOC539361	5920,43	1872,7	-3,16	-2,88	-3,49	-4047,73	similar to adipocyte determination and differentiation-dependent factor 1
Bt.18748.1.A1_a	LOC505696	59	11022,4	186,83	135,92	298,63	10963,41	similar to Protein tyrosine phosphatase, receptor type, B
Bt.4137.1.A1_at	LOC507436	798,5	2734,2	3,42	3,14	3,76	1935,7	similar to Putative lymphocyte G0/G1 switch protein 2
Bt.23318.1.S1_at	LOC510833	1743,47	7524,01	4,32	3,7	5,16	5780,54	similar to Collagen alpha 1(III) chain precursor
Bt.6651.1.S1_at	LOC781063	6730,01	1398,24	-4,81	-4,04	-5,93	-5331,77	similar to T-box 3 (ulnar mammary syndrome)
Bt.20430.1.A1_a	LOC537521	333,29	47,4	-7,03	-5,12	-11,14	-285,89	similar to KIAA1622 protein
Bt.3732.1.A1_at	---	2419,35	5269,13	2,18	2,07	2,3	2849,78	Transcribed locus
Bt.12510.3.S1_at	LOC509824 /// LC	41,1	312,42	7,6	5,34	13,06	271,32	similar to Os08g0528700 /// similar to Mucoepidermoid carcinoma translocated protein 1 (Transducer of regulated cAMP response element-binding protein 1) (Transducer of CREB protein 1)
Bt.10161.1.A1_a	---	529,99	21,11	-25,11	-14,66	-87,26	-508,88	Transcribed locus
Bt.9179.1.A1_at	LOC509283	585,42	1490,55	2,55	2,31	2,83	905,13	similar to chromosome 17 open reading frame 27
Bt.13443.1.S1_at	LOC531208	472,79	70,45	-6,71	-5,07	-9,82	-402,34	similar to KIAA0363
Bt.12263.1.S1_at	DLL4	2129,59	264,6	-8,05	-6,23	-11,35	-1864,99	delta-like 4 protein
Bt.16710.2.S1_at	---	578,61	1694,8	2,93	2,63	3,3	1116,19	Transcribed locus
Bt.24717.2.S1_a	MED6	705,02	247,04	-2,85	-2,55	-3,23	-457,98	mediator complex subunit 6
Bt.2824.1.S1_at	MGC137062	996,53	2559,56	2,57	2,35	2,83	1563,03	similar to Biogenesis of lysosome-related organelles complex-1, subunit 1 (BLOC-1 subunit 1) (GCN5-like protein 1) (RT14 protein)
Bt.28173.2.S1_at	LOC512700	308,93	11,53	-26,78	-12,16	-100000000	-297,39	similar to Flt3
Bt.12404.1.S1_at	CLPTM1L	3036,58	6569,22	2,16	2,01	2,34	3532,64	CLPTM1-like
Bt.13975.2.A1_a	LOC613972	9494,11	175,42	-54,12	-40,29	-82,34	-9318,69	Similar to Apolipoprotein D precursor (Apo-D) (ApoD)
Bt.22665.1.S1_at	GART	975,23	2353,7	2,41	2,19	2,68	1378,47	phosphoribosylglycinamide formyltransferase
Bt.11465.1.S1_at	hmg-coa-r	627,8	2222,01	3,54	3,06	4,18	1594,21	3-hydroxy-3-methylglutaryl CoA reductase
Bt.18578.1.A1_a	---	575,1	64,11	-8,97	-5,98	-17,73	-510,99	---
Bt.20581.2.S1_at	---	58,1	336,4	5,79	4,37	8,5	278,31	Transcribed locus
Bt.18169.1.A1_a	---	123,07	16,04	-7,67	-5,44	-12,93	-107,03	---
Bt.13986.1.S1_at	LOC404110	13071,65	5618,84	-2,33	-2,14	-2,55	-7452,81	EST00848 homolog
Bt.24907.1.A1_a	ADSS	5871	1128,65	-5,2	-4,34	-6,49	-4742,35	adenylosuccinate synthase
Bt.21102.1.S1_at	---	321,07	12,29	-26,13	-16,69	-59,75	-308,78	---
Bt.28173.3.A1_a	LOC512700	1737,37	10,77	-161,29	-66,41	-100000000	-1726,6	similar to Flt3
Bt.2638.1.S1_at	SERPINF1	260,55	14013,7	53,78	40,15	81,34	13753,15	serpin peptidase inhibitor, clade F (alpha-2 antiplasmin, pigment epithelium derived factor), member 1
Bt.12864.1.S1_at	MGC133682	1072,66	2361,96	2,2	2,02	2,41	1289,3	similar to 14 kDa phosphohistidine phosphatase (Phosphohistidine phosphatase 1)
Bt.18166.1.A1_a	LOC540709	1905,85	391,79	-4,86	-4,17	-5,81	-1514,06	similar to KIAA0941 protein
Bt.3026.1.A1_at	MGC137536	759,81	1844,55	2,43	2,21	2,68	1084,73	similar to Transcription elongation factor A protein 3 (Transcription elongation factor S-II protein 3) (Transcription elongation factor TFIIS.h)
Bt.26960.1.S1_at	---	931,79	2889,23	3,1	2,8	3,47	1957,43	CDNA clone MGC:165765 IMAGE:8011844
Bt.19334.3.S1_at	LOC517192	385,04	67,66	-5,69	-4,31	-8,31	-317,38	similar to jun D proto-oncogene
Bt.26755.3.S1_a	LOC783009	744,66	214,55	-3,47	-2,99	-4,12	-530,11	similar to KIAA0674 protein
Bt.29029.1.S1_at	MGC151590	1005,71	2471,53	2,46	2,25	2,7	1465,82	similar to transforming, acidic coiled-coil containing protein 2
Bt.15298.1.A1_a	---	205,17	8,91	-23,02	-9,58	-100000000	-196,26	Transcribed locus

probe set	GENE ID	baseline mean (LS	periment mean (L	fold change	lower bound of F	upper bound of F	difference of me	Gene Title
Bt.18577.2.A1_at	---	287,6	763,95	2,66	2,38	2,99	476,35	Transcribed locus
Bt.17000.1.A1_at	LOC510272	720,22	2589,48	3,6	3,04	4,37	1869,26	hypothetical LOC510272
Bt.12366.1.S1_at	MGC128891	889,66	2007,73	2,26	2,07	2,47	1118,07	similar to cyclin L2
Bt.10859.1.A1_at	MGC139506	2742,15	762,25	-3,6	-3,18	-4,13	-1979,9	similar to cAMP responsive element binding protein-like 2
Bt.9711.1.S1_at	LOC510065	2477,92	941,55	-2,63	-2,36	-2,96	-1536,37	hypothetical LOC510065
Bt.4688.1.S1_a_a	LOC510830	552,2	2288,81	4,14	3,49	5,08	1736,61	similar to KIAA1169 protein
Bt.22413.1.A1_at	MGC155172	151,27	846,95	5,6	4,45	7,54	695,68	Similar to TLE4 protein
Bt.19656.3.A1_at	BCL10	203,54	1,69	-120,47	-32,67	-100000000	-201,85	B-cell CLL/lymphoma 10
Bt.405.1.S1_at	FST	300,19	21,36	-14,05	-7,42	-125,3	-278,82	follistatin
Bt.15722.1.S1_at	FBL	5404,37	2322,02	-2,33	-2,12	-2,58	-3082,36	fibrillarin
Bt.5484.1.S1_at	vldlr	270,64	4058,25	15	12,78	18,12	3787,61	very low density lipoprotein receptor
Bt.3211.1.S2_at	GABARAPL1	7942,4	3551,16	-2,24	-2,06	-2,44	-4391,24	GABA(A) receptor-associated protein like 1
Bt.648.2.S1_at	MGC151609	1571,72	269,28	-5,84	-5,24	-6,57	-1302,44	similar to TRIP protein
Bt.27089.1.S1_at	---	2523,93	602,5	-4,19	-3,8	-4,65	-1921,42	Transcribed locus
Bt.22589.1.S1_at	MGC155183	320,18	1256,06	3,92	3,34	4,72	935,88	similar to group XIIA secreted phospholipase A2
Bt.1798.1.S1_at	MANBA	435,64	1170,81	2,69	2,4	3,05	735,18	mannosidase, beta A, lysosomal
Bt.9169.1.A1_at	LOC513730	7220,03	2671,01	-2,7	-2,47	-2,98	-4549,02	similar to notch 2 preproprotein
Bt.25475.1.A1_at	---	17,17	5243,9	305,44	190,16	775,1	5226,73	Transcribed locus
Bt.1452.2.A1_at	---	1561	469,49	-3,32	-2,86	-3,96	-1091,51	Transcribed locus
Bt.8879.1.A1_at	---	82,2	713,82	8,68	6,13	14,68	631,61	Transcribed locus
Bt.4336.1.S1_at	DF	1831,72	357,65	-5,12	-3,96	-7,2	-1474,07	D component of complement (adipsin)
Bt.17496.1.S1_at	LOC511508	3202,87	1198,28	-2,67	-2,4	-3,01	-2004,6	similar to KIAA0438
Bt.20359.1.S1_at	MGC148465	325,23	32,89	-9,89	-6,74	-18,3	-292,34	similar to IKAROS family zinc finger 3 (Aiolos)
Bt.14398.1.S1_at	MGC127772	138,62	8274,31	59,69	44,6	90,13	8135,7	similar to phosphatidylethanolamine-binding protein 4
Bt.4108.1.S1_at	MGC151609	6511,33	663,69	-9,81	-8,19	-12,19	-5847,64	similar to TRIP protein
Bt.4831.1.S1_at	NDP52	2379,61	966,85	-2,46	-2,22	-2,75	-1412,76	nuclear domain 10 protein
Bt.2257.1.S1_at	---	1561,84	4089,56	2,62	2,4	2,87	2527,71	Transcribed locus
Bt.7346.1.S1_at	LOC507464	105,65	1095,38	10,37	8,12	14,26	989,72	similar to keratin 15
Bt.16861.1.A1_at	LOC515128	282,76	1381,79	4,89	3,96	6,35	1099,03	hypothetical LOC515128
Bt.4203.1.S1_at	LOC506492	1014,49	3288,94	3,24	2,82	3,79	2274,46	F1Fo-ATP synthase complex Fo membrane domain f subunit
Bt.11179.1.S1_at	ITFG3	452,84	2519,07	5,56	4,58	7,09	2066,23	integrin alpha FG-GAP repeat containing 3
Bt.17939.1.S1_at	LOC540643	28,56	156,85	5,49	4,28	7,58	128,28	similar to Lamin-B1
Bt.9958.1.S1_at	IGFBP6	13807,12	1270,08	-10,87	-7,74	-18,25	-12537,04	insulin-like growth factor binding protein 6
Bt.5302.1.S1_a_a	MRVI1	142,67	411,32	2,88	2,53	3,34	268,64	murine retrovirus integration site 1 homolog
Bt.28975.1.S1_at	LOC538841	300,57	2547,91	8,48	7,57	9,6	2247,34	similar to Zinc finger SWIM domain-containing protein 6
Bt.5395.1.S1_a_a	CSPG2	13,26	159,71	12,04	6,78	52,12	146,44	chondroitin sulfate proteoglycan 2 (versican)
Bt.26030.1.A1_at	LOC789674	613,5	8349,51	13,61	12,77	14,56	7736	similar to Calpain 10
Bt.7142.1.S1_at	LOC617914	811,35	213,18	-3,81	-3,16	-4,76	-598,17	similar to OTTHUMP00000028701
Bt.27939.2.A1_a	LOC525346	1396,91	315,86	-4,42	-3,69	-5,5	-1081,05	similar to nuclear receptor coactivator-1
Bt.13324.1.S1_a	IDH1	336,47	31,2	-10,79	-8,2	-15,64	-305,28	isocitrate dehydrogenase 1 (NADP+), soluble
Bt.26692.1.S1_a	LOC615342	653	186,15	-3,51	-2,97	-4,27	-466,85	similar to BCL2/adenovirus E1B 19-kDa protein-interacting protein 3
Bt.8121.1.S1_x_a	BOLA	3888,25	37,27	-104,33	-59,36	-428,89	-3850,98	Classical MHC class I antigen
Bt.16738.1.A1_at	LOC540417	7372,64	1556,97	-4,74	-4	-5,79	-5815,67	similar to Iroquois related homeobox 3 (Drosophila)
Bt.7815.1.A1_at	---	543,28	120,16	-4,52	-3,71	-5,76	-423,12	Transcribed locus
Bt.7773.1.S1_x_a	BOLA	5435,34	116,43	-46,68	-27,67	-148,22	-5318,91	MHC class I heavy chain
Bt.27403.1.S1_at	LOC540987	4818,55	1863,2	-2,59	-2,41	-2,79	-2955,36	similar to Chromosome 5 open reading frame 5
Bt.16092.1.S1_at	---	860,19	2788,22	3,24	2,99	3,53	1928,03	Transcribed locus
Bt.18639.2.S1_at	FBXO32	252,41	43,67	-5,78	-4,45	-8,18	-208,74	F-box protein 32
Bt.29025.1.A1_at	LOC523809	7,02	127,55	18,18	8,21	100000000	120,53	similar to KIAA1959 protein
Bt.24501.1.A1_at	LOC539689	525,17	1539,45	2,93	2,62	3,31	1014,28	similar to Cartilage paired-class homeoprotein 1
Bt.17928.2.A1_at	LOC532126	3417,95	854,51	-4	-3,28	-5,09	-2563,44	similar to transmembrane protein 16A
Bt.2147.1.S1_at	---	166,84	1609	9,64	8,17	11,73	1442,16	Transcribed locus
Bt.24794.1.A1_at	C6orf106	2100,35	915,09	-2,3	-2,12	-2,49	-1185,26	Hypothetical protein LOC617655
Bt.1573.2.S1_a_a	FDX1	816,32	2396,68	2,94	2,66	3,28	1580,36	ferredoxin 1
Bt.5495.1.S1_at	BZW2	453,87	1231,38	2,71	2,4	3,11	777,51	basic leucine zipper and W2 domains 2
Bt.21662.1.S1_at	ATP6V0E2	641,73	89,68	-7,16	-4,97	-12,61	-552,05	ATPase, H+ transporting V0 subunit e2
Bt.27288.1.S1_at	---	65,43	424,41	6,49	4,84	9,74	358,99	Transcribed locus
Bt.3284.1.A1_a_a	MGC142824	207,29	1221,7	5,89	4,56	8,26	1014,4	similar to Not56-like protein
Bt.20296.1.S1_at	SFXN2	94,93	590,61	6,22	5,39	7,33	495,67	sideroflexin 2
Bt.20991.1.S1_at	POLR3D	357,06	775,36	2,17	2,05	2,3	418,3	polymerase (RNA) III (DNA directed) polypeptide D, 44kDa
Bt.1707.1.S1_at	VKORC1	3055,78	7698,62	2,52	2,28	2,81	4642,84	vitamin K epoxide reductase complex, subunit 1
Bt.18721.1.A1_at	---	290,95	57,43	-5,07	-3,89	-7,19	-233,52	Transcribed locus
Bt.5993.1.S1_at	KPNA2	1066,8	2856,88	2,68	2,4	3,03	1790,09	karyopherin alpha 2 (RAG cohort 1, importin alpha 1)
Bt.18639.1.A1_at	FBXO32	2140,76	563,98	-3,8	-3,29	-4,49	-1576,78	F-box protein 32

probe set	GENE ID	baseline mean (LS	periment mean (E	fold change	lower bound of F	upper bound of F	difference of me	Gene Title
Bt.9086.1.S1_at	AP1S1	9328,8	1477,88	-6,31	-5,65	-7,13	-7850,93	adaptor-related protein complex 1, sigma 1 subunit
Bt.22647.3.A1_at	LOC532952	147,61	18,74	-7,88	-5,43	-14,28	-128,87	similar to membrane-associated guanylate kinase-related 3 (MAGI-3)
Bt.27101.1.S1_at	---	915,82	175,87	-5,21	-4,02	-7,35	-739,95	Transcribed locus
Bt.8694.1.S1_at	LOC512110	7136	1862,62	-3,83	-3,27	-4,6	-5273,39	similar to Protein KIAA0195 (Transmembrane protein 94)
Bt.596.1.S1_at	PHYH	4454,61	1499,91	-2,97	-2,58	-3,49	-2954,7	phytanoyl-CoA 2-hydroxylase
Bt.8601.1.S1_at	LOC617280	145,18	729,96	5,03	3,9	7,03	584,78	similar to Rho guanine nucleotide exchange factor (GEF) 19
Bt.22373.1.A1_at	---	781,5	2068,17	2,65	2,38	2,98	1286,67	CDNA clone MGC:160111 IMAGE:8518814
Bt.4310.1.A1_at	MGC152252	250,54	21,83	-11,47	-7,39	-25,24	-228,71	similar to regulator of G-protein signalling 1
Bt.20989.1.S1_at	---	498,87	1625,29	3,26	2,82	3,85	1126,41	Transcribed locus
Bt.21044.1.A1_at	---	3277,47	1411,91	-2,32	-2,1	-2,58	-1865,56	Transcribed locus, moderately similar to XP_001092337.1 retinoic acid receptor, beta isoform 1 [Macaca mulatta]
Bt.16976.1.S1_at	---	294,19	71,37	-4,12	-3,35	-5,32	-222,82	Transcribed locus
Bt.269.1.S1_at	ATP2C1	2433,01	1028,74	-2,37	-2,13	-2,65	-1404,27	ATPase, Ca++ transporting, type 2C, member 1
Bt.13489.1.S1_at	---	1057,43	2524,51	2,39	2,17	2,64	1467,08	Transcribed locus
Bt.22458.1.S1_at	LOC512543	496,93	1945,13	3,91	3,52	4,39	1448,2	Hypothetical LOC512543
Bt.28780.2.A1_at	LOC505234	461,17	1718,87	3,73	3,32	4,23	1257,7	similar to FYVE, RhoGEF and PH domain-containing protein 4 (Actin filament-binding protein frabin) (FGD1-related F-actin-binding protein) (Zinc finger FYVE domain-containing protein 6)
Bt.27019.1.S1_at	---	31,21	506,93	16,24	9,74	47,73	475,71	Transcribed locus
Bt.12294.2.A1_at	AMIGO2	1232,77	98,83	-12,47	-10,43	-15,47	-1133,93	amphoterin induced gene 2
Bt.20014.1.S1_at	---	456,94	80,86	-5,65	-4,4	-7,89	-376,09	Transcribed locus
Bt.15808.1.S1_at	MGC142541	1383,51	235,93	-5,86	-4,7	-7,72	-1147,57	similar to membrane-associated RING-CH protein III
Bt.28390.1.S1_at	---	1417,7	576,51	-2,46	-2,2	-2,77	-841,19	CDNA clone MGC:139363 IMAGE:8278811
Bt.18965.1.A1_at	LOC537901	501,59	132,07	-3,8	-3,19	-4,68	-369,52	Similar to Na+-driven Cl-HCO3 exchanger
Bt.22465.1.S1_at	LOC615055	72,66	401,44	5,53	4,13	8,28	328,78	similar to EF-hand calcium binding domain 4A
Bt.8166.3.A1_s_a	CXXC5	94,7	1603,08	16,93	13,43	22,81	1508,37	CXXC finger 5
Bt.11030.1.S1_at	LOC514557	815,03	3195,79	3,92	3,3	4,82	2380,76	similar to OAF homolog (Drosophila)
Bt.3706.1.S1_at	MGC152079	253,37	783,07	3,09	2,72	3,55	529,7	similar to TSC22 domain family 4
Bt.7058.1.S1_at	LOC508088	888,09	2856,21	3,22	2,84	3,68	1968,12	similar to Nuclear distribution protein nudE homolog 1 (NudE)
Bt.23317.1.S1_at	LOC508221	3708,43	8494,43	2,29	2,11	2,5	4786	RPL13 protein-like
Bt.28362.1.S1_at	LOC613810	174,72	589,94	3,38	2,87	4,09	415,22	similar to serine/threonine protein kinase
Bt.1287.1.S1_at	PMM2	451,88	1575,94	3,49	3,04	4,07	1124,06	phosphomannomutase 2
Bt.28311.1.A1_at	LOC507708	1530,34	407,04	-3,76	-3,41	-4,17	-1123,29	similar to oxysterol-binding protein-like protein OSBPL10
Bt.18986.1.S1_at	LOC511682	1053,41	3849,9	3,65	3,26	4,16	2796,49	membrane-bound transcription factor site 1 protease-like
Bt.4597.1.S1_at	GPR68	34,5	294,64	8,54	5,43	19,7	260,14	G protein-coupled receptor 68
Bt.10541.1.S1_at	LOC535643	1174,25	3577,89	3,05	2,64	3,59	2403,64	similar to microtubule associated serine/threonine kinase 2
Bt.28481.1.A1_at	---	84,87	401,09	4,73	3,84	6,1	316,22	Transcribed locus
Bt.11413.1.S1_at	RAB7B	116,29	460,33	3,96	3,24	5,05	344,04	RAB7B, member RAS oncogene family
Bt.29280.1.S1_at	---	135,37	1906,06	14,08	8,53	39,35	1770,69	Transcribed locus
Bt.28082.1.S1_at	MGC139253	932,3	2810,64	3,01	2,6	3,57	1878,34	hypothetical LOC533562
Bt.7327.2.S1_a_a	MGC133692	3403,72	7982,69	2,35	2,12	2,62	4578,97	hypothetical LOC506714
Bt.10620.1.S1_at	LOC537203	1069,81	3808,92	3,56	2,97	4,43	2739,1	similar to DOCK180 protein
Bt.15358.1.S1_at	---	1516,96	525,82	-2,88	-2,5	-3,38	-991,15	Transcribed locus
Bt.15788.3.S1_at	LOC507402	41,12	228,56	5,56	4,11	8,51	187,44	Similar to Bone marrow stromal cell antigen 2
Bt.9078.2.S1_a_a	LOC505916	78,73	421,54	5,35	4,21	7,29	342,81	similar to spermidine synthase
Bt.10911.1.S1_at	LOC506495 /// LC	446,05	1027,57	2,3	2,08	2,57	581,53	hypothetical LOC506495 /// similar to zinc finger protein 665 /// hypothetical LOC619052 /// similar to Zinc finger protein Kr18 (HKr18)
Bt.23007.1.A1_at	MGC151906	751,54	297,85	-2,52	-2,24	-2,87	-453,69	Similar to Sorcin (22 kDa protein) (CP-22) (V19)
Bt.21957.1.S1_at	---	3350,26	1036,2	-3,23	-2,86	-3,7	-2314,07	Transcribed locus
Bt.22857.1.S2_at	TRB2	407,82	1687,56	4,14	3,52	5,01	1279,74	TRB-2 protein
Bt.2749.1.S1_at	LOC513497	525	2387,3	4,55	3,82	5,61	1862,31	similar to p21/WAF1
Bt.19625.1.A1_at	---	1172,68	260,64	-4,5	-3,81	-5,48	-912,04	Transcribed locus, weakly similar to NP_055525.3 protein-coupled receptor associated sorting protein 1 [Homo sapiens]
Bt.2367.1.A1_at	NT5E	37,65	6631,99	176,17	81,96	100000000	6594,34	5'-nucleotidase, ecto (CD73)
Bt.27984.1.S1_x_	IgCgamma	242,19	17,66	-13,71	-7,67	-62,03	-224,53	IgG2a heavy chain constant region
Bt.26227.1.A1_at	---	4738,96	1785,3	-2,65	-2,36	-3,02	-2953,66	Transcribed locus
Bt.5598.1.S1_at	C8ORF4	14400,93	4398,91	-3,27	-2,78	-3,96	-10002,02	chromosome 8 open reading frame 4
Bt.2506.1.S1_at	LOC506627	212,58	2697,21	12,69	10,55	15,87	2484,63	similar to dickkopf homolog 3
Bt.10105.1.S1_at	LOC523277	306,09	5,57	-54,98	-11,95	-100000000	-300,52	similar to membrane glycoprotein
Bt.16808.2.A1_at	MGC139757	507,98	23,54	-21,58	-12,61	-73,37	-484,44	similar to RAS-like, family 12 protein
Bt.4078.2.S1_a_a	RCN3	242,55	705,71	2,91	2,58	3,32	463,17	reticulocalbin 3, EF-hand calcium binding domain
Bt.6127.1.S1_at	GLB1	1114,09	2925,59	2,63	2,32	3,02	1811,5	galactosidase, beta 1
Bt.9925.1.S1_at	---	295,35	1548,53	5,24	4,57	6,16	1253,18	---
Bt.6354.1.S1_at	LOC539337	2575,37	604,44	-4,26	-3,91	-4,66	-1970,93	similar to wingless-type MMTV integration site family, member 10B
Bt.1422.1.S1_at	---	283,15	2067,54	7,3	5,53	10,74	1784,39	Transcribed locus
Bt.29102.1.S1_at	---	36,09	275,33	7,63	5,08	15,02	239,24	Transcribed locus
Bt.16326.1.S1_at	LOC515475	666,91	107,6	-6,2	-4,48	-9,97	-559,32	hypothetical LOC515475
Bt.28186.1.S1_at	---	973,55	324,12	-3	-2,69	-3,38	-649,43	Transcribed locus, strongly similar to XP_001106588.1 similar to angiogenic factor VG5Q isoform 1 [Macaca mulatta]

probe set	GENE ID	baseline mean (LS	periment mean (L	fold change	lower bound of F	upper bound of F	difference of me	Gene Title
Bt.5365.1.S1_at	LOC508208	424,39	128,11	-3,31	-2,79	-4,05	-296,28	similar to LATS, large tumor suppressor, homolog 2 (Drosophila)
Bt.27719.1.A1_at	SH3BP4	245,18	62,34	-3,93	-3,25	-4,95	-182,83	SH3-domain binding protein 4
Bt.22803.1.S2_at	LOC533307	1429,44	4162,83	2,91	2,54	3,4	2733,39	hypothetical LOC533307
Bt.10543.1.S1_at	LOC784675	1146,86	2926,94	2,55	2,31	2,83	1780,08	Similar to KIAA1462 protein
Bt.12588.1.S1_at	---	6979,05	2937,05	-2,38	-2,15	-2,66	-4042,01	Transcribed locus
Bt.24478.1.S1_at	LOC540132	796,7	226,82	-3,51	-2,93	-4,36	-569,88	Similar to TNE5
Bt.20968.1.S1_at	VSNL1	20,67	156,93	7,59	5,05	15,04	136,26	visinin-like 1
Bt.22046.1.S1_at	LOC540376	528,26	1358,51	2,57	2,28	2,94	830,25	similar to Alpha-methylacyl-CoA racemase (2-methylacyl-CoA racemase)
Bt.16770.1.A1_at	---	167,01	43,44	-3,84	-3,19	-4,8	-123,56	---
Bt.15905.1.S1_at	---	1616,51	687,61	-2,35	-2,12	-2,63	-928,91	Transcribed locus
Bt.9698.1.S1_at	MGC142910	1896,78	844,6	-2,25	-2,05	-2,48	-1052,18	similar to CSaids binding protein
Bt.8251.1.A1_at	LOC514192	317,1	976,96	3,08	2,63	3,69	659,86	similar to YEATS domain containing 2
Bt.13336.2.S1_at	SMC4L1	71,78	182,23	2,54	2,26	2,89	110,45	SMC4 structural maintenance of chromosomes 4-like 1 (yeast)
Bt.19227.2.A1_at	---	332,44	900,57	2,71	2,4	3,09	568,14	---
Bt.24660.1.S1_at	LRRC59	1745,76	4686,54	2,68	2,44	2,98	2940,78	leucine rich repeat containing 59
Bt.13383.1.S1_at	---	47,95	578,07	12,06	7,92	25,16	530,12	Transcribed locus
Bt.9556.1.S1_at	MEST	609,05	2204,93	3,62	3,3	3,99	1595,88	mesoderm specific transcript homolog (mouse)
Bt.20286.1.S1_at	---	1982,19	540,95	-3,66	-3,12	-4,43	-1441,25	CDNA clone MGC:154987 IMAGE:8563345
Bt.4850.2.S1_at	MGC140785	443,05	1932,08	4,36	3,86	4,98	1489,02	similar to 5-nucleotidase, cytosolic III
Bt.24459.1.A1_at	DCP1B	1285,88	537,71	-2,39	-2,16	-2,67	-748,17	DCP1 decapping enzyme homolog B (S. cerevisiae)
Bt.15952.1.A1_at	LOC512176 /// LO	673	134,01	-5,02	-4,11	-6,41	-538,99	similar to SEC14 and spectrin domains 1
Bt.19508.1.A1_at	LOC540179	292,67	1354,22	4,63	3,67	6,18	1061,55	similar to glypican 4
Bt.13313.2.S1_at	LOC525346	1294,19	273,45	-4,73	-3,73	-6,45	-1020,73	similar to nuclear receptor coactivator-1
Bt.11462.1.S1_at	SDC2	1432,46	514,48	-2,78	-2,45	-3,22	-917,98	syndecan 2
Bt.5888.1.S1_at	LOC782900	1169,22	3144,98	2,69	2,53	2,86	1975,76	similar to SNHG8 protein
Bt.27030.1.S1_at	LOC538640	14,73	1036,25	70,37	31,96	100000000	1021,53	similar to RBM35A protein
Bt.2871.2.A1_at	---	3404,94	1244,04	-2,74	-2,41	-3,17	-2160,9	Transcribed locus
Bt.10515.1.S1_at	MGC151821	1027,6	4574	4,45	3,98	5,03	3546,4	similar to NXN protein
Bt.9067.1.S1_at	---	668,65	1512,55	2,26	2,04	2,53	843,9	Transcribed locus
Bt.5237.1.S1_at	IGFBP4	1873,8	740,74	-2,53	-2,27	-2,84	-1133,06	insulin-like growth factor binding protein 4
Bt.27321.1.S1_at	---	285,06	720,66	2,53	2,23	2,9	435,6	Transcribed locus
Bt.11932.1.S1_at	---	2784,06	6441,93	2,31	2,15	2,5	3657,87	Transcribed locus
Bt.26635.1.S1_at	FZD1	2308,11	550,1	-4,2	-3,44	-5,35	-1758,01	frizzled homolog 1 (Drosophila)
Bt.13465.1.S1_at	MGC137215	376,85	962,11	2,55	2,25	2,93	585,26	similar to COMM domain containing 6
Bt.3714.2.S1_at	---	804,75	259,08	-3,11	-2,64	-3,75	-545,67	---
Bt.5455.3.S1_a_at	LOC513782	180,89	35,29	-5,13	-3,84	-7,61	-145,6	similar to PRPF40B protein
Bt.11212.1.S1_at	LOC781759 /// V	718,53	41,98	-17,12	-11,57	-32,56	-676,55	vasoactive intestinal peptide /// similar to vasoactive intestinal polypeptide
Bt.22111.1.S1_at	---	659,54	183,17	-3,6	-3,18	-4,12	-476,38	Transcribed locus
Bt.23659.1.S1_at	---	210,69	76,99	-2,74	-2,38	-3,2	-133,7	Transcribed locus
Bt.6817.1.S1_at	---	2819,98	197,46	-14,28	-10,83	-20,84	-2622,53	Transcribed locus
Bt.471.1.S1_at	THBD	3301,06	10,49	-314,84	-87,25	-100000000	-3290,57	thrombomodulin
Bt.7873.1.S1_at	LU	611,9	1655,17	2,7	2,37	3,14	1043,26	Lutheran blood group (Auberger b antigen included)
Bt.26602.1.S1_at	MGC139115	155,38	442,78	2,85	2,47	3,36	287,39	hypothetical LOC509157
Bt.21721.1.A1_at	MGC137635	48,31	195,17	4,04	3,23	5,35	146,87	similar to ubiquitin specific protease 2
Bt.8275.1.S1_at	---	131,4	2605,97	19,83	15,33	28	2474,57	Transcribed locus
Bt.27114.1.A1_at	---	1213,25	4045,38	3,33	3,11	3,58	2832,13	Transcribed locus
Bt.23619.1.S1_a_at	LOC540101	266,44	44,63	-5,97	-4,22	-10,09	-221,81	similar to MGC52980 protein
Bt.20113.1.S1_at	CASP6	368,27	982,87	2,67	2,41	2,98	614,6	caspase 6, apoptosis-related cysteine peptidase
Bt.9740.1.S1_at	---	483,92	1369,35	2,83	2,44	3,35	885,43	Transcribed locus
Bt.26218.1.A1_at	---	84,83	252,64	2,98	2,57	3,52	167,81	Transcribed locus
Bt.28209.1.S1_at	LOC540954	809,64	295,14	-2,74	-2,38	-3,22	-514,5	similar to RGM domain family, member B
Bt.2612.1.S1_at	TCTEL1	600,28	1525,38	2,54	2,29	2,84	925,1	TCTEL1 protein
Bt.27452.1.A1_at	---	113,02	7,94	-14,23	-7,97	-65,77	-105,08	Transcribed locus
Bt.3278.1.A1_at	LOC616742	610,59	1761,16	2,88	2,57	3,27	1150,57	similar to Ephrin-A5 precursor (EPH-related receptor tyrosine kinase ligand 7) (LERK-7) (AL-1)
Bt.19884.1.A1_at	PLA1A	1375,93	28,67	-47,99	-21,18	-100000000	-1347,26	phospholipase A1 member A
Bt.14572.1.A1_at	---	38,94	310,94	7,99	5,06	18,64	272	Transcribed locus
Bt.5847.1.S1_at	LOC504948	1386,8	307,26	-4,51	-3,58	-6,08	-1079,54	Similar to glycerol-3-phosphate dehydrogenase
Bt.13296.2.A1_at	MGC179470	644,68	2690,57	4,17	3,46	5,26	2045,89	hypothetical LOC534290
Bt.9791.1.S1_at	LOC414346	152,82	430,36	2,82	2,47	3,25	277,54	cyclophilin F
Bt.21409.1.A1_at	COL11A1	11,91	3147,83	264,29	142,27	1848,61	3135,91	collagen, type XI, alpha 1
Bt.7676.3.S1_at	IGF2	7783,07	1279,02	-6,09	-4,92	-7,89	-6504,05	insulin-like growth factor 2
Bt.17810.1.S1_a_at	RBP1	3667,44	243,99	-15,03	-12,33	-19,2	-3423,45	retinol binding protein 1, cellular
Bt.21014.1.S1_at	LOC529905	126,26	1361,69	10,78	8,08	16,09	1235,43	hypothetical LOC529905
Bt.11832.2.A1_at	---	409,57	91,52	-4,48	-3,45	-6,33	-318,05	Transcribed locus

probe set	GENE ID	baseline mean (LS	periment mean (L	fold change	lower bound of F	upper bound of F	difference of me	Gene Title
Bt.27058.1.A1_at	LOC511976	465,08	11,44	-40,66	-17,11	-100000000	-453,65	similar to integrin, alpha 8
Bt.9286.1.S1_at	MGC137407	473,85	1172,54	2,47	2,23	2,77	698,7	similar to LPS-induced TN factor
Bt.27803.1.A1_at	LOC522810	759,27	130,27	-5,83	-4,55	-8,09	-629,01	similar to testis expressed sequence 14
Bt.6612.1.S1_at	LOC507418	207,99	591,82	2,85	2,52	3,25	383,82	hypothetical LOC507418
Bt.18637.1.A1_at	LOC506860	975,12	2192,69	2,25	2,08	2,44	1217,57	similar to 6-pyruvoyl tetrahydrobiopterin synthase precursor (PTPS) (PTP synthase)
Bt.3715.1.S1_at	LOC789063	1743,69	4850,26	2,78	2,48	3,16	3106,57	similar to chromosome 6 open reading frame 86
Bt.23171.2.S1_at	PCBD1	5357,47	2186,4	-2,45	-2,17	-2,8	-3171,06	pterin-4 alpha-carbinolamine dehydratase/dimerization cofactor of hepatocyte nuclear factor 1 alpha (TCF1)
Bt.29481.1.A1_at	MGC139804	471,15	1282,06	2,72	2,4	3,12	810,91	hypothetical LOC509583
Bt.12414.1.S1_at	LOC508633	1677,53	31,6	-53,08	-27,73	-596,34	-1645,92	similar to CD8 beta antigen
Bt.3724.1.S1_at	---	3471,37	837,44	-4,15	-3,76	-4,6	-2633,93	Transcribed locus
Bt.15667.2.S1_at	LOC539361	1019,2	235,5	-4,33	-3,67	-5,27	-783,7	similar to adipocyte determination and differentiation-dependent factor 1
Bt.26769.1.S1_at	LOC531516	556,24	11,85	-46,95	-23,48	-11604,31	-544,39	similar to GTPase, IMAP family member 8
Bt.16441.1.A1_at	LOC508151	1241,34	2875,95	2,32	2,09	2,59	1634,61	similar to Desmoglein 2
Bt.5964.3.S1_at	---	344,62	63,19	-5,45	-4,2	-7,75	-281,43	Transcribed locus
Bt.19978.1.A1_at	---	2231,25	758,94	-2,94	-2,52	-3,52	-1472,31	Transcribed locus
Bt.11386.1.S1_at	LOC510844	1938,81	248,33	-7,81	-5,91	-11,36	-1690,48	similar to Alpha-fetoprotein enhancer-binding protein (AT motif-binding factor) (AT-binding transcription factor 1)
Bt.18822.1.A1_at	TRB2	1385,72	5957,36	4,3	3,67	5,18	4571,64	TRB-2 protein
Bt.22174.1.S1_at	LOC523661	1644,82	447,42	-3,68	-3,17	-4,34	-1197,4	similar to neural plakophilin-related arm-repeat protein (NPRAP)
Bt.21770.1.S1_at	SLC29A1	3941,9	400,45	-9,84	-7,25	-15,31	-3541,45	solute carrier family 29 (nucleoside transporters), member 1
Bt.28910.1.A1_at	---	236,68	27,23	-8,69	-5,9	-16,17	-209,45	---
Bt.27339.2.S1_at	LOC536741	18,7	289,68	15,49	9,04	52,55	270,98	similar to Mme protein
Bt.22234.1.S1_at	LOC505901	499,56	53,49	-9,34	-6,3	-17,72	-446,07	similar to protein kinase C-theta
Bt.8798.2.S1_at	LOC507093 /// LC	360,52	52,54	-6,86	-5,1	-10,33	-307,97	similar to retinaldehyde dehydrogenase 3 /// similar to aldehyde dehydrogenase 6
Bt.8888.1.A1_at	LOC523408	5151,19	1248,06	-4,13	-3,71	-4,63	-3903,13	similar to importin 8
Bt.6407.1.S1_at	LOC782137 /// M	139,65	706,11	5,06	4,52	5,71	566,46	hypothetical protein LOC613986 /// hypothetical protein LOC782137
Bt.10340.1.S1_at	---	2599,12	497,2	-5,23	-4,27	-6,68	-2101,92	Transcribed locus
Bt.1760.1.S1_at	MGC148716	450,23	3493,62	7,76	7,16	8,46	3043,38	similar to CGI-114 protein
Bt.6404.1.S1_at	LOC407241	1162,36	155,21	-7,49	-5,28	-12,82	-1007,16	Kruppel-like factor 15
Bt.4065.1.S1_at	---	609,83	242,74	-2,51	-2,22	-2,88	-367,09	Transcribed locus
Bt.13324.4.S1_at	IDH1	4856,95	1981,52	-2,45	-2,28	-2,64	-2875,44	isocitrate dehydrogenase 1 (NADP+), soluble
Bt.27918.1.S1_at	LOC505059	639,29	175,02	-3,65	-3,02	-4,57	-464,27	similar to Wtip protein
Bt.5098.1.S1_at	PTPN13	2446,88	800,06	-3,06	-2,65	-3,62	-1646,82	protein tyrosine phosphatase, non-receptor type 13
Bt.8337.1.S1_at	---	1427,99	356,86	-4	-3,56	-4,54	-1071,14	Transcribed locus
Bt.20226.1.A1_at	---	4913,22	2102,39	-2,34	-2,14	-2,57	-2810,83	Transcribed locus
Bt.2846.1.A1_at	MGC154996	179,1	627,1	3,5	2,86	4,48	448	similar to ras homolog gene family, member U
Bt.22982.1.A1_at	RTN1	309,63	1149,27	3,71	2,98	4,88	839,64	reticulon 1
Bt.21741.2.A1_at	LOC530184	1830,36	209	-8,76	-7,47	-10,54	-1621,36	similar to Ssbp3 protein
Bt.20519.1.A1_at	LOC507076 /// LC	11,37	599,7	52,73	27,87	473,84	588,33	similar to dopamine-oxygenase /// hypothetical protein LOC784321
Bt.28641.1.S1_at	---	138,88	24,18	-5,74	-4,69	-7,35	-114,7	Transcribed locus, moderately similar to XP_235326.4 similar to two AAA domain containing protein [Rattus norvegicus]
Bt.13413.2.A1_at	---	174,93	583,07	3,33	2,74	4,21	408,13	Transcribed locus
Bt.6661.1.S1_at	MGC128636	1737,33	5165,93	2,97	2,54	3,55	3428,6	similar to transcription elongation factor B (SIII), polypeptide 2
Bt.14204.1.A1_at	LOC538880	1640,33	5024,43	3,06	2,7	3,54	3384,1	similar to cytoplasmic polyadenylation element binding protein CPEB2b
Bt.2091.1.S1_at	MGC139459	603,94	4273,63	7,08	5,86	8,86	3669,69	similar to RTP801
Bt.19884.2.S1_at	PLA1A	402,24	6,27	-64,16	-24,32	-100000000	-395,97	phospholipase A1 member A
Bt.9786.1.S1_at	MGC139669	603,88	44,91	-13,45	-9,03	-25,94	-558,97	similar to Alpha-N-acetylgalactosaminide alpha-2,6-sialyltransferase 2 (GalNAc alpha-2,6-sialyltransferase II) (ST6GalNAc II) (Sialyltransferase 7B)
Bt.24266.2.S1_at	LOC534869	616,58	78,15	-7,89	-4,96	-18,73	-538,43	similar to KIAA0172
Bt.19598.1.A1_at	---	367,11	10,22	-35,91	-15,91	-100000000	-356,89	---
Bt.21939.1.S1_at	---	887,08	99,88	-8,88	-5,78	-19,09	-787,21	Transcribed locus
Bt.11260.2.S1_at	LOC511904	514,12	1195,68	2,33	2,06	2,65	681,56	similar to TGOLN2 protein
Bt.19329.2.S1_at	MGC139784	995,86	66,23	-15,04	-10,82	-24,45	-929,62	similar to EF-hand domain-containing protein 1 (Swiprosin-2)
Bt.6509.3.S1_a_at	LOC511043	34,57	199,95	5,78	4,08	9,84	165,38	similar to laminin 5 gamma 2 subunit
Bt.13028.1.S1_at	POSTN	59,15	315,87	5,34	4,66	6,22	256,72	periostin, osteoblast specific factor
Bt.13604.1.S1_at	---	306,29	691,95	2,26	2,04	2,51	385,65	Transcribed locus
Bt.5531.3.S1_at	BACE1	2302,43	829,55	-2,78	-2,38	-3,31	-1472,87	beta-site APP-cleaving enzyme 1
Bt.4750.1.S1_at	TKT	2020,1	5351,13	2,65	2,31	3,09	3331,04	transketolase
BtAffx.1.2.S1_at	ATP8A1	72,78	206,12	2,83	2,42	3,39	133,33	ATPase, aminophospholipid transporter (APLT), Class I, type 8A, member 1
Bt.28395.1.S1_at	MGC137245	690,37	149,51	-4,62	-3,52	-6,62	-540,86	similar to WD repeat domain 54
Bt.4937.1.S1_at	LOC505941	4157,56	9529,14	2,29	2,09	2,54	5371,59	similar to ribosome binding protein 1
Bt.13588.1.A1_at	MGC166278	240,77	986,79	4,1	3,23	5,56	746,02	similar to Phosphoserine aminotransferase 1
Bt.28145.1.S1_at	---	70,31	368,73	5,24	4,21	6,89	298,42	Polymorphic microsatellite locus (AFZ1)
Bt.8823.2.S1_a_at	MGC126999	329,75	1041,96	3,16	2,74	3,73	712,21	similar to Protein C9orf46
Bt.14054.1.A1_at	MGC127247	2369,42	715,63	-3,31	-2,92	-3,8	-1653,8	similar to interferon-related developmental regulator 1
Bt.11408.1.A1_at	---	148,3	1609,21	10,85	9,65	12,37	1460,9	Transcribed locus
Bt.13723.1.S1_at	MGC127182	54,19	311,92	5,76	4,13	9,42	257,73	Similar to sulfotransferase family, cytosolic, 1B, member 1

probe set	GENE ID	baseline mean (LS	periment mean (L	fold change	lower bound of F	upper bound of F	difference of me	Gene Title
Bt.11362.1.A1_at	---	292,55	12,39	-23,61	-11,61	-100000000	-280,16	Transcribed locus, strongly similar to XP_001100845.1 similar to cyclic AMP-regulated phosphoprotein, 21 kD isoform 1 isoform 1 [Macaca mulatta]
Bt.28617.1.S1_at	---	3114,54	233,13	-13,36	-10,98	-17	-2881,41	Transcribed locus, weakly similar to NP_001018155.1 [Danio rerio]
Bt.22304.1.S1_at	LOC614557	542,96	225,67	-2,41	-2,19	-2,65	-317,29	hypothetical LOC614557
Bt.28305.1.S1_at	LOC515280	3916,67	76,5	-51,2	-34,35	-100,15	-3840,17	similar to hepatocellular carcinoma antigen gene 520
Bt.18674.1.A1_at	---	8,81	550,96	62,56	31,43	5015,46	542,16	Transcribed locus
Bt.4775.1.S1_at	LOC525716	3383,71	1326,92	-2,55	-2,27	-2,9	-2056,79	S100B
Bt.2933.1.S1_at	LOC788205	325,79	1227,04	3,77	3,08	4,8	901,25	hypothetical protein LOC788205
Bt.21547.1.A1_at	MGC140246	181,66	885,44	4,87	3,91	6,39	703,78	similar to plakophilin 2a
Bt.6509.1.S1_at	LOC511043	16,78	289,29	17,24	10,12	56,48	272,51	similar to laminin 5 gamma 2 subunit
Bt.17954.1.A1_at	---	205,48	533,42	2,6	2,3	2,97	327,95	Transcribed locus
Bt.12058.1.A1_at	---	2665,65	1023,26	-2,61	-2,26	-3,05	-1642,39	Transcribed locus
Bt.3778.1.S1_at	LOC526461	499,97	7296,3	14,59	12,36	17,76	6796,33	similar to interferon induced transmembrane protein 5
Bt.11058.1.A1_at	PDP	1737,32	704,32	-2,47	-2,16	-2,86	-1033	pyruvate dehydrogenase phosphatase
Bt.20236.1.S1_at	ADAMTSL4	639,6	1557,21	2,43	2,14	2,81	917,61	thrombospondin repeat containing 1
Bt.21685.1.A1_at	---	342,87	61,72	-5,56	-4,6	-6,95	-281,15	Transcribed locus
Bt.12294.1.S1_at	AMIGO2	165,69	30,51	-5,43	-3,85	-9,05	-135,18	amphoterin induced gene 2
Bt.25921.1.A1_at	---	16,89	183,39	10,86	6,16	43,57	166,51	Transcribed locus
Bt.27800.1.A1_at	MGC152029	520,45	1187,51	2,28	2,04	2,57	667,06	similar to source of immunodominant MHC-associated peptides
Bt.24919.1.S1_at	---	58,55	323,1	5,52	3,98	8,91	264,54	Transcribed locus
Bt.21944.1.S1_at	MGC139976	88,03	383,1	4,35	3,63	5,37	295,07	similar to Syndecan-1 precursor (SYND1) (CD138 antigen)
Bt.17963.1.A1_at	ARL1	829,23	2114,83	2,55	2,3	2,86	1285,6	ADP-ribosylation factor-like 1
Bt.13162.1.S1_at	KRT5	78,2	9754,99	124,74	73,65	405,88	9676,79	keratin 5 (epidermolysis bullosa simplex, Dowling-Meara/Kobner/Weber-Cockayne types)
Bt.1521.1.S1_at	RDX	2268,71	5450,04	2,4	2,25	2,58	3181,33	radixin
Bt.10341.1.S1_at	---	222,23	611,01	2,75	2,36	3,28	388,77	Transcribed locus
Bt.4956.1.S1_at	COL11A1	52,55	496,54	9,45	5,56	31,03	443,99	collagen, type XI, alpha 1
Bt.29371.1.A1_at	---	7,03	138,62	19,72	8,65	100000000	131,59	Transcribed locus
Bt.13546.1.A1_at	---	267,74	37,05	-7,23	-4,63	-16,22	-230,69	Transcribed locus
Bt.8531.1.A1_at	MGC140202	1491,88	4608,54	3,09	2,83	3,38	3116,65	hypothetical LOC512206
Bt.13757.1.S1_at	---	2149,45	286,24	-7,51	-6,1	-9,7	-1863,22	Transcribed locus
Bt.126.1.S2_at	KCNJ2	11,09	116,92	10,54	5,59	84,89	105,83	potassium inwardly-rectifying channel, subfamily J, member 2
Bt.7541.1.S1_at	LOC789324 /// N	178,79	420,21	2,35	2,08	2,68	241,42	non-metastatic cells 4, protein expressed in /// similar to nucleoside-diphosphate kinase
Bt.21215.1.A1_at	LOC506721	77,39	5356	69,21	58,35	84,96	5278,61	similar to ALL1 responsive protein ARP1c
Bt.17982.1.S1_at	---	204,15	485,6	2,38	2,09	2,75	281,45	Transcribed locus
Bt.26942.1.S1_at	LOC530164	569,02	1485,04	2,61	2,26	3,07	916,02	similar to membrane glycoprotein SP55
Bt.13495.1.S1_at	---	102,99	6065,15	58,89	42,67	94,83	5962,16	Transcribed locus
Bt.16749.1.S1_at	LOC782382	101,02	525,42	5,2	3,8	8,17	424,4	similar to plexin A3
Bt.16925.1.A1_at	LOC515156 /// L(	40,89	203,23	4,97	4,16	6,11	162,34	similar to six transmembrane endothelial antigen of PAEC /// hypothetical protein LOC784147
Bt.10870.1.S1_at	---	159,18	17,79	-8,95	-5,62	-21,74	-141,38	Transcribed locus
Bt.11696.2.S1_at	---	301,69	678,51	2,25	2	2,56	376,82	Transcribed locus
Bt.21539.1.S1_at	MGC127316	459,85	1533,65	3,34	2,9	3,91	1073,81	similar to CG32066-PB
Bt.21115.1.A1_at	MGC143381	657,28	2334,47	3,55	2,88	4,61	1677,19	similar to SEC23A (S. cerevisiae)
Bt.2798.1.S1_a_at	TMSB10	1883,14	14080,93	7,48	5,71	10,81	12197,79	thymosin, beta 10
Bt.28143.1.S1_at	---	4680,34	1953,54	-2,4	-2,19	-2,64	-2726,8	---
Bt.27968.1.S1_at	MGC155048	11,31	2236,07	197,76	96,93	100000000	2224,76	similar to autoantigen
Bt.25966.1.A1_at	CBX6	6585,59	2644,41	-2,49	-2,3	-2,71	-3941,17	Chromobox homolog 6
Bt.28201.1.S1_at	MGC148280	26,77	193,45	7,23	4,54	17,15	166,68	similar to SQAW5801
Bt.26703.1.S1_at	---	1500,38	571,29	-2,63	-2,26	-3,11	-929,08	Transcribed locus
Bt.16063.1.A1_at	---	492,67	2323,04	4,72	4,02	5,65	1830,37	Transcribed locus
Bt.6351.1.S1_at	---	80,94	384,79	4,75	3,85	6,14	303,86	Transcribed locus, weakly similar to NP_001847.3 1 type XVI collagen precursor [Homo sapiens]
Bt.2582.1.S1_at	GALNT1	183,48	719,58	3,92	3,32	4,75	536,09	UDP-N-acetyl-alpha-D-galactosamine:polypeptide N-acetylgalactosaminyltransferase 1 (GalNAc-T1)
Bt.2129.1.S1_at	LOC786175 /// L(	24,95	205,18	8,22	5,55	15,78	180,22	similar to versican V0 splice-variant
Bt.8669.1.S1_at	---	263,4	906,83	3,44	2,85	4,3	643,43	Transcribed locus
Bt.2369.1.S1_at	MGC142882	1863,69	352,12	-5,29	-4,37	-6,65	-1511,57	similar to Ubiquitin specific peptidase 3
Bt.16056.1.A1_at	LOC525906	87,19	521,5	5,98	4,96	7,47	434,31	similar to Cas-Br-M (murine) ecotropic retroviral transforming sequence b
Bt.5451.1.S1_at	RAB5B	79,25	270,15	3,41	2,77	4,4	190,9	RAB5B, member RAS oncogene family
Bt.22869.1.S1_at	FABP5	43,13	1490,83	34,57	23,09	68,35	1447,71	fatty acid binding protein 5
Bt.21956.2.A1_at	---	392,19	871,75	2,22	2,04	2,43	479,57	---
Bt.20930.1.A1_at	LOC782162 /// L(	537,33	85,61	-6,28	-4,16	-12,53	-451,72	hypothetical protein LOC782162 /// similar to folate transporter/carrier
Bt.18945.1.A1_at	LOC525772	712,47	1650,76	2,32	2,12	2,55	938,29	similar to pleckstrin homology domain containing, family G (with RhoGef domain) member 1
Bt.30.1.S1_at	CRTL1	192	2320,12	12,08	10,91	13,52	2128,12	cartilage linking protein 1
Bt.24547.1.S1_at	---	402,18	40,11	-10,03	-6,16	-25,95	-362,07	Transcribed locus
Bt.17497.1.S1_at	---	352,41	857,01	2,43	2,12	2,83	504,6	Transcribed locus
Bt.13484.1.A1_at	PPP1R3C	918,49	342,67	-2,68	-2,34	-3,11	-575,82	protein phosphatase 1, regulatory (inhibitor) subunit 3C
Bt.22013.1.S1_at	PRKCH	713,3	64,01	-11,14	-8,39	-16,42	-649,29	protein kinase C, eta

probe set	GENE ID	baseline mean (LS	periment mean (L	fold change	lower bound of F	upper bound of F	difference of me	Gene Title
Bt.5911.1.S1_at	---	2115,53	790,11	-2,68	-2,38	-3,05	-1325,42	Transcribed locus
Bt.4551.1.S1_at	CTPS	315,39	4966,06	15,75	13,28	19,27	4650,67	CTP synthase
Bt.27343.1.A1_at	LOC534114	260,64	66,5	-3,92	-3,24	-4,91	-194,14	similar to Rab3A-interacting molecule
Bt.21473.1.A1_at	MPZL1	425,35	1847,2	4,34	3,42	5,93	1421,85	myelin protein zero-like 1
Bt.3560.1.S1_at	LOC786606	437,09	138,81	-3,15	-2,62	-3,91	-298,28	similar to SH3 domain binding protein
Bt.9449.1.S1_at	LOC510175	504,82	8,1	-62,34	-28,71	-100000000	-496,72	similar to Proline-rich cyclin A1-interacting protein
Bt.12444.2.S1_at	TEX261	549,94	196,03	-2,81	-2,39	-3,37	-353,91	testis expressed 261
Bt.16220.1.S1_at	LOC538491	8617,5	2385,81	-3,61	-3,2	-4,12	-6231,69	hypothetical LOC538491
Bt.4080.1.S1_at	LOC512530	2091,89	5846,02	2,79	2,36	3,4	3754,12	similar to SEC13-like 1
Bt.20510.1.S1_at	MGC127681	2530,48	1044,87	-2,42	-2,11	-2,81	-1485,6	similar to phospholemman precursor
Bt.21119.1.A1_at	LOC525346	579,78	93,45	-6,2	-4,22	-11,6	-486,32	similar to nuclear receptor coactivator-1
Bt.22600.1.A1_at	---	217,43	57,98	-3,75	-2,94	-5,13	-159,44	Transcribed locus
Bt.17162.1.A1_at	---	223,18	33,13	-6,74	-5,51	-8,59	-190,05	Transcribed locus
Bt.28583.1.S1_s_	COL1A1 /// LOC4	2592,43	15824,73	6,1	5,16	7,42	13232,3	collagen, type I, alpha 1 /// similar to pro alpha 1(I) collagen
Bt.11380.1.A1_at	---	5,1	139,84	27,4	11,46	100000000	134,73	Transcribed locus
Bt.21015.1.S1_at	MGC142781	289,86	859,03	2,96	2,49	3,65	569,16	carnitine acetyltransferase
Bt.719.1.A1_at	---	925,76	2249,51	2,43	2,22	2,68	1323,75	Transcribed locus
Bt.20511.1.S1_at	LOC783943 /// M	451,26	52,8	-8,55	-5,29	-21,43	-398,46	similar to Ral guanine nucleotide dissociation stimulator A
Bt.28687.1.A1_at	LOC618247	35,76	340,01	9,51	7,19	13,87	304,25	similar to ZMYM6 protein
Bt.10245.1.S1_at	MGC154964	4724,74	1864,15	-2,53	-2,25	-2,9	-2860,59	similar to p130
Bt.14228.1.S1_at	RPL35	2934,09	8285,91	2,82	2,59	3,11	5351,82	ribosomal protein L35
Bt.2888.1.S1_at	OSTF1	1271,07	5123,44	4,03	3,69	4,43	3852,37	osteoclast stimulating factor 1
Bt.15667.1.S1_a_	---	9446,04	3816,6	-2,47	-2,22	-2,8	-5629,44	---
Bt.15400.1.A1_at	---	1639,24	328,24	-4,99	-4,32	-5,87	-1311	---
Bt.6728.1.A1_at	Ndn	701,65	1584,71	2,26	2,01	2,57	883,06	necdin
Bt.11704.1.S1_at	---	184,19	1201,47	6,52	4,93	9,62	1017,28	Transcribed locus
Bt.28105.1.S1_at	LOC615534	3985,13	8900,44	2,23	2,04	2,46	4915,32	similar to Fibronectin type III domain containing 3B
Bt.4929.1.S2_at	GAA	307,07	967,27	3,15	2,68	3,79	660,2	glucosidase, alpha; acid
Bt.28741.1.A1_at	MGC152526	96,77	401,47	4,15	3,54	4,97	304,7	similar to hepatocellular carcinoma antigen 519
Bt.6002.1.S1_at	LOC505787	1152,51	378,31	-3,05	-2,59	-3,68	-774,2	similar to ABC-C transporter
Bt.1756.2.S1_at	---	7473,92	3223,49	-2,32	-2,03	-2,69	-4250,43	Transcribed locus
Bt.25063.1.A1_at	---	1793,2	426,04	-4,21	-3,49	-5,25	-1367,16	Transcribed locus
Bt.20596.1.S1_at	EVA1	10,57	641,75	60,7	22,94	100000000	631,18	epithelial V-like antigen 1
Bt.9217.1.A1_at	MGC151529	546,11	185,79	-2,94	-2,44	-3,66	-360,32	Similar to RT1-149 protein
Bt.21284.1.A1_at	---	3530,16	1455,61	-2,43	-2,25	-2,62	-2074,55	Transcribed locus
Bt.3371.1.S1_at	LOC510120	37,55	313,81	8,36	5,72	15,15	276,27	similar to MCM2 minichromosome maintenance deficient 2, mitotin (S. cerevisiae)
Bt.28189.1.S1_at	---	1163,24	2742,26	2,36	2,12	2,65	1579,02	Transcribed locus
Bt.6592.1.S1_at	CDH13	2721,52	6562,9	2,41	2,18	2,69	3841,38	cadherin 13, H-cadherin (heart)
Bt.29143.1.S1_at	MGC139389	36,67	213,94	5,83	4,1	9,86	177,27	similar to B-cell CLL/lymphoma 11A
Bt.24984.1.A1_at	---	252,31	39,87	-6,33	-4,1	-13,57	-212,44	Transcribed locus
Bt.23576.1.A1_at	LOC539655	2685,4	6043,53	2,25	2,02	2,53	3358,13	similar to PCTAIRE protein kinase 2
Bt.23654.1.S1_at	LOC614589	2050,19	4694,6	2,29	2,1	2,51	2644,41	similar to Zinc finger CCCH type antiviral protein 1 (Zinc finger CCCH domain-containing protein 2
Bt.4404.1.A1_at	TRYP8	19,75	333,98	16,91	10,23	47,39	314,22	pancreatic anionic trypsinogen
Bt.26048.1.A1_at	MGC133508	564,14	4209,94	7,46	6,54	8,65	3645,8	similar to Small EDRK-rich factor 1 (4F5) (m4F5)
Bt.24314.1.A1_at	FBP2	1982,42	499,63	-3,97	-3,38	-4,75	-1482,78	Fructose-1,6-bisphosphatase 2
Bt.22165.1.S1_at	MGC137948	55,31	948,62	17,15	14,43	21,07	893,3	similar to KIAA1914 protein
Bt.5679.1.S1_at	MGC137616	1809,27	693,31	-2,61	-2,3	-3,02	-1115,96	similar to Dynein light intermediate chain 1, cytosolic (Dynein light chain A) (DLC-A
Bt.16663.1.A1_at	---	3563,49	9,04	-394,33	-200,36	-12061,16	-3554,45	Transcribed locus
Bt.4596.2.S1_at	MGC139878	505,43	130,18	-3,88	-3,08	-5,17	-375,26	similar to Epidermal Langerhans cell protein LCP1
Bt.16385.1.A1_at	MGC127926	2225,74	76,49	-29,1	-20,58	-49,41	-2149,25	similar to 3-hydroxysteroid epimerase
Bt.4817.2.S1_at	MGC128478	70,08	674,1	9,62	5,49	38,21	604,01	similar to claudin 11
Bt.4407.1.S1_at	MGC137732	192,84	685,31	3,55	2,88	4,61	492,46	similar to CG7289-PA
Bt.15909.1.S1_at	MGC142520	2510,01	5973,49	2,38	2,18	2,62	3463,49	similar to Family with sequence similarity 98, member A
Bt.26594.1.S1_at	---	293,31	1671,92	5,7	4,38	8,03	1378,61	Transcribed locus
Bt.20118.1.S1_at	SAR1A	263,77	1291,73	4,9	4,01	6,21	1027,96	SAR1 gene homolog A (S. cerevisiae)
Bt.23129.3.S1_a_	LOC532572	3015,87	7573,92	2,51	2,21	2,91	4558,05	similar to Laminin gamma-1 chain precursor (Laminin B2 chain)
Bt.27645.1.A1_at	LOC506902	745,9	5905,72	7,92	6,72	9,59	5159,82	Similar to C20orf82
Bt.19862.2.S1_at	LOC518458	15,72	1060,38	67,45	39,37	233,12	1044,66	similar to semaphorin 6D
Bt.2964.1.S1_at	LOC787714 /// ZI	674,3	2567,59	3,81	3,1	4,91	1893,29	zinc finger protein 330 /// similar to Zinc finger protein 330
Bt.9268.1.S1_at	LOC537028	341,64	37,59	-9,09	-5,06	-41,25	-304,05	hypothetical LOC537028
Bt.4470.1.S1_at	RGS7	366,19	75,68	-4,84	-3,57	-7,47	-290,51	regulator of G-protein signaling 7
Bt.12688.1.A1_at	LOC785152	70,78	238,85	3,37	2,69	4,45	168,06	hypothetical protein LOC785152
Bt.27283.1.S1_x_	BOLA	4276,24	72,64	-58,87	-50,48	-70,51	-4203,6	Classical MHC class I antigen
Bt.2222.2.S1_at	LOC537096	813,85	279,41	-2,91	-2,4	-3,66	-534,44	similar to WD repeat and FYVE domain containing 3

probe set	GENE ID	baseline mean (LS	periment mean (L	fold change	lower bound of F	upper bound of F	difference of me	Gene Title
Bt.23733.1.A1_at	---	7,59	177,94	23,45	12,68	146,66	170,35	---
Bt.5083.1.S1_at	LOC781099 /// M	37,22	160,02	4,3	3,34	6,02	122,8	similar to solute carrier family 27 (fatty acid transporter), member 4 /// hypothetical protein LOC781099
Bt.19784.1.A1_at	---	979,28	402,03	-2,44	-2,11	-2,86	-577,24	Transcribed locus
Bt.27206.1.A1_at	---	6,8	129,79	19,09	9,27	100000000	122,99	Transcribed locus, moderately similar to XP_001149128.1 hypothetical protein [Pan troglodytes]
Bt.23493.1.S1_at	THBS	118,56	2031,08	17,13	13,6	23,04	1912,52	thrombospondin
Bt.29874.1.S1_at	EIF2C3	651,95	1609,23	2,47	2,15	2,88	957,28	eukaryotic translation initiation factor 2C, 3
Bt.7490.1.A1_at	MGC140483	2050,42	782,61	-2,62	-2,36	-2,92	-1267,81	similar to methylenetetrahydrofolate dehydrogenase (NADP+ dependent) 1-like
Bt.5692.2.S1_at	---	795,15	189,33	-4,2	-3,23	-5,97	-605,83	Transcribed locus
Bt.2587.2.S1_a_a	MGC140701	186,85	19,55	-9,56	-5,55	-33,81	-167,3	similar to Fumarate hydratase, mitochondrial precursor (Fumarase)
Bt.5970.1.S1_a_a	MGC127936	7986,24	3350,01	-2,38	-2,17	-2,64	-4636,23	similar to S100 calcium-binding protein A2 (S-100L protein) (CAN19)
Bt.15188.1.S1_at	---	37,63	868,63	23,08	11,85	368,51	831	---
Bt.11176.2.S1_at	MGC127803	727,56	208,39	-3,49	-2,83	-4,48	-519,17	similar to transmembrane protein 14A
Bt.24247.1.S1_at	---	424,28	127,21	-3,34	-2,73	-4,26	-297,07	Transcribed locus
Bt.25783.1.A1_at	SP2	613,3	200,71	-3,06	-2,59	-3,69	-412,6	Sp2 transcription factor
Bt.18203.1.A1_at	MGC151720	345,13	89,11	-3,87	-2,98	-5,48	-256,02	similar to C21ORF43
Bt.21405.1.S1_at	---	118,41	796,67	6,73	5,99	7,65	678,26	Transcribed locus
Bt.20129.1.S1_at	CUTL1	758,65	1766,6	2,33	2,1	2,6	1007,95	cut-like 1, CCAAT displacement protein (Drosophila)
Bt.5281.2.S1_a_a	---	399,58	912,35	2,28	2,03	2,59	512,77	CDNA clone MGC:139634 IMAGE:8280525
Bt.28642.1.A1_at	---	25,87	126,89	4,9	3,45	8,36	101,02	Transcribed locus
Bt.22534.1.S1_at	LOC534497	364,43	5379,66	14,76	13,06	16,94	5015,22	similar to peripheral myelin protein 22
Bt.4845.1.S1_at	WBSCR22	3406,7	1320,7	-2,58	-2,29	-2,95	-2085,99	Williams Beuren syndrome chromosome region 22 protein
Bt.3253.1.A1_at	LOC617871	1881,98	598,98	-3,14	-2,68	-3,78	-1283,01	hypothetical LOC617871
Bt.28632.2.S1_at	LOC540826	418,67	135,29	-3,09	-2,61	-3,78	-283,39	similar to ubiquitin E3 ligase SMURF2
Bt.26971.1.S1_at	---	82,21	1935,93	23,55	16,42	41,32	1853,72	Transcribed locus, moderately similar to XP_001088883.1 similar to NUAK family, SNF1-like kinase, 2 [Macaca mulatta]
Bt.5376.1.S1_at	YIF1A	1781,7	4038,11	2,27	2,08	2,47	2256,41	Yip1 interacting factor homolog A (S. cerevisiae)
Bt.24973.1.A1_at	LOC505941	2267,04	5440,7	2,4	2,2	2,64	3173,66	similar to ribosome binding protein 1
Bt.2039.1.S1_at	LOC514971	247,87	26,63	-9,31	-5,18	-44,48	-221,24	similar to cytochrome P450 2S1
Bt.13725.2.S1_at	---	1199,97	479,78	-2,5	-2,29	-2,74	-720,2	Transcribed locus, strongly similar to XP_001112553.1 similar to hyperparathyroidism 2 homolog isoform 2 [Macaca mulatta]
Bt.26461.1.A1_at	LOC511800	14768,65	826,17	-17,88	-14,46	-23,31	-13942,48	similar to KIAA1581 protein
Bt.22283.1.S1_at	---	1435,82	174,67	-8,22	-5,78	-13,95	-1261,15	Transcribed locus
Bt.16188.1.S1_at	CYYR1	11,05	1575,08	142,54	81,21	578,93	1564,03	Cysteine/tyrosine-rich 1
Bt.2886.1.S1_at	DKKL1	30,46	172,03	5,65	4,33	8	141,57	dickkopf-like 1 (soggy)
Bt.14000.1.S1_at	LOC789594	41,58	181,23	4,36	3,55	5,57	139,65	Hypothetical protein LOC789594
Bt.9068.1.S1_at	LOC404108	1106,46	2840,91	2,57	2,17	3,11	1734,44	non-muscle myosin heavy chain
Bt.18533.1.S1_at	MGC137608	497,98	35,33	-14,1	-7,37	-156,35	-462,66	similar to Cyclic-AMP-dependent transcription factor ATF-3 (Activating transcription factor 3) (Liver regeneration factor 1) (LRF-1)
Bt.15989.1.S1_at	IRF2	239,11	88,94	-2,69	-2,3	-3,23	-150,17	interferon regulatory factor 2
Bt.6898.2.S1_a_a	MGC138118	2,59	5254,92	2030,71	54,65	100000000	5252,33	similar to SPRY domain-containing SOCS box protein SSB-2
Bt.22576.3.S1_at	LOC782160	280,51	69,52	-4,04	-3,01	-6,02	-210,99	similar to Protein phosphatase 1, regulatory subunit 3D
Bt.29153.1.S1_at	---	1327,34	64,29	-20,65	-15,97	-29,08	-1263,06	---
Bt.9521.1.S1_at	LOC512924	399,58	26,21	-15,24	-9,57	-36,61	-373,37	similar to rhoHP1
Bt.19423.1.S1_at	ABCA1	534,45	1595,49	2,99	2,57	3,53	1061,03	ATP-binding cassette, sub-family A (ABC1), member 1
Bt.3196.1.S1_at	STRA6	345,85	20,99	-16,48	-7,57	-100000000	-324,87	stimulated by retinoic acid gene 6 homolog
Bt.13930.2.S1_at	LOC539979	261,96	56,45	-4,64	-3,6	-6,41	-205,51	similar to protein kinase
Bt.3276.1.A1_at	MGC137490	375,6	120,47	-3,12	-2,57	-3,93	-255,14	similar to rTS beta protein
Bt.15861.1.S1_at	---	58,68	174,75	2,98	2,57	3,5	116,07	Transcribed locus
Bt.3975.1.S1_at	LOC506522	864,2	2090,75	2,42	2,09	2,86	1226,55	similar to WD repeat domain 85
Bt.8724.1.S1_at	---	65,78	313,52	4,77	3,74	6,45	247,74	CDNA clone IMAGE:8473920
Bt.24206.1.A1_at	MGC157166	152,91	583,56	3,82	3,22	4,62	430,65	hypothetical LOC525916
Bt.17765.2.A1_at	---	353,14	40,19	-8,79	-5,22	-27,41	-312,95	Transcribed locus
Bt.9511.1.S1_at	---	564,59	196,93	-2,87	-2,39	-3,57	-367,66	Transcribed locus
Bt.10999.2.S1_at	MGC159894	843,72	294,21	-2,87	-2,38	-3,57	-549,51	similar to NCK adaptor protein 2
Bt.29257.1.A1_at	---	66,53	2628,55	39,51	27,11	72,45	2562,02	Transcribed locus
Bt.5788.1.S1_at	MGC155084	1662,09	377,64	-4,4	-3,74	-5,3	-1284,45	Similar to SAP-2=ERP/NET homolog
Bt.14201.1.S1_a_a	LOC784840 /// M	226,1	1026,04	4,54	4,16	4,98	799,94	hypothetical protein MGC134244 /// hypothetical protein LOC784840
Bt.23521.1.S1_at	MGC139846	1997,34	303,88	-6,57	-4,99	-9,63	-1693,46	similar to dual specificity phosphatase 26
Bt.4130.1.S1_at	F5	478,93	11,55	-41,47	-22,79	-224,18	-467,38	coagulation factor V (proaccelerin, labile factor)
Bt.21943.1.S1_at	LOC524460	1468,63	530,63	-2,77	-2,59	-2,96	-938	similar to UDP-Gal:glucosylceramide beta-1,4-galactosyltransferase
Bt.22200.1.S1_at	---	167,97	5210,47	31,02	25,31	39,97	5042,51	Transcribed locus
Bt.6113.1.S1_at	LOC524274	2628,37	878,13	-2,99	-2,69	-3,35	-1750,24	similar to Xeroderma pigmentosum, complementation group C
Bt.29796.1.S1_at	---	639,19	11716,52	18,33	13,45	28,54	11077,33	B4 cell-line anti-respiratory syncytial virus Ig lambda chain V region (IgL)
Bt.20293.1.S1_at	MGC127598	580,24	240,9	-2,41	-2,13	-2,77	-339,34	hypothetical protein MGC127598
Bt.4877.1.S1_at	LOC790012 /// P	628,24	1870,32	2,98	2,44	3,79	1242,08	phospholipase C, delta 1 /// similar to 1-phosphatidylinositol-4,5-bisphosphate phosphodiesterase delta 1 (Phosphoinositide phospholipase C) (PLC-delta-1) (Phospholipase C-delta-1) (PLC-III)
Bt.1694.1.S1_at	LOC539853	19,75	506,19	25,62	18,55	41,19	486,43	similar to gp50/Trop-2

probe set	GENE ID	baseline mean (LS	periment mean (L	fold change	lower bound of F	upper bound of F	difference of me	Gene Title
Bt.26713.1.S1_at	SLC38A5	88	1004,83	11,42	7,59	22,53	916,83	solute carrier family 38, member 5
Bt.5775.1.S1_at	MGC155110	922,96	4710,73	5,1	4,39	6,06	3787,77	similar to biliverdin-IX alpha reductase
Bt.21246.1.A1_at	---	15,51	2786,45	179,65	60,19	100000000	2770,94	Transcribed locus
Bt.17465.1.S1_at	MGC148990	919,33	2720,35	2,96	2,58	3,46	1801,02	similar to rhomboid-related protein
Bt.20947.1.S1_at	---	18,56	685,32	36,93	24,18	77,62	666,77	---
Bt.27104.1.A1_at	---	80,52	2737,32	33,99	19,66	122,92	2656,8	Transcribed locus
Bt.18995.1.A1_a	LOC514174	434,03	21,43	-20,26	-13,51	-39,98	-412,6	similar to cytoplasmic polyadenylation element-binding protein long form
Bt.15738.1.A1_at	---	1692,17	654,29	-2,59	-2,23	-3,07	-1037,88	Transcribed locus, strongly similar to XP_001113528.1 hypothetical protein LOC9728 isoform 2 [Macaca mulatta]
Bt.2349.1.S1_at	LOC512732	582,84	52,7	-11,06	-7,1	-24,3	-530,14	similar to stathmin-like-protein RB3
Bt.21113.1.S1_a	CPT1B	18,74	708,34	37,8	23,9	89,51	689,61	carnitine palmitoyltransferase 1B
Bt.656.1.S1_at	MGC143403	10440,05	3993,41	-2,61	-2,4	-2,85	-6446,64	similar to coronin, actin binding protein, 1C
Bt.3701.1.S1_at	LOC618459	679,18	1911,35	2,81	2,53	3,15	1232,17	hypothetical LOC618459
Bt.7196.1.S1_at	LOC404111	52,76	5740,32	108,8	76,31	188,99	5687,55	epidermal keratin VII
Bt.4394.1.S1_at	GUCY1B3	2374,73	878,58	-2,7	-2,24	-3,37	-1496,15	guanylate cyclase 1, soluble, beta 3
Bt.2904.1.S1_at	MGC126974	6101,91	2667,38	-2,29	-2,07	-2,54	-3434,54	hypothetical LOC507725
Bt.3823.1.S1_at	AVPI1	256,89	81,76	-3,14	-2,7	-3,71	-175,13	arginine vasopressin-induced 1
Bt.27481.1.A1_at	SPG3A	377,04	25,16	-14,99	-9,37	-36,44	-351,89	spastic paraplegia 3A (autosomal dominant)
Bt.8881.1.A1_at	LOC525946	11,76	121,7	10,35	6,68	22,19	109,94	similar to Ephrin type-A receptor 1 precursor (Tyrosine-protein kinase receptor EPH)
Bt.28084.1.S1_at	LOC517496	261,43	4766,45	18,23	13,76	26,83	4505,02	similar to KIAA1285 protein
Bt.14444.1.A1_at	LOC533295	69,35	314,72	4,54	3,48	6,48	245,37	Similar to Y53F4B.4a
Bt.10088.1.A1_at	---	676	146,64	-4,61	-3,59	-6,43	-529,36	Transcribed locus
Bt.2046.1.S1_at	ext1	38,6	1033,84	26,78	18,09	51,12	995,23	sushi repeat-containing protein
Bt.8552.1.S1_at	BOLA-DRA	1118,68	89,44	-12,51	-9,07	-19,9	-1029,24	major histocompatibility complex, class II, DR alpha
Bt.29921.1.S1_at	LOC614583	430,54	1592,69	3,7	3,16	4,47	1162,16	similar to SERTA domain containing 4
Bt.10214.1.S1_at	MGC140096	187,83	1648,82	8,78	7,7	10,17	1460,99	similar to DRAK1
Bt.24380.1.A1_at	MGC166193	729,53	1783,96	2,45	2,08	2,94	1054,42	similar to BTB (POZ) domain containing 5
Bt.9003.1.S1_at	KIAA1797	533,02	1406,55	2,64	2,27	3,13	873,53	hypothetical protein LOC506199
Bt.6033.1.S1_at	ST7	64,29	507,79	7,9	5,69	12,66	443,51	suppression of tumorigenicity 7
Bt.4793.1.S2_at	SLC12A2	3610,67	178,18	-20,26	-16,71	-25,65	-3432,49	solute carrier family 12 (sodium/potassium/chloride transporters), member 2
Bt.18894.1.A1_at	LOC785123	194,57	617,85	3,18	2,7	3,81	423,28	similar to putative RIN zinc finger protein
Bt.23135.1.S1_at	TAGLN2	5700,47	656,43	-8,68	-7,17	-10,92	-5044,04	transgelin 2
Bt.5141.1.S2_at	B4GALT1	716,99	3633,9	5,07	4,46	5,84	2916,91	UDP-Gal:betaGlcNAc beta 1,4- galactosyltransferase, polypeptide 1
Bt.4105.1.S1_at	MGC143272	417,27	2403,18	5,76	4,97	6,79	1985,91	similar to putative GPCR interacting protein GIP
Bt.21053.2.S1_at	MGC128630	1157,66	474,43	-2,44	-2,09	-2,92	-683,23	similar to synaptogyrin 1 isoform 1b
Bt.9840.1.S1_at	---	276,48	816,59	2,95	2,53	3,51	540,11	Transcribed locus
Bt.15788.1.S1_a	LOC507402	170,17	1538,06	9,04	7,45	11,42	1367,89	Similar to Bone marrow stromal cell antigen 2
Bt.6771.1.S1_at	LOC533149	248,57	896,22	3,61	2,93	4,68	647,65	hypothetical LOC533149
Bt.13422.1.A1_at	MGC152585	2711,38	783,85	-3,46	-2,8	-4,49	-1927,53	Hypothetical LOC507035
Bt.20936.1.S1_at	---	901,32	2940,89	3,26	2,83	3,82	2039,57	Transcribed locus
Bt.23.2.S1_at	SLC6A2	2527,53	10,77	-234,66	-112,24	-100000000	-2516,76	solute carrier family 6 (neurotransmitter transporter, noradrenalin), member 2
Bt.22435.1.S1_at	MGC133535	809,79	3193,65	3,94	3,1	5,31	2383,86	similar to FN5 protein
Bt.10813.1.S1_at	PDLIM4	1370	3324,34	2,43	2,06	2,93	1954,33	PDZ and LIM domain 4
Bt.22797.1.A1_at	---	981,22	45,46	-21,58	-13,4	-54,32	-935,76	Transcribed locus
Bt.1055.1.S1_at	LOC518563	706,11	1689,79	2,39	2,13	2,72	983,68	similar to HS6ST1 protein
Bt.2452.1.S1_at	LUM	415,21	2049,47	4,94	4,29	5,77	1634,26	lumican
Bt.24923.1.S1_at	LOC535060	29,44	1406,86	47,78	28,18	154,87	1377,41	hypothetical LOC535060
Bt.20035.2.A1_at	CXXC5	85,15	512,27	6,02	4,61	8,51	427,12	CXXC finger 5
Bt.26656.1.S1_at	LOC537631	299,13	22,95	-13,03	-8,84	-24,32	-276,18	similar to JNK3 beta2 protein kinase
Bt.26770.1.S1_at	MGC140759	310,32	918,76	2,96	2,61	3,39	608,44	similar to Transducin beta-like 2 protein (WS beta-transducin repeats protein) (WS-betaTRP) (Williams-Beuren syndrome chromosome region 13
Bt.28686.1.S1_at	MGC151721	702,82	27,68	-25,39	-15,12	-77,5	-675,14	similar to MAL2 proteolipid
Bt.15758.1.S1_at	PTGS2	2158,19	141,02	-15,3	-13,25	-18,05	-2017,17	prostaglandin-endoperoxide synthase 2 (prostaglandin G/H synthase and cyclooxygenase)
Bt.9108.1.S1_at	---	576,05	118,61	-4,86	-3,92	-6,28	-457,45	Transcribed locus
Bt.23502.1.S1_at	MGC159420	194,69	1048,97	5,39	4,42	6,81	854,28	similar to receptor activity-modifying protein 2
Bt.29907.1.S1_at	KLHDC8B	697,8	81,57	-8,56	-6,39	-12,75	-616,24	kelch domain containing 8B
Bt.9373.1.S1_at	---	123,55	402,82	3,26	2,58	4,36	279,27	Transcribed locus
Bt.5732.2.A1_at	---	3273,88	925,29	-3,54	-3,14	-4,02	-2348,59	Transcribed locus
Bt.3071.1.S1_at	LOC515784	3942,05	10196,63	2,59	2,23	3,07	6254,58	similar to P63 protein
Bt.18305.1.A1_at	---	37,29	3179,13	85,26	57,38	165,16	3141,84	---
Bt.19733.1.A1_at	---	377,79	99,14	-3,81	-3,1	-4,94	-278,65	Transcribed locus
Bt.26444.1.A1_at	---	611,07	47,02	-12,99	-8,9	-23,63	-564,05	Transcribed locus
Bt.20402.1.S1_at	PKD2	621,31	153,91	-4,04	-3,1	-5,66	-467,4	polycystic kidney disease 2 membrane protein
Bt.27400.1.S1_at	LOC523226	185,38	1086,18	5,86	5,14	6,78	900,8	similar to Protocadherin alpha subfamily C, 2
Bt.8867.1.S1_at	LOC536213	551,71	1626,51	2,95	2,53	3,53	1074,81	similar to CHKB protein
Bt.22573.1.A1_at	---	116,85	378,62	3,24	2,69	4,01	261,78	---

probe set	GENE ID	baseline mean (LS	periment mean (L	fold change	lower bound of F	upper bound of F	difference of me	Gene Title
Bt.8894.1.S1_at	---	631,31	199	-3,17	-2,49	-4,3	-432,3	Transcribed locus
Bt.4837.1.A1_at	ALDOC	4849,69	1642,59	-2,95	-2,63	-3,34	-3207,1	aldolase C, fructose-bisphosphate
Bt.21615.1.A1_at	MGC140693	518,85	19,54	-26,56	-15,2	-101,73	-499,31	similar to transmembrane protein 22
Bt.19332.2.A1_at	---	72,43	289,09	3,99	3,01	5,79	216,66	Transcribed locus
Bt.11481.1.A1_at	---	285,59	110,12	-2,59	-2,2	-3,14	-175,47	Transcribed locus
Bt.3391.1.S1_at	LOC781397	639,45	1640,08	2,56	2,28	2,93	1000,63	hypothetical protein LOC781397
Bt.20111.1.S1_at	LOC617439	1074,5	51,95	-20,68	-13,47	-43,8	-1022,55	similar to type I transmenmbrane protein
Bt.1165.1.S1_at	ADCY7	345,04	1801,94	5,22	4,61	5,99	1456,91	adenylate cyclase 7
Bt.4635.2.S1_a_at	CNN2	108,12	700,58	6,48	5,13	8,69	592,46	calponin 2
Bt.3948.1.S1_at	CDH3	148,75	788,44	5,3	4,42	6,55	639,69	cadherin 3, type 1, P-cadherin (placental)
Bt.25259.1.A1_at	LOC541187	29,71	420,03	14,14	11,83	17,48	390,31	similar to FIC1
Bt.22803.1.S1_at	TUBB	1877,75	4930,5	2,63	2,34	2,98	3052,75	tubulin, beta
Bt.23548.2.S1_at	MGC138006	66,77	920,73	13,79	10,34	20,48	853,96	hypothetical LOC513445
Bt.26637.2.S1_at	MGC138046	1324,76	117,38	-11,29	-9,56	-13,71	-1207,37	similar to chromatin modifying protein 4C
Bt.11770.1.S1_a_	SLC25A20	1067,37	2707,73	2,54	2,16	3,07	1640,36	solute carrier family 25 (carnitine/acylcarnitine translocase), member 20
Bt.12927.1.S1_at	HAS2	5,74	449,09	78,2	38,79	100000000	443,35	hyaluronan synthase 2
Bt.20979.1.S1_at	---	5494,85	1293,75	-4,25	-3,59	-5,13	-4201,1	Transcribed locus
Bt.21473.1.A1_a	MPZL1	619,76	2258,07	3,64	3,26	4,1	1638,3	myelin protein zero-like 1
Bt.5548.1.S1_at	SLC1A5	122,37	865,88	7,08	4,89	12,44	743,51	solute carrier family 1 (neutral amino acid transporter), member 5
Bt.29954.1.S1_at	GKAP1	890,65	294,8	-3,02	-2,5	-3,79	-595,85	G kinase anchoring protein 1
Bt.19329.1.A1_at	MGC139784	6198,13	335,14	-18,49	-15,3	-23,28	-5862,99	similar to EF-hand domain-containing protein 1 (Swiprosin-2)
Bt.27178.1.S1_at	LOC506539	311,84	688,4	2,21	2,02	2,42	376,56	similar to KIAA0999 protein
Bt.6362.1.A1_at	LOC785088	931,31	22,73	-40,97	-25,92	-96,84	-908,59	similar to hormone-sensitive lipase
Bt.24635.2.A1_at	IGFALS	682,22	2508,52	3,68	2,94	4,88	1826,31	insulin-like growth factor binding protein, acid labile subunit
Bt.5684.1.S1_at	LOC508877	222,78	613,99	2,76	2,3	3,39	391,21	hypothetical LOC508877
Bt.22498.1.A1_at	---	211,14	639,9	3,03	2,4	4,05	428,76	Transcribed locus
Bt.2849.1.S1_at	---	5,54	425,95	76,83	32,26	100000000	420,41	Transcribed locus
Bt.11178.1.S1_at	MGC128119	12576,38	2953,39	-4,26	-3,17	-6,42	-9622,98	similar to Glypican-3 precursor (Intestinal protein OCI-5) (GTR2-2) (MXR7)
Bt.10458.1.A1_at	---	8442,47	889,92	-9,49	-7,63	-12,42	-7552,54	Transcribed locus
Bt.7849.1.S1_at	MGC127504	2184,12	5029,41	2,3	2,04	2,63	2845,29	similar to Lysyl-tRNA synthetase (Lysine--tRNA ligase) (LysRS)
Bt.16976.2.A1_at	---	1420,22	454,12	-3,13	-2,6	-3,91	-966,1	Transcribed locus
Bt.13985.1.S1_at	---	677,69	135,75	-4,99	-3,87	-7,01	-541,95	Transcribed locus
Bt.29053.1.A1_at	---	2953,3	954,23	-3,09	-2,69	-3,64	-1999,07	Transcribed locus
Bt.9966.2.S1_a_at	LOC782818	4541,29	11193,84	2,46	2,12	2,93	6652,55	similar to procollagen alpha 2(V)
Bt.21362.1.S1_at	---	1639,71	635,67	-2,58	-2,25	-3,01	-1004,04	Transcribed locus
Bt.4357.1.S1_at	MGC139832	191,38	975,44	5,1	3,94	7,19	784,06	similar to Tetraspanin-7 (Tspan-7) (Transmembrane 4 superfamily member 2) (Cell surface glycoprotein A15) (T-cell acute lymphoblastic leukemia associated antigen 1) (TALLA-1) (Membrane component, X chromosome, surface marker 1) (CD231 antigen)...
Bt.23830.1.A1_at	---	568,63	170,45	-3,34	-2,69	-4,36	-398,18	Transcribed locus, moderately similar to XP_001104510.1 similar to gluconokinase-like protein isoform 1 [Macaca mulatta]
Bt.20330.1.S1_at	MGC139156	99,21	1383,73	13,95	11,42	17,82	1284,51	hypothetical LOC538575
Bt.14061.1.A1_at	MGC143209	150,99	19,96	-7,56	-4,78	-17,24	-131,03	hypothetical LOC534389
Bt.20402.2.A1_at	PKD2	1355,14	493,09	-2,75	-2,34	-3,32	-862,05	polycystic kidney disease 2 membrane protein
Bt.29922.1.S1_at	---	538,16	1244,34	2,31	2,02	2,69	706,18	Transcribed locus
Bt.12811.1.S1_at	UACA	4456,89	1558,09	-2,86	-2,72	-3,01	-2898,8	uveal autoantigen with coiled-coil domains and ankyrin repeats
Bt.199.1.S1_at	PNOC	6,09	1770,75	290,89	66,86	100000000	1764,67	prepronociceptin
Bt.25105.2.A1_at	LOC524375	374,03	87,97	-4,25	-3,62	-5,09	-286,06	similar to lymphocyte alpha-kinase
Bt.20436.1.S1_at	---	664,96	250,1	-2,66	-2,29	-3,15	-414,86	Transcribed locus
Bt.4544.1.S1_at	LOC535043	301,49	1576,54	5,23	4,16	7,04	1275,05	hypothetical LOC535043
Bt.7348.1.S1_at	---	831,24	200,72	-4,14	-3,16	-5,85	-630,52	Transcribed locus
Bt.599.1.S1_at	DSPG3	34,81	341,29	9,8	6,25	21,87	306,48	dermatan sulfate proteoglycan 3
Bt.22545.2.S1_at	MGC148755	2397,54	9050,1	3,77	3,13	4,75	6652,56	similar to fibulin-1 C
Bt.5528.1.S1_at	SLC7A5	43,46	495,88	11,41	5,76	452,32	452,42	solute carrier family 7 (cationic amino acid transporter, y+ system), member 5
Bt.2632.1.S1_at	SPP1	4621,17	4,77	-969,03	-395,13	-100000000	-4616,4	secreted phosphoprotein 1
Bt.20694.1.A1_at	LOC515749	167,32	17,96	-9,32	-6,18	-18,3	-149,36	similar to alpha-catenin related protein
Bt.22389.1.S1_at	LOC617336	4,6	2500,25	542,96	273,24	37438,69	2495,65	similar to WGAR9166
Bt.24801.1.A1_at	---	6409,23	21,39	-299,6	-172,83	-1117	-6387,84	Transcribed locus
Bt.28651.1.S1_at	LOC538697	350,91	888,86	2,53	2,23	2,9	537,95	similar to deleted in liver cancer 2 alpha
Bt.5160.1.S1_at	LOC513577	154,1	35,1	-4,39	-3,26	-6,66	-119	similar to U4/U6 snRNP-associated 61 kDa protein
Bt.16329.1.A1_at	LOC510050	158,45	564,17	3,56	3,14	4,08	405,72	similar to TG-interacting factor
Bt.1402.2.S1_at	GNAO1	773,63	20,14	-38,41	-22,06	-145,27	-753,49	guanine nucleotide binding protein (G protein), alpha activating activity polypeptide O
Bt.23174.1.S1_at	MGC127643	399,36	28,76	-13,89	-8,24	-42,18	-370,6	similar to CD74 antigen
Bt.1069.1.A1_at	PTPRR	666,73	1757,93	2,64	2,36	2,98	1091,2	protein tyrosine phosphatase, receptor type, R
Bt.24915.1.A1_at	CNTNAP3	252,43	62,07	-4,07	-3,05	-6,07	-190,36	cell recognition molecule CASPR3
Bt.17405.1.S1_at	---	285,51	84,29	-3,39	-2,68	-4,58	-201,21	Transcribed locus
Bt.22614.2.S1_at	---	2889,49	1069,6	-2,7	-2,27	-3,33	-1819,9	Transcribed locus

probe set	GENE ID	baseline mean (LS	periment mean (L	fold change	lower bound of F	upper bound of F	difference of me	Gene Title
Bt.14083.2.S1_at	MASP1	93,72	300,17	3,2	2,73	3,86	206,45	mannan-binding lectin serine peptidase 1 (C4/C2 activating component of Ra-reactive factor)
Bt.9399.1.S1_at	---	781,22	231,95	-3,37	-2,99	-3,82	-549,28	Transcribed locus
Bt.26122.2.S1_at	UXT	194,63	656,48	3,37	3,08	3,7	461,85	ubiquitously-expressed transcript
Bt.8319.3.S1_a_a	LOC515016	436,65	174,37	-2,5	-2,18	-2,91	-262,28	similar to mitochondrial tumor suppressor 1
Bt.19937.2.S1_at	LOC532189	541,18	1306,05	2,41	2,06	2,9	764,87	similar to carboxypeptidase D
Bt.20955.1.A1_at	---	1876,08	545,18	-3,44	-2,91	-4,16	-1330,9	Transcribed locus
Bt.1775.1.A1_at	---	1714,36	641,6	-2,67	-2,31	-3,15	-1072,76	Transcribed locus
Bt.29417.1.S1_at	TMEM30A	593,34	1777,96	3	2,79	3,22	1184,62	transmembrane protein 30A
Bt.4417.1.S1_at	CDH2	349,88	4736,05	13,54	11,41	16,55	4386,17	cadherin 2
Bt.22078.1.S1_at	LOC513520	2062,91	822,45	-2,51	-2,09	-3,08	-1240,46	similar to ATPase, H+ transporting, lysosomal accessory protein 2
Bt.6276.2.S1_at	LOC616537	281,17	90,24	-3,12	-2,48	-4,16	-190,92	similar to Rab6 protein
Bt.7337.2.S1_at	LOC781512	7,48	153,87	20,57	9,32	100000000	146,39	similar to ARAP2
Bt.24405.2.A1_at	LOC783765	275,08	46,65	-5,9	-4,12	-10,34	-228,43	tetraspanin similiar to uroplakin 1
Bt.16831.1.A1_at	LOC615978	2829,52	687,42	-4,12	-3,6	-4,75	-2142,1	similar to Chst2 protein
Bt.979.1.A1_at	MGC160128	138,81	7380,13	53,17	38,96	83,32	7241,32	similar to Myosin IB
Bt.8496.1.S1_at	MGC134517	823,2	1909,15	2,32	2,08	2,62	1085,96	similar to GDP-mannose pyrophosphorylase B
Bt.25109.1.S1_at	LOC533642	2680,75	7077,74	2,64	2,31	3,08	4396,98	Similar to Procollagen-lysine, 2-oxoglutarate 5-dioxygenase 2
Bt.4844.1.S1_at	PTN	103,93	1243,83	11,97	9,49	16,05	1139,91	pleiotrophin
Bt.23318.1.S2_at	LOC510833	675,36	5154,81	7,63	6,43	9,32	4479,45	similar to Collagen alpha 1(III) chain precursor
Bt.19254.1.A1_at	LOC506738	175,47	21,11	-8,31	-5,08	-22,76	-154,36	Similar to nucleoporin 155
Bt.15290.1.A1_at	---	888,68	21,31	-41,7	-29,7	-69,54	-867,37	Transcribed locus
Bt.23664.1.S1_at	LOC527211	455,14	1298,2	2,85	2,55	3,21	843,06	similar to polyamine oxidase
Bt.26501.1.S1_at	---	114,93	2504,75	21,79	18,41	26,61	2389,82	Transcribed locus
Bt.8617.1.S1_at	MGC139773	2170,63	537,15	-4,04	-3,53	-4,69	-1633,48	similar to chromosome 2 open reading frame 32
Bt.6619.1.S1_at	LOC614661	37,84	598,95	15,83	9,33	49,91	561,12	similar to coronin 6
Bt.26895.2.S1_at	LOC521099	6,8	428,29	63,02	23,39	100000000	421,5	hypothetical LOC521099
Bt.9930.1.S1_at	---	1543,8	496,51	-3,11	-2,64	-3,77	-1047,29	Transcribed locus
Bt.24373.1.S1_at	LOC618638	312,72	68,45	-4,57	-3,12	-8,38	-244,27	similar to tripartite motif-containing 47
Bt.14054.2.S1_at	MGC127247	256,91	36,77	-6,99	-4,83	-12,2	-220,14	similar to interferon-related developmental regulator 1
Bt.18434.1.A1_at	---	1244,58	271,53	-4,58	-4,11	-5,14	-973,04	Transcribed locus
Bt.8335.1.S1_at	---	804,19	2104,47	2,62	2,3	3,03	1300,28	Transcribed locus
Bt.4585.1.S1_at	ACAT2	425,06	1195,78	2,81	2,37	3,44	770,73	acetyl-Coenzyme A acetyltransferase 2
Bt.4107.1.S1_at	DSC2	1739,88	3772,8	2,17	2,02	2,33	2032,92	desmocollin 2
Bt.20076.1.S1_at	UBTF	427,31	1473,44	3,45	2,88	4,28	1046,13	upstream binding transcription factor, RNA polymerase I
Bt.19018.1.A1_at	---	256,39	7,72	-33,22	-16,5	-100000000	-248,67	Transcribed locus
Bt.28073.1.S1_at	LOC523223	419,71	1595,82	3,8	3,35	4,36	1176,11	similar to macrophage actin-associated-tyrosine-phosphorylated protein
Bt.28385.1.A1_at	LOC782489 /// M	25,1	1846,27	73,57	49,45	142,88	1821,18	similar to Cholinesterase precursor (Acylcholine acylhydrolase) (Choline esterase II) (Butyrylcholine esterase) (Pseudocholinesterase) /// hypothetical
Bt.12054.1.S1_at	---	5701,93	1208,02	-4,72	-4,3	-5,21	-4493,91	---
Bt.19409.1.A1_s_	---	1731,43	7283,91	4,21	3,55	5,15	5552,48	Transcribed locus
Bt.24364.1.A1_at	PRSS35	24,24	433,48	17,88	10,89	48,45	409,24	protease, serine, 35
Bt.13315.1.S1_at	LOC768237	1790,66	4938,96	2,76	2,44	3,17	3148,3	hypothetical protein LOC768237
Bt.20820.1.A1_at	LOC781032	3849,71	52,15	-73,83	-44,7	-209,78	-3797,56	similar to latent transforming growth factor beta binding protein 1 isoform LTBP-1L
Bt.13152.1.S1_s_	APP	91,91	1128,62	12,28	8,26	23,36	1036,71	amyloid beta (A4) precursor protein
Bt.373.3.S1_a_at	AMELX /// AMEL	373,47	2598,66	6,96	4,44	15,96	2225,19	amelogenin (amelogenesis imperfecta 1, X-linked) /// amelogenin, Y-linked
Bt.24694.1.A1_at	LOC511689	80,37	232,1	2,89	2,46	3,45	151,73	Similar to KIAA1237 protein
Bt.10458.2.S1_at	LOC513774	1587,54	175,79	-9,03	-6,72	-13,51	-1411,75	Similar to myasthenia gravis autoantigen gravin
Bt.13975.1.S1_a_	LOC613972	16284,08	983,58	-16,56	-12,8	-23,26	-15300,5	similar to Apolipoprotein D precursor (Apo-D) (ApoD)
Bt.23606.1.S1_at	ITPR1	6647,25	2032,66	-3,27	-2,48	-4,72	-4614,6	inositol 1,4,5-triphosphate receptor, type 1
Bt.27040.1.A1_at	---	306,23	64,28	-4,76	-3,13	-9,59	-241,94	Transcribed locus, moderately similar to XP_001067582.1 similar to BTB (POZ) domain containing 7 isoform 2 [Rattus norvegicus]
Bt.24810.1.S1_at	ADC	2455,1	195,85	-12,54	-10,03	-16,57	-2259,25	arginine decarboxylase
Bt.1976.1.S1_at	MGC139033	1495,9	601,14	-2,49	-2,07	-3,07	-894,76	similar to suppression of tumorigenicity 5
Bt.3551.1.S1_at	LOC518062	441,93	1594,92	3,61	3,07	4,31	1152,99	similar to Putative transporter C20orf59
Bt.21071.1.S1_at	---	2201,82	276,22	-7,97	-6,95	-9,28	-1925,6	Transcribed locus
Bt.25472.1.A1_at	LOC512714	115,5	11,85	-9,75	-6,19	-21,89	-103,65	similar to Lrrc34 protein
Bt.12217.1.S1_at	NTRK2	10,7	136,5	12,76	6,2	100000000	125,8	Neurotrophic tyrosine kinase, receptor, type 2
Bt.287.1.S1_at	RNASE6	129,95	8,67	-14,98	-7,44	-1496,53	-121,27	ribonuclease, RNase A family, k6
Bt.3410.1.S1_at	SYNGR2	728,56	2208,2	3,03	2,51	3,76	1479,64	synaptogyrin 2
Bt.20605.2.S1_at	---	24,84	438,04	17,64	10,98	43,55	413,2	Transcribed locus
Bt.9699.1.S1_at	CYP26	39,14	8398,32	214,57	87,99	100000000	8359,18	cytochrome P450 retinoic acid hydroxylase
Bt.12361.1.S1_at	LOC541100	1058,23	178,57	-5,93	-4,53	-8,56	-879,66	similar to Pleckstrin homology domain containing, family H (with MyTH4 domain) member 3
Bt.25578.1.A1_at	---	21,15	236,17	11,17	6,68	31,99	215,03	Transcribed locus
Bt.27655.1.S1_at	LOC534112	2664,87	313,28	-8,51	-7,36	-10,01	-2351,59	similar to connector enhancer of KSR2A
Bt.568.1.S1_at	IBSP	7900	11,05	-715,21	-311,66	-100000000	-7888,95	integrin-binding sialoprotein (bone sialoprotein, bone sialoprotein II)
Bt.13930.1.A1_at	LOC539979	501,93	118,45	-4,24	-3,05	-6,68	-383,49	Similar to protein kinase

probe set	GENE ID	baseline mean (LS	periment mean (L	fold change	lower bound of F	upper bound of F	difference of me	Gene Title
Bt.26992.1.A1_at	---	1433,18	3554,96	2,48	2,13	2,96	2121,78	Transcribed locus
Bt.9948.1.S1_at	NOTCH1	185,91	1396,59	7,51	5,93	10,09	1210,68	Notch homolog 1, translocation-associated (Drosophila)
Bt.20227.1.S1_at	---	149,67	1716,03	11,47	9,98	13,41	1566,36	Transcribed locus, moderately similar to XP_001092357.1 similar to solute carrier family 25 member 2 [Macaca mulatta]
Bt.4758.1.S1_at	FABP	42,56	2187,82	51,41	36,54	86,17	2145,26	fatty acid binding protein (heart) like
Bt.26404.1.S1_at	---	463,44	29,84	-15,53	-6,57	-100000000	-433,6	Transcribed locus
Bt.29420.1.S1_at	---	11,58	118,82	10,26	5,13	1743,88	107,24	Transcribed locus
Bt.5656.1.S1_at	FEZ1	1543,33	583,91	-2,64	-2,33	-3,02	-959,42	fasciculation and elongation protein zeta 1 (zygin I)
Bt.4038.1.S1_at	LOC524352	4235,08	1735,94	-2,44	-2,12	-2,87	-2499,14	similar to betaPix-bL
Bt.20393.1.S1_at	PDIA5	548,86	1985,19	3,62	3,07	4,34	1436,33	protein disulfide isomerase family A, member 5
Bt.13789.1.A1_at	CD14	154,8	12,37	-12,52	-8,45	-23,53	-142,44	CD14 molecule
Bt.1199.1.S1_at	LOC509687	2242,95	10861,73	4,84	3,98	6,19	8618,78	similar to OTTHUMP00000028924
Bt.8888.2.S1_at	LOC523408	632,4	109,12	-5,8	-4,78	-7,27	-523,28	similar to importin 8
Bt.20557.1.S1_at	---	1999,8	783,17	-2,55	-2,24	-2,97	-1216,63	Transcribed locus
Bt.7715.1.S1_at	LOC526884	602,37	1587,91	2,64	2,24	3,2	985,54	similar to WD-repeat protein 6
Bt.4854.1.A1_at	---	321,78	71,37	-4,51	-3,63	-5,84	-250,41	Transcribed locus
Bt.7576.1.S1_at	---	49,14	343,95	7	5,84	8,64	294,81	Transcribed locus
Bt.1178.1.S1_a_a	MGC159706	10984,16	173,39	-63,35	-45,72	-102,62	-10810,76	similar to Protein S100-A1 (S100 calcium-binding protein A1) (S-100 protein alpha subunit) (S-100 protein alpha chain)
Bt.2737.1.S1_at	MGC127744	15997,5	4366,29	-3,66	-2,91	-4,94	-11631,21	similar to Carbonic anhydrase III (Carbonate dehydratase III) (CA-III)
Bt.20725.1.A1_at	---	785,66	133,6	-5,88	-4,89	-7,29	-652,06	Transcribed locus
Bt.21504.1.A1_at	LOC540351	336,45	113,82	-2,96	-2,29	-4,1	-222,63	similar to Zyg-11 homolog B (C. elegans)-like
Bt.370.1.S1_at	AMD1	965,63	343,98	-2,81	-2,31	-3,56	-621,66	adenosylmethionine decarboxylase 1
Bt.21047.1.A1_at	---	173,62	21,95	-7,91	-4,75	-21,99	-151,67	Transcribed locus
Bt.4747.1.S1_at	NUP88	409,82	164,45	-2,49	-2,16	-2,9	-245,37	nucleoporin 88kDa
Bt.22770.1.S1_at	LOC511229	289,94	1002,7	3,46	2,95	4,12	712,76	similar to CARD8 protein
Bt.1178.1.S1_at	MGC159706	4036,33	65,64	-61,49	-34,63	-268,13	-3970,69	similar to Protein S100-A1 (S100 calcium-binding protein A1) (S-100 protein alpha subunit) (S-100 protein alpha chain)
Bt.17121.1.S1_at	---	2234,88	934,17	-2,39	-2,08	-2,78	-1300,71	---
Bt.28429.1.S1_at	---	3215,34	7476,86	2,33	2,06	2,66	4261,53	Transcribed locus
Bt.15784.1.S1_at	LOC521424 /// LC	427,03	4323,44	10,12	8,27	12,93	3896,41	similar to squamous cell-specific protein
Bt.24258.2.S1_at	LOC528150 /// LC	33,79	525,8	15,56	9,66	38,66	492,02	similar to Man9-mannosidase
Bt.4827.1.S1_at	---	800,59	2331,4	2,91	2,68	3,17	1530,8	---
Bt.25881.1.A1_at	MGC134325	960,33	380,66	-2,52	-2,21	-2,93	-579,67	Similar to transmembrane protein 53
Bt.17188.1.A1_at	---	221,46	10,94	-20,24	-11,11	-104,98	-210,53	Transcribed locus
Bt.13141.1.S1_at	BCL2	3824,23	331,77	-11,53	-9,27	-15,1	-3492,46	B-cell CLL/lymphoma 2
Bt.19491.1.S1_at	LOC787736	473,25	2031,67	4,29	3,81	4,87	1558,42	similar to selenoprotein SelM
Bt.16795.1.A1_at	SPAG6	204,6	5,67	-36,11	-15,25	-100000000	-198,93	sperm associated antigen 6
Bt.15939.1.A1_at	---	127,74	3736,6	29,25	26,04	33,26	3608,86	Transcribed locus
Bt.28035.1.S1_at	LOC518159	447,8	2352,76	5,25	4,65	5,99	1904,95	similar to Uncharacterized protein C20orf142
Bt.7760.1.S1_at	MGC139859	1184,48	3678,62	3,11	2,66	3,73	2494,14	similar to Glyoxylase 1
Bt.19850.2.S1_at	---	4867,89	1400,23	-3,48	-3,07	-3,96	-3467,65	Transcribed locus, weakly similar to XP_001084069.1 similar to acyl-CoA synthetase long-chain family member 1 isoform 4 [Macaca mulatta]
Bt.23401.1.S1_at	MGC127148	6141,01	255,36	-24,05	-20,06	-29,88	-5885,65	similar to Four and a half LIM domains protein 1 (FHL-1) (Skeletal muscle LIM-protein 1) (SLIM 1) (SLIM)
Bt.3362.1.S1_at	LOC522886	32,81	1625,51	49,54	20,33	100000000	1592,7	similar to periplakin
Bt.21923.1.A1_at	---	49,8	5037,8	101,16	72,73	165,24	4988	Transcribed locus
Bt.13336.1.A1_at	SMC4L1	146,46	382,86	2,61	2,23	3,16	236,4	SMC4 structural maintenance of chromosomes 4-like 1 (yeast)
Bt.12760.1.S1_at	INHBA	28,24	932,21	33,01	15,56	100000000	903,97	inhibin, beta A
Bt.29931.1.S1_at	LOC514928	722,21	1686,05	2,33	2,06	2,68	963,84	similar to Kinesin family member 1C
Bt.561.1.S1_at	MAP2K6	323,94	1233,75	3,81	3,28	4,48	909,81	mitogen-activated protein kinase kinase 6
Bt.12304.1.S1_at	ISG15	159,61	1455,79	9,12	5,68	21,8	1296,18	ISG15 ubiquitin-like modifier
Bt.3367.1.S1_at	NR1H2	1014,97	415,5	-2,44	-2,1	-2,92	-599,47	nuclear receptor subfamily 1, group H, member 2
Bt.11044.1.S1_at	ARPP-21	340,8	9,36	-36,4	-19,86	-206,44	-331,44	cyclic AMP-regulated phosphoprotein, 21 kDa
Bt.4797.1.S1_at	FKBP4	1862,58	700,38	-2,66	-2,26	-3,22	-1162,2	FK506-binding protein 4
Bt.7670.1.A1_at	LOC539020	5068,89	905,67	-5,6	-4,7	-6,82	-4163,23	similar to zinc finger protein
Bt.612.1.S1_at	LOC506406	248,83	735,36	2,96	2,62	3,35	486,54	similar to mitochondrial glutathione reductase
Bt.9781.1.S1_at	---	333,1	1526,74	4,58	3,95	5,4	1193,64	Transcribed locus, strongly similar to XP_001090650.1 hypothetical protein [Macaca mulatta]
Bt.4138.2.S1_at	---	697,64	1794,92	2,57	2,05	3,39	1097,28	---
Bt.24345.1.S1_at	C2	73,18	247,01	3,38	2,47	5,2	173,82	complement component 2
Bt.10107.1.S1_at	CBARA1	1820,77	529,83	-3,44	-2,96	-4,04	-1290,94	calcium binding atopy-related autoantigen 1
Bt.26895.1.S1_at	LOC521099	5,91	7042,62	1192,39	283,46	100000000	7036,71	hypothetical LOC521099
Bt.2750.1.S1_at	TFAP2A	40,16	415,45	10,34	7,67	15,61	375,28	transcription factor AP-2 alpha (activating enhancer binding protein 2 alpha)
Bt.9919.1.S1_at	MGC134370	11,85	667,31	56,31	26,1	100000000	655,46	similar to CG14120-PA
Bt.9672.1.S1_at	LOC514577	8,12	518,86	63,88	23,34	100000000	510,74	hypothetical LOC514577
Bt.22303.1.S1_at	---	391,83	1263,89	3,23	2,91	3,59	872,06	Transcribed locus
Bt.27634.1.A1_a	LOC534112	774,13	64,86	-11,93	-8,93	-17,72	-709,27	similar to connector enhancer of KSR2A
Bt.20316.1.S1_at	LOC525365	23,42	177,18	7,56	6,12	9,77	153,76	similar to diabetes related ankyrin repeat protein
Bt.18626.2.A1_at	---	1010,88	243,43	-4,15	-3,3	-5,47	-767,44	Transcribed locus

probe set	GENE ID	baseline mean (LS	periment mean (L	fold change	lower bound of F	upper bound of F	difference of me	Gene Title
Bt.27281.1.S1_at	---	2748,45	1001,34	-2,74	-2,4	-3,16	-1747,1	Transcribed locus
Bt.5301.1.S1_at	THBS	612,17	7469,23	12,2	10,04	15,43	6857,06	thrombospondin
Bt.15927.2.S1_at	MGC159964	46,84	270,31	5,77	4,03	9,76	223,47	similar to WD repeat domain, phosphoinositide interacting 1
Bt.13330.2.A1_at	MGC166250	3729,79	1360,25	-2,74	-2,42	-3,12	-2369,55	similar to pyruvate dehydrogenase kinase
Bt.1577.1.S1_at	C1QA	564,8	22,17	-25,47	-15,78	-64,38	-542,62	complement component 1, q subcomponent, A chain
Bt.1701.1.S1_at	LOC616222	382,58	1416,12	3,7	3,05	4,62	1033,55	similar to nonclathrin coat protein zeta-COP
Bt.27138.1.S1_at	---	1481,51	439,14	-3,37	-2,88	-4,01	-1042,37	---
Bt.2494.2.S1_a_a	SDC2	3536,03	537,06	-6,58	-5,63	-7,85	-2998,97	Syndecan 2
Bt.13853.2.S1_a_	MGC139227	420,42	141,3	-2,98	-2,46	-3,76	-279,12	similar to cell adhesion kinase beta
Bt.15953.1.S1_at	MGC138975	295,92	965,02	3,26	2,42	4,9	669,11	similar to mitochondrial ribosomal protein L14
Bt.24033.1.A1_at	LOC504760	624,58	1661,66	2,66	2,4	2,96	1037,08	similar to DEAD/H (Asp-Glu-Ala-Asp/His) box polypeptide RIG-I
Bt.25916.1.A1_at	HSF2BP	562,64	3349,3	5,95	4,71	7,93	2786,65	heat shock transcription factor 2 binding protein
Bt.5520.1.S1_at	IDH2	230,88	1755,11	7,6	5,87	10,57	1524,23	isocitrate dehydrogenase 2 (NADP+), mitochondrial
Bt.8053.1.S1_at	LOC506045	7406,59	3151,1	-2,35	-2,04	-2,76	-4255,49	hypothetical LOC506045
Bt.20774.1.A1_at	---	729,75	147,97	-4,93	-4,1	-6,08	-581,79	Transcribed locus
Bt.633.1.S1_at	SFXN1	2,9	425,79	146,78	45,73	100000000	422,89	sideroflexin 1
Bt.15939.2.S1_at	---	17,38	880,79	50,69	28,06	252,07	863,41	Transcribed locus
Bt.20891.1.S1_at	OAS1	1858,71	5360,77	2,88	2,67	3,12	3502,06	2',5'-oligoadenylate synthetase 1, 40/46kDa
Bt.18233.1.A1_s_	BCL2	3859,33	388,46	-9,93	-7,84	-13,36	-3470,87	B-cell CLL/lymphoma 2
Bt.2159.1.S1_at	MGC140063	215,3	6939,36	32,23	23,07	52,95	6724,06	similar to Transmembrane protein 45a (Dermal papilla derived protein 7)
Bt.25823.1.A1_at	---	246,83	71,75	-3,44	-2,46	-5,58	-175,08	Transcribed locus
Bt.3651.2.A1_at	LOC784977	281,36	4887,84	17,37	15,81	19,19	4606,48	similar to LOC387763 protein
Bt.13670.1.S2_at	ALPL	320,37	2405,92	7,51	6,41	8,98	2085,54	alkaline phosphatase, liver/bone/kidney
Bt.25090.1.A1_at	MGC143187	7,84	139,61	17,82	12,09	33,13	131,77	similar to Dimethylaniline monooxygenase [N-oxide-forming] 2 (Pulmonary flavin-containing monooxygenase 2) (FMO 2) (Dimethylaniline oxidase 2)
Bt.5392.1.S1_at	CD36	3424,3	316	-10,84	-9,57	-12,41	-3108,3	CD36 molecule (thrombospondin receptor)
Bt.17081.1.A1_at	MGC139114	17,09	2258,57	132,14	82,84	322,94	2241,48	similar to Rhombotin-2 (Cysteine-rich protein TTG-2) (T-cell translocation protein 2) (LIM-only protein 2)
Bt.19330.1.A1_s_	LOC616665	745,09	1858,84	2,49	2,25	2,77	1113,75	similar to Cdc42 effector, long
Bt.27339.1.A1_at	LOC536741	15,3	698,22	45,65	26,66	154,68	682,93	similar to Mme protein
Bt.347.1.S1_at	CHAD	9,7	221,81	22,86	13,44	73,22	212,1	chondroadherin
Bt.27401.1.A1_at	RNF128	45,74	237,56	5,19	4,13	6,85	191,83	ring finger protein 128
Bt.1742.1.S1_at	---	104,1	524,58	5,04	4,05	6,54	420,48	---
Bt.20418.1.A1_at	LOC534488	206,46	77,06	-2,68	-2,38	-3,02	-129,39	similar to solute carrier family 35, member A5
Bt.1424.1.S1_at	LOC520842	2041,74	5027,77	2,46	2,22	2,74	2986,03	similar to kruppel-like factor 4
Bt.20342.2.S1_a_	LOC533595	72,2	732,05	10,14	7,88	14,01	659,85	similar to Transducin-like enhancer of split 2 (E(sp1) homolog, Drosophila)
Bt.10135.2.S1_at	LOC534488	985,05	428,32	-2,3	-2,03	-2,61	-556,73	similar to solute carrier family 35, member A5
Bt.27621.1.A1_at	MGC155048	60,66	1196,84	19,73	12,54	44,94	1136,18	similar to autoantigen
Bt.2577.1.S1_at	LOC783506 /// L	6,28	1445,15	230,12	76,68	100000000	1438,87	similar to MGC127538 protein
Bt.19485.1.A1_at	---	613,11	2144,73	3,5	2,87	4,37	1531,62	Transcribed locus
Bt.21492.1.S1_at	LOC613647	696,07	231,55	-3,01	-2,64	-3,45	-464,52	similar to CDA04
Bt.2331.2.S1_at	MGC148675	337,01	15,99	-21,07	-12,78	-57,92	-321,02	similar to receptor activity-modifying protein 1
Bt.9140.1.S1_at	LOC526377	423,41	124,79	-3,39	-2,89	-4,04	-298,62	geminin-like
Bt.7478.1.S1_at	MGC140541	737,09	25,87	-28,5	-18,35	-62,51	-711,23	similar to heat shock protein, alpha-crystallin-related, B6
Bt.19601.1.S1_at	MGC142353	3512,41	1321,07	-2,66	-2,39	-3	-2191,34	similar to centrin 3
Bt.19805.1.A1_at	LOC786885 /// SI	666,6	2550,61	3,83	3,43	4,28	1884,01	solute carrier family 2 (facilitated glucose/fructose transporter), member 5 /// similar to glucose transporter 5
Bt.26784.2.S1_at	LOC538685	165,15	4,3	-38,36	-11,24	-100000000	-160,85	similar to KIAA1754 protein
Bt.5850.1.S1_at	---	934,08	345,65	-2,7	-2,24	-3,39	-588,44	Transcribed locus
Bt.6865.1.S1_at	LOC516598	10793,72	864,08	-12,49	-9,84	-16,88	-9929,64	similar to AXL receptor tyrosine kinase
Bt.28152.1.S1_at	---	233,78	12,71	-18,39	-10,37	-75,22	-221,07	Transcribed locus
Bt.21954.1.S1_at	---	6641,82	2786,4	-2,38	-2,13	-2,68	-3855,42	Transcribed locus, strongly similar to XP_001097236.1 hypothetical protein [Macaca mulatta]
Bt.6172.1.A1_at	LOC524109	8,66	258,82	29,89	15,75	258,5	250,17	similar to Protocadherin-19
Bt.17849.2.S1_at	LOC533166	303,01	106,84	-2,84	-2,22	-3,89	-196,17	similar to mosaic protein LR11
Bt.24725.1.S1_at	POLR2K	1143,57	469,64	-2,44	-2,03	-3,03	-673,93	polymerase (RNA) II (DNA directed) polypeptide K, 7.0kDa
Bt.12440.1.A1_at	IGFBP5	8657,49	542,65	-15,95	-13,99	-18,46	-8114,84	insulin-like growth factor binding protein 5
Bt.16391.1.A1_at	LOC782315	17,32	121,63	7,02	5,75	8,88	104,31	similar to IQ motif containing GTPase activating protein 2
Bt.16495.1.A1_at	LOC511602	7,68	1749,05	227,72	122,41	1578,3	1741,36	similar to alpha-5 type IV collagen
Bt.2096.1.S1_at	LOC505206	122,04	1530,09	12,54	9,7	17,47	1408,05	similar to pincher
Bt.24475.1.S1_at	LOC515758	49,94	483,12	9,67	6,94	15,54	433,18	hypothetical LOC515758
Bt.16094.1.S1_at	LOC509106	27,35	275,9	10,09	6,59	20,59	248,54	similar to enhancer of zeste homolog 2
Bt.3554.1.S1_at	LOC529049	8,11	154,46	19,03	9,08	100000000	146,35	similar to mannose receptor, C type 2
Bt.22586.1.A1_at	MGC129108	163,98	807,78	4,93	4,27	5,76	643,79	Similar to myo-inositol monophosphatase A3
Bt.3722.1.S1_at	---	71,84	401,32	5,59	3,85	9,67	329,48	CDNA clone IMAGE:8067330
Bt.20170.1.S1_at	EHD2	28,49	308,88	10,84	6,37	33,23	280,38	EH-domain containing 2
Bt.26797.1.S1_at	DENND2D	50,71	669,1	13,19	9,32	22,09	618,39	DENN/MADD domain containing 2D
Bt.18321.1.A1_at	MGC152413	270,75	1255,27	4,64	4,11	5,27	984,52	similar to guanine nucleotide binding protein beta subunit 4

probe set	GENE ID	baseline mean (LS	periment mean (L	fold change	lower bound of F	upper bound of F	difference of me	Gene Title
Bt.378.1.S1_at	ATP5I	2039,39	5246,99	2,57	2,13	3,24	3207,6	ATP synthase, H+ transporting, mitochondrial F0 complex, subunit e
Bt.1366.1.S1_at	CLEC3B	3466	11015,85	3,18	2,67	3,92	7549,85	C-type lectin domain family 3, member B
Bt.24260.2.S1_at	---	533,43	216,89	-2,46	-2,03	-3,04	-316,54	Transcribed locus
Bt.29185.1.S1_at	---	490,22	196,59	-2,49	-2,15	-2,96	-293,63	Transcribed locus
Bt.6244.1.S1_at	LOC505839	705,05	246,72	-2,86	-2,17	-4,12	-458,33	similar to ubiquitin specific protease 20
Bt.19937.1.S1_at	LOC532189	1228,14	3654,39	2,98	2,63	3,38	2426,25	similar to carboxypeptidase D
Bt.5401.1.S1_at	TGM2	12,84	1286,42	100,19	40,6	100000000	1273,58	transglutaminase 2 (C polypeptide, protein-glutamine-gamma-glutamyltransferase)
Bt.161.1.S2_at	DSG1	16,84	2541,01	150,89	93,95	378,18	2524,17	desmoglein 1
Bt.15740.1.A1_at	LOC534629	19,93	1064,79	53,43	30,97	189,21	1044,86	similar to tumor protein D52-like 1
Bt.25614.1.A1_at	TPP1	1086,79	2325,03	2,14	2,01	2,28	1238,25	Tripeptidyl-peptidase I
Bt.22568.1.S1_at	RPL29	2564,56	6650,24	2,59	2,26	3,04	4085,68	ribosomal protein L29
Bt.6133.2.A1_at	---	566,7	19,32	-29,34	-19,88	-55,02	-547,38	Transcribed locus, weakly similar to XP_001097766.1 glypican 3 isoform 4 [Macaca mulatta]
Bt.1491.1.S1_at	C1S	634,66	196,4	-3,23	-2,44	-4,74	-438,26	complement component 1, s subcomponent
Bt.3435.1.A1_at	LOC507975	22,44	7513,69	334,8	108,86	100000000	7491,24	hypothetical protein LOC507975
Bt.22760.1.S1_at	---	5000,47	1468,53	-3,41	-3,01	-3,87	-3531,95	Transcribed locus
Bt.25661.1.A1_at	LOC537027 /// LC	1460,48	377,6	-3,87	-3,25	-4,69	-1082,89	similar to Mitotic checkpoint serine/threonine-protein kinase BUB1 beta /// similar to BUB1 budding uninhibited by benzimidazoles 1 homolog beta
Bt.24607.2.S1_at	MGC128683	591,77	222,86	-2,66	-2,23	-3,28	-368,91	similar to Nucleolar protein 11
Bt.4106.1.S1_at	F3 /// LOC78400	159,48	1475,11	9,25	7,82	11,2	1315,64	coagulation factor III (thromboplastin, tissue factor) /// similar to F3 protein
Bt.648.3.S1_at	MGC151609	3911,1	685,19	-5,71	-4,55	-7,5	-3225,91	similar to TRIP protein
Bt.25228.1.A1_at	---	2420,78	963,51	-2,51	-2,01	-3,32	-1457,26	Transcribed locus
Bt.1404.1.S1_at	LOC514631	1794,03	381,2	-4,71	-3,93	-5,77	-1412,83	Similar to Cell division cycle associated 7-like
Bt.26901.2.S1_a	JPH2	114,47	356,16	3,11	2,39	4,31	241,69	junctophilin 2
Bt.8513.1.A1_at	LOC509610	1062,22	2568,76	2,42	2,26	2,58	1506,54	similar to N-acetylglucosamine-1-phosphate transferase
Bt.27243.1.A1_s	LOC533414	277,22	69,91	-3,97	-2,92	-6,13	-207,31	similar to RAD54B protein
Bt.14198.2.S1_at	LOC783295	536,03	133,64	-4,01	-3,16	-5,47	-402,39	hypothetical protein LOC783295
Bt.20822.1.A1_at	---	1341,68	588,45	-2,28	-2,01	-2,63	-753,23	Transcribed locus
Bt.5038.1.S1_at	FGF1	1229,9	20,37	-60,37	-37,88	-146,24	-1209,53	fibroblast growth factor 1 (acidic)
Bt.18325.2.A1_at	MGC151537	938,9	381,31	-2,46	-2,14	-2,89	-557,59	microtubule-associated protein 7
Bt.8330.1.S1_at	---	407,12	1321,16	3,25	2,86	3,71	914,04	Transcribed locus
Bt.5494.1.S1_at	CD44	276,94	2475,76	8,94	7,5	10,94	2198,82	CD44 molecule (Indian blood group)
Bt.10688.1.S1_at	LOC529661	67,43	932,12	13,82	9,85	22,66	864,7	similar to E2IG4
Bt.5334.1.S1_at	LAMR1	4241,73	12919,8	3,05	2,52	3,85	8678,07	laminin receptor 1 (ribosomal protein SA, 67 kDA)
Bt.8798.1.S1_at	LOC507093 /// LC	2329,95	333,42	-6,99	-6,12	-8,07	-1996,53	similar to retinaldehyde dehydrogenase 3 /// similar to aldehyde dehydrogenase 6
Bt.10283.1.S1_at	LOC537938	157,98	1645,75	10,42	8,35	13,65	1487,77	hypothetical protein LOC537938
Bt.3809.1.S1_at	LDHA	9185,4	3391,5	-2,71	-2,49	-2,95	-5793,89	lactate dehydrogenase A
Bt.28490.1.S1_at	---	319,13	65,57	-4,87	-3,3	-9,2	-253,57	---
Bt.27376.1.S1_at	BAG4	368,07	122,87	-3	-2,21	-4,47	-245,2	BCL2-associated athanogene 4
Bt.17447.1.A1_at	LOC541122	237,96	2719,48	11,43	10,43	12,56	2481,52	similar to chromosome 6 open reading frame 60
Bt.18229.1.A1_at	LOC507620	593,72	130,2	-4,56	-3,8	-5,6	-463,51	similar to partner and localizer of BRCA2
Bt.24112.1.A1_at	LOC511907	59,41	293,54	4,94	3,89	6,6	234,12	hypothetical LOC511907
Bt.19274.1.A1_at	MGC142642	10,59	241,08	22,76	11,3	2975,65	230,48	similar to C1q and tumor necrosis factor related protein 7
Bt.24124.1.A1_at	---	5,32	616,66	115,94	61,05	1076,16	611,34	Transcribed locus
Bt.27924.1.S1_at	RAP80	1256,18	408,25	-3,08	-2,48	-4,05	-847,92	receptor associated protein 80
Bt.981.3.S1_at	---	1396,35	402,61	-3,47	-3,06	-3,94	-993,74	Transcribed locus
Bt.16114.1.S1_at	---	293,2	77,05	-3,81	-2,72	-6,27	-216,15	Transcribed locus
Bt.18689.1.S1_at	LOC538401	194,11	1592,11	8,2	6,59	10,66	1397,99	similar to Arylsulfatase B precursor (ASB) (N-acetylgalactosamine-4-sulfatase) (G4S)
Bt.20518.1.A1_at	---	13,05	131,62	10,09	6,63	20,05	118,57	Transcribed locus
Bt.26606.1.S1_at	CHST1	675,17	1764,32	2,61	2,42	2,82	1089,14	carbohydrate (keratan sulfate Gal-6) sulfotransferase 1
BtAffx.1.13.S1_at	TAC3	61,45	2555,96	41,59	28,64	74,87	2494,51	tachykinin 3 (neuromedin K, neurokinin beta)
Bt.7347.1.S1_at	---	949,11	2218,79	2,34	2,05	2,72	1269,68	Transcribed locus
Bt.6154.1.S1_at	FHL3	904,77	284,9	-3,18	-2,53	-4,25	-619,87	four and a half LIM domains 3
Bt.11001.1.S1_at	---	1937,47	364,95	-5,31	-4,64	-6,13	-1572,52	Transcribed locus
Bt.15739.1.S1_at	MGC137017	316,03	895,33	2,83	2,45	3,3	579,3	similar to stimulated by retinoic acid 13
Bt.24351.1.A1_at	MGC142689	4,91	1338,09	272,67	114,82	100000000	1333,18	similar to limb expression 1
Bt.9211.1.S1_at	APBB1IP	1043,45	434,31	-2,4	-2,11	-2,75	-609,14	amyloid beta (A4) precursor protein-binding, family B, member 1 interacting protein
Bt.13235.1.S1_at	MGC148992	9,63	2153,59	223,56	99,8	100000000	2143,96	similar to RGC-32
Bt.13899.1.A1_at	LOC615535	6,58	656,28	99,68	43,95	100000000	649,69	similar to PDNP1
Bt.22741.2.A1_at	---	11,23	1347,53	119,96	67,77	506,14	1336,29	Transcribed locus
Bt.28388.1.S1_at	LOC514572	699,07	2353,86	3,37	2,76	4,31	1654,79	similar to Anaphase promoting complex subunit 4
Bt.20435.1.S1_at	LOC613935	220,19	2800,34	12,72	5,41	100000000	2580,15	similar to tumor suppressing subtransferable candidate 1
Bt.13734.1.A1_at	---	138,79	816,93	5,89	3,99	11,15	678,15	Transcribed locus
Bt.2039.2.S1_at	LOC514971	1712,15	21,92	-78,1	-30,24	-100000000	-1690,22	Similar to cytochrome P450 2S1
Bt.26423.1.A1_at	---	255,56	49,43	-5,17	-3,35	-11,16	-206,13	Transcribed locus
Bt.26107.1.A1_at	LOC540563	523,37	212,53	-2,46	-2,05	-3,01	-310,84	similar to ash1 (absent, small, or homeotic)-like

probe set	GENE ID	baseline mean (LS	periment mean (L	fold change	lower bound of F	upper bound of F	difference of me	Gene Title
Bt.16087.1.S1_at	MGC159943	22,09	836,94	37,88	27,67	59,28	814,85	similar to nidogen-2
Bt.5856.1.S1_at	---	460,91	94,54	-4,88	-3,57	-7,34	-366,37	Transcribed locus
Bt.18840.1.S1_at	LOC510708	62,78	1114,38	17,75	14,48	22,67	1051,59	similar to adenylate cyclase 2
Bt.12600.1.S1_at	---	953,59	161,63	-5,9	-4,86	-7,37	-791,96	Transcribed locus
Bt.23608.1.S1_s_	KRT8	2,16	1719,19	794,94	188,47	100000000	1717,03	keratin 8
Bt.8433.1.S1_at	LOC526045	1215,05	3199,1	2,63	2,17	3,33	1984,05	similar to SURF-4
Bt.23354.1.S1_at	MGC126963	3609,38	194,17	-18,59	-14,74	-24,86	-3415,21	similar to epoxide hydrolase 1
Bt.27140.1.S1_at	LOC535166	1080,42	92,6	-11,67	-9,88	-14,09	-987,82	similar to sulfatase 1
Bt.24460.1.S1_at	MGC143376	330,75	16,08	-20,57	-12,97	-47,9	-314,67	similar to zinc finger, CCHC domain containing 12
Bt.12360.1.S1_at	---	472,38	1242,3	2,63	2,31	3,01	769,92	Transcribed locus
Bt.20157.1.S1_at	LOC539561	3392,32	137,74	-24,63	-18,69	-35,62	-3254,58	similar to glutaminase liver
Bt.3227.1.S1_at	ASCC2	418,91	1247,59	2,98	2,5	3,6	828,69	activating signal cointegrator 1 complex subunit 2
Bt.14121.1.S1_at	---	5,96	757,51	127,18	66,82	1216,25	751,55	Transcribed locus
Bt.10343.1.A1_at	PALMD	2893,15	240,71	-12,02	-9,23	-16,89	-2652,44	palmdelphin
Bt.25077.1.S1_at	---	111,57	897,14	8,04	6,69	9,93	785,57	---
Bt.3989.1.S1_at	---	1265,02	2870,94	2,27	2,06	2,53	1605,92	Transcribed locus
Bt.16176.1.A1_at	---	51,25	2454,79	47,9	31,5	98,02	2403,54	Transcribed locus
Bt.22279.1.S1_at	LOC614739	3,31	1394,91	421,78	54,99	100000000	1391,61	hypothetical LOC614739
Bt.15623.1.S1_at	---	45,97	705,67	15,35	12,11	20,66	659,7	Transcribed locus, weakly similar to XP_001085012.1 similar to desmoplakin isoform I isoform 2 [Macaca mulatta]
Bt.12054.3.S1_at	LOC511748	1877,25	449,24	-4,18	-3,66	-4,79	-1428,02	similar to Yip1 domain family, member 1
Bt.16243.1.S1_at	MGC140079	11,62	3269,3	281,46	150,43	2066,06	3257,68	similar to chemokine-like factor superfamily 8
Bt.6591.1.S1_at	---	895,07	2351,13	2,63	2,19	3,27	1456,06	Transcribed locus
Bt.7130.1.S1_at	LOC534774	14,5	355,49	24,51	12,69	275,01	340,98	similar to aspartic-like protease
Bt.16415.1.S1_at	---	4,34	266,87	61,49	31,03	2104,73	262,53	Transcribed locus
Bt.9750.2.S1_a_a	SNRPG	1469,21	3513,63	2,39	2,17	2,63	2044,42	small nuclear ribonucleoprotein polypeptide G
Bt.21177.1.A1_s_	LOC511229	333,31	1347,22	4,04	3,64	4,5	1013,9	similar to CARD8 protein
Bt.6261.1.S1_at	LOC614323	32,89	463,54	14,09	10,68	20,33	430,65	similar to carbonic anhydrase
Bt.16063.2.S1_at	---	141,21	914,52	6,48	5,33	8,09	773,31	Transcribed locus
Bt.1819.1.S1_at	MGC127828	1133,17	2852,69	2,52	2,11	3,12	1719,52	similar to ubiquinol-cytochrome c reductase complex 7.2kDa protein
Bt.8829.1.S1_at	IFT122	929,69	323,92	-2,87	-2,49	-3,33	-605,77	WD repeat domain 10
Bt.13880.1.S1_at	LOC504445	155,26	3653,33	23,53	20,11	28,08	3498,07	similar to Dickkopf-1 (hdkk-1)
Bt.5026.1.S1_at	ANXA8	42,63	930,69	21,83	13,55	53,88	888,06	annexin A8
Bt.5324.1.S1_s_a	JSP.1	999,85	4106,16	4,11	3,74	4,51	3106,3	MHC Class I JSP.1
Bt.16815.1.S1_at	LOC513526	749,17	2673,98	3,57	3,13	4,1	1924,81	similar to U11/U12 snRNP 25K protein
Bt.12295.1.S1_at	PDPN	302,49	2788,44	9,22	7,47	11,83	2485,95	Podoplanin
Bt.20295.1.A1_at	---	572,56	22,75	-25,17	-16,48	-51,79	-549,81	Transcribed locus
Bt.14001.1.A1_at	---	345,69	20,75	-16,66	-10,51	-38,36	-324,94	Transcribed locus
Bt.23360.1.S1_at	LOC399559	1277,47	416,65	-3,07	-2,56	-3,82	-860,83	nicotinate phosphoribosyltransferase-like
Bt.21641.1.S1_at	MGC139340	9,11	1495,23	164,09	80,08	100000000	1486,12	similar to Ectoderm-neural cortex-1 protein (ENC-1) (p53-induced protein 10) (Nuclear matrix protein NRP/B)
Bt.10859.2.S1_at	MGC139506	737,15	131,3	-5,61	-4,46	-7,38	-605,85	similar to cAMP responsive element binding protein-like 2
Bt.2282.1.S1_a_a	LOC530071	186,27	31,45	-5,92	-4,57	-8,16	-154,82	similar to OTTHUMP00000016433
Bt.6552.1.S1_at	---	318,68	47,18	-6,75	-4,09	-19,35	-271,51	Transcribed locus
Bt.8191.1.S1_at	SLC9A3R1	472,82	1783,13	3,77	3,32	4,31	1310,31	solute carrier family 9 (sodium/hydrogen exchanger), member 3 regulator 1
Bt.17702.1.A1_at	---	2,89	414,19	143,55	49,74	100000000	411,31	Transcribed locus
Bt.800.1.S1_at	MAPK13	6,28	559,48	89,06	40,69	100000000	553,2	mitogen-activated protein kinase 13
Bt.21191.2.A1_at	MGC143198	1111,07	406,68	-2,73	-2,28	-3,39	-704,39	similar to phosphodiesterase 4D interacting protein (myomegalin)
Bt.21853.1.S1_at	AP1S1	1853,34	249,59	-7,43	-6,21	-9,07	-1603,74	Adaptor-related protein complex 1, sigma 1 subunit
Bt.554.1.S1_at	DMP1	18371,4	5722,07	-3,21	-2,58	-4,23	-12649,33	dentin matrix acidic phosphoprotein
Bt.166.1.S1_at	PENK	941,96	23,21	-40,58	-21,69	-282,87	-918,74	proenkephalin
Bt.11710.1.S1_at	MGC140046	606,28	1602,84	2,64	2,08	3,6	996,56	similar to phosducin-like 3
Bt.27202.1.A1_at	SOSTDC1	5,61	2612,75	465,39	218,04	100000000	2607,14	sclerostin domain containing 1
Bt.16874.1.A1_at	LOC617120	574,82	199,81	-2,88	-2,5	-3,32	-375,01	Hypothetical LOC617120
Bt.22194.1.S1_at	IER2	1634,47	497,12	-3,29	-2,57	-4,38	-1137,35	immediate early response 2
Bt.19862.1.A1_at	LOC518458	97,63	3245,35	33,24	28,13	40,18	3147,71	similar to semaphorin 6D
Bt.28423.1.S1_at	LOC541051	1831,73	24,16	-75,83	-39,25	-953,64	-1807,57	similar to KIAA0984 protein
Bt.6642.1.S1_a_a	---	901,21	239,42	-3,76	-3,14	-4,59	-661,79	Transcribed locus
Bt.13203.1.S1_at	---	2350,07	9,02	-260,42	-115,99	-100000000	-2341,04	Transcribed locus
Bt.2812.1.A1_at	MGC142413	43,67	156,29	3,58	3,14	4,1	112,62	similar to Zinc-finger protein neuro-d4 (D4, zinc and double PHD fingers family 1)
Bt.22757.1.S1_at	---	4813,13	1654,48	-2,91	-2,61	-3,25	-3158,65	Transcribed locus
Bt.25303.1.A1_at	---	107,65	565,93	5,26	3,98	7,44	458,28	Transcribed locus
Bt.373.2.S1_a_at	AMELX /// AMEL	4,49	3617,34	806,31	358,49	100000000	3612,85	amelogenin (amelogenesis imperfecta 1, X-linked) /// amelogenin, Y-linked
Bt.28295.1.S1_at	MGC159392	18,71	195,17	10,43	5,41	89,1	176,46	hypothetical LOC617670
Bt.1580.1.S1_at	LOC508224	35,99	428,08	11,9	8,42	19,61	392,1	similar to secretory granule, neuroendocrine protein 1 (7B2 protein)
Bt.26505.1.S1_at	---	12,59	422,03	33,51	22,55	63,73	409,44	Transcribed locus

probe set	GENE ID	baseline mean (LS	periment mean (L	fold change	lower bound of F	upper bound of F	difference of me	Gene Title
Bt.25257.1.A1_at	---	133,95	30,37	-4,41	-2,62	-12,12	-103,58	Transcribed locus
Bt.1976.2.S1_at	MGC139033	191,35	31,68	-6,04	-3,14	-45,1	-159,66	similar to suppression of tumorigenicity 5
Bt.24258.1.S1_at	LOC528150 /// LO	174,61	2352,23	13,47	11,98	15,22	2177,62	similar to Man9-mannosidase
Bt.9599.1.A1_at	MGC128671	489,09	1782,39	3,64	3,15	4,24	1293,29	Similar to Inositol hexakisphosphate kinase 2 (InsP6 kinase 2) (Inositol hexakisphosphate kinase 2) (P(i)-uptake stimulator) (PiUS)
Bt.21319.1.A1_at	---	71,05	2522,42	35,5	25,46	57,52	2451,37	Transcribed locus, weakly similar to NP_001036812.1 repeat domain 5 [Xenopus tropicalis]
Bt.13911.1.S1_s_	---	13,07	214,64	16,42	9,57	53,07	201,57	---
Bt.21475.3.S1_a_	LOC786013	536,44	1357,32	2,53	2,21	2,96	820,88	similar to Ded protein
Bt.9640.1.A1_at	SPON1	26,85	900,23	33,52	23,25	58,78	873,38	Spondin 1, extracellular matrix protein
Bt.28168.1.A1_at	MGC166050	8,18	146,18	17,88	9,18	210,22	138	similar to insulin gene enhancer binding protein Isl-1
Bt.13030.2.S1_at	COL2A1	248,85	709,45	2,85	2,44	3,43	460,6	collagen, type II, alpha 1
Bt.16639.1.A1_at	---	6030,1	709,15	-8,5	-6,86	-10,95	-5320,95	Transcribed locus
Bt.18204.2.A1_at	SGLT5	9,43	311,36	33,02	17,45	259,93	301,93	Na+/glucose cotransporter-related protein
Bt.26637.1.A1_at	---	991,64	67,63	-14,66	-9,69	-28,85	-924,01	Transcribed locus
Bt.18955.2.A1_at	---	150,25	2,81	-53,38	-23,28	-100000000	-147,44	Transcribed locus
Bt.7728.1.A1_at	---	2187,67	343,23	-6,37	-5,52	-7,42	-1844,44	Transcribed locus
Bt.21215.2.S1_at	LOC506721	21,78	458,53	21,05	13,44	46,48	436,75	similar to ALL1 responsive protein ARP1c
Bt.13587.2.S1_a_	LOC521539	220,94	1626,83	7,36	6,09	9,12	1405,89	Similar to mannosidase, alpha, class 2A, member 1
Bt.28430.1.S1_at	---	10	313,64	31,36	17,03	176,09	303,64	---
Bt.19936.1.A1_at	---	187,88	916,49	4,88	4,21	5,7	728,61	Transcribed locus
Bt.115.1.S1_at	DDC	130,14	3090,29	23,75	19,63	29,61	2960,15	dopa decarboxylase (aromatic L-amino acid decarboxylase)
Bt.7418.1.S1_at	LOC511800	5972,5	262,34	-22,77	-17	-33,73	-5710,16	similar to KIAA1581 protein
Bt.18969.1.S1_at	---	1767,1	295,64	-5,98	-4,84	-7,62	-1471,46	Transcribed locus
Bt.4438.1.S1_at	PRKAR1B	198,48	29,11	-6,82	-4,29	-16,56	-169,37	protein kinase, cAMP-dependent, regulatory, type I, beta
Bt.8712.1.S1_at	STIM1	3117,53	1197,32	-2,6	-2,16	-3,27	-1920,21	stromal interaction molecule 1
Bt.9288.1.S1_at	LOC510738	18,08	1001,4	55,4	36,92	108,13	983,33	similar to FLJ00258 protein
Bt.14209.1.A1_at	---	13,29	1329,13	99,98	46,11	100000000	1315,84	Transcribed locus
Bt.18203.2.S1_at	MGC151720	277,9	60,84	-4,57	-2,74	-13,14	-217,06	similar to C21ORF43
Bt.24925.1.A1_at	---	9,44	530,46	56,18	18,45	100000000	521,02	---
Bt.7700.1.S1_at	ACTN1	133,9	1097,56	8,2	6,7	10,33	963,67	actinin, alpha 1
Bt.16187.1.A1_at	LOC538461	290,66	86,7	-3,35	-2,95	-3,81	-203,96	similar to Kelch repeat and BTB (POZ) domain containing 6
Bt.29801.1.S1_at	---	42,92	3666,75	85,44	48,03	362,53	3623,83	B4 cell-line anti-respiratory syncytial virus Ig lambda chain V region (IgL)
Bt.25009.1.S1_at	---	76,63	837,96	10,94	4,9	100000000	761,33	Clone NG010006A21G10 mRNA, complete sequence
Bt.19181.1.A1_at	LOC532572	92,45	805,21	8,71	7,21	10,76	712,76	similar to Laminin gamma-1 chain precursor (Laminin B2 chain)
Bt.5515.1.S1_at	NT5E	17,05	5539,93	324,99	215,31	644,04	5522,88	5'-nucleotidase, ecto (CD73)
Bt.4882.1.S1_at	FKBP9	2249,41	5906,32	2,63	2,11	3,47	3656,92	FK506 binding protein 9
Bt.2725.1.S1_at	UBE2C	11,16	251,88	22,56	11,54	297,31	240,71	ubiquitin-conjugating enzyme E2C
Bt.16036.1.S1_at	MGC139020	102,5	2018,52	19,69	15,92	25,31	1916,01	similar to SH3BGRL2 protein
Bt.11454.1.A1_at	---	372,99	6,47	-57,67	-29,78	-705,04	-366,53	Transcribed locus
Bt.7980.1.S1_at	LASP1 /// LOC78	3374,97	8385,24	2,48	2,12	2,99	5010,27	LIM and SH3 protein 1 /// similar to LIM and SH3 protein 1
Bt.12179.1.S1_at	LOC518469	41,53	1141,05	27,48	19,58	44,75	1099,52	similar to RP5-1022P6.2
Bt.7808.1.A1_at	---	93,74	1594,98	17,02	12,99	24,01	1501,24	Transcribed locus
Bt.543.1.S1_at	NR2F1	1855,45	100,05	-18,55	-12,55	-34,03	-1755,4	nuclear receptor subfamily 2, group F, member 1
Bt.3139.1.A1_at	---	6694,83	78	-85,83	-56,13	-176,26	-6616,83	Transcribed locus
Bt.11017.1.S1_at	LOC540504	126,9	915,35	7,21	5,95	8,92	788,45	similar to Nesprin-2 (Nuclear envelope spectrin repeat protein 2) (Syne-2) (Synaptic nuclear envelope protein 2) (Nucleus and actin connecting element protein) (Protein NUANCE)
Bt.3236.1.A1_at	LOC782247	6,36	386,5	60,74	34,03	260,32	380,14	similar to RhoGEF protein
Bt.26081.1.A1_at	LOC514646	343,59	25,34	-13,56	-9,5	-22,66	-318,25	similar to Acyltransferase like 1
Bt.21203.1.S1_at	---	173,52	952,97	5,49	4,72	6,44	779,45	Transcribed locus
Bt.13702.1.S1_at	---	287,24	2496,17	8,69	7,52	10,1	2208,92	Transcribed locus
Bt.11013.1.S1_at	---	43,22	399,55	9,24	6,85	13,64	356,33	Transcribed locus
Bt.11476.1.S1_at	MGC128664	3194,04	67,19	-47,53	-34,2	-75,8	-3126,84	similar to Beta-1,3-N-acetylglucosaminyltransferase lunatic fringe (O-fucosylpeptide 3-beta-N-acetylglucosaminyltransferase)
Bt.22596.1.A1_at	---	41,92	409,21	9,76	8,1	12,01	367,29	Transcribed locus
Bt.14239.1.A1_at	MGC155329	52,56	953,37	18,14	13,9	25,39	900,82	similar to enhancer of filmentation 1
Bt.64.1.S1_at	NDUFB7	276,35	3003,19	10,87	5,47	765,54	2726,84	NADH dehydrogenase (ubiquinone) 1 beta subcomplex, 7, 18kDa
Bt.20853.1.S1_a_	LOC506769	715,87	36,61	-19,56	-12,9	-38,47	-679,27	similar to src kinase associated phosphoprotein 1
Bt.648.1.A1_at	MGC151609	3657,57	734,45	-4,98	-4,23	-5,91	-2923,12	similar to TRIP protein
Bt.227.1.A1_at	GSTA2	41,66	579,2	13,9	10,48	20,01	537,54	glutathione S-transferase A2
Bt.25236.1.A1_at	LOC786844	25,48	974,56	38,25	25,28	75,55	949,08	similar to adlican
Bt.4277.1.A1_at	---	53,42	1154,52	21,61	16,84	29,38	1101,1	Transcribed locus
Bt.20905.1.S1_at	LOC504509	439,85	27,82	-15,81	-11,39	-24,9	-412,03	similar to Zeta-chain (TCR) associated protein kinase
Bt.8436.1.S1_at	IFI6	399,34	4064,3	10,18	8,66	12,07	3664,95	interferon, alpha-inducible protein 6
Bt.21958.1.A1_at	LOC508963	794,62	289,15	-2,75	-2,07	-4,04	-505,46	hypothetical LOC508963
Bt.18132.1.A1_at	LOC516290	6,8	320,49	47,12	21,98	100000000	313,69	similar to FLJ00261 protein
Bt.13435.1.A1_at	LOC539445	132,51	718,1	5,42	4,59	6,45	585,59	similar to serine/threonine protein kinase MASK

probe set	GENE ID	baseline mean (LS	periment mean (L	fold change	lower bound of F	upper bound of F	difference of me	Gene Title
Bt.4912.1.S1_at	PI16	175,1	65,41	-2,68	-2,21	-3,38	-109,69	peptidase inhibitor 16
Bt.3399.2.S1_at	---	20,47	935,86	45,72	31,12	82,9	915,39	Transcribed locus
Bt.12625.1.S1_at	LOC615883	79,78	1309,37	16,41	13,31	20,86	1229,59	similar to SLIT3
Bt.2410.1.A1_at	---	23,48	209,43	8,92	6,08	15,65	185,95	Transcribed locus
Bt.22459.1.S1_at	LOC785319	70,67	2219,79	31,41	24,2	43,42	2149,12	similar to Neural cell adhesion molecule 1, 180 kDa isoform precursor (N-CAM 180) (NCAM-180)
Bt.25989.1.A1_at	GJB6	4,52	758,74	167,78	63,84	100000000	754,21	gap junction protein, beta 6
Bt.5046.2.A1_a_a	LOC506670	275,97	17,93	-15,39	-9,53	-36,67	-258,04	similar to Solute carrier family 7, (cationic amino acid transporter, y+ system) member 13
Bt.10144.1.A1_s_	MGC142564	23,14	508,88	21,99	16,39	32,28	485,74	similar to T-lymphoma invasion and metastasis inducing protein 1 (TIAM1 protein)
Bt.16415.3.A1_at	---	2,83	416,95	147,18	57,14	100000000	414,12	Transcribed locus
Bt.4670.1.S1_at	LOC539596	60,94	1014,59	16,65	11,95	26,08	953,65	similar to Transforming growth factor-beta induced protein IG-H3 precursor (Beta IG-H3) (Kerato-epithelin) (RGD-containing collagen associated
Bt.25187.1.A1_at	LOC615535	15,34	383,57	25	18,46	37,07	368,22	Similar to PDNP1
Bt.13184.1.S1_at	---	4,59	521,4	113,51	62,04	565,94	516,81	Transcribed locus
Bt.4177.3.A1_at	LOC781194	7,72	261,76	33,91	20,86	83,09	254,04	Similar to KIAA1568 protein
$	1338 genes satisfied the comparison filtering criteria							

Appendix 2:

Understanding Pulp Biology for Routine Clinical Practice.
Stéphane Simon, Paul Cooper, Philip Lumley, Ariane Berdal, Phillip Tomson, Anthony J Smith. ENDO (Lond Engl) 2009;3(3)

Aim: To review the latest developments in the field of pulp biology, particularly those elements of specific interest to clinical dentists, whilst highlighting the importance of maintaining pulp vitality for conservative dentistry. Pulp biology is crucial to everyday practice in dentistry and the knowledge acquired, especially in the last five years on the pulp healing process, has highlighted simple but effective applications. However, difficulties in communication between biologists and clinicians, mostly due to the complexity of biology as a discipline, are a significant obstacle to therapeutic developments and their application on a larger scale.
Methods: A literature review was undertaken on the current understanding of the biology of the dentine-
pulp complex, especially in the context of conservative dentistry.
Results: Novel biotechnological insights have recently been discovered, including the presence of stem cell-like cells within the tooth and their potential roles in reparative and regenerative processes. A greater understanding is also developing regarding the structure of the dentine-pulp complex, both macroscopically and microscopically, which may have important consequences for therapeutic choices.
Conclusions: The emergence of new adhesive systems, together with disinfecting molecules, represents a first step towards the application of new biological approaches to the treatment of pulpal disease. Improved understanding of the many pathophysiological processes of the dentine-pulp complex and the development of new materials, which are being adapted to clinical conditions, has led to significant advances for the therapeutic principles underpinning conservative dentistry.

Appendix 3:

Molecular characterization of young and mature odontoblasts.
Simon S, Smith AJ, Lumley PJ, Berdal A, Smith G, Finney S, Cooper PR.
Bone. 2009 Oct;45(4):693-703.

The odontoblast is the secretory cell responsible for primary, secondary and tertiary reactionary dentinogenesis. We provide evidence that the changes in secretory activity of odontoblasts reflect differential transcriptional control and that common regulatory processes may exist between dentine and bone.

Introduction: Based on the hypothesis that differential dentine secretion (primary and secondary dentinogenesis) is associated with changes in the transcriptional control within the cell, we have investigated the transcriptome of odontoblasts at young and mature stages and subsequently used this information to identify key regulatory intracellular pathways involved in this process.

Materials and Methods: We used microarray analysis to compare the transcriptome of early stage (primary dentinogenesis) and late stage (secondary dentinogenesis) odontoblasts from 30 month old bovine teeth. Secondarily, we used post-array sqRT-PCR to confirm the differential expression of 23 genes in both populations of odontoblasts. Finally, immunohistochemistry was performed on bovine and murine tissues with antibodies to DMP1 and anti-phospho p38 proteins.

Results: DMP-1 and osteocalcin gene expression were up-regulated in the mature odontoblasts, whereas collagen I, DSPP, TGF-beta1 and TGF-beta1R gene expression were down-regulated. Microarray analysis highlighted 574 differentially regulated genes (fold change>2 - $p<0.05$). This study supports further existing similarities between pulp cells and bone cells. Using post-array Sq-RT-PCR we characterized transcript levels of genes involved in the p38 MAP kinase pathway (PTPRR, NTRKK2, MAPK13, MAP2K6,MKK3). Differential p38 gene activation was confirmed by immunohistochemistry for p38 protein in murine teeth. Finally, immunohistochemistry for DMP1 indicated that odontoblasts involved in primary and secondary dentinogenesis may coexist in the same tooth.

Conclusion: As established in bone cells, the transcriptome of the odontoblast was shown here to evolve with their stage and functional maturity. Identification of the involved signalling pathways, as highlighted for p38, will enable the deciphering of physiology and pathology of mineralized tissue formation.

Appendix 4:

The MAPK pathway is involved in odontoblast stimulation via p38 phosphorylation. Simon S., Smith A.J., Berdal A., Lumley P.J., Cooper P.R.
Journal of Endodontics. Accepted for Publication -*In Press*

We have previously shown that the *p38* gene is highly expressed in odontoblasts during active primary dentinogenesis, but is drastically down-regulated as cells become quiescent in secondary dentinogenesis. Based on these observations, we hypothesized that p38 expression might be upregulated, and the protein activated by phosphorylation, when odontoblasts are stimulated such as during tertiary reactionary dentinogenesis. We stimulated immortalized, odontoblast-like MDPC-23 cells, alone or in combination, with heat-inactivated *Streptococcus mutans*, EDTA-extracted dentine matrix proteins (DMPs), or growth factors, including transforming growth factor (TGF)-ß1, tumor necrosis factor-α (TNF-α), and adrenomedullin (ADM). We used ELISA to measure the resulting phosphorylation of the p38 protein, as well as its degree of nuclear translocation. Our results suggest that the p38-MAPKinase pathway is activated during odontoblast stimulation in tertiary dentinogenesis by both p38 phosphorylation and enhanced nuclear translocation. Data indicate that odontoblast behaviour therefore potentially recapitulates that during active primary dentinogenesis.

Appendix 5:

Evaluation of a new laboratory model for pulp healing: preliminary study. Simon S, Cooper P, Smith A, Picard B, Ifi CN, Berdal A. Int Endod J. 2008 Sep;41(9):781-90.

Aim: To assess the feasibility of using the mouse as an in vivo model for studying pulpal healing in response to restorative procedures.
Methodology: Direct pulp capping on maxillary first molar teeth with mineral trioxide aggregate (MTA), overlaid with light-cured composite resin, was performed on nineteen 3-month-old mice. For control teeth, the composite resin was placed in direct contact with the pulp. Animals were killed at 3 days, 1 week, 2 weeks, 5 weeks and 11 weeks postoperatively. Extracted dental tissues were subsequently analysed by haematoxylin and eosin staining, immunohistochemistry for dentine sialophosphoprotein (DSPP) expression, scanning electronic microscopy and X-ray analysis to determine both pulpal response and dentine bridge formation.
Results: Of the 19 mice initially used, 16 were subsequently studied. Histological analyses of pulps directly exposed to MTA for up to 2 weeks demonstrated a distinct structural change in the extracellular matrix. By weeks 5 and 11, a dentine bridge was present in all MTA-treated specimens in which DSPP immunoreactivity was clearly apparent. Scanning electronic microscopy and X-ray analysis enabled confirmation of calcification of the dentine bridge, and demonstrated that it had a globular surface morphology as opposed to the tubular appearance associated with orthodentine.
Conclusions: This is the first description of the utilization of a murine model for study of in vivo pulpal repair. This approach provides a novel opportunity to enable the use of genetically modified animals to explore cellular and molecular processes during reparative events.